# EXPERIMENTAL AND NUMERICAL INVESTIGATIONS OF MINIMUM QUANTITY LUBRICATION WITH HYBRID NANO-FLUID ON MACHINABILITY OF TITANIUM ALLOY

*By*

**Prianka Binte Zaman**

A Thesis
Submitted to the
Department of Industrial & Production Engineering
in Partial Fulfilment of the
Requirements for the Degree
of
DOCTOR OF PHILOSOPHY IN INDUSTRIAL & PRODUCTION ENGINEERING

DEPARTMENT OF INDUSTRIAL & PRODUCTION ENGINEERING
BANGLADESH UNIVERSITY OF ENGINEERING & TECHNOLOGY
DHAKA, BANGLADESH

March 2021

The thesis titled **"Experimental and Numerical Investigations of Minimum Quantity Lubrication with Hybrid Nano-Fluid on Machinability of Titanium Alloy"** submitted by **Prianka Binte Zaman**, Student No. 0412084001P, Session- April 2012, has been accepted as satisfactory in partial fulfillment of the requirement for the degree of Doctor of Philosophy in Industrial & Production Engineering on March 9, 2021.

## BOARD OF EXAMINERS

| | | |
|---|---|---|
| 1. | Dr. Nikhil Ranjan Dhar<br>Professor<br>Department of Industrial & Production Engineering<br>BUET, Dhaka | Chairman |
| 2. | Dr. Nikhil Ranjan Dhar<br>Head<br>Department of Industrial & Production Engineering<br>BUET, Dhaka | Member<br>(Ex-officio) |
| 3. | Dr. A. K. M. Masud<br>Professor<br>Department of Industrial & Production Engineering<br>BUET, Dhaka | Member |
| 4. | Dr. Firdous Sarwar<br>Associate Professor<br>Department of Industrial & Production Engineering<br>BUET, Dhaka | Member |
| 5. | Dr. Shuva Ghosh<br>Associate Professor<br>Department of Industrial & Production Engineering<br>BUET, Dhaka. | Member |
| 6. | Dr. A. K. M. Bazlur Rashid<br>Professor<br>Department of Materials and Metallurgical Engineering<br>BUET, Dhaka | Member |
| 7. | Dr. Vishal Santosh Sharma<br>Professor<br>Department of Industrial & Production Engineering<br>Dr. B.R. Ambedkar National Institute of Technology<br>Jalandhar-144011, India. | Member<br>(External) |

## Declaration

It is hereby declared that this thesis or any part of it has not been submitted elsewhere for the award of any degree or diploma.

Prianka Binte Zaman

**This work is dedicated**
**to my loving**

***'Family'***

# Table of Contents

# List of Tables

# List of Figures

# List of Symbols

| | | |
|---|---|---|
| V | : | Cutting speed |
| f | : | Feed rate |
| d | : | Depth of cut |
| C | : | Nano-particle concentration |
| TT | : | Tool-type |
| D | : | Nozzle diameter |
| $\theta_P$ | : | Nozzle angle (Primary) |
| $\theta_S$ | : | Nozzle angle (Secondary) |
| P | : | Air pressure |
| Q | : | Oil flow rate |
| T | : | Cutting temperature |
| F | : | Main cutting force |
| $R_a$ | : | Average surface roughness |
| VB | : | Average flank wear |
| VS | : | Average auxiliary flank wear |
| r | : | Nose radius of the insert |
| $\Delta t$ | : | Temperature difference |
| V | : | Voltage applied to the heater |
| R | : | Heater resistance |
| $\Delta r$ | : | Radial clearance |
| A | : | Heat transfer area |
| $Q_c$ | : | Heat input |
| $Q_i$ | : | Incidental heat transfer at $\Delta t$ |
| $Q_e$ | : | Heat conduction through oil |
| K | : | Thermal conductivity of oil |
| t | : | Say bolt universal seconds |
| $\nu$ | : | Kinematic viscosity |
| $\dot{q}_p$ | : | Rate of heat generation by plastic deformation |
| $\eta$ | : | Is the fraction of plastic deformation energy |
| $\dot{\sigma}$ | : | Material flow stress tensor |
| E | : | Plastic strain rate |
| P | : | Material density |
| $C_p$ | : | Specific heat |
| $\dot{q}_f$ | : | Friction forces |
| $\eta_f$ | : | Fraction of dissipated energy |
| J | : | Equivalent heat conversion factor |
| $\tau$ | : | Shear stress computed by Coulomb‘s law |
| $\dot{\gamma}$ | : | Slip strain rate |
| $\beta$ | : | Frictional heat going into the workpiece |
| $E_f$ | : | Heat absorption coefficient |
| $\varepsilon$ | : | Equivalent plastic strain |
| $\dot{\varepsilon}$ | : | Strain rate normalized with a reference strain rate $\dot{\varepsilon}_0$ |
| T | : | Instantaneous temperature |
| $T_M$ | : | Melting temperature |
| $T_R$ | : | Reference temperature |
| $\varepsilon^f$ | : | Fracture strain |
| $D_1$ | : | Initial fracture strain |
| $D_2$ | : | Exponential factor |

| | | |
|---|---|---|
| $D_3$ | : | Triaxiality factor |
| $D_4$ | : | Strain rate factor |
| $D_5$ | : | Temperature factor |
| $\sigma_m$ | : | Average of the three normal stress |
| $\bar{\sigma}$ | : | Von-Mises equivalent stress |
| W | : | Damage parameter |
| $\Delta\varepsilon$ | : | Accumulated increment of equivalent plastic strain |
| Nu | : | Nusselt number |
| Re | : | Reynolds number |
| Pr | : | Prandtl number |
| $LN_2$ | : | Liquid Nitrogen |
| $CO_2$ | : | Carbon di Oxide |
| MQL | : | Minimum Quantity Lubrication |
| MQCL | : | Minimum Quantity Cooling Lubrication |
| SJMQL | : | Single Jet Minimum Quantity Lubrication |
| DJMQL | : | Double Jet Minimum Quantity Lubrication |
| NP | : | Nano particle |
| NF | : | Nano-fluid |
| HNF | : | Hybrid Nano-Fluid |
| SQL | : | Small Quantity Lubrication |
| HPC | : | High-Pressure Coolant |
| MRR | : | Material Removal Rate |
| BUE | : | Built-up-edge |
| PVD | : | Physical Vapor Deposition |
| CVD | : | Chemical Vapor Deposition |
| CBN | : | Cubic Boron Nitride |
| PCBN | : | Poly Crystalline Cubic Boron Nitride |
| PCD | : | Poly Crystalline Diamond |
| MWCNT | : | Multi-walled Carbon Nanotube. |
| DOE | : | Design of Experiment |
| RSM | : | Response Surface Methodology |
| ANOVA | : | Analysis of Variance |
| MAPE | : | Mean Absolute Percentage of Error |
| FEM | : | Finite Element Modeling |
| ALE | : | Arbitrary Eulerian-Lagrangian |
| SEM | : | Scanning Electron Microscope |

## Acknowledgment

First of all, I would like to express her deepest and heartfelt gratitude to the Almighty for surrounding her with kindness and blessing. I am extremely grateful to my respected supervisor Dr. Nikhil Ranjan Dhar, Professor, Department of IPE, BUET for his constant encouragement, guidance, support and advice throughout this research. I am also thankful to all the teachers and employees of the Department of IPE, BUET who directly or indirectly helped me. My sincere appreciation goes to the examiners of my doctoral thesis Dr. A. K. M. Masud, Dr. Ferdous Sarwar, Dr. Shuva Ghosh, Dr. A.K.M. Bazlur Rashid and Dr. Vishal Santosh Sharma for their valuable suggestions to improve the content of this thesis.

I also thank Director, DAERS, BUET for providing the research fund and machine shop facilities for carrying out this research work. I express my heartfelt gratitude to all the staff members of Central Machine Shop, especially Mr. Manik Chandra Dey for their help in conducting the experimental work. The help extended by Dr. Shakhawat H. Firoz, Head, Department of Chemistry, BUET for allowing me to use "Nano-chemistry Research Lab" facilities for the preparation of hybrid nano-fluid is also sincerely acknowledged. I am thankful to the technicians of the ME and GCE department, BUET for their help regarding the nano-fluid characterization and SEM respectively. Special thanks go to my fellow researchers: Shanta Saha, Imran Hasan Tusar and Nazma Sultana for their availability during experimental work and their inspirations at various stages of this research.

Last but not the least, I am intensely indebted to my parents, parents-in-law, husband and daughter for their selfless love, encouragement and sacrifices which inspire and motivate me to complete this research.

## Abstract

Titanium alloy, particularly Ti-6Al-4V, is extensively utilized in versatile engineering applications such as aerospace, automobile, biomedical, chemical and other manufacturing industries owing to their enviable and inimitable mechanical properties. But their machinability is usually considered to be poor because of low thermal conductivity, low elastic modulus, high hardness and high chemical reactivity. In the area of manufacturing, any attempt to improve the machinability of such hard-to-machine material is encouraged. Application of cutting fluids can reduce the cutting temperature and friction which heading to prolonged tool life and improved machining performance. But, conventional cutting fluids application techniques are known for being expensive, polluting and a non-sustainable part of modern manufacturing processes. Manufacturing industries are now being forced to implement economical, ecological and sustainable cooling strategies. Minimum Quantity Lubrication (MQL) technique is a modern technique, where a very small amount of coolant/ lubricant is delivered to the cutting zone as a form of a mist which can improve the machinability. However, the performance of MQL should be enhanced when utilized for machining hard-to-machine materials. Optimum selection of MQL delivery system parameters and improved cutting fluid can enhance its performance. Nano-fluid which comprises superior tribological and thermo-physical properties is a promising alternative to MQL fluid. This fluid can effectively improve the cooling and lubrication efficiency of MQL. Moreover, hybrid nanofluid can be a better choice due to its synergistic effects of integrating multiple nanoparticles. Optimization of process parameters, nano-fluid concentration and tool type also helps to achieve the ultimate machining performance.

In this study, a double jet MQL delivery system has been designed and fabricated for delivering mist directly towards the chip-tool and work-tool interfaces in turning Ti-6Al-4V alloy. Hybrid nano-fluid has also been prepared and applied through the MQL technique. The performance of the newly designed double jet MQL system and hybrid nano-fluid-based MQL has been systematically investigated. Double jet MQL combined with hybrid nano-fluid has performed the best compared to dry, single jet MQL with conventional cutting fluid and double jet MQL with conventional cutting fluid. Finally, process parameters have been optimized due to achieve an overall efficient manufacturing system for turning Ti-6Al-4V alloy. This thesis also presents a finite element model of turning Ti-6Al-4V alloy by carbide insert. Based on this model the effects of hybrid nano-fluid-based MQL application on temperature distribution and chip formation were investigated in simulations. The chip-tool interface temperature distribution and chip morphology in simulation show a good agreement with the measured value. This study revealed the promising behavior of nano-fluid-based double jet MQL in turning Ti-6Al-4V alloy by coated and uncoated carbide inserts within a specified range of cutting parameters. Nano-fluid-based MQL has an enormous opportunity to enhance the machinability of Ti-6Al-4V alloy considering environmental issues and should be explored further.

# Chapter-1

## Introduction

Titanium is the ninth richest element present in the outer layer of the earth and the fourth richest metal used for structural work [Donachie, 2000]. "Commercially pure" titanium comprises acceptable mechanical properties to be used for various purposes, but in most of the applications, titanium alloy is used. Titanium and its various alloys have extensive applications in different sectors because of their unique blend of favorable mechanical properties. Moreover, Ti-6Al-4V is recognized as the workhorse of the titanium industry, as it accomplishes more than 50% of entire titanium applications. Initially, this alloy was formulated for low weight and high strength products of the aerospace industry in the 1950s [Liu and Shin, 2019]. It is also applicable for making different automotive parts [Joshi, 2006]. The biocompatibility of Ti-6Al-4V alloy makes it useful for medical applications [Lepicka and Gradzka-Hahlke, 2016]. High corrosion resistance makes it the best alloy for use in the chemical processing and marine industry [Lepicka and Gradzka-Hahlke, 2016]. Some other usages of this alloy are different sports equipment, electronics equipment and some consumer products [Froes et al., 2019], etc. This versatile area of application is feasible because of its favorable mechanical properties such as high strength and toughness, better formability, biocompatibility, outstanding fatigue properties, ability to endure extreme temperature, excellent corrosion resistance [Cui et al., 2011].

However, the higher cost of raw materials and machining of this material confines its use in diverse sectors. High cutting temperature, tool wear, cutting force and low product quality are the major problems regarding the machining of Ti-6Al-4V alloy. Machinability of a material can be described as, the ease of cutting material with a specific tool under a specific operating condition [Black and Payton, 2003]. Materials having superior machinability offer good material removal rates as well as require less power, time and cost to achieve a satisfactory part quality. Some output responses of machining such as chip morphology, metal removal rate (MRR), cutting temperature, cutting forces,

cutting tool life and part quality may be utilized to assess machinability [Che-Haron, 2001; Che-Haron and Jawaid, 2005]. The emerging applications of Ti-6Al-4V alloy enforce the scientific researchers and manufacturing industry around the globe to study the improvement of their machinability [Mondal et al., 2020]. Machinability can be enhanced by selecting appropriate cutting fluid types and their application methods along with optimum cutting parameters and proper tool-type [Ezugwu and Wang, 1997; Kosaraju and Anne, 2013; Settineri and Faga, 2008]. This research intends to design and develop an advanced, eco-friendly and economic cooling system that will help to enhance the machinability of Ti-6Al-4V alloy and as a consequence, the application of this alloy is widely expanded.

## 1.1 Literature review

### 1.1.1 Problems regarding Ti-6Al-4V alloy machining

The combination of different properties of Ti-6Al-4V alloy makes its machining very difficult [Davim, 2014]. Due to the high strength, hot hardness and high shear angle of titanium alloys, chip formation can be delayed and small chips are formed during machining. So, higher stress (cutting force per unit area) in the cutting zone arises for smaller contact areas (about 1/3 of steel at the same cutting conditions) [Calamaz et al., 2008; Lepicka and Gradzka-Hahlke, 2016]. Additionally, for high shear angle during machining of titanium alloy saw-toothed chips are formed, which cause cyclic cutting forces and tool chatter [Armendia et al., 2010; Veiga et al., 2013]. Cutting force is increased with the increase of feed rate and depth of cut, due to the increase of chip load. During the machining of titanium alloy high-frequency cyclic force is occurred which is correlated with the segmentation frequency of the chip formation [Sun et al., 2009]. Besides, high cutting force and the cutting temperature are formed during Ti-6Al-4V machining due to its hot hardness [Pervaiz et al., 2019].

In addition to this, heat cannot be rapidly dispersed from the cutting zone towards the chips or workpiece due to its low thermal conductivity (7.2 W/mK), and most of the heat is transported towards the cutting tool. A concentrated heat on the cutting edge of the tool and high chip-tool interface temperature is observed [Koenig, 1979]. The low elastic modulus of titanium and its alloys cause large deflection of the workpiece under tool pressure, for which Ti-6Al 4V alloy deflected at a very high amount (almost two folds

compared to steel machining) because of its low elastic modulus [Gupta and Laubscher, 2017; Donachie, 2003]. The cyclic nature of cutting force due to serrated chip formation along with the low elastic modulus of the work material produces severe chatter vibration in the cutting tool which exaggerates the cutting force, temperature and tool wear [Komanduri and Hou, 2002]. Surface quality is also reduced due to the rubbing of the machined surface by the tool [Marigoudar and Kanakuppi, 2013].

Also, Ti-6Al 4V alloys are highly chemically reactive, which facilitates the tool to react with the workpiece. Due to this reaction, different types of tool wear like adhesion and diffusion wear can happen [Donachie, 2000]. Additionally, work material showed the tendency of being welded with the tool and form BUE [Ezugwu and Wang, 1997; Machado and Wallbank, 1990]. Though the BUE protects the tool's cutting edge initially, abrupt failure of the tool can happen. High chemical reactivity is the cause of reacting to this alloy with environmental elements and form oxides, hydrides, and nitrides on the outer layer of the machined part. Fatigue strength of the machined surface decreased, due to this hard outer layer and the tool wear also enlarged [Donachie, 2003].

### 1.1.2 Effects and control of high cutting temperature

Due to plastic deformation occurred during metal cutting, enormous heat and stress are generated due to the conversion of mechanical energy into thermal energy which consequently raises the temperature of the cutting tooltips and the work-surface near the cutting zone [Trent, 1983]. High temperature is generated in the vicinity of the nose and cutting edges of the tool. The primary detrimental effect of cutting temperature is the wear of a tool [Geoffrey et al., 1989]. Heat is generated from the combined effect of three heat sources during machining, which is shown in Fig.1.1. The primary heat source (A-B) is at the shear plane due to the intensive plastic deformation of the work material during machining. The friction at the tool-chip interface also causes the generation of heat, which is called the secondary heat source (A-C). Finally, in the tertiary heat source (A-D), the heat is generated at the tool-work-piece interface due to rubbing contact between the tool flank face and the newly machined surface of the work-piece [Inasaki, 2007]. The temperature of the rake face is the maximum temperature in real machining operations and it causes tool wear, which is mainly because of the secondary heat source. The rubbing in the tertiary heat source mainly affects the surface roughness of the machined part and also the cutting temperature and force.

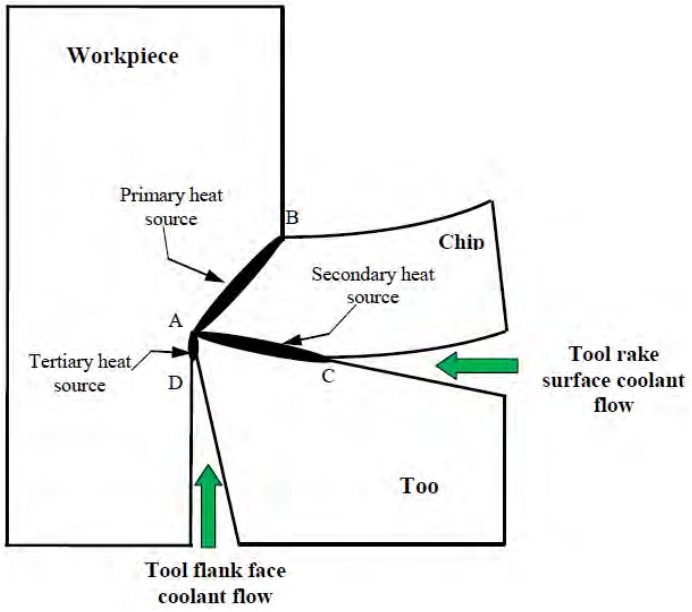


**Fig.1.1** Heat sources in the orthogonal machining process

At such high temperature and pressure, the bonding strength of the tool substrate deteriorates and different thermal wear (diffusion and plastic deformation), as well as mechanical wear (abrasion and attrition), are occurred. Chipping of the cutting edge or breakage of the tool nose and premature tool failure may also happen by plastic deformation and thermal fracturing which lead to dimensional inaccuracy, increase in cutting forces [Ezugwu et al., 2003; Koenig, 1979]. The high cutting temperature also causes mechanical and chemical damage to the finished surface. If the high cutting temperature is not controlled, surface integrity may be hampered by oxidation and inducing residual stresses, micro-cracks and structural changes [Reedand Clark, 1983]. This problem increases further with the increase while machining for high material removal and difficult-to-machine materials.

During Ti-6Al-4V alloy machining high heat is generated due to its high strength and hardness. Moreover, for low thermal conductivity, most of the heat is dissipated in the tool. The combined effects of these two phenomena increase the cutting zone temperature. When the high temperature is created during titanium machining, element diffusion from a tool into the chip and chip into a tool may happen, which eventually causes crater wear. Moreover, carbon deficiency occurred due to carbon diffusion; make the cutting edge brittle and susceptible to catastrophic fracture [Deng et al., 2008]. Frictional force, temperature, and tool wear highly depend on the frictional coefficient at the tool-chip interface, which is affected by the process parameters and the work-tool combinations. With the increase of cutting parameters, the amount of this cutting temperature increases.

High cutting velocity results in very high temperature which reduces the dimensional accuracy and tool life by plastic deformation and rapid wear of the cutting points [Chattopadhyay and Chattopadhyay, 1982]. Kosaraju et al. [2012] performed an analysis, where the effect of different process parameters on machinability performance characteristics of titanium was examined. Cutting speed is the most significant process parameter, that highly affecting the process responses. MRR is proportional to speed, feed, and depth of cut. So, acquiring high MRR is very difficult for high cutting temperature and consequent tool wear. The directional cutting forces during titanium machining are highly affected by the tool material, configurations like principal cutting edge angle and cutting edge radius and also the cutting process parameters [Antonialli et al., 2010; Wyen and Wegener, 2010]. Cutting force mainly depends on the friction of the interfaces, area of the interfaces and the shear strength of the work materials [Lee et al., 2002; Merchant, 1945]. At high-speed cutting where high temperature is generated, cutting force decreases due to thermal softening of the material. On the other hand, with the extensive increment of cutting speed, a huge amount of tool wear can happen and cutting force is increased further.

At high cutting temperature, titanium and its alloys become highly chemically reactive and it reacts with the cutting tool and quickly deforms the tool during machining, hindering its machinability [Kumar and Jerold, 2013; Yang and Liu, 1999]. Different tool material reacts differently with the titanium and its alloys. Flank wear, crater wear, notch wear and chipping are the basic failure criteria of the tool during machining of these materials. Plastic deformation is another criterion of tool failure during titanium machining, which is more active in high-speed machining. Because high compressive stress and huge heat are generated during high-speed machining [Ezugwu and Wang, 1997]. They also suggested that straight grade cemented carbide tools are the best choice among other available tools for continuous cutting of titanium alloys whereas, for some interrupted cutting, HSS tools maybe work better. But their performance is not sufficient to machine titanium and its alloys. So, the innovation of new tool materials is essential for better efficiency.

Titanium and its alloys are generally used for sophisticated parts of various sectors which requires maximum reliability. The surface finish is an index to measure the service life of a component. In contrast, achieving the required surface finish is not very easy for the products machined from titanium and its alloys. High cutting temperature,

built-up-edge formation, serrated chip formation, micro-crack formation, plastic deformation are the main causes of deterioration of the surface finish [Ezugwu and Wang, 1997]. The optimum process parameters, appropriate cutting tool and proper coolant (with the delivery method) are essential due to achieve lower product roughness, lower cutting temperature, higher tool life and lower production cost [Ramana et al., 2011]. Generally, the surface roughness is reduced when machining at high speed [Namb and Paulo, 2011]. In another study by Kumar and Jerold [2013], it can be concluded that among the process parameters, the feed rate is most important for the roughness, then comes cutting speed and depth of cut. Kosa and Ney [1989] suggested that in machining ductile metals, the heat and temperature developed due to plastic deformation and rubbing of the chips with the tool may cause continuous built-up of welded debris which affects machining operation. During machining difficult-to-machine materials tools will be subjected to high frictional heat and chips will have a tendency to stick and cause severe built-up edge formation. Due to high reactivity and high cutting temperature during titanium machining, built-up-edge (BUE) formation is usual, which can affect the surface finish of the product [Hutchison et al., 2001]. Therefore, it is essential to reduce the cutting temperature as far as possible.

Machining performance can be improved by reducing the heat generation in the cutting zone and removing the generated heat from this area. Heat generation can be controlled by an appropriate selection of work-tool combination, process parameters, cutting fluid and machine tools. But for a specific work-tool, process parameter and machine tools, the generated heat can be removed from the cutting zone by using cutting fluid, which primarily acts as coolant and lubricant [Hutchison et al., 2001]. As a coolant, it dissipates heat from the work-piece and cutting zone. As a lubricant, it reduces the contact length and friction in the chip-tool and work-tool interfaces through their ball bearing and rolling effect, which ultimately minimizes cutting force and chatter. At high cutting speed, high heat is generated and machinability can be improved by the cooling action of the cutting fluid. Whereas low cutting speed force is very high and machinability can be improved by the lubricating action. The cutting tool material used to cut titanium and its alloys should comprise different qualities, such as high hot hardness, chipping resistance, toughness, fatigue resistance, lower reactivity, high compressive strength and better thermal conductivity [Machado and Wallbank, 1990]. But, without using coolant most of the available tools fail to properly cut titanium and its alloys [Davim, 2014]. The cooling and lubricating performance of cutting fluid may improve the wear condition,

reduce the friction coefficient and as a result cutting temperature, frictional force, surface roughness and dimensional accuracy are reduced and tool life is extended [Liu et al., 2011].

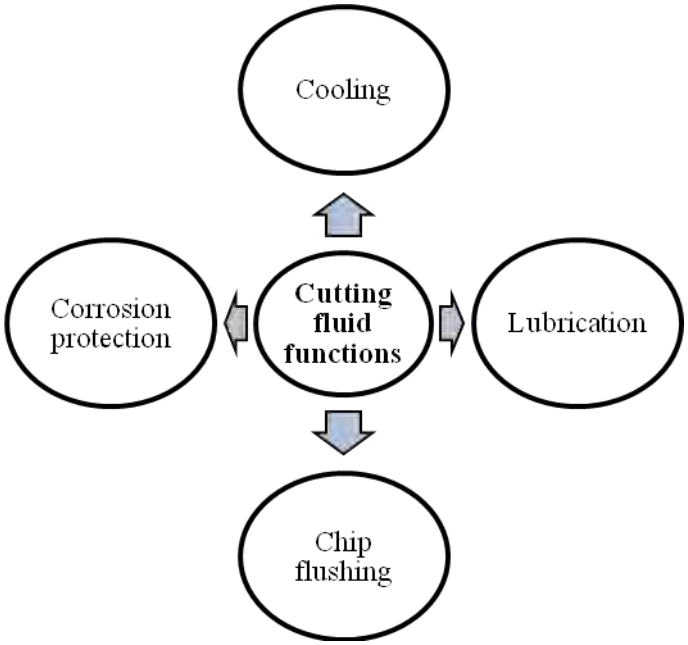


**Fig.1.2** Functions of cutting fluid in machining [Rong and Wang, 2016]

The freshly machined surface is very susceptible to corrosion and surface finish can be hampered by this. Cutting fluid can prevent the surface from corrosion. It's the tertiary but important task function of cutting fluid. The additional function of cutting fluid is flushing away the produced chips from the cutting zone to prevent the built-up edge formation and rubbing the machined surface. There are four basic functions of cutting fluid in machining, which are mentioned listed in Fig.1.2. Additionally, cutting fluids also help in the machining of ductile materials by reducing or preventing the formation of a built-up edge (BUE), which degrades the surface finish [Heginbotham, W. B. 1961]. Ultimately, it can be said that the overall functions of cutting fluids help to enhance the machinability of any machining process. Due to achieving an effective and efficient cutting fluid application, accurate selection of the type of fluids (thermal properties to dissipate heat, physical properties to easy penetration) and the application methods (for proper penetration to the heat zone) is crucial [Mannekote and Kailas, 2012]. The selection of appropriate cooling methods and cutting fluid highly depends on the work-tool combination and process parameters. Basic types of cutting fluids are oil-based, water-based and gas-based. Cutting fluid can be applied by conventional cooling methods. An

enormous quantity of fluid is used in these techniques, which is not only uneconomical but also very harmful for the environment and people. Despite the good performance of the cutting fluid, manufacturing industries are being obligated to implement environment-friendly cooling strategies. Several sustainable and environmentally friendly cooling techniques for reducing the cutting temperature can be used for machining difficult-to-cut materials. Cryogenic cooling, compressed air/ gases cooling and MQL are some recently invented methods of them [Chetan et al., 2016].

### 1.1.3 Effects of conventional cooling methods

In conventional cooling huge amount of cutting fluid is applied with or without using additional pressure. One of the most common conventional ways of cooling is the flood cooling method, where the fluid is applied without pressure. Because of the ineffective penetration of the fluid into the cutting zone, the amount should be very large for achieving the required performance. The other upgraded conventional cooling technique is high-pressure cooling (HPC), where the fluid is applied with high pressure. The efficiency and effectiveness of the latter technique are much better due to the proper penetration of the fluid in the area of interest. The required amount of fluid in HPC is slightly less than the flood cooling. Coolants/lubricants can remove heat mainly from the interfaces to elevate the machining performance. The main purpose of using coolant is to reduce the contact area on the tool-chip and tool-work interfaces, which can reduce the friction and consequently the tool wear. The other purpose of using cutting fluid is flushing away the chips, which is very essential [Hadad and Sharbati, 2016]. Coolant is applied by a conventional/flood cooling method without additional pressure. In high-pressure cooling (HPC) system coolant is applied at high pressure and its effectiveness is better. A huge amount of coolant is used in these techniques, which is not only uneconomical but also very harmful for the environment and people.

Machining with coolant gives better performance with better product quality compared to dry cutting. By the flood cooling method, a copious amount of coolant (more than 100 L/hr) continuously flows towards the cutting zone, which eventually cools the tool and workpiece and also lubricates the chip-tool and work-tool interfaces [Revuru et al., 2017]. Chip flushing is also done by flood cooling. The flood cooling method is effective to improve the machining situation for various types of machining, like milling, grinding, etc. [Ezugwu and Wang, 1997]. Muthukrishnan and Davim [2011] applied a

Water-soluble servo cut S coolant by flood cooling technique and studied its influence on the tool wear of TTI 15 ceramic insert during machining of the Ti-6Al-4Valloy. The study reveals that flood cooling can reduce the wear of the tool also the adhesion of the work material on the tool. Due to these reasons, tool life can be improved by around 30 % and the surface finish ultimately gets better compared to dry cutting. Few researchers investigated the performance of a conventional cooling system in comparison with argon enriched environment when Ti-6Al-4V alloy was turned by an uncoated carbide insert. They concluded that machining under an argon enriched environment deteriorated the machinability concerning cutting temperature, tool life, surface roughness and cutting force [Ezugwu et al., 2005a]. Deiab et al. [2014] compared six different environments when they were applied during machining Ti-6Al-4V alloy. When surface roughness ($R_a$) was a concern, flood cooling performs approximately equal or slightly better than dry, MQL, MQCL, cooled air and cryogenic cooling at low speed- feed combination but its performance deteriorates with the increase of feed. When considered the flank wear, flood cooling performs better than dry, MQL, MQCL, cooled air and worst than cryogenic cooling. But, at a higher speed-feed combination, the effect of dry, MQL, MQCL, cooled air have deteriorated. In the case of power consumption, it performs better than dry cutting only. Khatri and Jahan [2018] performed high-speed milling of Ti-6Al-4V alloy under dry, flood and MQL condition to explore the mechanism of tool wear for uncoated and coated carbide tools. The result showed that the cumulative wear in flood cooling is less than dry but greater than MQL condition. However, the flood cooling method is the most widely used in standard machining and used as the point of reference for all experiments. Most of the literature discussed further according to advanced cooling for machining titanium alloys consider flood cooling as well as dry-machining as a benchmark.

During the machining of titanium alloys, a high cutting temperature is produced. At a higher speed, feed and depth of cut, the higher cutting temperature was generated. For reducing the temperature, typically flood cooling is used effectively. But sometimes, when the fluid comes close to the high heat, it creates the vapor and subsequently impedes the generally low-pressure coolant from entering the cutting zone. As a result, the reduced cooling effect has happened and higher flank wear and nose wear were observed [Ezugwu et al., 2009]. The concept of HPC is to penetrate the coolant into the chip-tool interface due to the action of high pressured coolant flow and increase the chip curling, which reduces the interface area and also takes away the BUE from the cutting edge. Chip

breakability is increased and the disposal of chips becomes very easy [Ezugwu and Wang, 1997]. The surface integrity of a machined part is very important to estimate product quality and sustainability. The ultimate benefit of HPC is the improvement of product quality and tool life. Several researchers applied this technique in the machining of Ti–6Al–4V alloy and got a very positive outcome in respect of the machinability performance.

Compared to conventional wet cooling, HPC produced less cutting temperature, force, coefficient of friction, contact length and enhanced chip breakability in turning Ti-6Al-4V alloy. Eventually, surface finish, productivity and tool life were improved. Water-based coolant outperformed the oil-based coolant regarding chip breakability, tool life and productivity. On the contrary, Neat oil HPC did not offer reduced the main cutting force and specific energy due to better lubrication effect [Nandy et al., 2009]. A larger nozzle diameter was showed improved and proper cooling due to an increment of broken chips and chip curling in turning Ti-6Al-4V alloy by an uncoated microcrystalline insert. [Shankar et al., 2015]. Higher coolant pressure facilitates the proper coolant penetration in HPC during different machining of Ti-6Al-4V alloy. Chip breakability, chip serration frequency and average shear-band thickness were increased and the disposal of chips becomes very easy with the application of high-pressure coolant. Better heat transfer happened and consequently, surface roughness and tool life got better in the case of HPC. Additionally, lower speed provides a better effect of HPC [Da Silva et al., 2013; Palanisamy et al., 2009a, 2009b]. The increase of coolant flow rate in addition to high pressure produced less cutting temperature, tool wear and discontinuous chip. But, cutting force was slightly increased by HPC compared to conventional flood cooling [Klocke et al., 2012]. Ezugwu et al. [2019] compared the performance of three types of coolant in HPC during turning Ti-6Al-4V alloy in respect of chip-formation, tool life, tool failure modes and surface quality. Dicyclohexylamine based coolant performs better at higher pressure, whereas, triethanolamine-based coolant works better at lower pressure and an ester-based coolant has the lowest performance due to its oxidation tendency. Water can also be performed as HPC cutting fluid and improved tool life significantly, reduced surface roughness and chip size [Hadzley et al., 2013].

HPC with a specially designed tool holder outperformed dry and overhead flood cooling regarding chip formation and tool wear during turning Ti-6Al-4V alloy by carbide insert [Taylor et al., 2018]. Several researchers worked on turning Ti-6Al-4V alloy and compared the performance of HPC applied by a specially designed double-flow nozzle

with totally dry cutting. Cutting temperature, force, and surface roughness were reduced and tool life was increased by using HPC [Khan et al., 2017; Mia et al., 2017]. Hammond et al. [2011] compared a focused HPC technique for milling of Ti-6Al-4V alloy and inspect its efficacy with different cooling methods used in machining based on literature. From the study, it was evident that the HPC strategy performed better than other methods regarding tool wear. The basic reason they mentioned was the same as previous, such as superior chip flushing and lesser chip-tool contact length. Bermingham et al. [2014] investigated to recognize the advantage of HPC over flood cooling during the milling and drilling of sophisticated titanium parts similar to aircraft containing deep-pocketed thin walls. In this work, both the end mill and drill bit have an internal through spindle/tool coolant delivery system. For drilling, internal fluid flow is essential. Under HPC condition tool wear could be kept under control (70% less compared to flood cooling), for which MRR could be increased without sacrificing the tool life. Arai and Ogawa [1997] investigated the effect of HPC in drilling Ti–6Al–4V alloy compared to conventional flood cooling by a drill with an internal oil channel. The study reveals that HPC provides lower tool wear, cutting forces and cutting temperature during machining. This cooling technique is very effective in controlling the cutting temperature even during a deep hole drilling. But the rigidity of the drill bit is the prime requirement during drilling operation with HPC. Multiple coolant flow can increase the performance of the HPC system further. HPC technique in turning Ti–6Al–4V by uncoated tool not only beneficial compared to dry machining but also the cryogenic cooling method. Bermingham et al. [2012] executed a direct comparison of cryogenic cooling and high-pressure emulsion cooling methods during turning of Ti–6Al–4V as an alternative to dry cutting. Tool life was significantly enhanced by both of the methods than dry cutting. But between these two effective techniques, HPC provided proper coolant penetration in the cutting zone irrespective of nozzle position, superior chip breakability and enhanced tool life.

Based on the literature it can be revealed that the high-pressure cooling system used in machining is very effective for the reduction of cutting temperature, cutting force, tool wear with improved tool life and surface finish. Due to improved chip breakability, chip removal becomes very easy. This technique is very effective for difficult-to-cut materials. Liu and Liu [2018] reviewed some papers regarding the quality improvement of Ti-6Al-4V alloy products under HPC. Coolant type, coolant pressure and the injection position affect the cooling performance of HPC and deserve investigation for better

performance. However, this technique has a very large negative impact on the economy and environment because of using a high amount of cutting fluid. Additionally, a huge amount of cutting fluid creates huge fumes around the cutting zone, which can obstruct the machining area's visibility and create problems during machining.

### 1.1.4 Effects of sustainable cooling methods

At the age of sustainable machining, approach industries were devoted to reducing the amount of cutting fluid consumption significantly. An enormous quantity of fluid, which is used in conventional techniques, can cause environmental pollution and health hazards during their application and disposal. Moreover, they are uneconomical due to their huge amount. In general, the cost associated with the huge amount of cutting fluid application is about 16% of the total manufacturing cost, which is about 4 times compared to the cost of tooling in machining, which can be visualized in Fig.1.3.

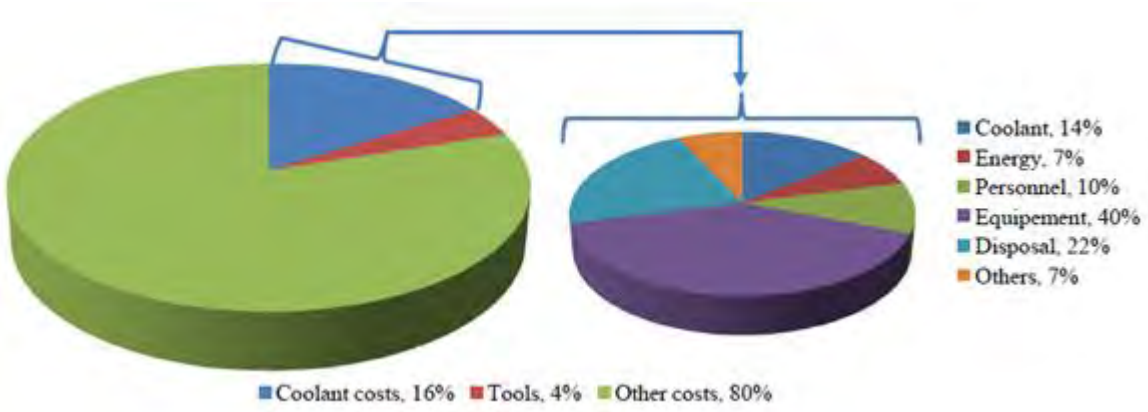


**Fig.1.3** Cutting fluid costs in metal machining-Redrawn from [Osman et al., 2019]

For machining difficult-to-cut materials, cutting fluid cost may be increased up to 20~30% of the total manufacturing cost [Chetan et al., 2016; Hadad and Sharbati, 2016]. The disposal cost of the cutting fluids comprises a large portion of the total coolant system cost. From the viewpoint of cost, ecological and human health issues, manufacturing industries are now being forced to implement strategies to reduce the amount of cutting fluids used in their production lines. Recently, Krolczyk et al. [2019] presented a review article regarding the ecological trends of using cutting fluid in machining due to achieve sustainability. Without using any kind of cutting fluid during machining, which is called dry machining can be a great option for reducing the environmental pollution, health problems of operators along with the cost of machining. This method is also called green machining. But in dry machining, some benefits of using coolant are not offered [Sreejith

and Ngoi, 2000]. In the search towards sustainable machining other than dry cutting recently, various methods like vegetable oil-based coolant application [Heisel et al., 1998], cryogenic cooling with $LN_2$ or $CO_2$ [Dhar et al., 2002; Dhar et al., 2006c], compressed air cooling [Boswell and Chandratilleke, 2009] and MQL application [Dhar and Khan, 2010] have been adopted. These methods are considered able to reduce environmental pollution and health hazards along with minimizing the problems regarding dry machining. Compressed air cooling may be a feasible alternative to harmful liquid-based cooling but for low convective heat removal rate, this method is not sufficient for acute heat generation in metal cutting [Boswell and Chandratilleke, 2009].

Dry machining is the best approach to eradicate the adverse effects of using the cutting fluid and also to reduce the machining costs due to the complete elimination of cutting fluid [Klocke and Eisenblaetter, 1997; Krolczyk et al., 2017; Sreejith and Ngoi, 2000]. This method is eco-friendly, provides cleaner production and also facilitates-boosting sustainability [Liang et al., 2019]. But, due to friction and adhesion between tool and workpiece during dry machining, high cutting temperature and low tool life are going to happened [Wu et al., 2012]. So, this machining requires expensive high heat and wear-resistant tools and rigid machines. Moreover, it is restricted to the cutting of low-strength material with moderate cutting conditions [Goindi and Sarkar, 2017]. For dry machining of Ti-6Al-4V alloy appropriate cutting conditions and tools needed to be selected for better machining performance. High temperature during machining of this alloy is the prime cause of extreme tool failure [Cantero et al., 2005]. Usually, less than 60 m/min of cutting speed is recommended in industrial applications for the machining of titanium alloys [Che-Haron, 2001]. By using the cemented tungsten carbide tool up to 60 m/min speed can be used for machining Ti-6Al-4V. But, it's not appropriate for machining this alloy over 30 m/min by HSS tools [López De Lacalle et al., 2000]. Therefore, higher productivity cannot be achieved by the dry cutting of this alloy. For high-speed dry machining of Ti-6Al-4V alloy advanced cutting tool can be a great alternative. This may be possible by introducing advanced tool materials [Corduan et al., 2003], using various coatings for tools [Che-Haron and Jawaid, 2005] and the application of textured tools [Ze et al., 2012]. The latter is the most recent technique of advanced tools.

Elmagrabi et al. [2008] performed high-speed milling of Ti-6Al-4V alloy under dry conditions within a range of feed rate and depth of cuts. Results showed that coated tools perform better than uncoated carbide tools regarding tool life. Surface roughness was not

susceptible to these two types of tools. Feed rate and depth of cut affect the surface roughness more. In another work [Jawaid et al., 2000], PVD-TiN and CVD-TiCN+$Al_2O_3$ coated tools were compared in the face milling of this material and the CVD tool performed better regarding MRR and tool life. Nevertheless, both of the tools experienced extreme chipping at the cutting edge and flaking at the rake surface of the tool. Li et al. [2017] carried out an ultra-high-speed face milling of Ti-6Al-4V by using (Ti, Al)N-TiN coated cemented carbide tools at a small depth of cut and feed rate under dry condition. The chips were susceptible to be burned at higher speeds. Larger cutting temperatures, cutting forces, cutting power, specific cutting energy and rapid tool wear were evident at higher speeds. Massive surface peeling in the rake face, huge abrasive wear and adhesion wear at the flank surface were the usual wear type at ultra-high-speed titanium alloy milling. In the case of the dry turning of this alloy, the uncoated tool produces lower surface roughness compared to PVD coated tool at low-speed cutting, whereas PVD coated tool was preferred for high-speed cutting. These results confirm the requirements of using a coated tool at higher speed conditions [Ramana and Aditya, 2017]. Ultra-hard tools like CBN and PCD tools provide better tool life and surface finish compared to coated tungsten carbide tools during high-speed dry machining of titanium alloy. PCD tool is more effective than the two hard tools mentioned above. Although these hard tools are more costly compared to coated carbide, they are utilized when surface finish and tool wear are concerned [Nabhani, 2001].

Liang et al. [2018] carried out a comparative study where Micro milling by AlCrN, AlTiN and TiN coated and the uncoated cutting tool was performed. AlTiN-based and AlCrN-based tools produced less flank wear and edge chipping compared to other tools. Coated micro drills were failed due to coating delamination and cutting edge chipping. In another research [Wang and Ezugwu, 1997], noteworthy advancement in tool life was claimed for the PVD coated Single layered TiN and multi-layered TiN/TiCN/TiN tool perform better compared to the uncoated tool during continuous turning of Ti-6Al-4V. At lower speed and higher feed rate TiN coated tool perform better than other coated tool, while, at low feed rate and high-speed TiN/TiCN/TiN coated tool outperformed TiN coated tool. Choudhary and Paul [2019] perform performance analysis (combining specific cutting energy, dimensional deviation and average flank wear criteria) among 5 types of PVD coated and uncoated tungsten carbide tools during turning and declared the uncoated tool as the best option for machining this alloy. Because the coated tool did not provide

that much significant improvement in machining. Recently, various researchers have studied the use of textured tools during the dry machining of Ti-6Al-4V alloy. Compared to the non-textured tool, a special texture created on the rake face of the tool can improve the tribological conditions at the chip-tool interface, chip-tool contact area was reduced, friction at the interface was reduced and the heat dissipation area was increased. Ultimately, reduce the chip shape irregularity, tool wear, cutting temperature, forces, surface roughness and enhance machinability [Ranjan and Hiremath, 2019; Zhang et al., 2020]. Textured grooves at the rake surface of the tools are better compared to the conventional tool and textured grooves at the flank surface concerning temperature, force, friction coefficient and chip thickness ratio because of reduced friction at the chip-tool interface. But, tool life was better for the textured tool at the flank, due to the reduction of rubbing at the tool-workpiece interface [Ze et al., 2012].

The process parameter plays an important role in enhancing the machinability of the Ti-6Al-4V alloy. Li et al. [2012] analyzed the variation of serrated chip morphology concerning cutting speed, feed, axial depth of cut and radial depth of cut during dry milling by CVD coated tungsten carbide end mill of this material. The study showed that with the increase of speed saw-tooth chip pitch, height and serration ratio were increased but chip thickness decreased. Feed rate was the second parameter affecting the saw-tooth chip formation, whereas the depth of cut has very little impact. Hernández et al. [2018] conducted an experimental study, the effect of different process parameters (speed and feed rate) on-chip morphologies and geometries in dry turning of Ti-6Al-4V by WC-Co inserts coated with $TiCN/Al_2O_3$. For a range of specific speed-feed rate combination chip was continuous but when speed increased and feed decreased segmented chips were formed. The adiabatic shear band and the back surface of the chips have different microstructural grain alignment and these became more distinct with the increase of cutting speed. Pradhan et al. [2019] assessed the effect of cutting speed on force components, surface roughness, tool wear, chip-tool contact length and chip segmentation when machining Ti-6Al-4V alloy by uncoated carbide tool. The result shows that with the increase of cutting speed, force components reduced up to a certain point after that they increased. Surface roughness, tool wear, cutting temperature were minimum and the chip shape also evenly helical in that medium speed, higher temperature, force and irregular chips were observed in other cases. Jia and Zhu [2018] examined the effect of process parameters on tool wear and roughness in turning Ti-6al-4V alloy by PCBN cutting tool.

Tool wear increased with the increase of cutting parameters. On the other hand, roughness increased with the increase of feed rate but with the increase of cutting speed and depth of cut roughness decreased up to a certain limit and then it increased. Tool wear is mostly affected by speed, whereas roughness is mostly affected by feed rate. In another paper [Liu et al., 2019], tool wear, as well as chip morphology, were investigated concerning speed and radial depth of cut in case of dry milling of this alloy. Optimum cutting parameters were identified considering lower tool wear and higher MRR. Vijay and Vijayan [2013] experimented with milling Ti-6Al-4V and select optimum speed, feed and depth of cut.

Dry machining of difficult-to-cut material is possible, but it requires high-cost tools as well as rigid machine tools to withstand the severity of machining [Arulraj et al., 2014]. Some experimental investigations have been carried out using different kinds of tool materials under dry cutting. But, the generation of high cutting temperature and tool wear is always a prime concern in the dry machining of Ti-6Al-4V [Revuru et al., 2018], which in turn can hamper the product quality and productivity. In that case, dry machining is not suitable for machining of hard-to-cut materials with high cutting parameters, especially where machining efficiency and/or high surface quality are required [Cantero et al., 2005]. Cryogenic cooling is an eco-friendly and effective cooling technique for difficult-to-cut material [Khanna et al., 2019], where liquid cryogen is directly impinged into the cutting interfaces because of improving machining performance. As the liquid cryogen temperature is very low, this method provides better cooling performance rather than lubrication [Dhar et al., 2002b]. The most popular cryogens are nitrogen and carbon dioxide used in liquid form. Nitrogen remains liquid at -196°C at atmospheric pressure and carbon dioxide remains liquid at room temperature by a minimum pressure of 57 bar [Cordes et al., 2014]. In machining, liquid cryogens are utilized to reduce the temperature of the cutting zone less than the softening temperature of the tool material and improve tool life significantly. Consequently, enhanced material removal rate, less tool wear and better surface finish of the machined part could be achieved [Dhar et al., 2006c]. Additionally, no harmful residue is left after using this gaseous coolant and does not require any costly disposal system. So, this method fulfills most of the requirements of sustainable machining and can be considered as an alternative to conventional cooling strategy [Kopac, 2009; Sun et al., 2015]. To improve the performance of the Ti-6Al-4V alloy, cryogenic cooling can be utilized efficiently. Adhesion–dissolution–diffusion wear and edge depression during Ti-6Al-4V machining were minimized under cryogenic

conditions because of the effective minimization of cutting temperature. So, for all the machining conditions, cryogenic cooling produces less tool flank and crater wear, subsequently higher productivity without compromising the environmental safety compared to wet cooling and dry cutting. A significantly larger positive effect of cryogenic machining can be achieved under moderate cutting velocity [Venugopal et al., 2007a]. In a similar study, Venugopal et al. [2007b] revealed that, in turning of Ti-6Al-4V alloy using uncoated carbide inserts under moderate cutting speed, cryogenic cooling improved the tool life by about 3.4 times of dry turning, whereas by wet cooling tool life can be double of dry machining. With the increase of cutting speed, the performance of cooling environments was reduced but wet cooling became ineffective to reduce wear.

Cryogenic cooling is very effective to improve machining performance [Dhar et al., 2006d]. It can reduce the chemical reactivity due to lower cutting temperature and improved the chip breakability due to the high speed of $LN_2$ flow during high-speed milling of Ti-6Al-4V alloy. Consequently, the thermal wear of the tool was reduced and the surface finish was enhanced [KE et al., 2009]. During CNC milling of the Ti-6Al-4V alloy, tool life was extended and surface roughness, power consumption and specific machining energy were reduced when cryogenic cooling was employed compared to dry and flood cooling [Mia and Dhar, 2019a; Shokrani et al., 2016a, 2016b]. In the drilling of Ti-6Al-4V alloy, Ahmed and Kumar [2016] utilized $LN_2$-based cryogenic cooling and compared its performance with wet cooling. Lower cutting temperature, tool wear, thrust force, torque, the mean surface roughness, improvement in hole quality and less serration and uniform segmentation in chip morphology were observed during cryogenic machining. In the reaming of Ti-6Al-4V alloy, the cutting temperature, thrust force and torque were reduced by the application of $LN_2$-based cryogenic cooling. Moreover, surface quality and cylindricity were also got better with better chip breakability during cryogenic cooling that was observed than a conventional flood cooling [Ahmed and Pradeep Kumar, 2017]. In turning of Ti-6Al-4V using CrN-coated carbide cutting tools cryogenic cooling with $LN_2$ was compared with dry cutting and tool life enhancement was accomplished under cryogenic cooling [Yousfi et al., 2017]. Lee et al. [2015] investigated the performance of cryogenic-assisted milling with or without preheating of Ti-6Al-4V workpiece compared to dry machining using soft (Si) and hard (CrTiAlN) coated cutting tool. Tool life was enhanced more for a soft-coated tool than a hard-coated tool. As proved in earlier literature, cutting force slightly increased due to the hardening of the work-piece for the

use of cryogenics. This problem can be reduced by preheating of the workpiece and cutting force was reduced by around 65 %. During the rough turning of Ti-6Al-4V with coated carbide tool, cryogenic cooling was able to improve the life of the tool also reduce the repulsion force and coefficient of friction at the tool-workpiece interface than traditional cooling technique. Here, the effect of cryogenic cooling on chip formation and average surface roughness was very insignificant and also the positive effect of $LN_2$ was reduced at higher cutting parameters [Dhar et al., 2002a; Rotella et al., 2014; Tirelli et al., 2014]. Caudill et al. [2014] performed an $LN_2$ based cryogenically cooled burnishing operation to improve the surface finish. They found better results compared to flood-cooled and dry operations and consequently, the functional performance of the machined component during its service life was also getting better.

The coolant nozzle position and delivery method were proved to be very sensitive for cryogenic cooling ($LN_2$) compared to the high-pressure cooling technology. Optimum coolant delivery, nozzle position and number can enhance the performance [Bermingham et al., 2012]. Hong et al. [2001] claimed that effective lubrication can be achieved by using $LN_2$ if properly applied. The effectiveness of LN2 can be further enhanced by using techniques to lift the chip from the rake face for allowing the coolant to properly reaching the area of interest. In their research, a customized nozzle assembly was used to deliver two focused jets of $LN_2$ applied selectively towards the rake and/or the flank surface. The reduction of feed force and coefficient of friction at the chip-tool interface confirmed the lubricating behavior and the simultaneous double jet was more effective. Additionally, a special compact coolant delivery system can prevent the wastage of excess $LN_2$ and pre-cooling of the workpiece. In another research [2016], Aramcharon employed a newly designed modular cryogenic system to facilitate effective penetration of coolant in the area of interest during the turning of Ti-6Al-4V alloy with coated carbide inserts. Overall machining performance was improved in terms of the friction between tool-chip interface, chip formation process and tool wear. Moreover, the process becomes more stable due to easier chip removal of a smaller radius curvature of helically shaped chips. Any standard tool holder can be integrated with this new coolant delivery system. The electron beam melted Ti-6Al-4V was semi-finish turned under cryogenic cooling and dry cutting. Cutting temperature was considerably less in the case of cryogenic machining where the cutting force components were similar for both of the cases [Bordin et al., 2015]. Mia and Dhar [2019] also compared single and dual jet cryogenic systems for machining Ti-6Al-4V

alloy. The latter method significantly reduced specific cutting energy, temperature, roughness, and increased tool life.

When liquid cryogens ($LN_2$ and $LCO_2$) were applied during machining of Ti-6Al-4V alloys, both were efficient compared to dry and wet cutting but $CO_2$ seems to be more effective in reducing the force components, surface roughness and chip serration frequency [Kumar and Jerold, 2013]. A comparative analysis was performed by Tapoglou et al. [Tapoglou et al., 2017] in milling of Ti-6Al-4V among dry cutting, emulsion flood cooling, medium pressure through the tool, MQL, compressed air, cryogenic $CO_2$ and cryogenic $CO_2$ combined with compressed air or MQL. Tool life was found to be best under emulsion flood cooling. But among eco-friendly alternatives, $CO_2$ plus MQL performed the best. Pittalà [2018] studied the effect of size and position of the internal coolant channels for delivering the $CO_2$ cryogenic coolant in case of end milling of Ti-6Al-4V on tool temperature and tool wear, where larger size and middle of the flute radial hole provide more effective results. Karkade and Patil [2018] evaluated the performance of compressed $CO_2$ gas cooling compared to dry turning and found that surface integrity was improved by the former technique, though the cutting force was increased may be due to work hardening. Ross and Ganesh [2019] experimentally examined the influence of Cryogenic $CO_2$ in reducing temperature compared to the traditional cooling method and found the former process more effective in end milling of Ti-6Al-4V alloy. In the face milling of this alloy, Cryogenic $CO_2$ was better than conventional flood cooling in terms of tool life. With the increase of $CO_2$ flow rate more positive effect was evident [Sadik et al., 2016].

There are various limitations of using cryogenic cooling. Equipment cost and the cost of $LN_2$ or liquid $CO_2$ are very high [Mia et al., 2019]. Moreover, they are not reusable, unlike conventional cutting fluids. Due to the extremely low temperature of the cryogenic environment work hardening can occur, which consequently produces higher cutting force and poor dimensional quality [Revuru et al., 2017]. At ambient pressures, solid $CO_2$ is generated from the liquid $CO_2$, which may restrict the flow of coolant towards the cutting zone [Biermann et al., 2015]. For that reason, a specially designed application system and proper insulation should be used for applying cryogenic coolant near the cutting zone [Shokrani et al., 2016c] ensuring the minimum use of cryogenic coolant and maximize efficiency. Cryogenic coolant flow can be obstructed due to the frozen action of the nozzle [Sharma et al., 2009]. The handling of cryogenic coolant in liquid and gaseous forms is

also very difficult [Yasa et al., 2012]. For these safety issues, its use is limited to a research purpose rather than being popular for practical industrial applications [Yasa et al., 2012]. Their maintenance along with their consistent supply is the major difficulty against their use.

Minimum Quantity Lubrication (MQL) machining is an easy to use, economical, eco-friendly and effective alternative to conventional cooling, also called near-dry machining [Amini et al., 2015; Astakhov, 2008; Dhar et al., 2006b; Khan et al., 2009] or micro-lubrication [Dureja et al., 2015]. Usually, the cutting fluid amount is varied between 10-500 ml/h [Dhar and Khan, 2010; Silva et al., 2005]. Thus, the amount of cutting fluid consumption is significantly low in the case of MQL compared to conventional flood cooling where the usual fluid consumption is around 1200 l/h [Silva et al., 2005]. For machining Ti-6Al-4V, especially in turning and milling MQL outperforms the greenest dry machining condition. Liu et al. [2013] have studied the turning of this alloy, where tool wear was reduced noticeably by MQL than dry machining. A tribo-chemical layer was formed on the cutting tool insert during MQL machining. This protective layer formation along with the cooling lubrication effects of MQL eventually protects the tool. In milling Ti-6Al-4V, average surface roughness and cutting force components (feed, normal and axial) were reduced when machining under MQL conditions compared to dry [Krishnaraj et al., 2017]. MQL method was not only better than dry cutting but also found effective compared to flood cooling in turning of Ti-6Al-4V alloy, where the PCD tool was successfully utilized [Revankar et al., 2014]. For drilling of Ti-6Al-4V with different carbide tools, MQL by usual external nozzle delivery could not effectively reduce cutting temperature [Zeilmann and Weingaertner, 2006]. When internal MQL was used it became effective. Through the drill bit gave around 50% lower temperature than obtained by applying MQL with the external nozzle. In this research, all three coated tools produce less temperature than the uncoated one under external MQL condition. The performance of MQL is extensively related to the types of cutting fluid used [Khan et al., 2009]. As a very low amount of liquid is used in MQL conditions, it mainly increases the interface lubrication. Although MQL was established as an effective and efficient alternative to dry and flood cooling, eco-friendly cold air and cryogenic cooling performed better compared to MQL in different aspects because cooling capability is less for MQL than conventional and cryogenic cooling [Boswell and Islam, 2016]. For machining difficult-to-cut materials such as titanium and its alloy, where temperature control is the prime concern due to the

excessive heat generation during machining, traditional MQL systems become less effective [Su et al., 2007]. Still today huge research has been conducted for the performance improvement of MQL [Brinksmeier et al., 1999].

### 1.1.5 Performance enhancement of MQL technique

The cooling and lubrication ability of this method varies depending on the work-tool combination and tool configuration. Besides this, appropriate cutting parameters (cutting speed, feed rate depth of cut) facilitate chip removal and penetration of the mist jet at the cutting zone. The appropriate cutting condition under MQL machining highly depends on the work-tool combination [Dhar et al., 2006b]. Singh et al. [2019b] also perform optimization of cutting parameters like cutting speed, feed rate and depth of cut under MQL turning of Ti-6Al-4V alloy using a specific tool concerning minimum tool wear, cutting temperature, roughness and force. In the case of the micro-milling of the Ti-6Al-4V part using tungsten carbide micro-tool under minimum quantity lubrication, Hassanpour et al. [2016] analyzed the effect of feed rate, spindle speed and axial depth of cut on the cutting force and surface integrity. The cutting speed was found as the most influential factor, which can reduce the cutting force and eventually the surface roughness. When Mello et al. [2017] performed the grinding operation of Ti-6Al-4V by silicon carbide wheel under MQL and flood cooling, the surface finish was finer under MQL at a low depth of cut. But at a higher depth of cut, flood cooling performs better compared to others.

Upadhyay et al. [2012] reviewed various articles and identified several MQL parameters (i.e. mist spray techniques, air pressure, air/ oil flow rate, nozzle diameter, nozzle stand-off distance, nozzle position/angle, etc.) which have a vital impact on MQL performance. Mist formation and impingement of mist into the appropriate places highly depend on the appropriate selection of these MQL parameters, which is a prerequisite to a highly efficient MQL system [Mia et al., 2017a]. In conventional coolant applications, large volumes of cutting fluid are applied in the machining area, therefore, the number, direction and position of the nozzle are usually not very critical. But in the MQL system, a minute amount of fluid is used [Dhar et al., 2006b]. So, its appropriate pin-pointed impingement at the area of interest is high affects its efficiency. When the cutting fluid jet closely reaches the chip-tool and work-tool interfaces, it can work properly for removing heat from the above-mentioned interfaces and the tool surfaces and also lubricate the

interfaces to reduce the friction. Ultimately, similar or superior performance compared to other effective cooling methods can be achievable by MQL [Dhar et al., 2006a; Yan et al., 2012]. The efficient MQL process can enhance the product quality and tool life, which in turn reduces the manufacturing cost, which is applicable for not only carbon steel but also hard-to-cut alloy [Dhar et al., 2006b; Sarikaya and Güllü, 2015, 2014; Sarıkaya et al., 2016]. MQL jet can be delivered by an external nozzle or through-the-tool or tool holder towards the heat-affected zone [Dhar et al., 2006b]. Using an external nozzle is easy but less effective. Through-the-tool or tool holder better lubrication at the point of interest but investment cost is higher. Obikawa et al. [2006] studied the effect of the internal and external flank supply of MQL into the cutting zone on the cutting temperature and tool wear. Compared to the external MQL, the internal supply reduces the tool wear considerably due to the superior application of the oil mist. At a fixed oil flow rate, temperature and tool wear were reduced with the upsurge of MQL air pressure. Multiple MQL mist flow in the heat-affected zones during machining was proved to be more effective than single mist flow regarding various process responses, like cutting temperature, cutting force and surface roughness, etc. [Hadad and Sadeghi, 2013; Masoudi et al., 2018]. Masoudi et al. [2018] also compared single nozzle performance at the rake and flank surface and reported that the rake nozzle has shown a better reduction of friction and consequently the surface roughness. But the opposite results have been shown in another article. In the case of the single nozzle, MQL flank nozzle cooling has resulted in longer tool life and lower surface roughness in comparison with dry and MQL rake nozzle [Attanasio et al., 2006; Sharma et al., 2009]. For flank spray coolant supplied from the auxiliary flank to the tooltip at an angle of 45° with the rake surface is proved to be more effective than the common (directly below the nose of the tool) flank nozzle [Obikawa et al., 2008].

Huang et al. [2018] investigated the effect of oil flow rate and air pressure on different responses in MQL machining and found that surface roughness and cutting force decrease with the increase of fluid flow rate. On the other hand, with the increase of pressure, force decreases but roughness increases. Yan et al. [2012] studied the effect of air pressure and fluid flow rate on tool wear and surface roughness in the case of milling forged steel. They stated that tool life and productivity were enhanced when air pressure increased due to better impingement of MQL mist in the cutting zone. Furthermore, tool life and surface finish were improved with a higher flow rate. Liu et al. [2011] determined

appropriate MQL oil quantity, air pressure and position of nozzle regarding cutting force and cutting temperature in the end-milling of Ti–6Al–4V alloy under fixed cutting parameters. The study concludes that within a specific range of parameters, too high or too low air pressure and spraying distance cannot facilitate the mist penetration into the contact zones. Additionally, the oil flow rate increment benefitted the MQL performance up to a specific value. The coupling effect of MQL and nozzle parameters with the cutting parameters were not studied in this work, which is very important to investigate. In another paper, Damir et al. [2017] reported the effect of oil and airflow rate, nozzle orientation and nozzle stand-off distance on the machining performance compared to flood and dry milling of titanium alloys. The study revealed that lower cutting force, surface roughness and tool temperature were acquired using higher air, oil flow-rate, lower distance and a 45° nozzle angle concerning the feed direction due to better atomization and penetration of the fluid jet into the cutting zone. Appropriate selection of different MQL parameters is a prerequisite to a highly efficient MQL system.

The performance of the MQL system could be further enhanced by using different additives with MQL liquids, such as solid lubricant, nano-fluid, ionic liquid, etc. Recently nano-fluids have been extensively utilized by the MQL system to enhance the machining performances of different materials [Abbas et al., 2019; Rapeti et al., 2016; Sen et al., 2019a]. It is a new type of fluid that consists of different nanoparticles dispersed into different base fluids having improved viscosity and thermal conductivity compared to the base fluid [Li et al., 2017]. Nanoparticles like Cu, ZnO, $MoS_2$, $Al_2O_3$, CNT, diamond, hBN and xGnP, etc. can be dispersed into water, vegetable oil or synthetic oil, etc. Nano-particles are mixed into lubricants to enhance the lubricating and cooling properties over an extensive range of temperatures. Nano-fluids can reduce the friction between two contact surfaces and cool the heat-affected zone during machining. Nano-particles present in the nano-fluid can easily penetrate the contacting surfaces, retain the oil particles and create an elastohydrodynamic lubrication effect. Besides, the enhanced thermal conductivity of the nano-fluid helps to easily cool the cutting zone. For that reason, highly efficient nano-lubricants can reduce the cutting fluid amount required for machining, which eventually reduces the cost and saves the environment as well as ensures improved machining performance [Sayuti et al., 2014]. Nano-fluid-based MQL is mostly used in milling, drilling and grinding of Ti-6Al-4V alloy.

Singh et al. [2019a] examined the influence of graphene enriched nano-fluid and textured tools on machining Ti-6Al-4V alloy. Tool life was increased as well as the main cutting force and the temperature was reduced under nano-fluid compared to dry machining. Kim et al. [2015] reported that nanofluid-based MQL can effectively reduce the forces, burrs and surface roughness in micro- end milling of Ti-6Al-4V alloy when they utilized hexagonal boron nitride (hBN) particles to produce nano-fluid. Mosleh et al. [2019] performed a study for orbital drilling of Ti-6Al-4V alloy by tungsten carbide tool and used MoS2 and hBN nanoparticles with MQL aerosol. Lower surface temperatures and less variation of frictional torques were created when using nanofluid with MQL. Hegab et al. [2018b] evaluated the performance of multi-walled carbon nanotubes (MWCNTs) dispersed into vegetable oil applied through the MQL technique during Ti–6Al–4V turning. Compared to conventional MQL (without nanoparticle) MWCNT nano-fluid enhanced MQL offered better results regarding tool wear and power consumption. Lee et al. [2010] have studied the effect of nanodiamond and paraffin oil-based MQL in mesoscale grinding of Ti-6Al-4V. Grinding forces and surface roughness were significantly reduced by the nano-fluid MQL approach compared to dry and pure MQL techniques. Ground surface integrity could be more perfect with the smaller-sized nano-diamond particles. Hegab et al. [2018a] investigated the nanofluid performance compared to conventional MQL and found that surface quality was improved for all concentrations of MWCNT nanoparticle but the improvement of surface roughness was not proportional to nano-particle concentration. So, with smaller particle size and higher nanoparticle concentration, its performance got better. Nam and Lee [2018] also second this previous statement. In their research, they have experimentally investigated the effect of different sized and shaped nano-fluid enhanced MQL in micro-drilling of Ti-6Al-4V alloy and compared with compressed air and conventional MQL performance. The study also found that friction at the drilling area, drilling torque, drill bit wear was reduced and drilled hole quality was improved. Different concentrations of Water-based $Al_2O_3$ nanofluid were applied through MQL in the grinding of Ti-6Al-4V alloy and compared with conventional coolant and pure water by Setti et al. [2012]. The study revealed that grinding forces were reduced significantly for all concentrations of nanoparticles, but the surface finish has been found to improve for a higher concentration. Eltaggaz and Deiab [2018] studied the effect of nanoparticle concentration on the performance of MQL during turning of Ti–6Al–4V alloy. Different concentration (0, 2, 4 % wt) of $Al_2O_3$ was applied by MQL and found that

the maximum concentration of nano-particles offered the best results regarding tool flank wear and coefficient of friction.

When this method was compared with the wet cooling technique it showed diverse results. Setti et al. [2015a] analyzed the performance of the water-based $Al_2O_3$ nanofluid-based MQL technique for the grinding operation of Ti-6Al-4V alloy. In terms of normal and tangential force, nano-fluid-based MQL outperformed flood and conventional MQL cooling techniques. In the case of surface integrity, nano-fluid-based MQL was found superior to MQL with soluble oil but inferior to wet cooling. In other research, Setti et al. [2015b] analyzed the grinding performance of Ti–6Al–4V alloy, when $Al_2O_3$ and CuO nano-particles with water nano-fluid were applied by the MQL method in terms of chip formation and coefficient of friction. Nano-fluid-based MQL provides superior performance compared to dry, wet and MQL with soluble oil techniques and between two nano-fluids $Al_2O_3$ based nanofluid improved the grindability of Ti–6Al–4V more. The type of nano-particle affects the most on the performance of nano-fluid-based MQL. Nguyen et al. [2015] explored the usability of lamellar-type graphite nano-platelets in MQL machining of Ti-6Al-4V. When applied to the above-mentioned nano-enhanced MQL into the cutting zone, each layer of the lamellar-type structure can easily penetrate the chip-tool and work-tool interfaces to provide better lubrication. Milling tool life was improved, micro-chipping and tool fracture was reduced compared to traditional pure MQL and dry cutting. The big advantage of the lamellar shape of having a micro-sized diameter while having a nano-sized thickness restricts them to penetrate through the skin and breath through the nose. Songmei et al. [2017] used vegetable oil-based nano-fluid with MQL in Ti-6Al-4V milling to enhance the machining performance. The type and concentration of nanoparticles were varied in this work. Finally, it can be said that the performance relation with nano-particle concentration depends on the type of cutting fluid, machining operation, cutting conditions, size of the nanoparticle, range of their concentration, etc. A huge experimental investigation is required to find out the appropriate concentration of the nano-particles.

Kim et al. [2017] performed micro-end milling of Ti-6Al-4V under nano-diamond enhanced nanofluid MQL. Lower concentration (0.1 wt.%) of nanofluid was better for reducing the cutting force, tool wear and friction, whereas higher concentration (1.0 wt.%) nano-fluid was better for reducing surface roughness. In another study, Kim et al. [2017] compared combined cryogenic cooling ($LN_2$) and MQL with vegetable oil-based nanofluid

(0.5 wt.% hBN) with wet cooling in case of turning the Ti-6Al-4V alloy intending machinability improvement. Concerning the cutting force, the coefficient of friction, and the surface roughness combined with cryogenic cooling and nanofluid MQL significantly improved the performance compared to wet conditions. A face milling experiment for Ti-6Al-4V alloy under MQL with graphite nanofluid compared to dry, wet, MQL, cryogenic and MQL plus cryogenic conditions have been studied by Park et al. [2017]. MQL and cryogenic methods were better than dry and wet cutting. Initially, the cryogenic method was better than nano-fluid-based MQL, but after some time workpiece got hardened and exessive tool wear was evident. Nano-fluid-based MQL showed its influence to reduce tool wear even at high temperatures when oil may be vaporized but nanoparticles were penetrated the cutting interfaces and reduce friction. This method also showed the lowest peak to valley ratio for serrated chip formation, which recognizes this coolant condition as the best for titanium machining.

Sharma et al. [2016] reviewed various articles to evaluate the performance of MQL during machining using conventional and nanofluids and concluded that machining could be better when using nano-fluids-based MQL compared to dry wet and conventional MQL method. The use of hybrid nano-fluids was suggested for the machining operations to achieve further improvement. In machining Ti–6Al–4V alloy, significant progress has been made in MQL machining with nano-fluids which comprise superior tribological and thermo-physical properties. Furthermore, MQL with hybrid nanofluid performs better than pure nano-fluid-based MQL. Because hybrid nanofluid contains multiple types of nano-particles and have better thermo-physical properties than pure nano-fluid due to the physical synergistic effects of integrating multiple nanoparticles [Devarajan et al., 2018]. Current studies have established the improved tribological performance of hybrid nano-fluid as a coolant in the machining of various difficult-to-cut materials in respect of several machining indices [Xie et al., 2016; Zhang et al., 2016]. The use of MQL with hybrid nano-fluid for machining titanium alloy is rare. Very recently Jamil et al.[2019] used $Al_2O_3$–CNT-based hybrid nano-fluid enhanced MQL in the machining of Ti-6Al-4V alloy and acquired huge improvement in reducing the surface roughness, cutting force and tool wear compared to cryogenic machining.

### 1.1.6 Summary of the Review

From the literature review, it is realized that the high cutting temperature is the major cause for the low machinability of the Ti-6Al-4V alloy. Cutting fluid reduces the high cutting temperature, consequently reduce the cutting force, tool wear and surface roughness. However, the conventional flood cooling technique is not much efficient due to the formation of a high-temperature vapor blanket, which restricts the coolant to flow into the cutting zone. A high-pressure coolant (HPC) jet can penetrate the cutting zone as well as helps with easy chip removal, which makes it efficient. But both of these two methods require a huge amount of coolant and are considered to be uneconomical and environmentally hazardous. Dry machining can be a green and sustainable solution but it requires costly high heat and wear-resistant cutting tools as well as rigid machines due to acquiring tool vibration. Cryogenic cooling was the most efficient and eco-friendly method for improving the machinability of the Ti-6Al-4V alloy. But, this method is very expensive and difficult to handle liquid cryogen. Moreover, work hardening due to extreme cooling sometimes negatively affect the cutting force and product quality.

MQL has appeared as a promising, eco-friendly, economical, and effective solution for various machining compared to dry and flood cooling. Application of nano-particle (mono and hybrid) in MQL base fluid can improve its cooling and lubrication performance further. It is a new research trend with ever-growing attention among various researchers around the world. This is still in the developing stage and the performance of this system varies with process parameters, mist parameters and type of cutting tool and type of nanoparticle used. There is a great need to explore the workability and suitability of nano-fluid-based MQL when machining Ti-6Al-4V. Moreover, the use of hybrid nanofluid for enhancing the performance of MQL is very rare. This research intends to understand the influence of different MQL parameters, cutting parameters and cutting tool types on the machinability of Ti-6Al-4V alloy regarding various responses. Additionally, the current work proposes to evaluate the effect of MQL with hybrid nanofluid compared to other environments. On top, this study proposes to fill the gap in the available literature regarding the optimal MQL conditions, cutting conditions, tool type and nanoparticle concentration for machining Ti-6Al-4V alloy under hybrid nano-fluid-based MQL.

## 1.2 Objectives of the Present Work

The objectives of the present research are as follows:

(i) Design and development of a suitable double jet MQL delivery system towards the rake and flank surface of the cutting tool simultaneously.

(ii) Preparation and characterization of hybrid nano-fluid using carbon nano-tube (CNT) and aluminum oxide ($Al_2O_3$) with cutting oil.

(iii) Systematic investigation to study the effects of MQL with hybrid nanofluid on machinability of turning titanium (Ti-6Al-4V) alloy by different carbide inserts (coated and uncoated) in respect of chips morphology, cutting temperature, cutting forces, tool wear, tool life, surface roughness and dimensional accuracy.

(iv) Development of empirical models for predicting cutting temperature, cutting force and surface roughness as a function of significant process parameters based on the experimental results and their validation. Optimize process parameters for improving the machinability of Ti-6Al-4V alloy considering multi-objectives.

(v) Development of a finite element model (FEM) to observe the chip morphology and temperature distribution in turning Ti-6Al-4V alloy by carbide insert under different cooling environments and its validation based on experimental results.

## 1.3 Outline of the Thesis

The machinability of titanium alloy can be improved by the application of an MQL jet using a proper coolant applied through an efficient nozzle. Keeping that in view, the present research work has been taken up to explore the role of the MQL system on the major machinability characteristics in turning of Ti-6Al-4V alloy by carbide inserts under different machining conditions as well as to develop a finite element model for machining under different cooling conditions.

**Chapter 1** begins with the introduction followed by a comprehensive survey of previous work regarding the effect of high cutting temperature on the machinability of Ti-6Al-4V alloy, measures for controlling temperature, the effect of different conventional and sustainable cooling techniques and techniques for MQL performance improvement.

This chapter also contains the objective of the present work along with the outline of the thesis.

**Chapter 2** presents the experimental conditions and procedure of the machining carried out with the measurement of quality characteristics. Calibration of tool-work thermocouple for Ti-6Al-4V alloy and carbide inserts are also presented in the chapter. The design and fabrication of the double jet MQL delivery system for impinging the mist towards the cutting zones are thoroughly described in this chapter. Synthesis and characterization of hybrid $Al_2O_3$-MWCNT nano-fluid as an alternative to conventional MQL fluid is also described in this chapter. The effects of double jet MQL and the prepared hybrid $Al_2O_3$-MWCNT nano-fluid compared to single jet MQL and conventional MQL fluid regarding various machinability indices are presented in chapter 2.

**Chapter 3** presents the modeling of the machinability responses in turning Ti-6Al-4V alloy regarding process parameters, nanoparticle concentration of hybrid nanofluid and tool-type. Ultimately the process and nano-fluid parameters along with tool type have been optimized considering the multiple responses, such as cutting temperature, cutting force and surface roughness.

**Chapter 4** focuses on finite element modeling which has been developed by using ABAQUS/Explicit software. The model development procedure adopted for turning Ti-6Al-4V alloy under different cooling environments has been thoroughly described in this chapter.

**Chapter 5** demonstrates the detailed discussion on experimental results and potential explanations are acquired.

Finally, the conclusion and recommendations for future work are highlighted in **Chapter 6.** References and publication lists are provided at the end.

# Chapter 2

# Experimental Investigations

In this present research work, an advanced, eco-friendly and economic manufacturing system has been developed for the machinability enhancement of Ti-6Al-4V alloy and consequently expands its applications. Machining under MQL was the basis for starting this research. Afterward, several steps have been completed to fulfill the ultimate objective. The major steps of the experimental investigation are as follows:

(i) Development of an efficient double jet MQL nozzle and preparation of a hybrid nano-fluid.

(ii) To evaluate the performance of a double jet MQL system with hybrid nano-fluid compared to dry and conventional MQL system.

Huge experimentation has been conducted in turning Ti-6Al-4V alloy and different responses have been collected at different stages of the experimentation for further analysis. Details of experimentation and data analysis procedures have been described in this chapter.

## 2.1 Experimental Procedure and Conditions

The experimentation has been carried by turning Ti-6Al-4V alloy, having an initial diameter of 100 mm and a length of 800 mm in a manual lathe machine (KL-3280C/2000) with a maximum power of 10hp. Ti-6Al-4V is an α+β alloy, which has high strength and is heat treatable to acquire more strength. Hence, they are typically used in different high-strength applications [Ezugwu and Wang, 1997]. This alloy also consists of superior corrosion resistance and biocompatibility but machinability is very low [Davim, 2014]. Commercially available coated and uncoated tungsten carbide inserts (ISO designation SNMG 120408) have been used in turning operation. The coated carbide insert has a multi-layered CVD-coating of TiN-TiCN-$Al_2O_3$-TiN (outermost). This tool usually provides enhanced machining performance regarding tool wear, surface finish and thermal

stability [Mia and Dhar, 2019]. Inserts have been mounted in a PSBNR 2525 M12 tool holder, which provided the required working tool geometry of -6°, -6°, 6°, 6°, 15°, 75°, 0.8 mm. In this research, turning has been done under dry and MQL conditions. A simple MQL setup has been used, where an aerosol is formed by mixing a very little amount of cutting fluid (unit of ml/hr) with the compressed air and finally, applied into the interfaces to cool and lubricate. Continuous and proper impingement of the MQL jet towards the chip-tool and work-tool interface zones where the highest temperatures exist is the prime concern for an effective MQL system. The schematic view of the experimental set-up has been shown in Fig.2.1.

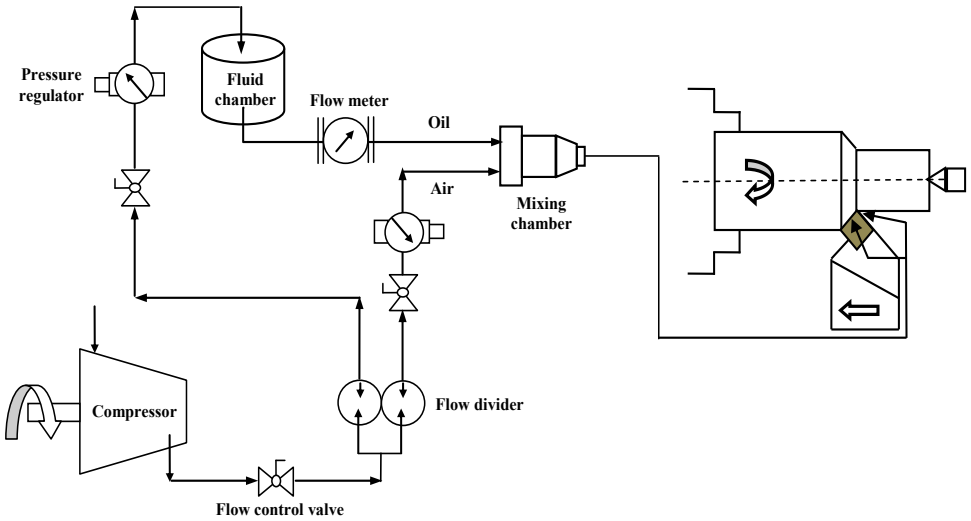


**Fig.2.1** Schematic view of the experimental set-up

The major components of the MQL delivery system are a compressor, fluid chamber, mixing chamber and micronozzle. For regulating pressure and flow rate, pressure regulator and flow meter are used respectively in the appropriate position. Compressed air is supplied by the compressor, which can develop a maximum pressure of 25 bars. Part of compressed air directly flows to the mixing chamber and the rest is to the fluid chamber to flow the fluid out of the container towards the mixing chamber. The capacity of the fluid chamber is 1 liter. It is connected to the compressor by a flexible pipe through the inlet port to keep the fluid inside the chamber under constant pressure. It is required to maintain the flow of cutting fluid into the mixing chamber through a flow control valve at a constant rate over a long period during machining. The capacity of the fluid chamber has been kept at one liter because up to the rate of 200 ml/hr it can continue for 5 hrs. The photographic view of the experimental setup has been presented in Fig.2.2.

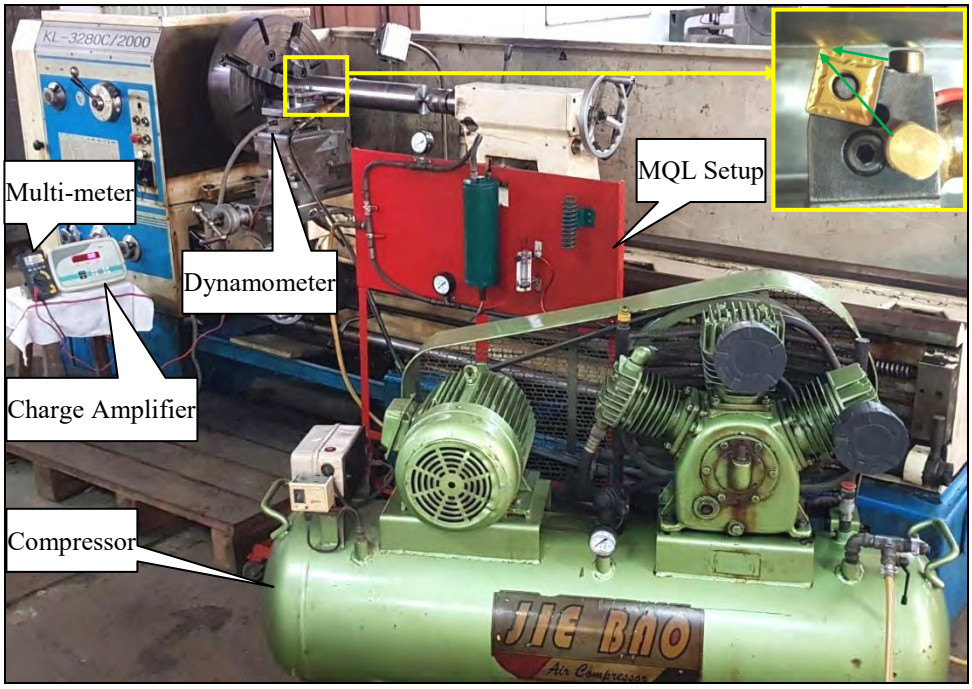


**Fig.2.2** Photographic view of the experimental set-up

The mixing chamber is used to develop air-oil mist by mixing the compressed air and cutting fluid. Oil has flowed towards the mixing chamber through the central tube and flowed out through the small radial holes at the end of the tube. On the other hand, the air has flowed to the front chamber by the inlet tube and entered the mixing chamber by the holes situated in the partition plate. Sudden expansion at the inlet and contraction at the outlet of the mixing chamber results in turbulence in the air-flow.

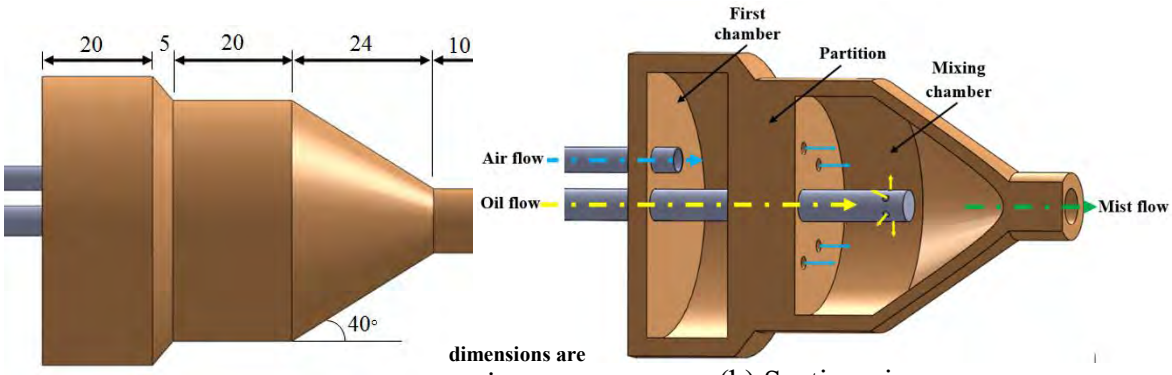


(a) Front view (b) Section view

**Fig.2.3** Mixing chamber (a) front view and (b) section view

The front view and section view of the mixing chamber is shown in Fig.2.3. In the mixing chamber, oil and air convene at the perpendicular direction, which assists the complete and proper mixing of air with cutting fluid in the chamber to form an air-oil mist. The tapered shape of the mixing chamber facilitates easy flowing of the mist to the nozzle

which is connected with the outlet port of the mixing chamber. Prepared mist from the mixing chamber has been delivered towards the machining zone through a micro nozzle.

The experimental work has been divided into three parts. The first stage of the investigation has been involved in the design of a double jet MQL delivery system. The influential process parameters for MQL performance are nozzle diameter, nozzle angle (primary and secondary), air pressure and oil flow rate [Singh et al., 2020]. Cutting process parameters have been set at fixed values throughout the first stage. At the end of this stage, Optimum MQL and nozzle parameters concerning multiple responses, such as cutting temperature, cutting force and surface roughness have been determined. Machining conditions for the first stage of the investigation have been presented in Table 2.1.

**Table 2.1** Machining conditions for designing double jet MQL delivery system

| | | |
|---|---|---|
| **MQL supply** | | |
| Nozzle Diameter | : | 0.5 ~1.5 mm |
| Primary Nozzle Angle | : | 10 ~ 20° (+ Angle with nozzle top surface) |
| Secondary Nozzle Angle | : | 10 ~ 20° (- Angle with nozzle top surface) |
| Air Pressure | : | 5 ~20 bar |
| Oil Flow Rate | : | 50 ~ 200 ml/hr |
| **Environment** | : | MQL (VG-68 Cutting oil) |
| **MQL Application technique** | : | Double Jet Micro Nozzle |
| **Process parameters** | | |
| Cutting velocity, V | : | 75 m/min |
| Feed rate, f | : | 0.14 mm/rev |
| Depth of cut, d | : | 1.0 mm |

The second stage of the investigation has been involved in the evaluation of the newly designed optimum double jet nozzle for MQL supply. As well as the prepared hybrid $Al_2O_3$-MWCNT based nanofluid has been evaluated as MQL liquid. The turning experiment has been carried out for dry and MQL conditions (with an external single jet, double jet nozzle and double jet nozzle with hybrid nano-fluid delivery) at a fixed cutting speed (V), feed rate (f) and depth of cut (d) condition for coated and uncoated carbide inserts. Here, the performance of hybrid nano-fluid based MQL with a double jet micro nozzle on the machinability characteristics of Ti-6Al-4V alloy regarding the chip formation, cutting temperature, cutting force, surface roughness, tool wear and dimensional deviation with time has been studied compared to traditional single jet MQL, double jet MQL (with cutting oil) and completely dry condition. It is expected from this comparison that hybrid nano-fluid-based MQL with double jet micro nozzle outperforms

the other three conditions. The experimental conditions for this stage have been given in Table 2.2.

**Table 2.2** Machining conditions to study the effects of MQL with hybrid nano-fluid

| | | |
|---|---|---|
| **MQL supply** | | |
| Nozzle Diameter | : | 0.5 mm |
| Primary Nozzle Angle | : | 20° |
| Secondary Nozzle Angle | : | 15° |
| Air Pressure | : | 20 bar |
| Oil Flow Rate | : | 50 ml/hr |
| **Environment** | : | - Dry<br>- MQL (VG-68 Cutting oil)<br>- MQL (hybrid nanofluid) |
| **MQL Application technique** | : | - External Single Jet<br>- Double Jet Micro Nozzle |
| **Process parameters** | | |
| Cutting velocity, V | : | 73 m/min |
| Feed rate, f | : | 0.14mm/rev |
| Depth of cut, d | : | 1 mm |
| **Nanoparticle concentration** | : | 1 vol % |

**Table 2.3** Machining conditions for optimization of process parameters

| | | |
|---|---|---|
| **MQL supply** | | |
| Nozzle Diameter | : | 0.5 mm |
| Primary Nozzle Angle | : | 20° |
| Secondary Nozzle Angle | : | 15° |
| Air Pressure | : | 20 bar |
| Oil Flow Rate | : | 50 ml/hr |
| **Environment** | : | MQL with hybrid nanofluid |
| **MQL Application technique** | : | Double Jet Micro Nozzle |
| **Process parameters** | | |
| Cutting velocity, V | : | 40 ~ 110 m/min |
| Feed rate, f | : | 0.10 ~ 0.18 mm/rev |
| Depth of cut, d | : | 0.5~1.5 mm |
| **Nanoparticle concentration** | : | 0.5~1.5 vol % |
| **Tool-type** | : | Uncoated and coated carbide inserts |

The third stage of the work involved modeling and optimization of process parameters (cutting speed, feed rate, depth of cut, nano-fluid concentration and tool-type, etc.) for efficient and effective machining of Ti-6Al-4V alloy regarding cutting temperature, cutting force and surface roughness. The ranges of cutting parameters have been chosen within the feasible range based on literature [Kechagias et al., 2020; Sartori et al., 2018; Venkata Ramana, 2017], where the feasible range of cutting speed was 30~120 m/min, the feed rate was 0.1~0.343 mm/rev and depth of cut was 0.25~1.6 for machining Ti-6Al-4V alloy by using uncoated, PVD coated and CVD coated cutting tool under

various cooling/lubrication environments including dry and MQL. For hybrid $Al_2O_3$-MWCNT nano-fluid 0.125~1.5 vol % of nanoparticle concentration was previously used by Asadi et al. [2018]. Table 2.3 briefly showed the conditions for the third stage of the investigation. Detailed description of this third stage has been presented in chapter 3.

In the present research work, various responses have been measured under all the machining conditions. Machining chips were collected to study their morphology. In turning Ti-6Al-4V alloy serrated chips are usually produced. Scanning Electron Microscopy (SEM) has been done for all the chips. Afterward, the segmentation degree, Gs and slip angle, υ of the serrated chips have been determined. The chip segmentation degree, Gs has been calculated by utilizing the following equation [Rao et al., 2011].

$$G_s = \frac{H-C}{H} \quad \text{.....} \quad \textbf{(2.1)}$$

where H is the chip thickness and C is the continuous chip thickness of a serrated chip. All the parameters of a serrated chip have been shown in Fig.2.4.

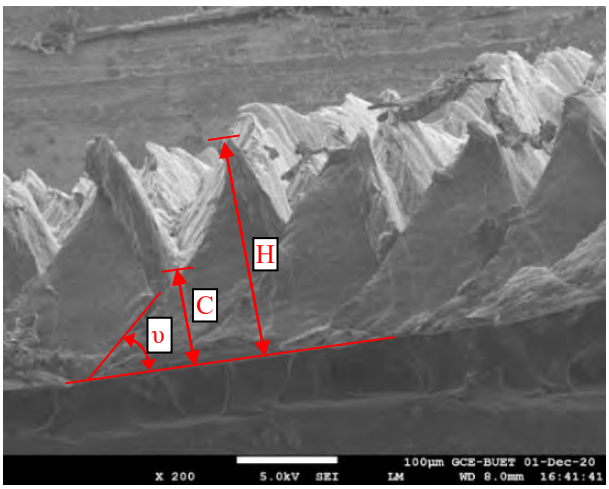


**Fig.2.4** SEM of serrated chips

The cutting temperature has been measured by a simple tool-work thermocouple technique, where tool and work material serve as two dissimilar metals. For a specific experimental run, a cutting temperature reading has been collected from 15 mm of tuning operation and the most stable reading has been collected. During machining, the chip-tool interface has formed the hot junction. Two Cu wires have been used to connect the tool with a distant part of the workpiece passing through the multimeter, which eventually completes the thermoelectric circuit. A Cu rod connected with the end of a Cu wire has been used to touch the work-piece at the time of operation. This part has served as the cold

junction (room temperature) if the Cu rod along with the wires has been virtually ignored. Insulations of the tool and work-piece from the lathe machine parts are mandatory for preventing the generation of parasitic emf and electrical short circuits. Leather has been used to insulate the workpiece from four jaw self cantered chuck and a mica sheet has been used to insulate the tool holder from the tool post. This technique is simple but reliable for measuring average cutting temperature over the entire contact area but high local temperatures at a specific point of contact cannot be observed. This method can be used for a wide range of temperatures. The tool-work thermocouple loop has been schematically shown in Fig.2.5. To apply the tool-work thermocouple technique for temperature measurement, proper calibration to relate the voltage generation with the actual temperature for a specific work-tool combination is essentially required. For calibration of the tool-work junction, a long tubular chip and tungsten carbide insert has been brazed together at one end. The free ends of the chip and tungsten carbide insert have been connected through the digital multi-meter (SANWA-digital multi-meter-CD772). The brazed junction of the tool-work thermocouple and a reference thermocouple (chromel-alumel) were placed contiguous to each other.

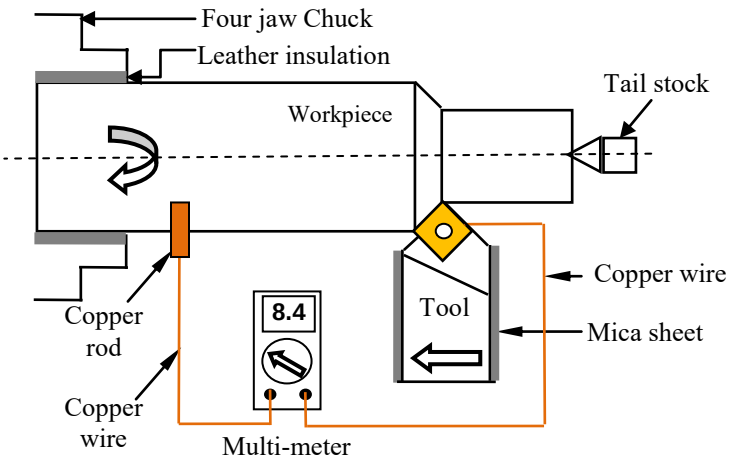


**Fig.2.5** Schematic diagram of the tool-work thermocouple

Afterward, the junction has been heated and the brazed junction served as the hot junction of the thermocouple. Thermoelectric voltage is generated in the tool-work thermocouple. This voltage was recorded by the multi-meter, at the same time the temperature (°C) of the hot junction was directly measured by the reference thermocouple using a digital thermometer (Eurotherm, UK). Corresponding voltage and temperature have been recorded during heat application and plotted. The photographic view of the

setup for tool-work thermocouple calibration used in the present investigation has been shown in Fig.2.6.

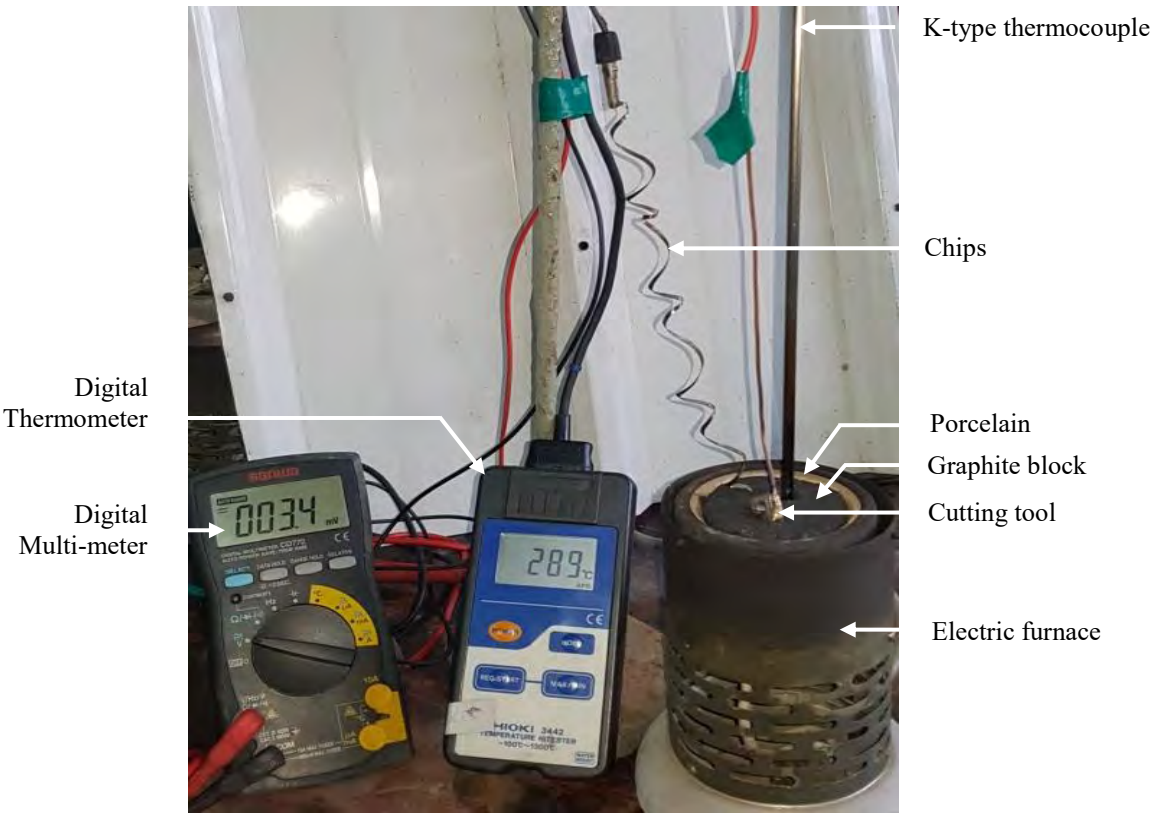


**Fig.2.6** Photographic view of the tool-work thermocouple calibration set up

The variation of temperature with different thermoelectric voltage (mV) for the thermocouple of tungsten carbide (tool material) and Ti-6Al-4V alloy has been plotted in Fig.2.7. Almost linear relationships between the temperature and voltage have been obtained with more than 99% accuracy. The regression equation used to determine the chip-tool interface temperature from the thermocouple voltage has been shown in Eq. 2.2:

**Temperature (°C) for Coated tool**= 46.82 + 71.98 Voltage (mV)

**Temperature (°C) for Uncoated tool**= 81.28 + 83.5 Voltage (mV) **.....(2.2)**

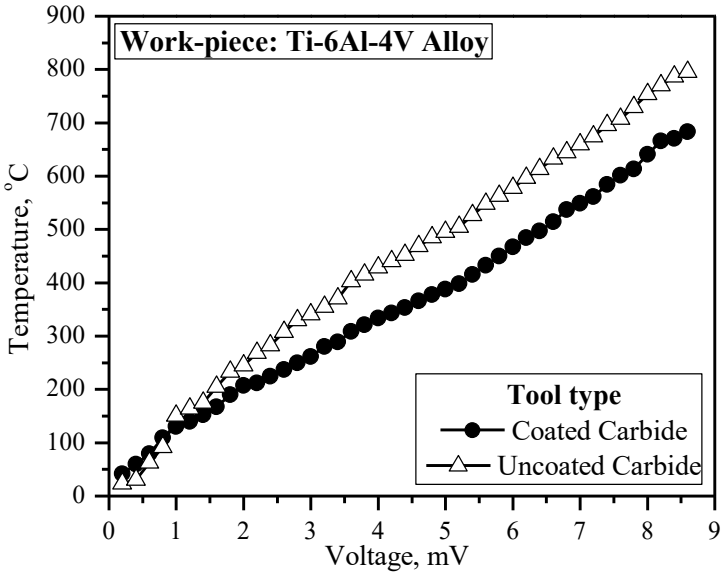


**Fig.2.7** Variation of temperature with various thermoelectric voltage

The force acting on a cutting tool during the process of metal cutting is the fundamental importance in the design of cutting tools. The determination of cutting forces is essential for several important requirements:

(i) to estimate the power requirements of a machine tool

(ii) to estimate the straining actions that must be resisted by the machine tool components, bearings, jigs and fixtures

(iii) to evaluate the role of various parameters in cutting forces

(iv) to evaluate the performance of any new work material, tool material, environment, techniques, etc. concerning machinability (cutting forces)

The main cutting force (F) was monitored by a KISTLER dynamometer (9257B). The tool post has been fixed into the dynamometer during machining and the dynamometer has been coupled with a charge amplifier. Stable reading has been taken as force data. For the evaluation of the machined surface roughness, $R_a$ (Arithmetical mean roughness) was measured by a Talysurf type roughness checker (Surtronic 3+, Rank Taylor Hobson Limited, UK) using a widely used cut-off length of 0.8 mm and total evaluation length of 4 mm after each experimental run. The measurement was repeated thrice at different locations, at an approximately equally distant position on the cylindrical machined surface. The average of these three values has been calculated for each given value of surface roughness. Tool wear is the progressive failure of the cutting tool owing

to the usual cutting operation. Due to high cutting temperature and force, the cutting tool is affected severely. If the cutting force becomes too large, the tool fractures. If the cutting temperature becomes too high, the tool material softens and fails. Cutting tools also often fail prematurely, randomly and catastrophically by mechanical breakage and plastic deformation under adverse machining conditions caused by intensive pressure and temperature and/or dynamic loading at the tooltips particularly if the tool material lacks strength, hot hardness and fracture toughness. However, in the present investigations, the tool failure mode has been mostly gradual wear. The geometrical pattern of tool wear that is generally observed in turning by carbide inserts is schematically shown in Fig.2.8.

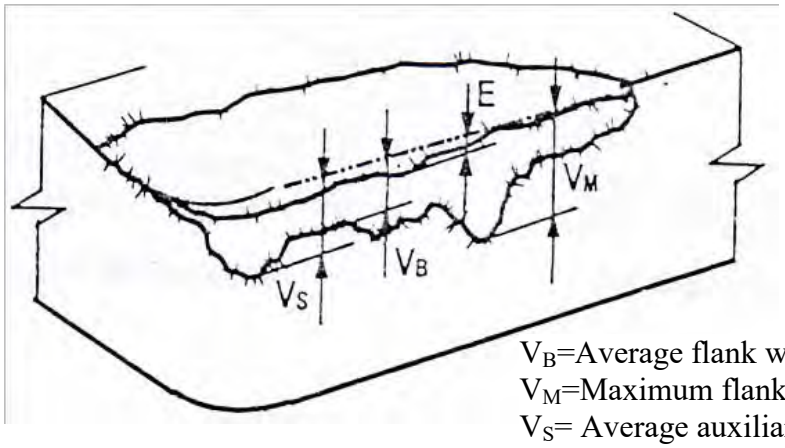


$V_B$=Average flank wear
$V_M$=Maximum flank wear
$V_S$= Average auxiliary flank wear

**Fig.2.8** Schematic view of a general pattern of wear [Khan, 2015]

Principal flank wear ($V_B$), which intensifies the cutting temperature, cutting forces and also provoke vibration and chatter during machining. On the other hand, the auxiliary flank wear ($V_S$) affects the surface finish and dimensional accuracy of the machined parts. Tool wear is considerably influenced by the temperature and nature of interactions of the tool-work interfaces which depend upon the machining conditions for a given tool-work combination. Tool life is calculated based on ISO Standard 3685 for tool life. The cutting tool was rejected for further machining considering one or a combination of the following rejection criteria [ISO 3685: ―Tool life testing with single-point turning tools," 1976]:

- Average flank wear ≥ 0.3 mm
- Maximum flank wear ≥ 0.4 mm
- Nose wear ≥ 0.3 mm
- Notching at the depth of cut line ≥ 0.6 mm
- Surface roughness value ≥ 1.6 µm
- Excessive chipping (flaking) or catastrophic fracture of the cutting edge.

Tool wears have been analyzed under different environments for specific machining conditions. During machining for each case, the insert was withdrawn at regular

intervals and then the tool wears at the auxiliary and principal flank face of the tool were measured using an optical microscope (Carl Zeiss, Germany) fitted with a precision micrometer of least count 1μm. The study has been continued until any of the above-mentioned criteria has been fulfilled. The rejected tools were finally examined in the scanning electron microscope (SEM) and the micrographs have been analyzed further. The dimensional deviation under different cooling environments has been measured concerning the variation in diameter of the machined workpiece. After one full pass of turning of about 200 mm length with specific cutting speed, feed rate and depth of cut, the variation of job diameter has been measured by using the outer caliper.

## 2.2 Desirability based RSM technique

RSM (Response Surface Methodology) is a powerful, systematic and rigorous mathematical tool has been initiated by Box and Wilson [1951]. This technique can be utilized to do experimental design, evaluate the effects of process parameters on the process output responses, identify significant parameters and interactions contributing to the response being measured, establish a correlation between the significant parameters and the responses and ascertain optimum process parameters settings meant for superior process performance within the limits selected for the experimental design [Goethals Jr. and Cho, 2011]. Afterward, multi-response optimization can be accomplished with desirability analysis. In this research, desirability-based RSM has been employed for designing the double jet MQL delivery system and process parameter optimization for the efficient turning of Ti-6Al-4V alloy. Commercial statistics software package MINITAB 17 has been used for this purpose. In the first stage of RSM, systematic data are generated and summarized for evaluation by a well-chosen experimental design. Considering the limited resources of any problem area, experimental design can generate the maximum required information with the minimum amount of experimentation, which saves both time and money as well as ensure a valid, justifiable, and acceptable conclusion (Montgomery, 2009). Time and cost-saving by reducing the number of the experimental run is an advantage of RSM [Boyaci, 2005]. Box- Behnken designs (BBD) and central composite design (CCD) are appropriate for fitting the second-order polynomial model of the response surface design [Manohar et al., 2013]. The second-order polynomial model is required for optimization purposes. BBD is more popular in real industrial research, because of its economic nature [Khuri and Mukhopadhyay, 2010]. It's an incomplete three

levels of factorial designs. Two levels of factorial design combined with incomplete block design in a specific method provide this BBD. By using experimental data, empirical statistical models can be developed to approximate the relationship between process parameters and responses. Although empirical equations developed by RSM are approximate models, they are subsequently used for predicting process responses and used as objective functions and constraint functions in the case of parameter optimization. The empirical models developed from the experimental data can be linear or quadratic. If the independent or input variables $X_1$, $X_2$, $X_3$,…. $X_n$ affects the response variable (Y) and all the variables are quantifiable then the response surface can be defined as Eq. 2.3.

$$Y = f(X_1, X_2, X_3 \ldots X_n.) + e \quad \text{…….....…….....} \quad \textbf{(2.3)}$$

Where f is the response function which is unidentified and possibly very complex and $e$ is the experimental error. Experimental error is needed to be distributed normally with zero means. With the experimental results, empirical (approximation) process models are developed where the significant process parameters (discrete or continuous) are linked with the process responses which are assumed to be continuous. The empirical model is of the 'black box' type. The true response function f is indefinite. An appropriate approximation for f depends upon the experimenter‘s ability.

When the "operability region" is very small for a problem area that confirms a little curvature in the function, f, then a first-order model can be used to approximate the true response surface. This type of model is generally called the main effect model, which is shown in the following Eq. 2.4.

$$Y = \{ b_o + b_1X_1 + b_2X_2 + b_3X_3 + \ldots \} + e \quad \textbf{.....……...……..…..(2.4)}$$

The interaction effect of the input variables, if significant, can be included in the first-order model as described below.

$$Y = \begin{Bmatrix} b_o + b_1X_1 + b_2X_2 + b_3X_3 + b_{12}X_1X_2 \\ + b_{23}X_2X_3 + b_{13}X_1X_3 + \ldots\ldots \end{Bmatrix} + e \quad \textbf{....……..…(2.5)}$$

When the first-order model (with or without the interaction term) is inadequate to approximate the true response surface then the second-order model is required [Khuri and Mukhopadhyay, 2010]. The general second-order model is as follows:

$$Y = \left\{ \begin{matrix} b_o X_o + b_1 X_1 + b_2 X_2 + b_3 X_3 + b_{12} X_1 X_2 + b_{23} X_2 X_3 + \\ b_{13} X_1 X_3 + b_{11} X_1^2 + b_{22} X_2^2 + b_{33} X_3^2 + ..... \end{matrix} \right\} + e \quad \text{..... (2.6)}$$

Where Y is the estimated response based on a second-order equation. The second-order model is very flexible and the parameters $b_0$, $b_1$, $b_2$, $b_3$, $b_{12}$, $b_{23}$, $b_{13}$, $b_{11}$, $b_{22}$ and $b_{33}$ can be calculated by the least-squares regression method. Regression analysis is found in the successful technique to perform the trend analysis of responses concerning various combinations of design variables.

Analysis of variance (ANOVA) [Lin and Ho, 2003] can be used to find out the model significance and the significant model terms, which were responsible for the variation of the responses. The calculated P-value < 0.05 indicates that the model and model terms are significant with a 95% confidence interval. Percent contribution ($P_i$) of the model and model terms on different output responses can also be determined from ANOVA based on Adj SS (adjusted sum of squares) values by using Eq. 2.7 [Singh et al., 2011]:

$$P_i = \frac{SS_i}{\sum SS_i} \times 100\% \quad \text{..... (2.7)}$$

where SS=sum of squares. i= model terms.

The lack-of-fit value forms the ANOVA table should be > 0.05, which proves that this value is insignificant compared to the pure error value and the proposed predictive models have been fitted the experimental data very well [Sachin et al., 2019]. The $R^2$ value is another important criterion to decide the validity of the regression model [Montgomery, 2001]. This indicates the proportion of variance in the response variable that can be explained by the input variables. If this value is 90 % or more, the relationship established by the empirical models is highly acceptable. The $R^2$ value of the final regression model should close to the $R^2$ (adjusted) value which is preferable in an ideal situation. This confirms that no insignificant terms have been added to the regression model. Besides, $R^2$ (predicted) value indicated how well the developed model can predict the responses for new observations within the range of process parameters.

The residual plots [Majumder et al., 2017] can be utilized to examine the normality and the randomness of the residual values of the formulated empirical models. A 4 in 1 residual plot has been drawn along with the formulated model. These are normal

probability plots, a histogram of the residuals, a residual versus fitted value and residual versus observation order. Data follow a straight line closely on the normal probability plot and a bell-shaped histogram of the residuals with no skewness and outlier confirm the normality of the data used for the development of the model. On the other hand, even and random distribution of the data point on both sides of the 0 residual value line with constant variance and no specific pattern on the residual versus fitted value and observation order plot verify the randomness of the residual values. Evaluation of the normality and the randomness of the residual values is required to verify the characteristics of a good model and reliable experimental data.

Verification of the model with experimental data is the utmost necessity before using these models for optimization of the process parameters [Koç and Kaymak-Ertekin, 2009]. A validity test has to be conducted before using this for optimization purposes. Any formulated empirical model is considered to be valid if it can predict response data with a reasonable error using a new set of input combinations that were not used during the model formulation by conducting additional experimental runs. The prediction accuracy of an empirical model can be numerically evaluated by different error measures. Among them mean absolute percentage of error (MAPE) is an effective, simple and widely used method for model validation [Myttenaere et al., 2016]. MAPE is the average of the absolute percentage error where percentage errors for each experimental run are totaled irrespective of their signs. As it is an error measure, its lower value confirms better model performance. MAPE for the models was computed by utilizing Eq. 2.8 [Boyd et al., 2019].

$$\text{MAPE} = \frac{1}{n}\sum_{t=0}^{n}\frac{|\text{Actual}_t - \text{Predicted}_t|}{\text{Actual}_t} \times 100 \quad \text{..... (2.8)}$$

By utilizing various plots constructed during empirical modeling, the effects of process parameters on the responses can be visually evaluated. In the main effect plots, the individual effect of each process input on the process outputs has been demonstrated. The steeper slope of the line means the greater magnitude of the main effect. If the effect of one input variable on the output variable changes depending on the level of another input variable, then the interaction effects are significant. Parallel lines imply no significant interaction effect and the non-parallel lines imply the interaction effect. There is little prior research where the environment and tool type were considered concurrently.

As a final point, using the empirical models of the responses process parameters optimization can be accomplished. In manufacturing, it is very important to optimize the process parameters. Enhanced productivity, reduced production cost and hazard-free operation are a by-product of an optimized process [Xiong et al., 2016]. An effective and efficient manufacturing process offers low temperature, low force, low tool wear and high material removal rate without compromising the product quality. The situation of multiple, partially/full conflicting objectives in the optimization problem is called the multi-criteria optimization (MCO) or multi-response optimization (MRO). Nowadays, multi-response optimization (MRO) has gain greater importance among various researchers and manufacturing industries [Bhushan, 2013; Gupta et al., 2016; Sarikaya and Güllü, 2015]. MRO is very complex, because, different responses have been measured on a different scale. Different techniques like grey relational analysis incorporated with the Taguchi method, desirability function (DF) approach based RSM, Pareto optimization, the genetic algorithm can be used for Optimization. The first two methods are very easy to use and between them, the DF method is more flexible than grey-based Taguchi. Because it can select any value of the variables within the range whereas grey-based Taguchi can select the value of the level. The computation time of this method is very less. Different software programs such as Minitab, Design-Expert have adopted the DFs approach for their response optimizer system. DFs of Derringer and Suich type (Derringer and Suich, 1980) are used in this software. Every response has been translated by an individual DF into a unit-less desirability value (d) that varies over the range $0 \leq d \leq 1$. Typical desirability functions for maximizing, target and minimize the response has been shown in Fig.2.9. Desirability, d=1 represents the ideal situation (improvement beyond this point is impossible) and d=0 means a completely unacceptable situation. Typical desirability functions are shown in Fig. 2.9 (a), (b) and (c) respectively.

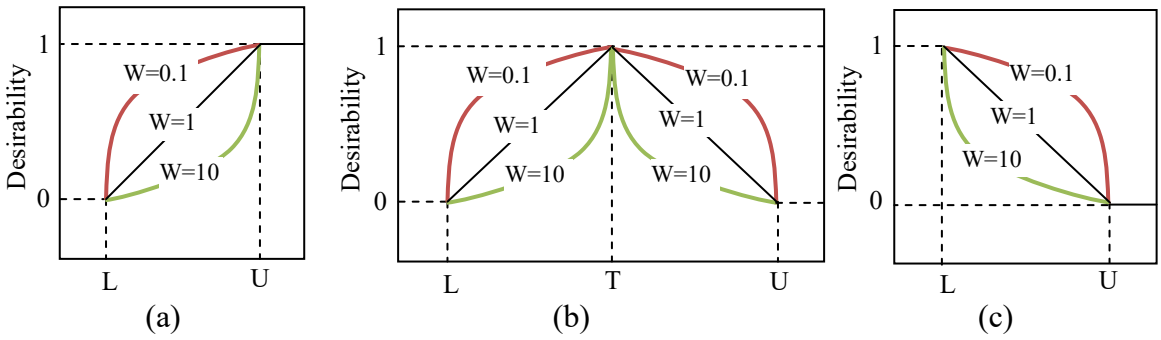


**Fig.2.9** Desirability functions for (a) maximize the response, (b) target the response and (c) minimize the response

The desirability function shape for each response is defined by the weight (from 0.1 to 10). 0.1 weight means less emphasis on the target than the bound, whereas 1 means equal emphasis of both and 10 means more emphasis on the target than the bound. Usually, lower weight offers higher desirability but it does not affect the optimum results. In this article, all of the objectives needed to be minimized, so, the desirability function is given in Fig. 2.9 (c) is used for all of the cases. Composite or overall DF also has a value between 0 to 1, which is calculated by the weighted geometric mean of the individual DFs according to Eq. 2.9. Derringer [1994] develops this weighted case of the DFs, where the weights are the relative importance (or priorities) to the individual responses.

$$D = (d_1^{w1} \times d_2^{w2} \times \cdots \times d_n^{wn})^{1/n} \quad \textbf{(2.9)}$$

This composite DF implies a single objective for the multi-response problem [Ehrgott, 2005]. The combination of parameter settings, which has given the maximum total desirability has been considered to be optimal. This DF approach is very simple to apply and also the relative importance of various responses can be considered, which is very useful for the practical case of process improvement. Larger values of the 'importance' correspond to more important responses. This 'importance' value affects the optimization results and also composite desirability.

## 2.3 Design and fabrication of double jet MQL delivery system

The purpose of an MQL delivery system is to direct cutting fluid to the optimal position to achieve maximum fluid flow at the area of interest and reduce mainly the temperature and frictional coefficient of the matting surfaces. Heat reduction can happen by the fluid vaporization at the cutting zone and conduction through the flow of the compressed air. And as a result, other indices are improved. In MQL, disposal of the cutting fluid is not needed because of full evaporation of the coolant and the cost associated with this action is also eliminated. The nozzle of the MQL delivery system fulfills the purpose of increasing the fluid velocity by contracting the cross-sectional area of the jet stream. The MQL delivery system has been designed and developed so that the nozzle spray pattern, covering area, air pressure and coolant flow rate can be controlled and keep constant throughout the cut. The expected result of this arrangement is effective cooling with economical coolant dispensing. It is important to properly position the coolant delivery system to achieve the following:

(i) Impinging cutting fluid to the tool/workpiece and tool/chip interfaces

(ii) Consistent coolant flow prevents alternative heating and cooling of the tool and reduces the possibility of thermal shock.

(iii) Flushing the chips out of the cutting zone. This is one of the most important functions of the fluid and may require positioning one or more fluid lines just to move chips out of the cutting zone

Besides the tool-work-piece combination and cutting conditions, heat generation in metal cutting depends on the type of cutting fluids and their application methods. The effectiveness of any cooling technique depends on how closely the coolant jet can reach the chip-tool and work-tool interfaces. Since a minute amount of fluid is used in the MQL system, the appropriate pin-pointed impingement of fluid mist in the area of interest mostly affects the efficiency of the MQL system. So, the goal of the MQL is simple, apply just enough fluid to fully lubricate the cutting zone using the least amount of oil as possible. Usually, coolant mist in MQL is supplied by a single nozzle along the rake surface to the chip-tool interface, which is evaporated after application and the tool-work-piece rubbing interface remains untreated. Oil mist supplied from two nozzles (along with the rake and flank surface of the cutting tool) is more effective than the single nozzle. By this multiple mist supply, the coolant reaches as close to the chip-tool and work-tool interfaces as possible and cools the above-mentioned interfaces and both the rake and auxiliary flank of the tool effectively as well.

In this work, a double jet micronozzle has been designed by which two well-controlled and focused MQL jets have directly impinged into the chip-tool and the work-tool interfaces. The secondary coolant flow through the auxiliary flank face facilitates coolant penetration in the work tool interface which causes better surface finish along with low temperature, force and tool wear. Similar coolant flow direction and destination were used in the case of cryogenic cooling of Ti-6Al-4V turning [Hong et al., 2001]. The proposed double jet nozzle includes a PSBNR-2525 M12 (Sandvik) type tool holder with an inlet connection adapter and two specially designed micro nozzles. The Inlet nozzle is permanently joined by brazing which guides the MQL mist from the mixing chamber towards the double jet micro nozzle for final delivery. The axis of above mentioned three nozzles are intersected in a common point and are pair-wise perpendicular. Two

cylindrical-shaped closed-end primary and secondary coolant feed nozzles were attached at the top face and front face of the tool holder to deliver the well-controlled and focused MQL mists towards the tooltip through the rake surface (chip-tool interface) and flank surface (work-chip interface) of the tool respectively. The primary nozzle jet creates a positive angle with the nozzle top surface. Whereas, the secondary nozzle jet creates a negative angle with the nozzle top surface. Fig.2.10 shows the double jet micro nozzle, the primary nozzle angle and the secondary nozzle angle.

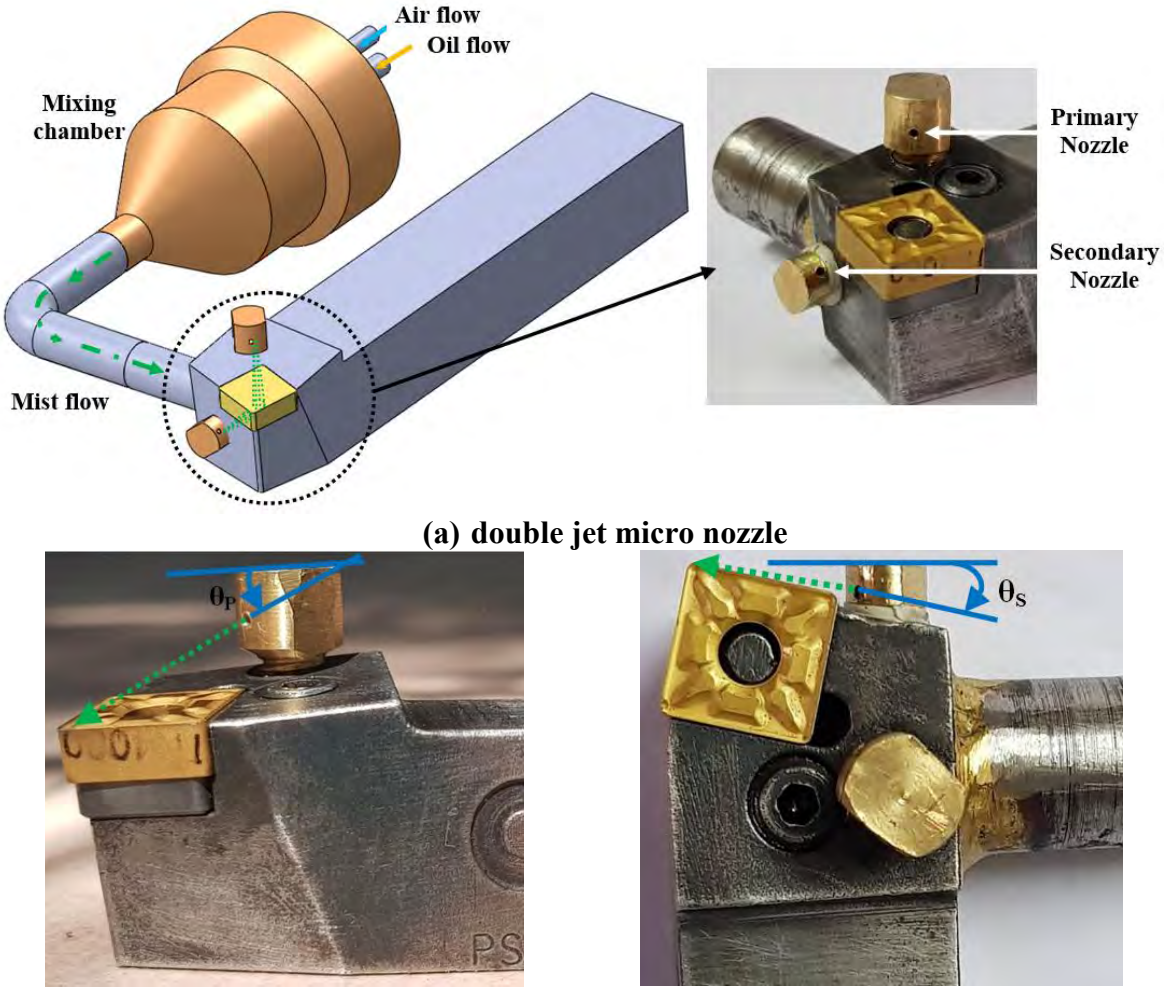


**(a) double jet micro nozzle**

**(b) primary nozzle angle** **(c) secondary nozzle angle**

**Fig.2.10** Photographic view of (a) double jet micro nozzle (b) primary nozzle angle and (c) secondary nozzle angle.

In previous research [Banerjee and Sharma, 2019] regarding multiple nozzle MQL turning of Ti-6Al-4V alloy, a larger oil proportion in rake nozzle was beneficial for lower cutting energy whereas a larger proportion in the flank nozzle was beneficial for surface roughness and tool wear. An equal amount of oil mist in two nozzles provides a moderate amount of responses. Hence, in this research equal oil distribution was tried to maintain. The primary and the secondary nozzles have equal travel distances from the inlet port. The

main oil mist flow is divided into two approximately equal amount and flow out through these two nozzles. As a very low amount of fluid is delivered during MQL, a slight change of nozzle position may hamper its cooling performance terribly. For the traditional nozzle, it should be positioned at an angle with the rake surface of the tool before every run and need to be maintained strictly throughout the machining time. This problem further increases if two nozzles for double flow are required. The major benefits of using a double jet nozzle are the elimination of nozzle setup time as well as potential nozzle orientation errors, which provide consistent cooling throughout the machining operation without constant inspection. However, the determination of the optimum nozzle diameter, nozzle angle, air pressure and coolant flow rate is mandatory for an effective and efficient MQL system.

In this work, RSM has been used for empirical modeling of the process responses regarding the MQL parameters based on experimental data and then optimize the MQL parameters for the required value of the responses. The second-order model is appropriate for optimization purposes. For double jet MQL delivery designing, the influential process parameters for jet performance are nozzle diameter, nozzle angle (primary and secondary), air pressure and oil flow rate while cutting temperature, cutting force and surface roughness were selected as process responses. The range of parameters has been selected based on literature and pilot experiment. Table 2.4 shows the input parameters and their levels as considered for experimentation. With the MQL parameters and their levels selected, the Box-Behnken experimental design was created by using MINITAB 17 software and experiments were executed. Multiple response values were collected for further analysis. Table 2.5 shows the experimental design with corresponding responses.

**Table 2.4** MQL parameters with their levels

| Sl.No | Variable | Symbols | Unit | Lower Level | Upper Level |
|---|---|---|---|---|---|
| 1 | Nozzle diameter | D | mm | 0.5 | 1.5 |
| 2 | Primary Nozzle angle | $\theta_P$ | $^o$ | 10 | 20 |
| 3 | Secondary Nozzle angle | $\theta_S$ | $^o$ | 10 | 20 |
| 4 | Air pressure | P | Bar | 5 | 20 |
| 5 | Oil flow rate | Q | ml/hr | 50 | 200 |

**Table 2.5** Box-Behnken experimental design with corresponding responses

| Run Order | D | θp | θs | P | Q | T (°C) | F(N) | Ra (μm) |
|---|---|---|---|---|---|---|---|---|
| **1** | 0.5 | 10 | 15 | 12.5 | 125 | 653.99 | 471.38 | 2.87 |
| **2** | 1.5 | 10 | 15 | 12.5 | 125 | 661.37 | 486.08 | 2.25 |
| **3** | 0.5 | 20 | 15 | 12.5 | 125 | 663.83 | 462.56 | 1.58 |
| **4** | 1.5 | 20 | 15 | 12.5 | 125 | 671.20 | 477.26 | 2.09 |
| **5** | 1.0 | 15 | 10 | 5.0 | 125 | 644.16 | 491.96 | 1.86 |
| **6** | 1.0 | 15 | 20 | 5.0 | 125 | 644.16 | 490.98 | 1.31 |
| **7** | 1.0 | 15 | 10 | 20.0 | 125 | 676.12 | 492.94 | 1.25 |
| **8** | 1.0 | 15 | 20 | 20.0 | 125 | 653.99 | 488.04 | 1.51 |
| **9** | 1.0 | 10 | 15 | 12.5 | 50 | 658.91 | 484.12 | 2.48 |
| **10** | 1.0 | 20 | 15 | 12.5 | 50 | 671.20 | 467.46 | 2.05 |
| **11** | 1.0 | 10 | 15 | 12.5 | 200 | 658.91 | 483.14 | 2.21 |
| **12** | 1.0 | 20 | 15 | 12.5 | 200 | 653.99 | 479.22 | 1.39 |
| **13** | 0.5 | 15 | 10 | 12.5 | 125 | 658.91 | 479.22 | 1.94 |
| **14** | 1.5 | 15 | 10 | 12.5 | 125 | 666.28 | 492.94 | 2.05 |
| **15** | 0.5 | 15 | 20 | 12.5 | 125 | 649.08 | 480.20 | 1.74 |
| **16** | 1.5 | 15 | 20 | 12.5 | 125 | 653.99 | 493.92 | 1.55 |
| **17** | 1.0 | 15 | 15 | 5.0 | 50 | 646.62 | 490.98 | 2.23 |
| **18** | 1.0 | 15 | 15 | 20.0 | 50 | 666.28 | 480.20 | 1.66 |
| **19** | 1.0 | 15 | 15 | 5.0 | 200 | 636.78 | 489.02 | 1.31 |
| **20** | 1.0 | 15 | 15 | 20.0 | 200 | 658.91 | 490.98 | 1.69 |
| **21** | 1.0 | 10 | 10 | 12.5 | 125 | 663.83 | 490.98 | 2.09 |
| **22** | 1.0 | 20 | 10 | 12.5 | 125 | 673.66 | 479.22 | 1.86 |
| **23** | 1.0 | 10 | 20 | 12.5 | 125 | 653.99 | 487.06 | 2.25 |
| **24** | 1.0 | 20 | 20 | 12.5 | 125 | 661.37 | 476.28 | 1.47 |
| **25** | 0.5 | 15 | 15 | 5.0 | 125 | 646.62 | 482.16 | 1.94 |
| **26** | 1.5 | 15 | 15 | 5.0 | 125 | 639.24 | 490.00 | 2.04 |
| **27** | 0.5 | 15 | 15 | 20.0 | 125 | 653.99 | 474.32 | 2.09 |
| **28** | 1.5 | 15 | 15 | 20.0 | 125 | 676.12 | 495.88 | 1.62 |
| **29** | 1.0 | 15 | 10 | 12.5 | 50 | 656.45 | 485.10 | 2.01 |
| **30** | 1.0 | 15 | 20 | 12.5 | 50 | 663.83 | 490.98 | 1.58 |
| **31** | 1.0 | 15 | 10 | 12.5 | 200 | 658.91 | 494.90 | 1.78 |
| **32** | 1.0 | 15 | 20 | 12.5 | 200 | 644.16 | 482.16 | 1.29 |
| **33** | 0.5 | 15 | 15 | 12.5 | 50 | 653.99 | 465.50 | 2.33 |
| **34** | 1.5 | 15 | 15 | 12.5 | 50 | 661.37 | 493.92 | 2.17 |
| **35** | 0.5 | 15 | 15 | 12.5 | 200 | 646.62 | 484.12 | 2.13 |
| **36** | 1.5 | 15 | 15 | 12.5 | 200 | 653.99 | 478.24 | 1.86 |
| **37** | 1.0 | 10 | 15 | 5.0 | 125 | 636.78 | 490.98 | 2.26 |
| **38** | 1.0 | 20 | 15 | 5.0 | 125 | 663.83 | 474.32 | 1.90 |
| **39** | 1.0 | 10 | 15 | 20.0 | 125 | 676.12 | 483.14 | 2.13 |
| **40** | 1.0 | 20 | 15 | 20.0 | 125 | 666.28 | 483.14 | 1.51 |
| **41** | 1.0 | 15 | 15 | 12.5 | 125 | 668.74 | 468.44 | 2.20 |
| **42** | 1.0 | 15 | 15 | 12.5 | 125 | 666.28 | 464.52 | 2.44 |
| **43** | 1.0 | 15 | 15 | 12.5 | 125 | 668.74 | 470.40 | 2.08 |
| **44** | 1.0 | 15 | 15 | 12.5 | 125 | 668.74 | 468.44 | 2.33 |
| **45** | 1.0 | 15 | 15 | 12.5 | 125 | 666.28 | 467.46 | 2.26 |
| **46** | 1.0 | 15 | 15 | 12.5 | 125 | 666.28 | 464.52 | 2.13 |

Based on the experimental results, empirical modeling of process responses regarding MQL parameters has been performed by using the commercial statistics software package MINITAB 17 and validated. The predictive empirical models developed for different responses are shown in Eq. 2.10 to 2.12.

$$\mathbf{T} = 479.1 + 31.47\ D + 5.275\ \theta p + 5.949\ \theta s + 8.704\ P + 0.2405\ Q - 24.49\ D\times D - 0.1762\ \theta s\times\theta s - 0.1329\ P\times P - 0.001380\ Q\times Q + 1.967\ D\times P - 0.2458\ \theta p\times P - 0.01147\ \theta p\times Q - 0.1493\ \theta s\times P + 0.01475\ \theta s\times Q \quad \text{..... (2.10)}$$

$$\mathbf{F} = 694.8 - 12.70\ D - 6.799\ \theta p - 14.104\ \theta s - 8.813\ P - 0.1249\ Q + 21.72\ D\times D + 0.1127\ \theta p\times\theta p + 0.5145\ \theta s\times\theta s + 0.2171\ P\times P + 0.001445\ Q\times Q + 0.915\ D\times P - 0.2287\ D\times Q + .1111\ \theta p\times P + 0.00849\ \theta p\times Q - 0.01241\ \theta s\times Q + 0.00566\ P\times Q \quad \text{..... (2.11)}$$

$$\mathbf{R_a} = 0.767 - 1.344\ D - 0.0891\ \theta p + 0.4635\ \theta s + 0.0402\ P + 0.00021\ Q - 0.01584\ \theta s\times\theta s - 0.005901\ P\times P - 0.000031\ Q\times Q + 0.1130\ D\times\theta p - 0.0380\ D\times P - 0.00550\ \theta p\times\theta s + 0.00540\ \theta s\times P + 0.000422\ P\times Q \quad \text{..... (2.12)}$$

**Table 2.6** ANOVA for the cutting temperature

| Source | DF | Adj SS | Adj MS | F-Value | P-Value | % Contribution |
|---|---|---|---|---|---|---|
| Model | 14 | 4606.32 | 329.02 | 71.17 | 0.000 | 96.98 |
| Linear | 5 | 2689.49 | 537.90 | 116.36 | 0.000 | 56.63 |
| D | 1 | 199.81 | 199.81 | 43.22 | 0.000 | 4.21 |
| θp | 1 | 236.07 | 236.07 | 51.07 | 0.000 | 4.97 |
| θs | 1 | 163.65 | 163.65 | 35.40 | 0.000 | 3.45 |
| P | 1 | 1814.60 | 1814.60 | 392.53 | 0.000 | 38.21 |
| Q | 1 | 275.35 | 275.35 | 59.56 | 0.000 | 5.80 |
| Square | 4 | 1037.47 | 259.37 | 56.11 | 0.000 | 21.84 |
| D×D | 1 | 353.48 | 353.48 | 76.46 | 0.000 | 7.44 |
| θs×θs | 1 | 182.97 | 182.97 | 39.58 | 0.000 | 3.85 |
| P×P | 1 | 527.27 | 527.27 | 114.06 | 0.000 | 11.10 |
| Q×Q | 1 | 568.03 | 568.03 | 122.87 | 0.000 | 11.96 |
| 2-Way Interaction | 5 | 879.36 | 175.87 | 38.04 | 0.000 | 18.51 |
| D×P | 1 | 217.56 | 217.56 | 47.06 | 0.000 | 4.58 |
| θp×P | 1 | 339.94 | 339.94 | 73.53 | 0.000 | 7.16 |
| θp×Q | 1 | 74.03 | 74.03 | 16.01 | 0.000 | 1.56 |
| θs×P | 1 | 125.45 | 125.45 | 27.14 | 0.000 | 2.64 |
| θs×Q | 1 | 122.38 | 122.38 | 26.47 | | 2.58 |
| Error | 31 | 143.31 | 4.62 | | | 3.02 |
| Lack-of-Fit | 26 | 134.24 | 5.16 | 2.85 | 0.123 | 2.83 |
| Pure Error | 5 | 9.07 | 1.81 | | | 0.19 |
| Total | 45 | 4749.63 | | | | 100.00 |

**Model Summary**

S=2.15009 $R^2$=96.98% $R^2$ (adj)= 95.62% $R^2$ (pred)= 91.72%

For all the responses, the Full quadratic model has been reduced to a more suitable model with only significant terms ($p < 0.05$) by using a backward elimination technique considering hierarchy criterion (If a statistically insignificant term is a part of an interaction term or a higher-order term, then the term stays in the model). ANOVA for reduced models for each response has been shown in Table 2.6, 2.7 and 2.8. The influence of each term in the final model on the responses as well as the percent contribution of each term has been determined by calculated based on Adj SS (adjusted sum of squares) values from the ANOVA tables. Plots for the residual analysis of the final models have also been presented followed by the ANOVA tables.

**Table 2.7** ANOVA for the cutting force

| Source | DF | Adj SS | Adj MS | F-Value | P-Value | % Contribution |
|---|---|---|---|---|---|---|
| Model | 16 | 4082.22 | 255.14 | 67.07 | 0.000 | 97.37 |
| Linear | 5 | 1176.85 | 235.37 | 61.87 | 0.000 | 28.07 |
| D | 1 | 739.57 | 739.57 | 194.40 | 0.000 | 17.64 |
| θp | 1 | 374.62 | 374.62 | 98.47 | 0.000 | 8.94 |
| θs | 1 | 19.45 | 19.45 | 5.11 | 0.031 | 0.46 |
| P | 1 | 8.64 | 8.64 | 2.27 | 0.143 | 0.21 |
| Q | 1 | 34.57 | 34.57 | 9.09 | 0.005 | 0.82 |
| Square | 5 | 2326.97 | 465.39 | 122.33 | 0.000 | 55.50 |
| D×D | 1 | 257.40 | 257.40 | 67.66 | 0.000 | 6.14 |
| θp×θp | 1 | 69.28 | 69.28 | 18.21 | 0.000 | 1.65 |
| θs×θs | 1 | 1443.87 | 1443.87 | 379.53 | 0.000 | 34.44 |
| P×P | 1 | 1300.92 | 1300.92 | 341.96 | 0.000 | 31.03 |
| Q×Q | 1 | 576.25 | 576.25 | 151.47 | 0.000 | 13.74 |
| 2-Way Interaction | 6 | 578.40 | 96.40 | 25.34 | 0.000 | 13.80 |
| D×P | 1 | 47.06 | 47.06 | 12.37 | 0.001 | 1.12 |
| D×Q | 1 | 294.12 | 294.12 | 77.31 | 0.000 | 7.02 |
| θp×P | 1 | 69.39 | 69.39 | 18.24 | 0.000 | 1.66 |
| θp×Q | 1 | 40.58 | 40.58 | 10.67 | 0.003 | 0.97 |
| θs×Q | 1 | 86.68 | 86.68 | 22.78 | 0.000 | 2.07 |
| P×Q | 1 | 40.58 | 40.58 | 10.67 | 0.003 | 0.97 |
| Error | 29 | 110.33 | 3.80 | | | 2.63 |
| Lack-of-Fit | 24 | 82.63 | 3.44 | 0.62 | 0.804 | 1.97 |
| Pure Error | 5 | 27.69 | 5.54 | | | 0.66 |
| Total | 45 | 4192.54 | | | | 100.00 |

**Model Summary**

S=1.95047 $R^2$=97.37% $R^2$ (adj)= 95.92% $R^2$ (pred)= 93.24%

For cutting temperature, P is the most influential factor with a 34.01% contribution followed by Q×Q and P×P with 10.65% and 9.88 % contribution. For cutting force, θs×θs was the most affecting term with 26.19% followed by P×P and D with 23.6%and 13.41% respectively. For surface roughness, θs×θs was a highly influencing term with a

contribution of 23.52%, followed by θp and P×P with 20.86% and 16.52% contribution. Other terms of the models were considered to be less significant. The lack-of-fit value for all the models is greater than 0.05. So, the proposed predictive models have been fitted with the experimental data very well. Table 2.8 ANOVA for the surface roughness.

**Table 2.8** ANOVA for the surface roughness

| Source | DF | Adj SS | Adj MS | F-Value | P-Value | % Contribution |
|---|---|---|---|---|---|---|
| Model | 13 | 5.51470 | 0.42421 | 31.81 | 0.000 | 92.82 |
| Linear | 5 | 2.35065 | 0.47013 | 35.25 | 0.000 | 39.56 |
| D | 1 | 0.06126 | 0.06126 | 4.59 | 0.040 | 1.03 |
| θp | 1 | 1.37476 | 1.37476 | 103.08 | 0.000 | 23.14 |
| θs | 1 | 0.28623 | 0.28623 | 21.46 | 0.000 | 4.82 |
| P | 1 | 0.12076 | 0.12076 | 9.05 | 0.005 | 2.03 |
| Q | 1 | 0.50766 | 0.50766 | 38.06 | 0.000 | 8.54 |
| Square | 3 | 2.29833 | 0.76611 | 57.440 | 0.000 | 38.68 |
| θs×θs | 1 | 1.55027 | 1.55027 | 116.24 | 0.000 | 26.09 |
| P×P | 1 | 1.08865 | 1.08865 | 81.62 | 0.000 | 18.32 |
| Q×Q | 1 | 0.30927 | 0.30927 | 23.19 | 0.000 | 5.21 |
| 2-Way Interaction | 5 | 0.86573 | 0.17315 | 12.98 | 0.000 | 14.57 |
| D×θp | 1 | 0.31923 | 0.31923 | 23.93 | 0.000 | 5.37 |
| D×P | 1 | 0.08122 | 0.08122 | 6.09 | 0.019 | 1.37 |
| θp×θs | 1 | 0.07563 | 0.07563 | 5.67 | 0.023 | 1.27 |
| θs×P | 1 | 0.16403 | 0.16403 | 12.30 | 0.001 | 2.76 |
| P×Q | 1 | 0.22563 | 0.22563 | 16.92 | 0.000 | 3.80 |
| Error | 32 | 0.42679 | 0.01334 | | | 7.18 |
| Lack-of-Fit | 27 | 0.33899 | 0.01256 | 0.71 | 0.744 | 5.71 |
| Pure Error | 5 | 0.08780 | 0.01756 | | | 1.48 |
| Total | 45 | 5.94150 | | | | 100.00 |

**Model Summary**

S=0.115487 $R^2$=92.82% $R^2$ (adj)= 89.90% $R^2$ (pred)= 85.23%

The $R^2$ value of the final regression model of cutting temperature was 96.98%, which is very close to the $R^2$ (adj) value of 95.62%. Similarly, the $R^2$ and $R^2$ (adj) values of the final regression model of cutting force were 97.37 % and 95.92%, whereas for surface roughness these values were and 92.82% and 89.90% respectively. For all of these responses, $R^2$ and $R^2$ (adj) values were also very close. $R^2$(pred) values for temperature, force and roughness were 91.72%, 93.24% and 85.23% respectively. Based on different $R^2$ values for all the models depicted that these models were highly acceptable and can be used to predict the responses.

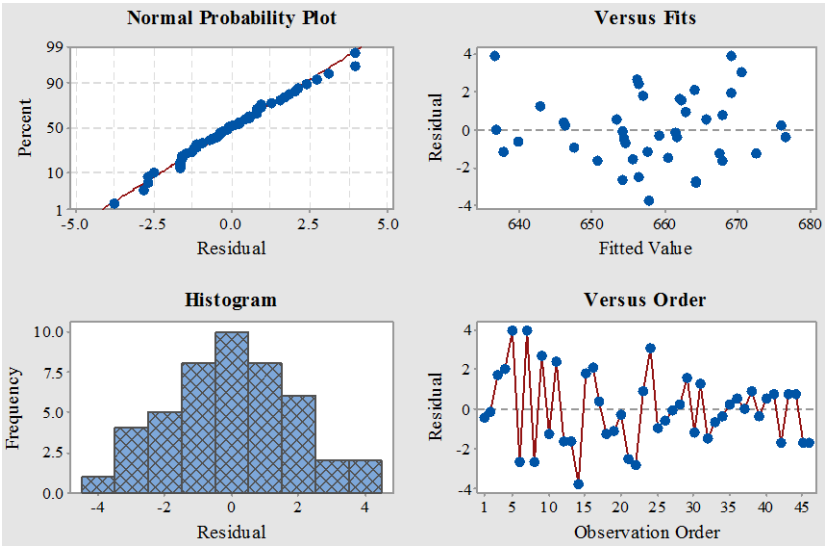


**(a) Cutting temperature**

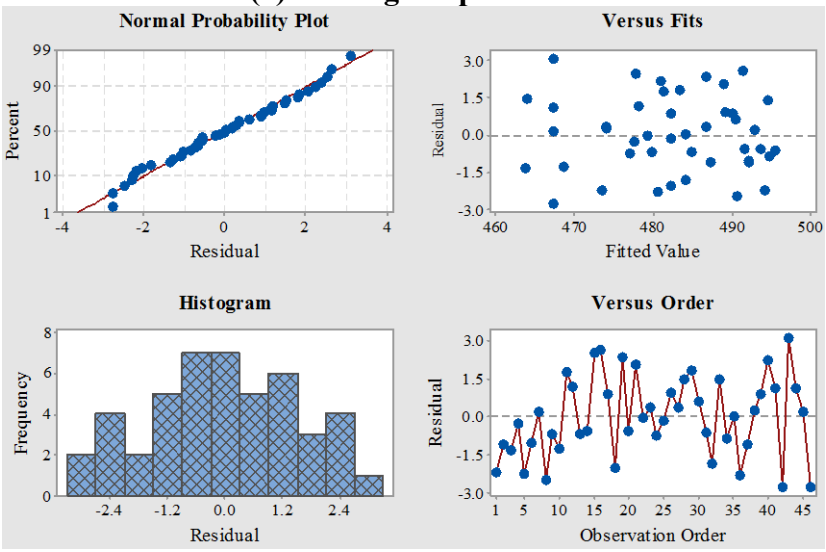


**(b) Cutting force**

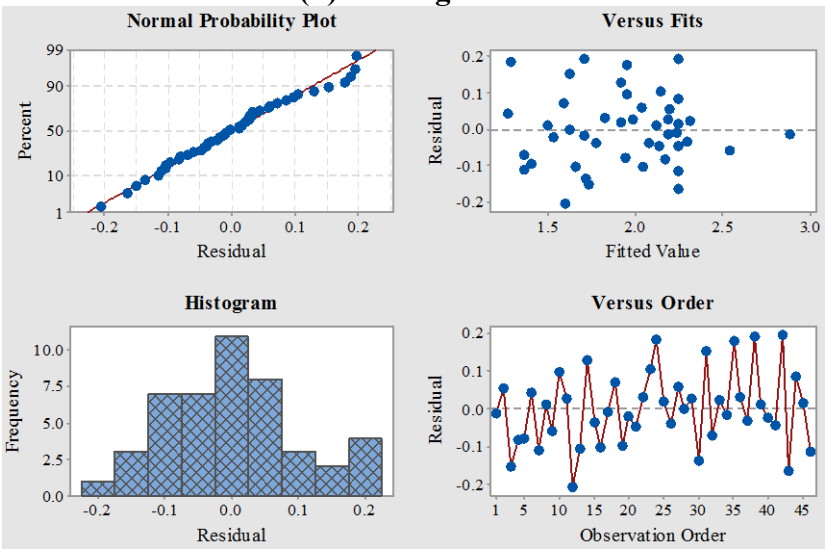


**(c) Surface roughness**

**Fig.2.11** Residual plots for (a) cutting temperature, (b) cutting force and (c) surface roughness.

Residual plots for different responses have been presented in Fig.2.11. Fig.2.11 (a) shows the cutting temperature. In the normal probability plot, most of the points have been fall along the straight line and the histogram depicts a fairly normal distribution of the residuals. No skewness and outlier of the data were observed from the histogram of residuals. These confirm the appropriateness of the proposed model. In the residual versus fitted value plot, the residuals have been allocated fairly evenly and randomly across all the fitted (estimated) values and the residual points appear to be randomly distributed on both sides of the line representing 0 residual value with constant variance. In the residual versus observation order plot, no particular trend or pattern has not been evident. The residuals have fluctuated randomly around the centerline which confirms the non-significance of the experiment order on the residual. It can be concluded that the normality and the randomness of the residual values confirmed by the previously mentioned plots, verified the characteristics of a good model and reliable experimental data [Saha and Mondal, 2016]. Fig.2.11 (b) and (c) have been shown the residual plot for cutting force and surface roughness. From these plots, similar conclusions can be drawn. The MQL parameters for the validity test of the empirical models have been shown in Table 2.9.

**Table 2.9** MQL parameters used for validity test

| Test | **D** | **$\theta_P$** | **$\theta_S$** | **P** | **Q** |
|---|---|---|---|---|---|
| 1 | 0.5 | 10 | 10 | 5.0 | 50 |
| 2 | 0.5 | 10 | 20 | 5.0 | 200 |
| 3 | 0.5 | 15 | 15 | 12.5 | 125 |
| 4 | 0.5 | 20 | 10 | 20.0 | 50 |
| 5 | 0.5 | 20 | 20 | 20.0 | 200 |
| 6 | 1.0 | 10 | 10 | 5.0 | 50 |
| 7 | 1.0 | 10 | 20 | 5.0 | 200 |
| 8 | 1.0 | 20 | 10 | 20.0 | 50 |
| 9 | 1.0 | 20 | 20 | 20.0 | 200 |
| 10 | 1.5 | 10 | 10 | 5.0 | 50 |
| 11 | 1.5 | 10 | 20 | 5.0 | 200 |
| 12 | 1.5 | 15 | 15 | 12.5 | 125 |
| 13 | 1.5 | 20 | 10 | 20.0 | 50 |
| 14 | 1.5 | 20 | 20 | 20.0 | 200 |
| 15 | 1.5 | 20 | 10 | 20.0 | 200 |

In Fig.2.12, the experimental responses have been compared with the fitted responses obtained from the predictive models. The results obtained from the models seem to be very close to the experimental results. The Mean Absolute Percentage of Error (MAPE) for the responses has been calculated as 3.93%, 1.27% and 5.78% respectively. Based on the percentage error it can be concluded that the temperature and force model has

been predicted the responses more accurately than the roughness model but all the models are acceptable for correlating the responses with the MQL parameters with a reasonable error.

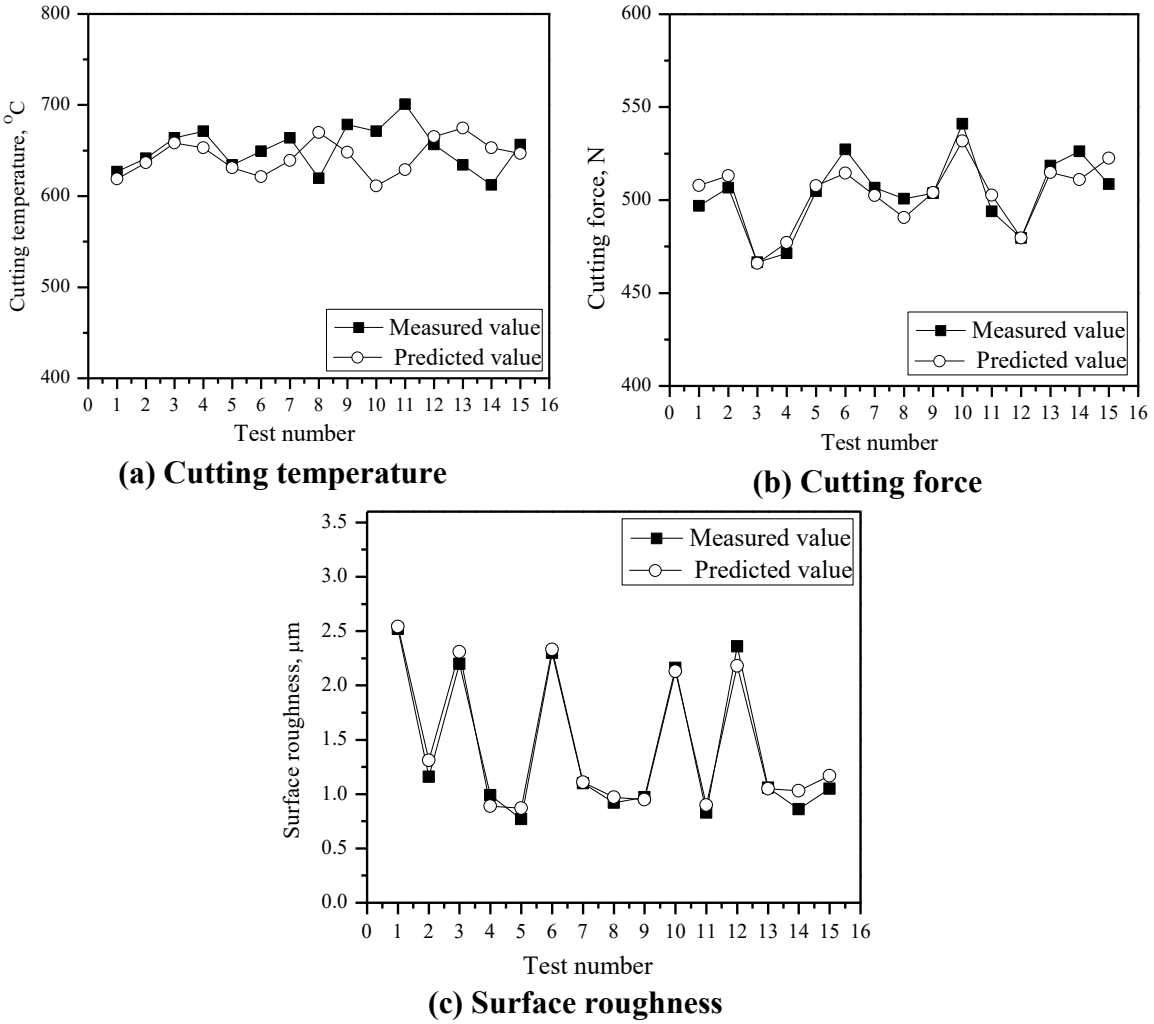


**Fig.2.12** Comparison of measured and predicted (a) cutting temperature (b) cutting force and (c) surface roughness.

The effects of MQL parameters on different process responses have been analyzed by using main and interaction effect plots. Different MQL parameters have different effects on the machining responses. Two types of parameters affected the MQL performance such as nozzle-related parameters like diameter, impingement angle, standoff distance, etc. and the other is spray-related parameters, such as air pressure, oil flow rate, etc. After analyzing their effect on the machinability, optimum parameter settings needed to be determined. Nozzle diameter and angle are important for accurate impingement of the MQL oil mist. Whereas, air pressure and oil flow rate affect the mist particle size, distribution and velocity. The cooling and lubrication capacity of the MQL jet is strongly

influenced by the mist droplet size, distribution and velocity [Duchosal et al., 2013] as well as the impingement direction of the mist jet. So, all the MQL parameters and also their interactions have a significant effect on the cooling and lubrication performance of the MQL.

Heat in the cutting zone negatively affects the tool life and machined surface. For achieving an economic and efficient MQL based machining process, the cooling and lubrication performance of an MQL system has to be understood [Sharma et al., 2009]. Different MQL parameters have a different effect on cutting temperature. The main effect and interaction plot for temperature regarding various process inputs have been shown in Fig.2.13.

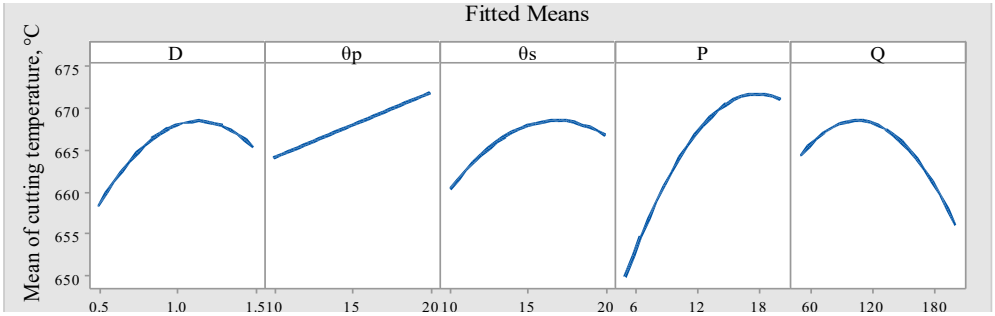


**(a) Main effect plot**

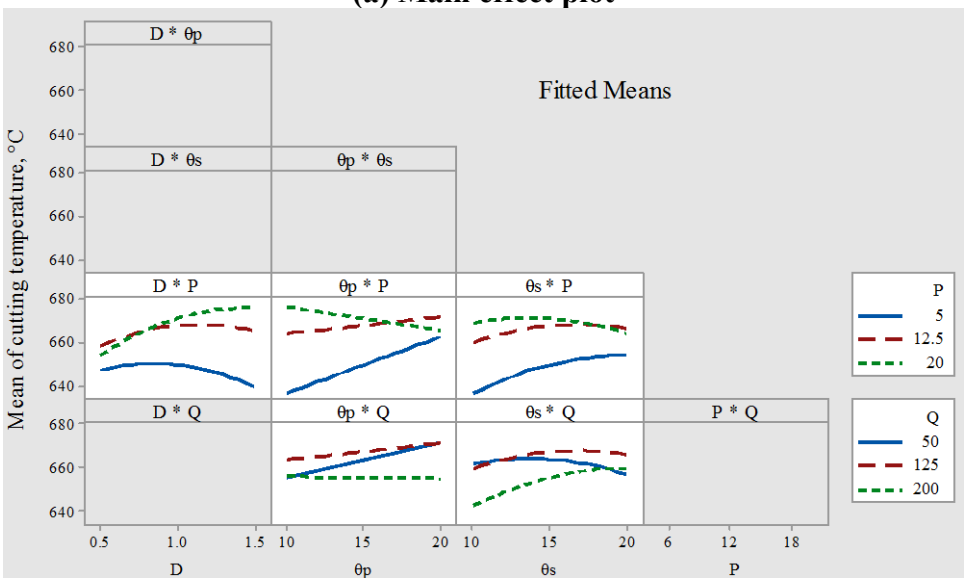


**(b) Interaction plot**

**Fig.2.13** (a) Main effect and (b) interaction plot for cutting temperature

From the main effect plot, it can be seen that for low diameter nozzle penetration of the oil mist is effective and for this reason with a diameter of 0.5 mm cutting temperature is minimum and temperature increased with the diameter due to improper penetration. But for a nozzle diameter of 1.5 mm temperature slightly decreased, because bulk cooling may

happen in this situation. Temperature increases with the increase of primary nozzle angle, so it can be concluded that a 10° angle of the nozzle impinges the oil mist towards the chip-tool interface precisely. A secondary nozzle with a 20° angular outlet provides accurate mist flow towards the work-tool interface. With the increase of air inlet pressure, spray angle is increased, mist droplet diameter is decreased [Huang et al., 2018], the number of droplets and droplet velocity is increased [Park et al., 2010; Rohit et al., 2018], which helps the droplet to penetrate the interfaces. But, greater than certain air pressure, smaller mist particles may spring back from the tool and work surface due to the conservation of momentum effects and could not penetrate the interfaces [Liu et al., 2011], which may increase the tool wear and consequently increased the cutting temperature. But at the highest air pressure (20 bar) broken chips were created and also removed BUE from the cutting edge. This may lead a portion of oil mist particles to enter into the chip-tool interface and so, temperature increment was slightly slowed down. With the increase of flow rate droplet diameter was decreased and velocity was increased [Lin and Ho, 2003]. Due to the spring back effect of the oil droplet, they could not enter into the interface and eventually the generated heat could dissipate and also frictional heat was produced for lower lubrication. Ultimately, tool wear and the cutting temperature were increased. But when the flow rate was largely increased then the temperature was reduced due to bulk cooling action. There are some significant interaction effects of the input factors for the cutting temperature. Such as the interaction effect of D×P implies that for low pressure 1.5 mm nozzle produces less cutting temperature but for high pressure 0.5 mm nozzle produces less temperature. Due to these interaction effects, the selection of one parameter depends on other parameters. In that case, for the selection of optimum levels of the inputs, interaction effects have to be considered in conjunction with the main effects.

The cutting force depends on various MQL parameters and also cutting temperature. Sometimes higher cutting temperatures ease the machining process and due to this reason, cutting force reduces. The main effect and interaction plot for force regarding various process inputs have been shown in Fig.2.14.

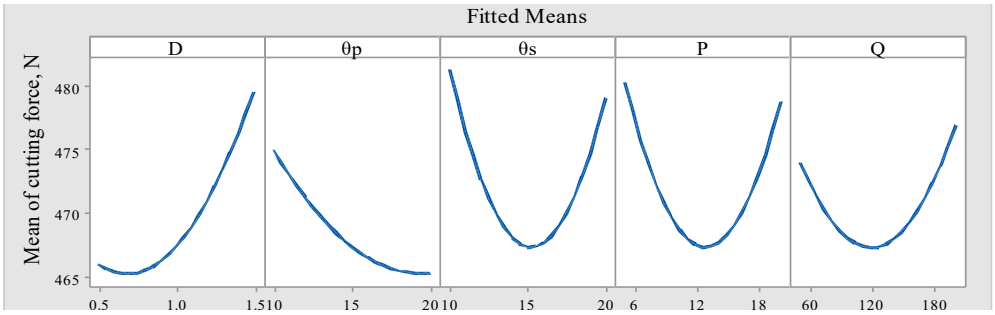


**(a) Main effect plot**

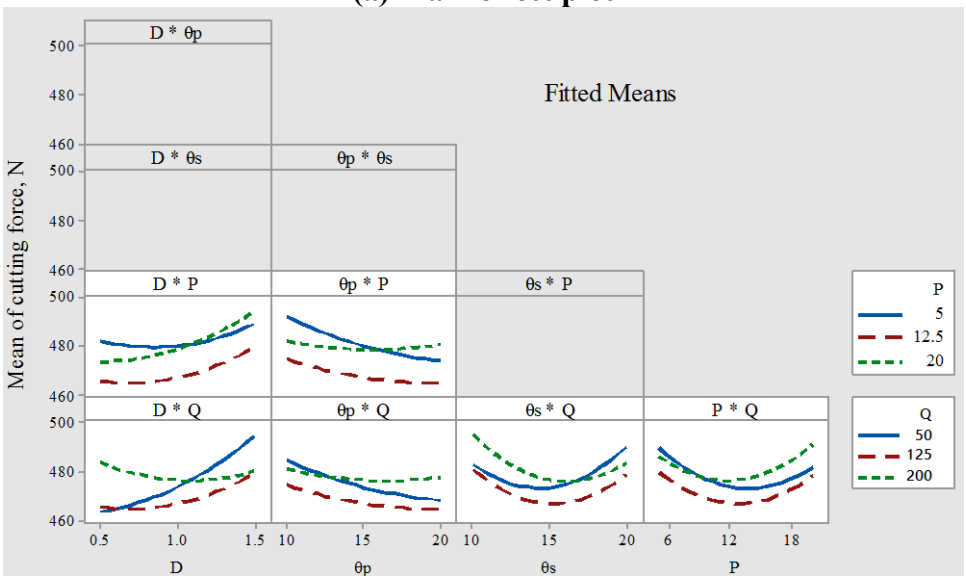


**(b) Interaction plot**

**Fig.2.14** (a) Main effect and (b) interaction plot for cutting force

From the main effect plot, it can be seen that for low diameter nozzle penetration of the oil mist is effective and for this reason with a diameter of 0.5 mm cutting force was minimum and cutting force was increased with the increase of nozzle diameter due to improper penetration. Although the nozzle diameter of 1.5 mm cutting temperature was reduced slightly due to bulk cooling but cutting force was not reduced due to lack of proper cooling and lubrication at the interfaces. Cutting force was minimum for a primary nozzle angle of 20° and a secondary nozzle angle of 15°. With the increase of air pressure, cutting force reduces may be due to temperature enhancement. But at high pressure, a discontinuous chip was formed, which may increase vibration and cutting force. As a result, the cutting force was increased for the highest air pressure. The oil flow rate showed a similar effect as air pressure. Here also, at the first stage cutting force was reduced with the increase of oil flow rate. But when the oil flow rate was increased extremely, bulk cooling was happened and cutting force was increased due to lack of effective cooling at the interface. There are some significant interaction effects of the input factors for the cutting force. Such as the interaction effect of D×P implies that for low pressure 1 mm

nozzle produces less cutting force but for high pressure 0.5 mm nozzle produces less force. Due to these interaction effects, the selection of one parameter depends on other parameters. In that case, for the selection of optimum levels of the inputs, interaction effects have to be considered in conjunction with the main effects.

Surface roughness depends on various MQL parameters and also cutting temperature and force. The surface finish was highly improved for the use of a secondary nozzle towards the work-tool interface. The main effect and interaction plot for roughness regarding various process inputs have been shown in Fig.2.15. From the main effect plot, it can be seen that for large diameter nozzle provide better surface roughness. Because for larger diameter nozzle mist droplet diameter was larger. Larger droplets wetted and protect the machined surface perfectly and improve the surface quality. Surface roughness was minimum for a primary nozzle angle of 20°, due to less cutting force was provided at this condition. A secondary nozzle angle of 20° was provided minimum roughness.

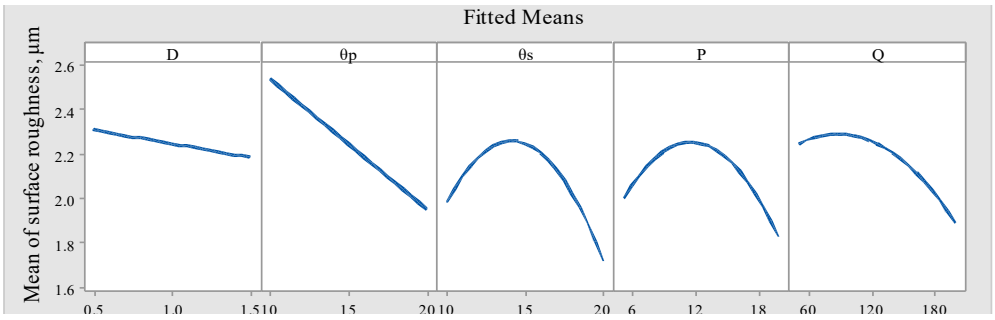


**(a) Main effect plot**

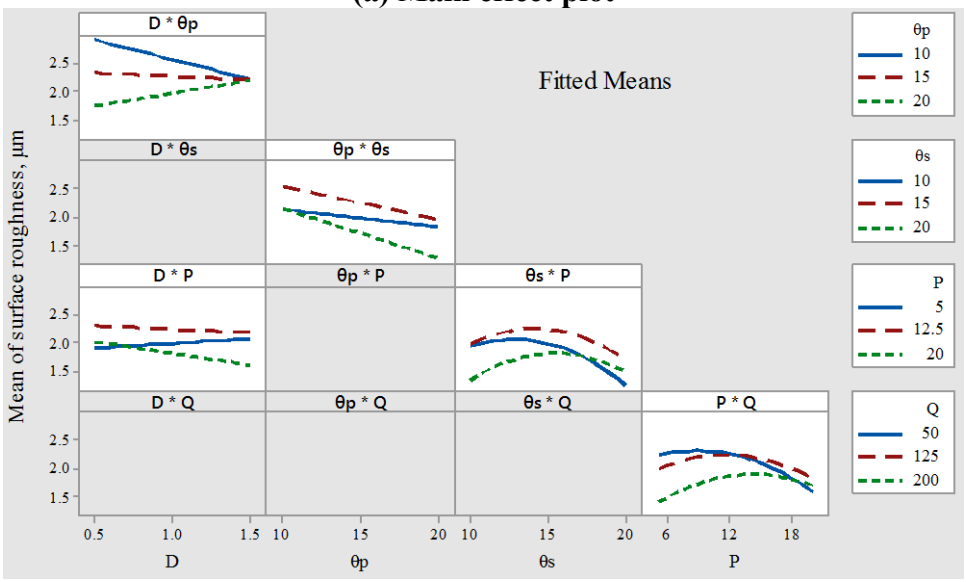


**(b) Interaction plot**

**Fig.2.15** (a) Main effect and (b) interaction plot for surface roughness

A secondary jet aimed at this direction covers up most of the machined surface and improves the surface finish. With the increase of air pressure, surface roughness increases due to improper penetration of coolant. Because higher pressure produced smaller droplets that may not effectively penetrate at the interfaces. But at the highest pressure discontinuous chips were formed and cutting force was increased but roughness was decreased. Usually, when continuous chips were formed, machined surface quality is better. But if BUE is formed with continuous chips, then surface quality may deteriorate due to the scratching effect of the BUE on the work material during machining. Additionally, continuous chips may be entangled in the machining region, which may rub against the machined surface and worsen the surface finish. So, during MQL assisted machining, when high air pressure was applied, it may remove the BUE and the surface finish was getting better. Additionally, discontinuous chips were formed due to an increase in chip curling. Discontinuous chips were easily removed from the machining zone and the machined surface was saved from the rubbing marks of the entangled chips, which ultimately improve the surface quality. With the increase of oil flow rate surface roughness was slightly increased or remain similar due to ineffective cooling and lubrication. But when the flow rate was extremely high, it may wet the machined surface and saved the machined surface to deteriorate. So, the excessive oil flow rate was reduced the surface roughness greatly. There are some significant interaction effects of the input factors for the surface roughness. For example, the first interaction effect D×θp implies that, For the primary angle of 10°, a 1.5 mm nozzle is better than a 0.5 mm nozzle, whereas for a 20° angle, a 0.5 mm nozzle is better than a 1.5 mm nozzle. For the 15° nozzle angle, the diameter change did not affect the roughness. Due to these interaction effects, the selection of one parameter depends on other parameters. In that case, for the selection of optimum levels of the inputs, interaction effects have to be considered in conjunction with the main effects.

The machinability of Ti-6Al-4V alloy will be enhanced when the output responses like cutting temperature, force and surface roughness will be minimized. The composite desirability approach has been employed for optimization in this research, which is a widely used optimization method when multiple responses are involved [Manjaiah et al., 2019]. Using the 'Response Optimizer' of MINITAB 17, a combination of optimum coolant parameter settings has been identified for the minimum value of all the responses simultaneously based on their fitted empirical models. The weight and importance value

for all the responses have been assigned as 1. The Optimization plots for selecting the optimum cooling parameter settings for minimum cutting temperature, force and roughness simultaneously have been shown in Fig.2.16.

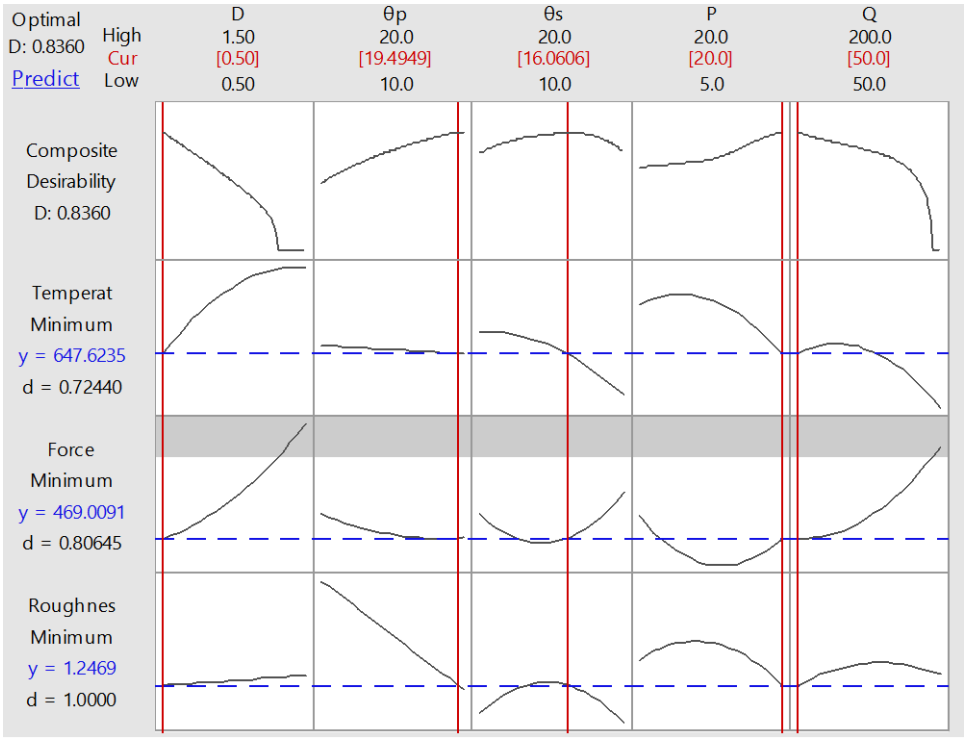


(a)

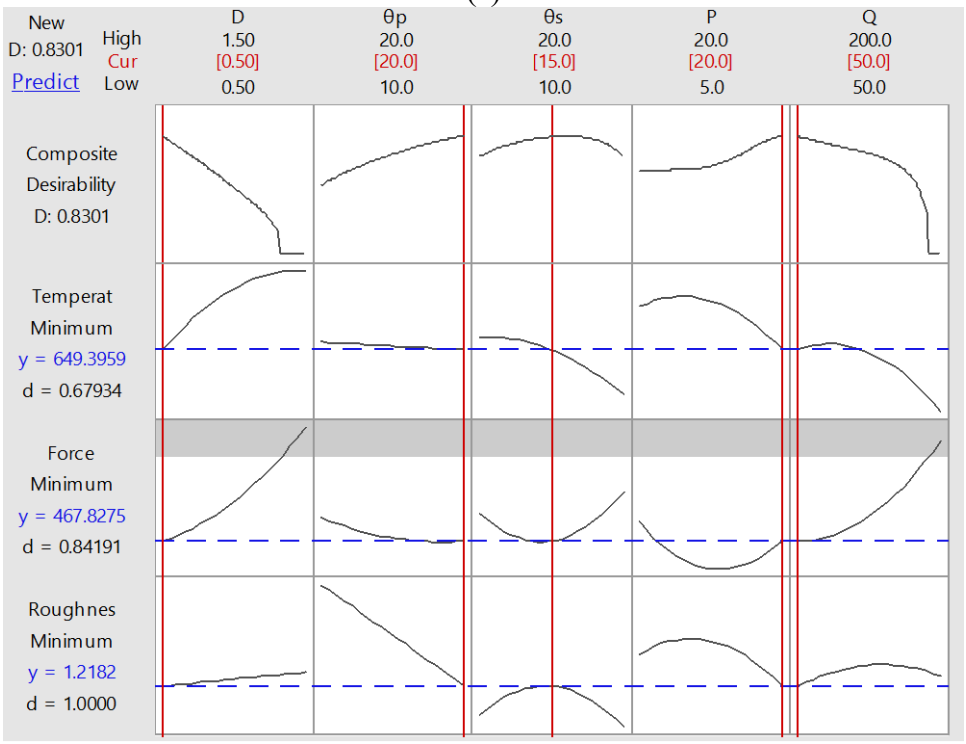


(b)

**Fig.2.16** Optimization plot to minimize temperature, force and roughness (a) preliminary output and (b) final feasible output.

Nozzle diameter of 0.5 mm, primary nozzle angle of 19.49°, secondary nozzle angle of 16.06°, 20 bar air pressure and 50 ml/hr oil flow rate have been selected as optimum when considering all the responses simultaneously. Composite desirability was 0.836, which means the optimum input parameter settings can achieve favorable results for all the responses concurrently. Individual desirability for minimizing temperature was 0.7244, for minimizing force was 0.80645 and for minimizing roughness was 1. The values of individual desirability indicate that the optimum parameter settings were more effective for reducing the surface roughness, followed by force and temperature. For the final selection of the nozzle angles nearest angles such as 20° and 15° have been selected. In that case, two individuals and the final composite desirability was slightly decreased but was at a highly acceptable level. The final composite desirability achieved was 0.8301, which is an acceptable value confirmed previously [Sachin et al., 2019]. The optimum MQL parameters determined in this section have been used throughout the further experiment.

## 2.4 Preparation and Characterization of Nano-fluid

Nano-fluids are engineered colloidal suspensions of tiny nanometer-sized (anyone principal dimension < 100nm) solid additives called nano-particles in the base fluids, like water, mineral oil, vegetable oil, ethylene glycol, or their proportionate mixture [Taylor et al., 2013]. Different carbon-based, ceramic, metallic, semiconductor type, polymeric and lipid-based nanoparticles and a mixture of two nanoparticles can be used for fabricating nano-fluids. Nano-fluids are considered as 'smart fluid' due to their augmented thermo-physical properties and heat transfer characteristics, which can be controlled by controlling the nanoparticle concentration in the base fluid [B. Li et al., 2017]. Nanofluids were first proposed by Choi and Eastman [1995] and have become very popular at present. Thermal performance, such as thermal conductivity and the convection heat transfer coefficient of the nanofluid can be largely improved compared to simple base fluids [Yu et al., 2008]. Improved load-carrying capacity, anti-wear and friction reduction properties of the lubricating oils with nanoparticle additives have been revealed by various tribology researches [Jatti and Singh, 2015; Yu and Xie, 2012]. For the aforementioned properties, nano-fluids have become very popular in some cooling and/or lubricating application in a wide variety of applications including manufacturing, transportation, energy, and electronics, etc. The performance of nanofluids can be further improved by dispersing two

different types of nanoparticles in the base fluid, which is called hybrid nano-fluid. Due to synergistic effect of different nano particles, hybrid nano-fluid comprises better thermal characteristics compared to conventional nano-fluid. A trade-off between advantages and disadvantages of the single nano-fluids was happened when hybrid nano-fluid is prepared [Minea and Moldoveanu, 2018]. Although nanoparticles are very small in size, they have a high surface area to volume ratio. Due to their large surface area, their heat-dissipating capacity increases to a great extent.

There are several techniques for the fabrication of nano-fluids, such as a single-step method and a two-step method [Yu and Xie, 2012]. In the single-step method production of nanoparticles and their dispersion into a base-fluid to make nano-fluid is done in a single step by the direct evaporation process. Here, under vacuum condition source material is vaporized followed by a vapor that is condensed via contact between the vapor and a flowing liquid [Choi and Eastman, 2001]. By maintaining the continuous liquid flow nanoparticle agglomeration can be minimized and good dispersion can be assured. However, this method is very expensive and the volume is also limited due to the limited space in the vacuum chamber. Recently, the two-step physical process is the most commonly used technique of nano-fluid preparation. In this process, nanoparticles are synthesized first in the form of dry powder. Nowadays, various nanoparticles are commercially available and can be used for making nano-fluid. The inert gas condensation technique has already been established to commercially produce huge quantities of nano-powders [Suryanarayana and Prabhu, 2006]. In the second processing step, the manufactured or purchased nano-particles are dispersed into an appropriate base fluid such as water, ethylene glycol and engine oil, etc. For mixing magnetic stirring can be used. Due to enhance the stability of the nano-fluid addition of surfactant or ultra-sonication method can be used. This method is more economical than the one-step method due to the comparatively low price of available nanoparticles. However, the nanofluid prepared by this method usually has a stability problem. All the nanofluids slowly settle down after a period based on the nano-particle type, base fluid, surfactant used, ultrasonication/ magnetic stirring time. The useful time of the nanofluid is before sedimentation.

In this research, Hybrid $Al_2O_3$-MWCNT based nanofluid has been used as MQL fluid. MWCNT has higher thermal conductivity (3000W/m K) which enhance the thermal conductivity significantly and provide best heat transfer performance. On the other hand, $Al_2O_3$ based nano-fluid has the higher anti friction property compared to other common

nano-particles and provide better surface quality. So, $Al_2O_3$-MWCNT based nanofluid has higher heat transfer and lubrication property. As mentioned earlier, the two-step physical process is the easiest one and also the least expensive. So, it has been used to synthesize hybrid $Al_2O_3$-MWCNT based nanofluid. The stability of a single MWCNT based nano-fluid can be increased by the addition of an oxide nano-particle with it [Yang et al. 2020]. So, the stability of $Al_2O_3$-MWCNT hybrid nano-fluid should be more than a single MWCNT based nano-fluid. The MWCNT was purchased from Tanfeng Tech. Inc. China, which has a mean diameter of 10-20 nm and a length of 5-15 μm. MWCNT has a density of 2.1 gm/cm$^3$. The $Al_2O_3$ nanoparticle powder has been purchased from Sigma-Aldrich Chemicals Pvt. Ltd, INDIA, which has a mean diameter of <50 nm and has a density of 3.9 gm/cm$^3$. Hybrid nano-fluid with a concentration of 0.5%, 1% and 1.5% were prepared by dispersing 80% $Al_2O_3$ and 20% MWCNT into the base fluid. Generally, more $Al_2O_3$ volume proportions provide better absorbance of hybrid nano-particles into a base fluid [Asadi et al., 2018]. The weight of nanoparticles required was calculated by using Eq. 2.13:

$$\%\ \text{volume concentration} = \frac{V_{Al2O3}+V_{CNT}}{V_{Al2O3}+V_{CNT}+V_{VG\,68}} = \frac{\left(\frac{m}{\rho}\right)_{Al2O3}+\left(\frac{m}{\rho}\right)_{CNT}}{\left(\frac{m}{\rho}\right)_{Al2O3}+\left(\frac{m}{\rho}\right)_{CNT}+V_{VG\,68}} \quad \textbf{.....(2.13)}$$

where ρ is the density in gm/cm$^3$and m is the mass in gm. The masses of $Al_2O_3$ and MWCNT nanoparticles used for preparing a volume of 100 ml nanofluid were determined and presented in Table 2.10.

**Table 2.10** Masses of nano-particles used for preparing 100 ml of nanofluids

| Nano-particle concentration, % | Mass (gm) | |
|---|---|---|
| | MWCNT (20%) | $Al_2O_3$ (80%) |
| 0.5 | 0.21 | 1.57 |
| 1 | 0.42 | 3.15 |
| 1.5 | 0.64 | 4.75 |

For the preparation of specific concentration nanofluid, the required amount of commercially available $Al_2O_3$ and MWCNT nanoparticles have been dispersed into the VG 68 cutting oil. Then 2 hours of ‗Magnetic stirring' with the rotational speed of 700 rpm were used to mixing the nanoparticle with the oil followed by 1hr of 'Ultrasonic agitation' with the frequency of 20 kHz for preventing the agglomeration of the fluid. Both of these above-mentioned methods were used by several researchers due to preparing stable nanofluids [Krishna and Rao, 2016]. The duration of these processes is an important

factor, on which the thermal properties of nanofluid depends [Leong et al., 2016]. The Nano-fluid preparation procedure is shown in Fig.2.17.

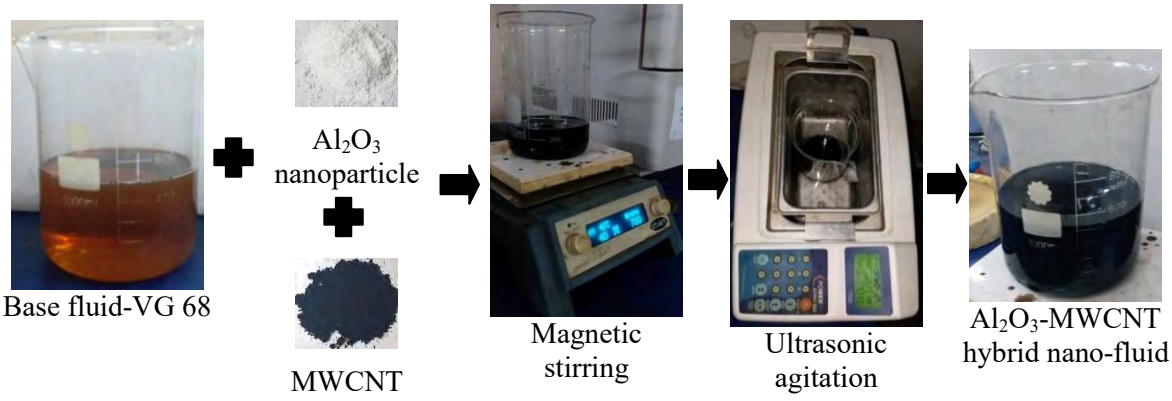


**Fig.2.17** Nano-fluid preparation procedure

No surfactant was used in this experiment because for oil-type base fluid it is not essential for stable dispersion. Moreover, the surfactant can create fumes when applying the nano-fluid at the high-temperature zone and also affect the thermal properties of the nano-fluid. MWCNT nanofluid sample was kept for observation and no visible settlement of particle was not observed even after 3 hours. The hybrid nano-fluid prepared are assumed to be isentropic, Newtonian in behavior and their thermo-physical properties are uniform and constant with time all through the fluid sample.

Thermal conductivity is a very significant property of nanofluid, used as a coolant. Different parameters affect the thermal conductivity of nanofluids, such as the type of particle and the base fluid [Wang et al., 1999], the morphology and concentration of particle [Mirmohammadi et al., 2019], temperature [Das et al., 2003], additives used or not [Eastman et al., 2001] clustering of the particle [Zhu et al., 2006], the acidity of nanofluid [Xie et al., 2002] and so on. Morphology of the particle means shape, size, texture, etc. Due to the enhancement of thermal conductivity of nano-fluid compared to a base fluid, nanofluid is attracted by the sectors where the cooling action is very necessary. It is expected that any solid particle usually enhances the thermal conductivity of the fluid. Because solid particle has greater thermal conductivity compared to liquid.

There are several methods used for measuring the thermal conductivity of nanofluids, such as transient hot-wire techniques, the steady-state parallel-plate method, cylindrical cell method, temperature oscillation technique, etc [Paul et al., 2010]. The cylindrical cell method is one of the most common steady-state methods used for

measuring the thermal conductivity of fluids. In this technique, two coaxial cylinders are used, where a heater is placed inside the inner cylinder and the outer cylinder is cooled by water. The fluid is kept in between the cylinders. Using Fourier‘s law with the temperature of the coaxial cylinders, the thermal conductivity of the liquid samples in the gap could be calculated. Plug and jacket type apparatus is based on the concept of cylindrical cell method, which was previously used for measuring the thermal conductivity of the nanofluids [Vajjha and Das, 2009]. In this research, plug and jacket type bench-top apparatus (H471) supplied by P.A. Hilton Ltd has been used, which is completed with a console for the control and display of temperature and heat input. Here, the inner cylinder is called a plug and the outer cylinder is called a jacket. In between the heated plug and a water cooling jacket, there is a small radial clearance (0.3mm). This small clearance is filled by the fluid, whose thermal conductivity is needed to be examined. The clearance is very small, so no natural convection has happened to the working fluid. The fluid is there as a form of a lamina of face area $\pi d_m L$ ($0.133 m^2$) and thickness of $\Delta r$ (0.3mm) and transfers heat from the plug to the jacket.

For minimizing thermal inertia and temperature variation the plug is manufactured from aluminum anodized (mean diameter 39 mm, effective length 110 mm). A cylindrical heating element of resistance 55 Ω (may vary for different apparatus) is used to heat the plug. For measuring the temperature, a thermocouple is inserted into the plug close to the external surface. The plug has an inlet and an outlet for the test fluid and the fluid is injected by a syringe. By using two 'O' rings the plug is held centrally in the water jacket. For the cleaning purpose 'O' rings can be easily removed. The cylindrical jacket is manufactured from nickel-plated brass which has a water inlet and an outlet. The jacket is cooled by a continuous supply of water at a rate of 3 liters/min. A K-type thermocouple is attached to the inner sleeve of the jacket. The thermocouples have measured the temperature of the hot and cold faces of the test fluid lamina. A small console (aluminum and plastic coated) is connected to the plug/jacket assembly and controls the voltage supplied to the heating element. To determine the power input an analog voltmeter (0-60V) is used and a digital temperature indicator with a selector switch displays the temperature of the plug and jacket with $0.1^{o}$ C resolution. Calibration of the equipment by a fluid with known thermal conductivity is necessary before evaluating the sample.

For thermal conductivity measurement of hybrid $Al_2O_3$-MWCNT nano-fluids, the plug and jacket assembly unit was dismantled, cleaned and reassembled. The nanofluid

was then injected into the radial space of the apparatus. Sufficient liquid must be passed through the clearance space such that there is no air pocket. Water was passed through the jacket and the heater adjusted to give a temperature difference and heat transfer rate. when stable the voltage and the plug and jacket temperatures were observed. The incidental heat transfer at the given temperature difference is deducted from the total heat input and considering that the rest was passing through the fluid lamina.

Here,

$t_1$ = Plug temperature

$t_2$ = Jacket temperature

$\Delta t$ =Temperature difference

V= Voltage applied to the heater

R= Heater resistance

$\Delta r$ = Radial clearance

A ($\pi d_m L$) = Heat transfer area

Electrical heat input, $Q_e = \frac{V^2}{R}$ **……..…….....……..….....(2.14)**

Incidental heat transfer at $\Delta t$ (from the graph) = $Q_i$

Heat conduction through oil, $Q_c = Q_e - Q_i$ **…….....……..……..…..….....(2.15)**

Thermal conductivity of oil, $K = \frac{Q_c \Delta r}{A \Delta t}$ **……..…….....……..….....(2.16)**

The thermal conductivities of different nanofluid samples calculated are shown in Fig.2.18.

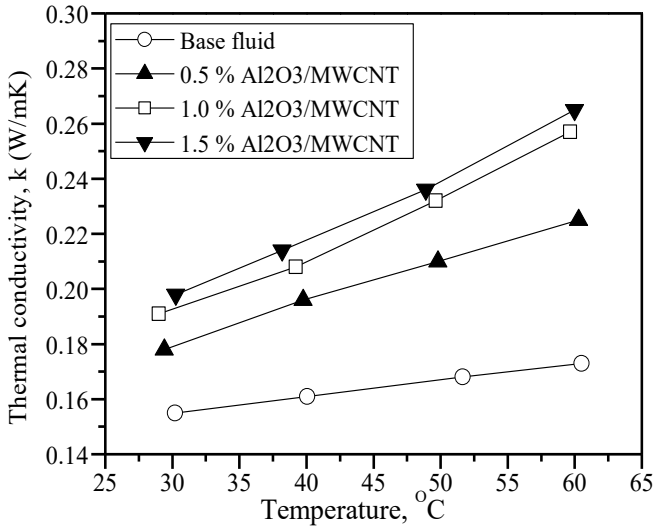


**Fig.2.18** Thermal conductivity of the base fluid and nano-fluids

Dynamic viscosity is a physical property of a fluid that indicates its resistance to flow or shear and a measure of fluid's adhesive/cohesive or frictional properties. It is a very important property of fluid when analyzing liquid behavior and fluid motion near solid boundaries. Nanofluid viscosity was not investigated thoroughly as the other thermal properties, but it is one of the most critical parameters of nanofluids. For the cooling application of nanofluid, thermal conductivity increment is necessary. On the other hand, less increment or constant viscosity is more acceptable, which indicates a higher ratio of thermal conductivity and viscosity. Some crucial factors like temperature, nanoparticle volume fraction, particle size, morphology, dispersion method, etc. influence the viscosity of nanofluids [Mahbubul et al., 2012; Mishra et al., 2014].

There are several techniques for evaluating the viscosity of nano-fluids, such as rotational viscometer [Pastoriza-Gallego et al., 2011], vibration viscometer [Lee et al., 2011], falling ball viscometer [Feng and Johnson, 2012], efflux cup viscometers [Kumar et al., 2018; Seyedzavvar et al., 2019], etc. In this research efflux cup type say-bolt universal viscometer (Koehler- SV3000), has been utilized for the measurement of viscosity of all the samples. In this viscometer, the temperature of the liquid holding vessel and the orifice is controlled by submerging them in a thermostatically controlled oil bath. Test liquid is placed in the vessel and the temperature is set. The temperature can be set between 21 to 99°C. When the temperature reaches the specific value, the orifice is opened. The viscosity is the efflux time in seconds, required by the fluid to pass from a vessel through an orifice under precisely controlled conditions to fill a 60 cc container. Time is counted by using a stopwatch. The universal orifice has dimensions of 0.176 cm in diameter and 1.225 cm in length. The efflux time required by using a universal orifice is called Say bolt universal seconds (SUS), and it is a measure of viscosity.

Say bolt universal seconds (t) can be converted to kinematic viscosity (v) by using Eq. 2.17 and Eq. 2.18:
When,

$$When\ t < 100\ secs, v = 0.22 \times t - \frac{195}{t} centistokes \quad \textbf{.....(2.17)}$$

$$When\ t > 100\ secs, v = 0.22 \times t - \frac{180}{t} centistokes \quad \textbf{.....(2.18)}$$

For all the samples kinematic viscosity decreased with the increase of temperature. Also with the increase of nanoparticle concentration from 0.5 to 1.5 vol % viscosity has been increased. Kinematic viscosity of the base fluid and nano-fluids has been presented in Fig.2.19.

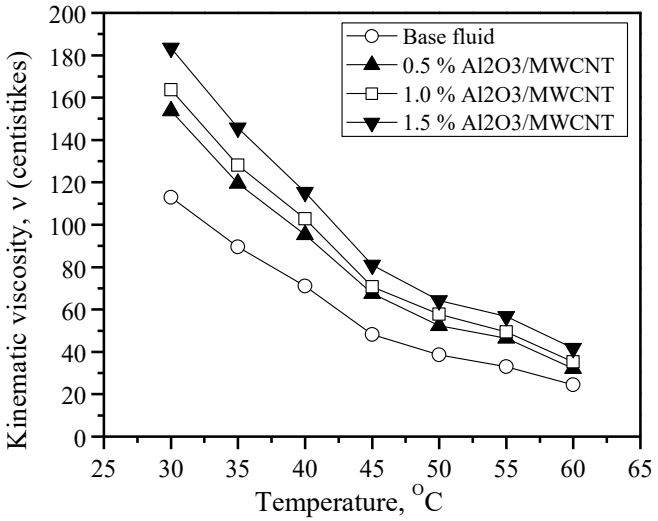


**Fig.2.19** Kinematic viscosity of the base fluid and nano-fluids

## 2.5 Experimental results

A systematic investigation has been carried out due to study the performance of a double jet MQL using hybrid nano-fluid on machinability of turning titanium (Ti-6Al-4V) alloy by different carbide inserts (coated and uncoated) compared to dry machining, single jet MQL, double jet MQL regarding chips morphology, cutting temperature, cutting force, tool wear, tool life, surface roughness and dimensional accuracy. Machining conditions for this analysis have been presented in Table 2.2.

### 2.5.1 Chip morphology

For assessing the performance of a machining operation chip morphology can be studied. Chips were collected for turning Ti-6Al-4V alloy by uncoated and coated carbide inserts under various cooling conditions for analyzing their color, shape and serration characteristics. The color and shapes of the chips produced in different environments have been shown in Table 2.11.

Table 2.11 Shape and color of chips produced during turning Ti-6Al-4V

| Runs | Cutting tool | Environment | Cutting fluid | Chip color | Chip shape |
|---|---|---|---|---|---|
| 1 | Uncoated | Dry | - | Golden | Ribbon |
| 2 | Uncoated | SJMQL | Cutting oil | Metallic | Helical& ribbon |
| 3 | Uncoated | DJMQL | Cutting oil | Metallic | Helical |
| 4 | Uncoated | DJMQL | Hybrid nano-fluid | Metallic | Short helical |
| 5 | Coated | Dry | - | Golden | Ribbon |
| 6 | Coated | SJMQL | Cutting oil | Metallic | Helical & ribbon |
| 7 | Coated | DJMQL | Cutting oil | Metallic | Helical |
| 8 | Coated | DJMQL | Hybrid nano-fluid | Metallic | Short helical |

The SEM of the chips has been done to study the serration characteristics which have been shown in Fig.2.20 and Fig.2.21.

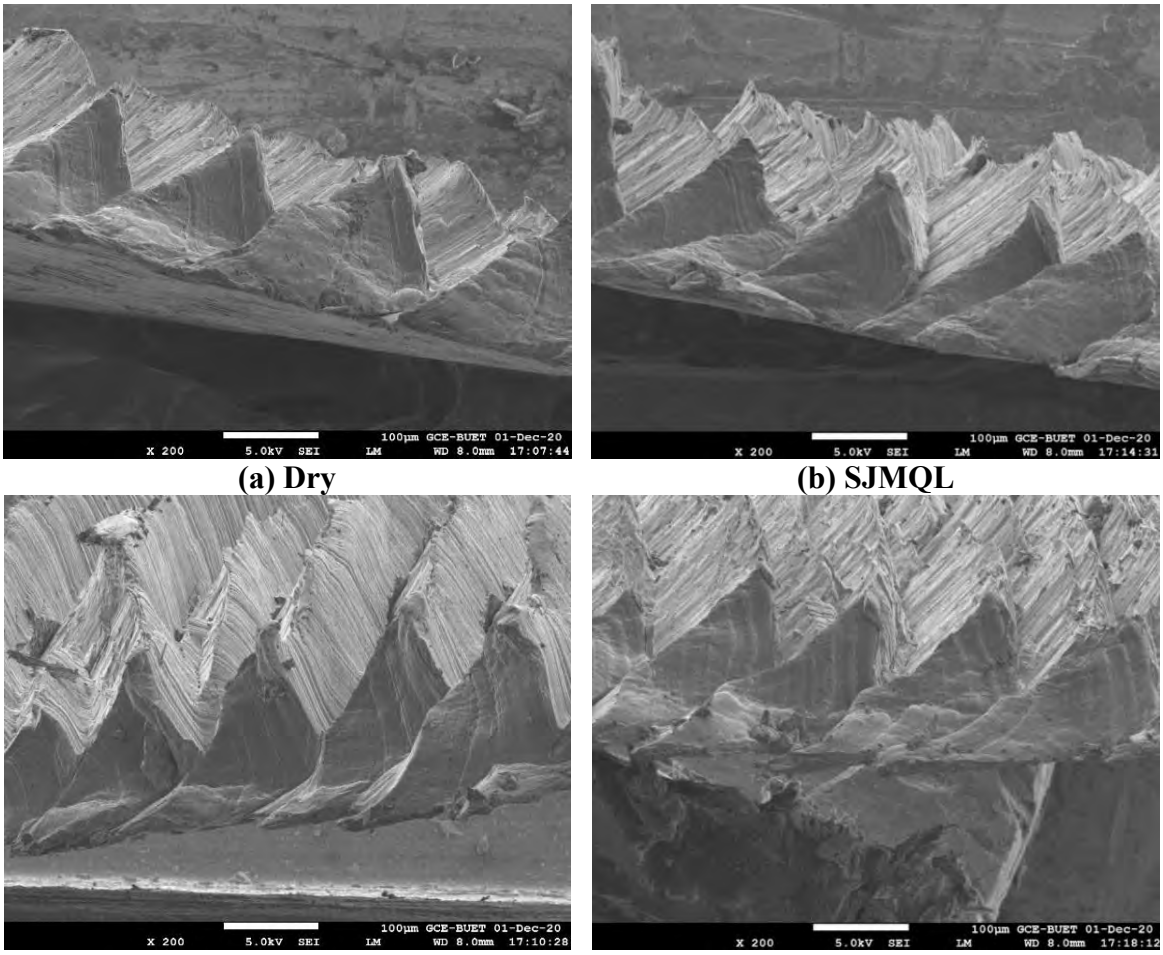


**(a) Dry** **(b) SJMQL**

**(c) DJMQL** **(d) DJMQL with HNF**

**Fig.2.20** SEM of chips produced in turning Ti-6Al-4V alloy by uncoated carbide insert under (a) Dry, (b) SJMQL, (c) DJMQL and (d) DJMQL with HNF

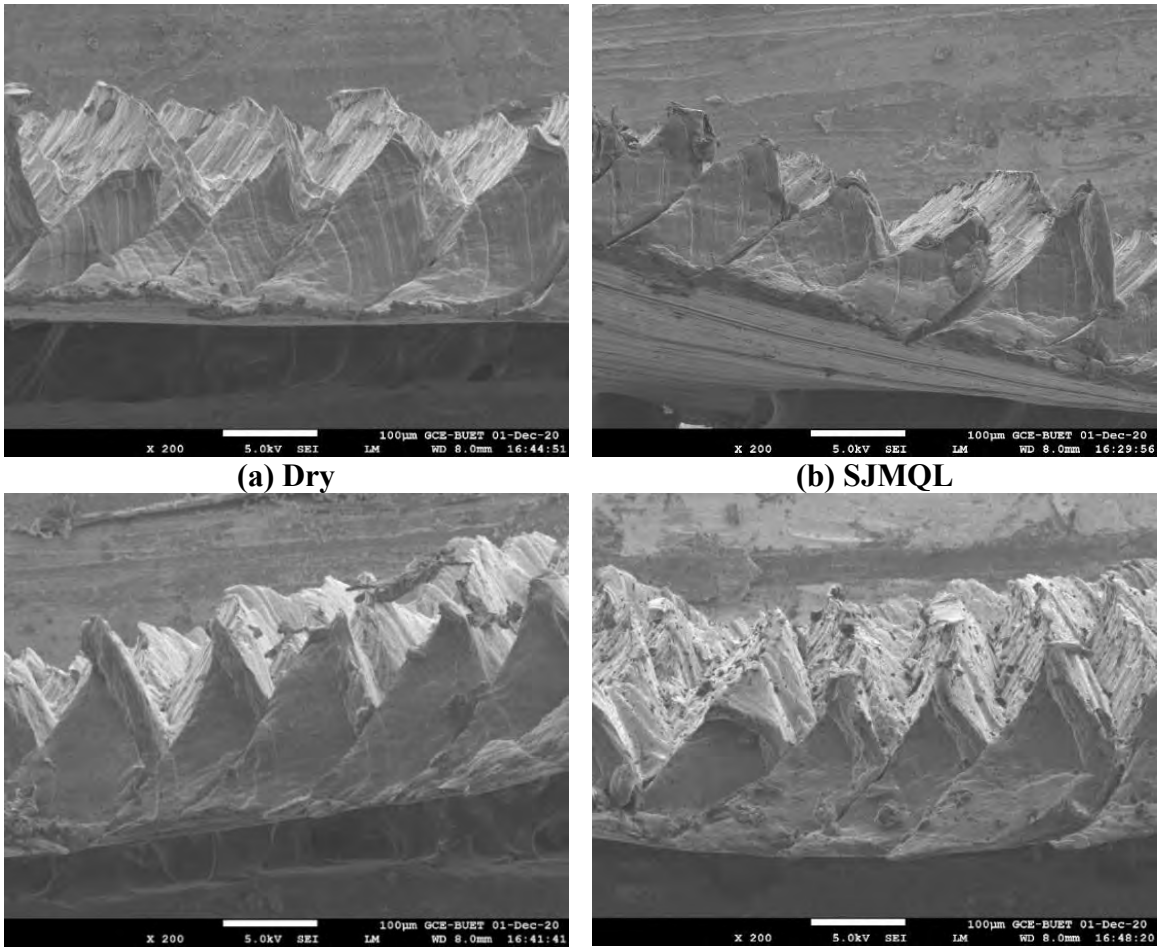


**(a) Dry** **(b) SJMQL**

**(c) DJMQL** **(d) DJMQL with HNF**

**Fig.2.21** SEM of chips produced in turning Ti-6Al-4V alloy by coated carbide insert under (a) Dry, (b) SJMQL, (c) DJMQL and (d) DJMQL with HNF

Variation of chip segmentation degree and slip angle of serrated chips during turning Ti-6Al-4V alloy by uncoated and coated carbide insert under different cooling environments have been presented in Fig.2.22.

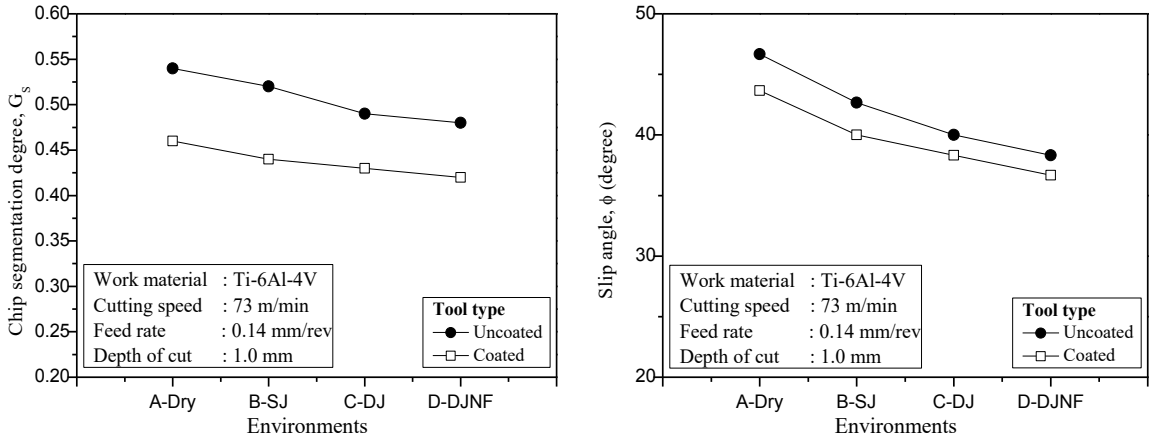


**(a) chip segmentation degree** **(b) slip angle**

**Fig.2.22** Variation of (a) chip segmentation degree and (b) slip angle in turning Ti-6Al-4V alloy by uncoated and coated carbide inserts under different environments.

### 2.5.2 Cutting temperature

Cutting temperature (average chip tool interface temperature) is the most important index for assessing the machinability of any material. Variation of cutting temperature with machining time for uncoated and coated carbide insert under different cooling environments has been shown in Fig.2.23.

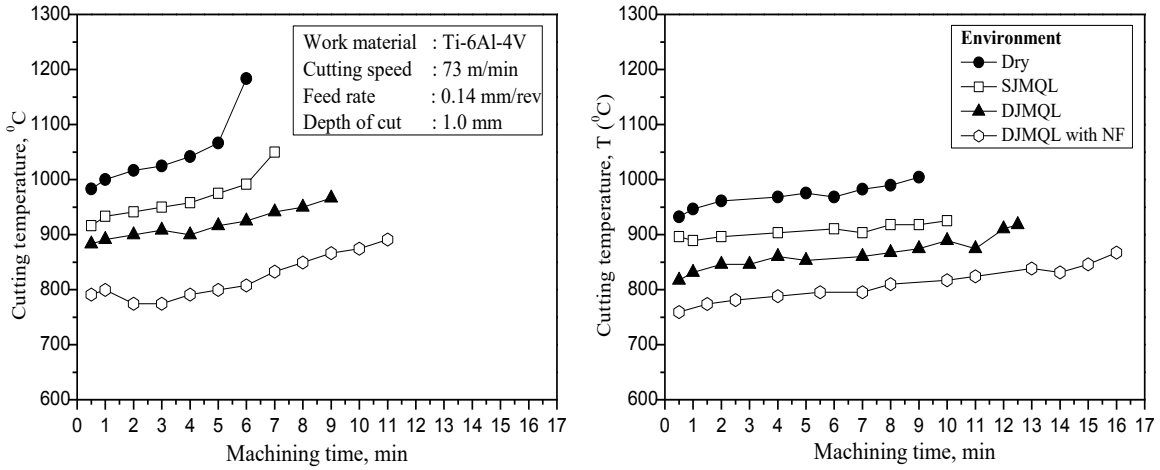


**(a) Uncoated carbide insert** **(b) Coated carbide insert**

**Fig.2.23** Variation of cutting temperature (T) with machining time for (a) uncoated and (b) coated carbide insert under different cooling environments

### 2.5.3 Cutting force

The force required for a cutting tool is directly correlated to the power consumption during the cutting of a specific work-material. It also affects the productivity, quality of product and the overall economy in machining. The variation of the main cutting forces with time observed during turning titanium alloy with uncoated and coated carbide inserts are shown in Fig.2.24.

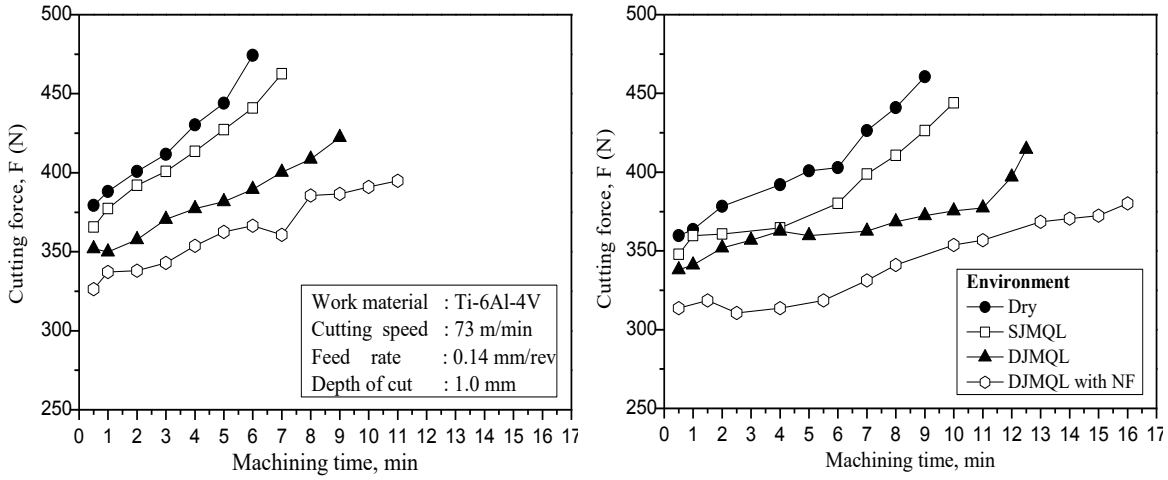


**(a) Uncoated carbide insert** **(b) Coated carbide insert**

**Fig.2.24** Variation of main cutting force (F) with machining time for (a) uncoated and (b) coated carbide insert under different cooling environments

### 2.5.4 Tool wear and tool life

Cutting tool life significantly affects the productivity and economy of machining. Cutting temperature, cutting force and surface roughness was increased with the increase of tool wear. Tool life is determined based on 300 µm of average principle flank wear. The growth of average principal flank wear while turning Ti-6Al-4V alloy by uncoated and coated carbide inserts at a specific speed, feed and depth of cut under different cooling environments have been shown in Fig.2.25. New cutting edges were used for each environmental run. Initially, high tool wear was observed irrespective of the environment. Afterward, tool wear became stable and gradually increased with time. Cutting continues until the average principal flank wear reaches 300 µm.

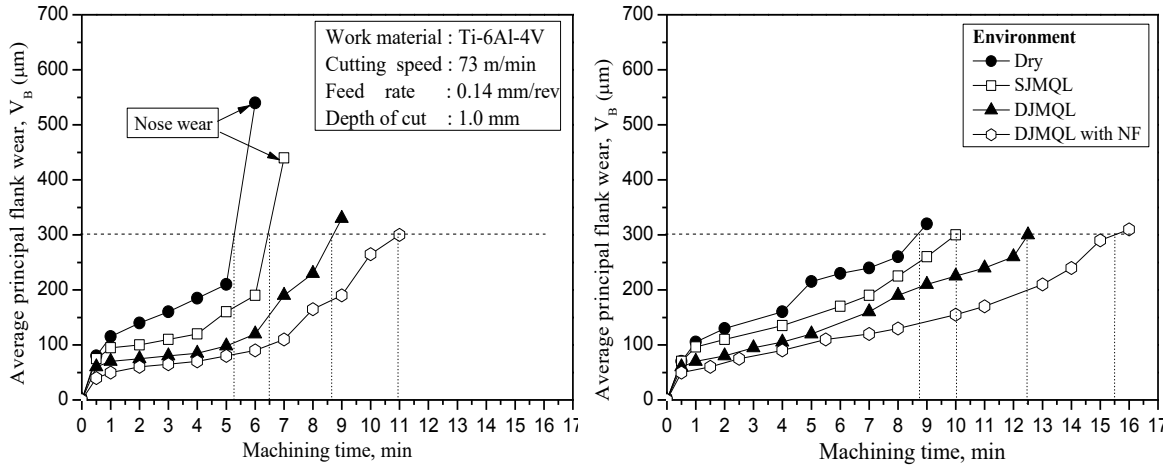


**(a) Uncoated carbide insert** **(b) Coated carbide insert**

**Fig.2.25** Growth of average principal flank wear ($V_B$) with machining time for (a) uncoated and (b) coated carbide insert under different cooling environments

The growth of average auxiliary flank wear ($V_S$) with machining time observed while turning Ti-6Al-4V alloy by coated and uncoated carbide inserts under previous conditions and environments have been shown in Fig.2.26

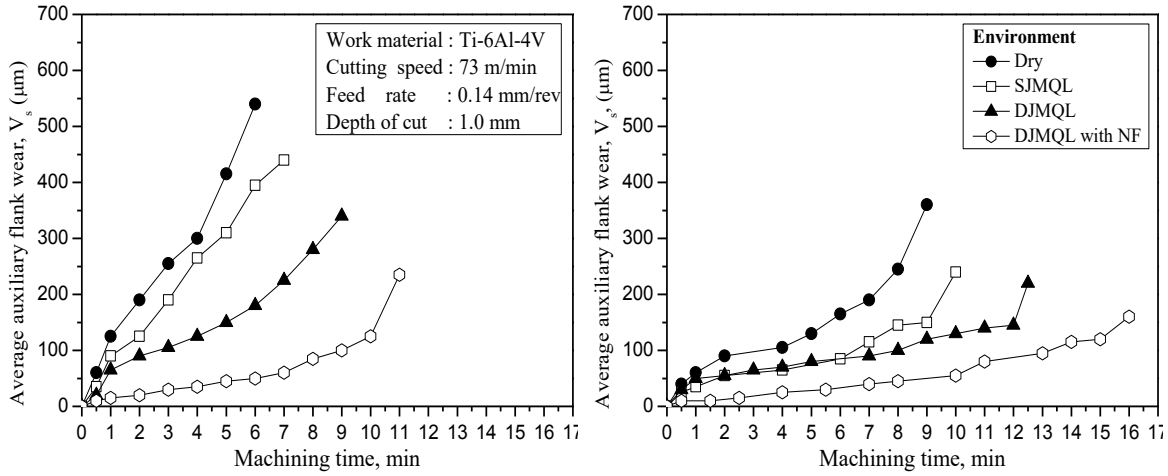


**(a) Uncoated carbide insert** **(b) Coated carbide insert**

**Fig.2.26** Growth of average auxiliary flank wear ($V_S$) with machining time for (a) uncoated and (b) coated carbide insert under different cooling environments

The pattern and extent of wear developed at the tooltips for machining Ti-6Al-4V alloy have been observed under Scanning Electron Microscope to see the actual effects of different environments on the wear of the carbide inserts.

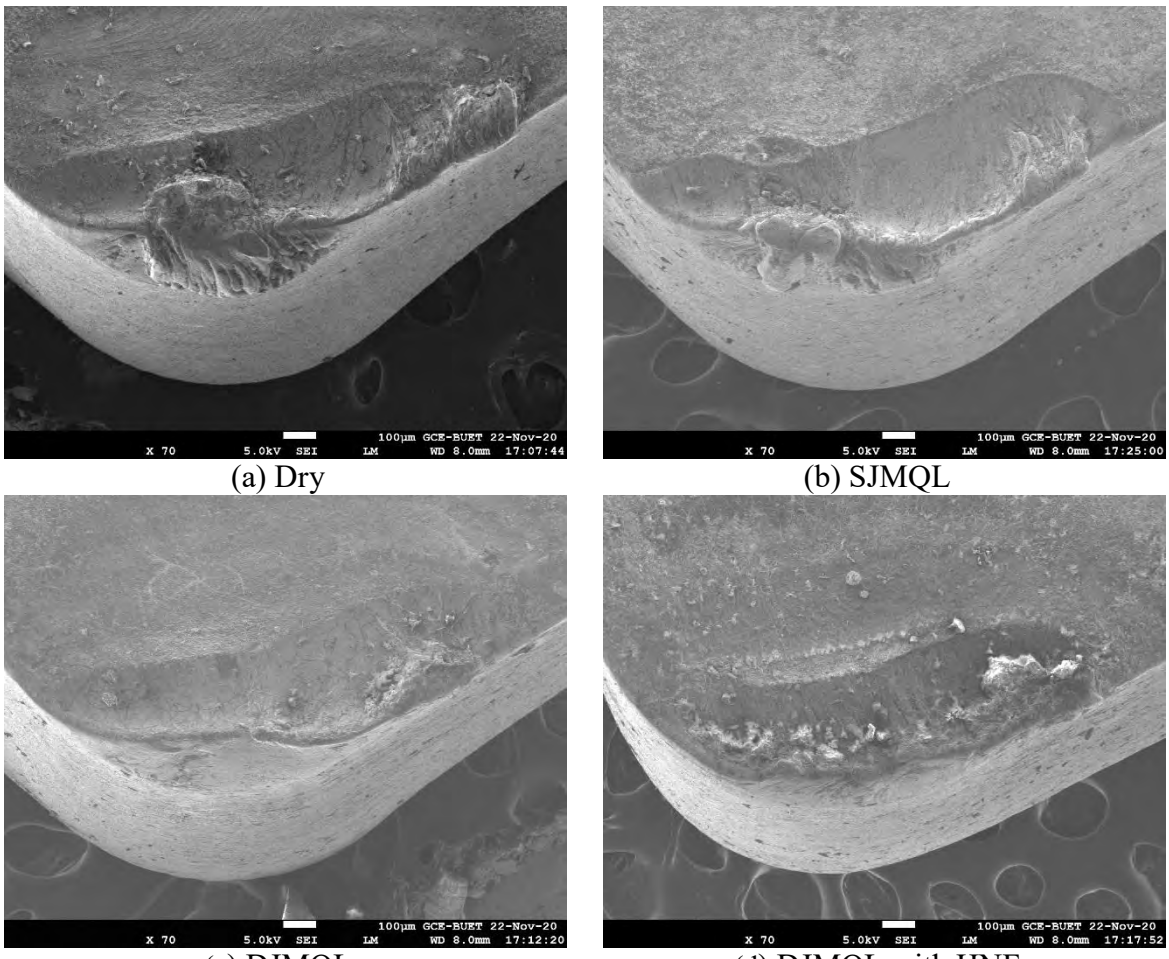


(a) Dry (b) SJMQL

(c) DJMQL (d) DJMQL with HNF

**Fig.2.27** SEM of worn-out uncoated carbide insert under different cooling environments

The SEM of tool wear for different cooling environments when turning Ti-6Al-4V alloy at V=73 m/min, f=0.14 mm/rev and d=1 mm using uncoated and coated carbide inserts have been shown in Fig.2.27 and Fig.2.28.

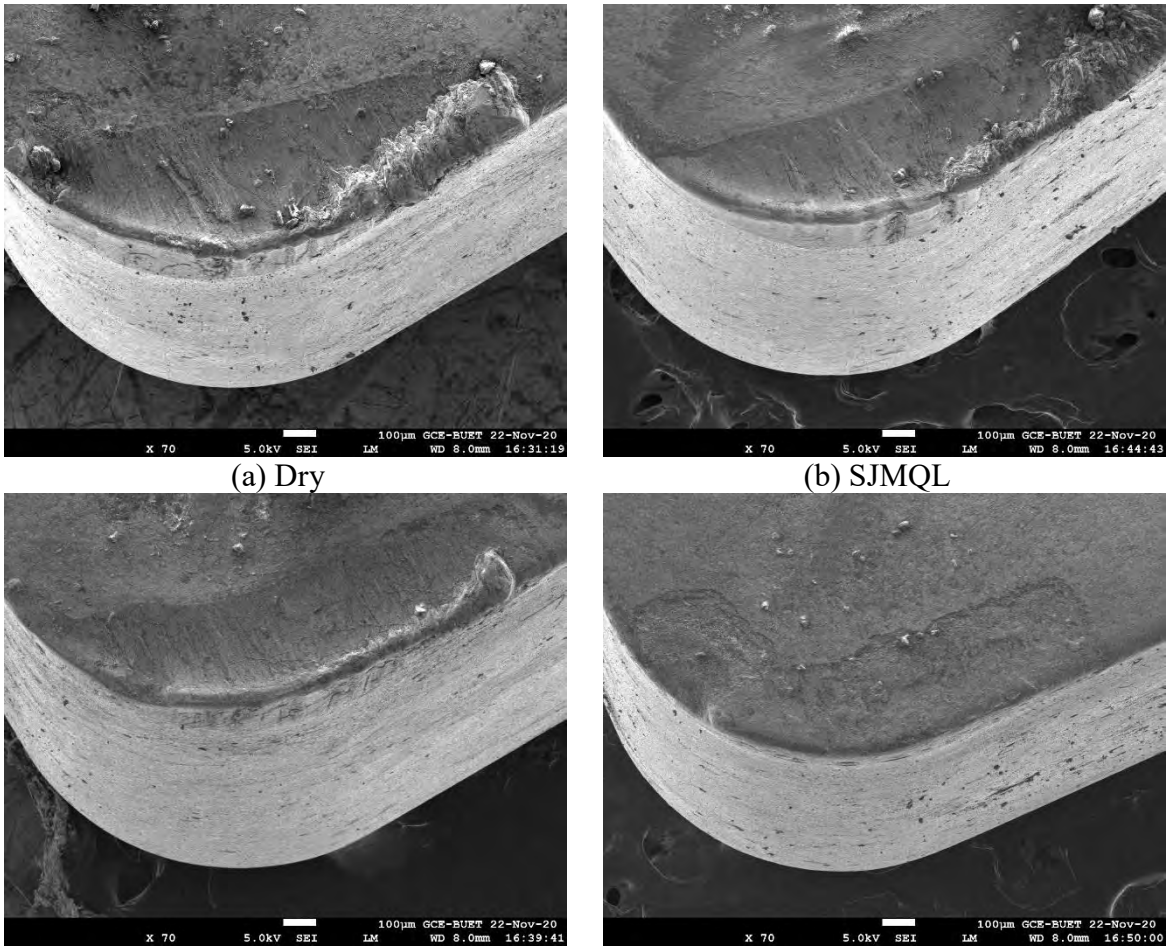


(a) Dry (b) SJMQL

(c) DJMQL (d) DJMQL with HNF

**Fig.2.28** SEM of worn-out coated carbide insert under different cooling environments

### 2.5.5 Surface roughness

The surface roughness of a machined product is extremely allied with the cutting tool wear. Cutting temperature and cutting force also have relations with the surface roughness. Variation of surface roughness ($R_a$) with machining time for uncoated and coated carbide insert under different cooling environments has been shown in Fig.2.29.

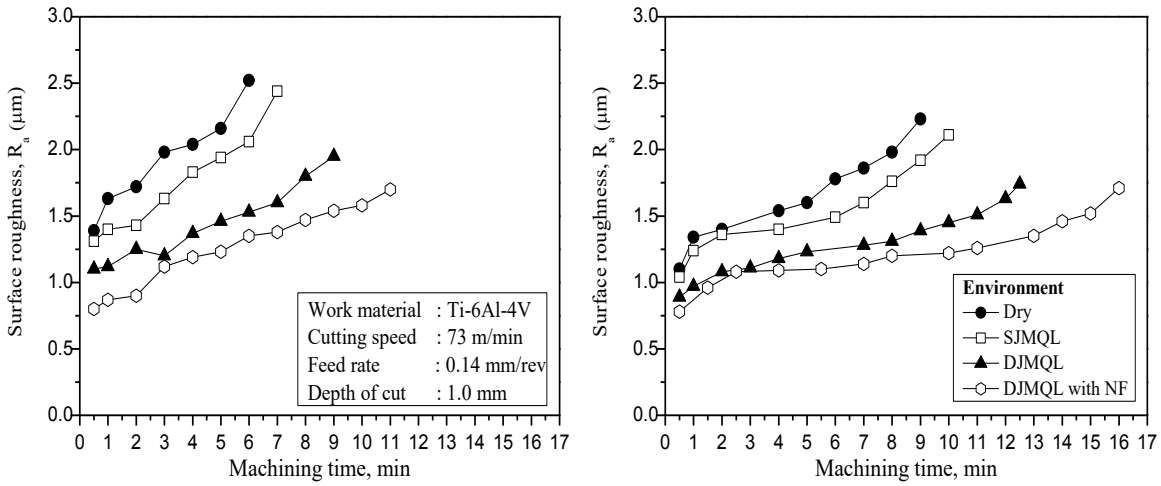


**(a) Uncoated carbide insert** **(b) Coated carbide insert**

**Fig.2.29** Variation of surface roughness ($R_a$) with machining time for (a) uncoated and (b) coated carbide insert under different cooling environments

### 2.5.6 Dimensional deviation

Variation of dimensional deviation with machining time for uncoated and coated carbide insert under different cooling environments has been presented in Fig.2.30.

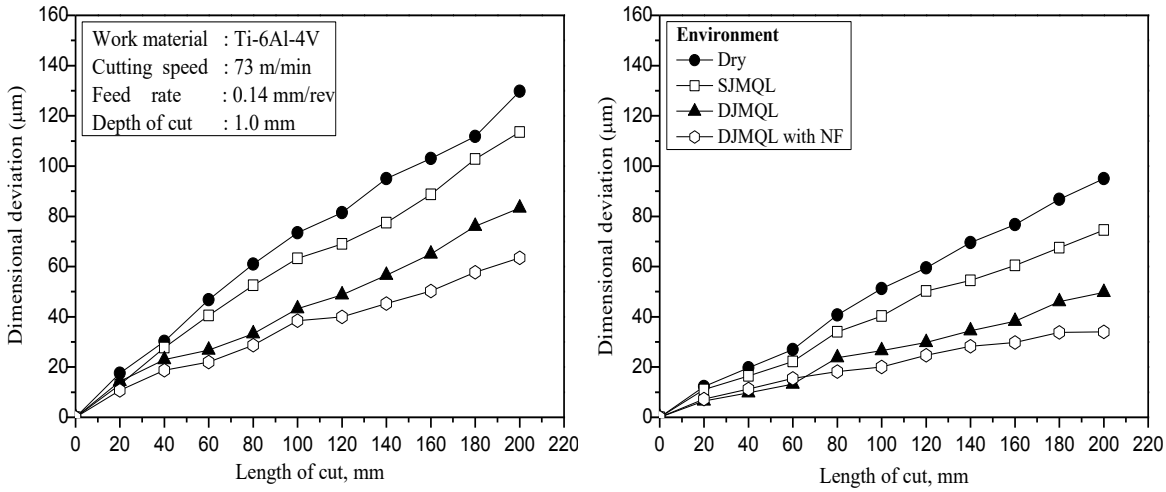


**(a) Uncoated carbide insert** **(b) Coated carbide insert**

**Fig.2.30** Variation of dimensional deviation with machining time for (a) uncoated and (b) coated carbide insert under different cooling environments

# Chapter 3

## Optimization of Process Parameters

Process input optimization intending low production cost without negotiating the quality of the machined part is the primary goal of the current manufacturing industry. Enhanced product quality, reduced production cost and hazard-free operation is a by-product of an optimized process [Xiong et al., 2016]. For turning cutting speed, feed rate and depth of cut are the primary process parameters but the work-tool combination and cutting environment play an important role in enhancing the process performance. Cutting temperature, force, tool wear, tool life, surface roughness are the process responses by which process performance can be measured. Selecting an optimum setting of process inputs considering all the important responses simultaneously according to their importance is a rising necessity in manufacturing. The optimization of machining parameters was initialized by Taylor [1907], who has first presented an optimum cutting speed for maximizing productivity. Optimization of process parameters has become a popular area for many researchers after Gilbert's analytical method for optimization of cutting speed for maximizing productivity and minimizing cost in case of turning operation [Gilbert, 1950]. Nowadays, optimum process input selection for different operations is a vast area of manufacturing research. Because, without reducing product cost and enhancing the quality of the product, no one can sustain in this competitive world.

The initial step for the optimum process input selection is to discover the relationship between process inputs and outputs by creating mathematical models. Mathematical models usually of two types, such as, mechanistic and empirical [Box and Draper, 1987]. In the mechanistic model input-output relationship for the cutting process is developed analytically and empirical models are formulated based on experimental data. For different metal cutting processes, a suitable mechanistic model is rare to find [Luong and Spedding, 1995]. Thus, empirical models are usually utilized for the optimization of process parameters in metal cutting processes. Response Surface Methodology (RSM) is a

statistical regression technique, widely used in metal cutting process modeling before optimization.

## 3.1 Empirical modeling of machining responses

RSM has been used for empirical modeling of the process responses regarding different process inputs based on experimental data. Optimization of the process inputs has been done for the required value of the process responses. The second-order model is appropriate for optimization purposes. Experimentation has been carried out for investigating the effect of process inputs on cutting temperature, cutting force and surface roughness in turning Ti-6Al-4V. Response modeling and process parameter optimization have been done. The final selected process parameters and their levels for this research have been shown in Table 3.1.

**Table 3.1** Process parameters with their levels

| Sl.No | Variable | Symbols | Unit | Lower Level | Upper Level |
|---|---|---|---|---|---|
| 1 | Cutting Speed | V | m/min | 40 | 110 |
| 2 | Feed rate | f | mm/rev | 0.10 | 0.18 |
| 3 | Depth of cut | d | mm | 0.5 | 1.5 |
| 4 | Nano-particle concentration | C | % | 0.5 | 1.5 |
| 5 | Tool-type | TT | - | C | UC |

* C= Coated carbide insert, UC=Uncoated carbide insert

With the process inputs and their levels selected for parameter optimization, Box-Behnken experimental design was created by using MINITAB 17 software. Total 54 experimental runs were executed and multiple responses such as cutting temperature, force and surface roughness values were collected. Table 3.2 shows the experimental design with corresponding responses.

**Table 3.2** Box-Behnken experimental design with corresponding responses

| Run | V | f | d | C | TT | T | F | Ra |
|---|---|---|---|---|---|---|---|---|
| **1** | 75 | 0.14 | 0.5 | 0.5 | C | 788.21 | 216.58 | 0.90 |
| **2** | 75 | 0.14 | 1.0 | 1.0 | UC | 796.88 | 371.42 | 0.84 |
| **3** | 40 | 0.14 | 1.0 | 1.5 | C | 634.90 | 385.14 | 0.94 |
| **4** | 110 | 0.18 | 1.0 | 1.0 | C | 898.34 | 389.06 | 0.91 |
| **5** | 75 | 0.14 | 1.0 | 1.0 | C | 752.22 | 367.50 | 0.76 |
| **6** | 40 | 0.14 | 0.5 | 1.0 | UC | 613.18 | 235.20 | 1.02 |
| **7** | 110 | 0.18 | 1.0 | 1.0 | UC | 972.23 | 419.44 | 1.02 |
| **8** | 40 | 0.18 | 1.0 | 1.0 | C | 617.62 | 427.28 | 1.01 |
| **9** | 75 | 0.10 | 1.0 | 1.5 | UC | 818.59 | 317.52 | 0.82 |
| **10** | 40 | 0.14 | 1.5 | 1.0 | C | 678.08 | 548.80 | 0.94 |
| **11** | 75 | 0.10 | 1.0 | 0.5 | C | 766.62 | 307.72 | 0.62 |
| **12** | 40 | 0.14 | 1.5 | 1.0 | UC | 684.99 | 558.60 | 1.12 |
| **13** | 110 | 0.14 | 0.5 | 1.0 | UC | 947.18 | 212.66 | 0.88 |
| **14** | 75 | 0.10 | 1.5 | 1.0 | UC | 835.29 | 441.00 | 0.82 |
| **15** | 75 | 0.18 | 1.0 | 1.5 | UC | 877.04 | 428.26 | 1.11 |
| **16** | 75 | 0.14 | 0.5 | 1.5 | UC | 812.74 | 207.76 | 0.94 |
| **17** | 75 | 0.14 | 1.5 | 1.5 | UC | 877.04 | 512.54 | 1.06 |
| **18** | 75 | 0.14 | 0.5 | 1.5 | C | 773.82 | 189.14 | 0.84 |
| **19** | 75 | 0.18 | 1.0 | 1.5 | C | 855.16 | 413.56 | 1.02 |
| **20** | 110 | 0.14 | 1.0 | 0.5 | C | 922.82 | 356.72 | 0.74 |
| **21** | 75 | 0.14 | 1.5 | 0.5 | C | 855.16 | 521.36 | 1.03 |
| **22** | 40 | 0.10 | 1.0 | 1.0 | C | 581.63 | 294.00 | 0.60 |
| **23** | 110 | 0.14 | 1.0 | 1.5 | C | 951.61 | 349.86 | 0.68 |
| **24** | 75 | 0.10 | 1.0 | 0.5 | UC | 841.13 | 336.14 | 0.70 |
| **25** | 110 | 0.10 | 1.0 | 1.0 | UC | 913.78 | 293.02 | 0.58 |
| **26** | 75 | 0.14 | 1.0 | 1.0 | UC | 826.94 | 372.40 | 0.92 |
| **27** | 75 | 0.14 | 1.5 | 0.5 | UC | 899.58 | 538.02 | 1.16 |
| **28** | 40 | 0.18 | 1.0 | 1.0 | UC | 629.88 | 443.94 | 1.13 |
| **29** | 75 | 0.18 | 0.5 | 1.0 | C | 766.62 | 234.22 | 1.00 |
| **30** | 75 | 0.18 | 1.5 | 1.0 | UC | 899.58 | 607.60 | 1.12 |
| **31** | 75 | 0.14 | 1.0 | 1.0 | C | 766.62 | 354.76 | 0.77 |
| **32** | 75 | 0.18 | 0.5 | 1.0 | UC | 841.13 | 244.02 | 1.08 |
| **33** | 40 | 0.14 | 1.0 | 0.5 | C | 692.48 | 387.10 | 0.90 |
| **34** | 110 | 0.14 | 1.5 | 1.0 | UC | 958.03 | 543.90 | 0.92 |
| **35** | 110 | 0.14 | 0.5 | 1.0 | C | 879.63 | 201.88 | 0.74 |
| **36** | 75 | 0.18 | 1.0 | 0.5 | UC | 899.58 | 431.20 | 1.06 |
| **37** | 40 | 0.10 | 1.0 | 1.0 | UC | 604.83 | 317.52 | 0.78 |
| **38** | 75 | 0.18 | 1.0 | 0.5 | C | 862.35 | 421.40 | 0.98 |
| **39** | 110 | 0.14 | 1.0 | 0.5 | UC | 1010.64 | 372.40 | 0.94 |
| **40** | 75 | 0.10 | 1.0 | 1.5 | C | 795.41 | 299.88 | 0.61 |
| **41** | 40 | 0.14 | 0.5 | 1.0 | C | 596.03 | 216.58 | 0.90 |
| **42** | 75 | 0.18 | 1.5 | 1.0 | C | 819.17 | 570.36 | 1.00 |
| **43** | 40 | 0.14 | 1.0 | 1.5 | UC | 654.93 | 393.96 | 0.98 |
| **44** | 75 | 0.14 | 1.0 | 1.0 | UC | 810.24 | 370.44 | 0.96 |
| **45** | 75 | 0.10 | 0.5 | 1.0 | UC | 760.14 | 149.94 | 0.72 |
| **46** | 110 | 0.14 | 1.5 | 1.0 | C | 869.55 | 524.30 | 0.80 |
| **47** | 40 | 0.14 | 1.0 | 0.5 | UC | 671.63 | 412.58 | 1.14 |
| **48** | 75 | 0.10 | 1.5 | 1.0 | C | 752.22 | 423.36 | 0.68 |
| **49** | 75 | 0.14 | 1.0 | 1.0 | C | 759.42 | 369.46 | 0.82 |
| **50** | 75 | 0.14 | 0.5 | 0.5 | UC | 868.69 | 245.00 | 1.02 |
| **51** | 110 | 0.10 | 1.0 | 1.0 | C | 855.16 | 268.52 | 0.40 |
| **52** | 75 | 0.10 | 0.5 | 1.0 | C | 685.28 | 146.02 | 0.60 |
| **53** | 75 | 0.14 | 1.5 | 1.5 | C | 826.36 | 496.86 | 1.02 |
| **54** | 110 | 0.14 | 1.0 | 1.5 | UC | 1002.29 | 365.54 | 0.84 |

Utilizing the data of Table 3.2, the final reduced empirical model for temperature, force and roughness has been created by using the MINITAB 17 software with the backward elimination technique, where insignificant terms based on $p > 0.05$ have been removed. The predictive empirical models developed for different responses have been presented in Eq.3.1 to 3.6.

$$T_{coated} = 354.7 + 7.492\ V + 759.0\ f + 133.9\ d - 402.4\ C - 0.01763\ V\times V + 192.9\ C\times C - 1.093\ V\times d \quad \textbf{.....(3.1)}$$

$$T_{uncoated} = 338.1 + 8.369\ V + 759.0\ f + 133.9\ d - 402.4\ C - 0.01763\ V\times V + 192.9\ C\times C - 1.093\ V\times d \quad \textbf{.....(3.2)}$$

$$F_{coated} = -87.5 - 1.254\ V + 2637\ f + 200.7\ d - 66.4\ C + 0.00579\ V\times V - 7010\ f\times f + 25.5\ C\times C + 821\ f\times d \quad \textbf{.....(3.3)}$$

$$F_{uncoated} = -70.4 - 1.254\ V + 2637\ f + 200.7\ d - 66.4\ C + 0.00579\ V\times V - 7010\ f\times f + 25.5\ C\times C + 821\ f\times d \quad \textbf{.....(3.4)}$$

$$R_{a\ coated} = 0.355 - 0.002393\ V + 11.50\ f - 0.573\ d - 0.556\ C - 24.31\ f\times f + 0.3294\ d\times d + 0.2644\ C\times C \quad \textbf{.....(3.5)}$$

$$R_{a\ uncoated} = 0.483 - 0.002393\ V + 11.50\ f - 0.573\ d - 0.556\ C - 24.31\ f\times f + 0.3294\ d\times d + 0.2644\ C\times C \quad \textbf{.....(3.6)}$$

ANOVA tables for the reduced models for all responses have been presented in Tables 3.3, 3.4 and 3.5. The influence of each term in the final model on the responses as well as the percent contribution of each term has been determined by calculated based on Adj SS (adjusted sum of squares) values from the ANOVA tables. It can be depicted that, cutting speed was the most contributing terms with 79.04% contribution to the temperature. For surface roughness, the feed rate has the most contribution (54.87%) followed by tool-type (14.44%). The lack-of-fit value (> 0.05) also implies that this value is insignificant compared to the pure error value. So, the proposed predictive models have been fitted with the experimental data very well. Plots for the residual analysis of the final models have also been presented followed by the ANOVA tables. The $R^2$ value of the final empirical model for temperature was 97.98 %, which is very close to the $R^2$(adj) value of 97.57 %. Similarly, the $R^2$ and $R^2$(adj) values of the final regression model of cutting force were 99.37 % and 99.24%. In the case of roughness, these values were 94.41 % and 93.41% respectively. For all the cases, these two values were very close which is preferable in an ideal situation. $R^2$(pred) values for temperature, force and roughness were 96.79%, 99.05% and 91.93 % respectively. Based on different $R^2$ values for all the models depicted that these models were highly acceptable and can be used to predict the responses.

**Table 3.3** ANOVA for the cutting temperature

| Source | DF | Adj SS | Adj MS | F-Value | P-Value | % Contribution |
|---|---|---|---|---|---|---|
| **Model** | 9 | 640419 | 71158 | 237.54 | 0.000 | 97.98 |
| **Linear** | 5 | 589040 | 117808 | 393.27 | 0.000 | 90.12 |
| V | 1 | 516584 | 516584 | 1724.47 | 0.000 | 79.04 |
| f | 1 | 22120 | 22120 | 73.84 | 0.000 | 3.38 |
| d | 1 | 16141 | 16141 | 53.88 | 0.000 | 2.47 |
| C | 1 | 1650 | 1650 | 5.51 | 0.023 | 0.25 |
| TT | 1 | 32545 | 32545 | 108.64 | 0.000 | 4.98 |
| **Square** | 2 | 42797 | 21398 | 71.43 | 0.000 | 6.55 |
| V×V | 1 | 5973 | 5973 | 19.94 | 0.000 | 0.91 |
| C×C | 1 | 29778 | 29778 | 99.40 | 0.000 | 4.56 |
| **2-Way Interaction** | 2 | 8583 | 4291 | 14.33 | 0.000 | 1.31 |
| V×d | 1 | 2930 | 2930 | 9.78 | 0.003 | 0.45 |
| V×TT | 1 | 5653 | 5653 | 18.87 | 0.000 | 0.86 |
| Error | 44 | 13181 | 300 | | | 2.02 |
| **Lack-of-Fit** | 40 | 12623 | 316 | 2.26 | 0.222 | 1.93 |
| **Pure Error** | 4 | 557 | 139 | | | 0.09 |
| **Total** | 53 | 653600 | | | | 100 |

**Model Summary**

S=17.3078 $R^2$=97.98% $R^2$ (adj)= 97.57% $R^2$ (pred)= 96.79%

**Table 3.4** ANOVA for the cutting force

| Source | DF | Adj SS | Adj MS | F-Value | P-Value | % Contribution |
|---|---|---|---|---|---|---|
| **Model** | 9 | 699003 | 77667 | 769.10 | 0.000 | 99.37 |
| **Linear** | 5 | 693394 | 138679 | 1373.28 | 0.000 | 98.57 |
| V | 1 | 4358 | 4358 | 43.15 | 0.000 | 0.62 |
| f | 1 | 85885 | 85885 | 850.48 | 0.000 | 12.21 |
| d | 1 | 597778 | 597778 | 5919.54 | 0.000 | 84.98 |
| C | 1 | 1445 | 1445 | 14.31 | 0.023 | 0.21 |
| TT | 1 | 3929 | 3929 | 38.90 | 0.000 | 0.56 |
| **Square** | 3 | 3453 | 1151 | 11.40 | 0.000 | 0.49 |
| V×V | 1 | 605 | 605 | 5.99 | 0.018 | 0.09 |
| f×f | | 1509 | 1509 | 14.95 | 0.000 | 0.21 |
| C×C | 1 | 486 | 486 | 4.81 | 0.034 | 0.07 |
| **2-Way Interaction** | 1 | 2156 | 2156 | 21.35 | 0.000 | 0.31 |
| f×d | 1 | 2156 | 2156 | 21.35 | 0.000 | 0.31 |
| Error | 44 | 4443 | 101 | | | 0.63 |
| **Lack-of-Fit** | 40 | 4314 | 108 | 3.34 | 0.124 | 0.61 |
| **Pure Error** | 4 | 129 | 32 | | | 0.02 |
| **Total** | 53 | 703446 | | | | 100.00 |

**Model Summary**

S=10.0491 $R^2$=99.37% $R^2$ (adj)= 99.24% $R^2$ (pred)= 99.05%

**Table 3.5** ANOVA for the surface roughness

| Source | DF | Adj SS | Adj MS | F-Value | P-Value | % Contribution |
|---|---|---|---|---|---|---|
| **Model** | 8 | 1.45820 | 0.182275 | 94.98 | 0.000 | 94.41 |
| **Linear** | 5 | 1.28756 | 0.257513 | 134.18 | 0.000 | 83.36 |
| V | 1 | 0.16834 | 0.168338 | 87.71 | 0.000 | 10.90 |
| f | 1 | 0.84750 | 0.847504 | 441.60 | 0.000 | 54.87 |
| d | 1 | 0.04420 | 0.044204 | 23.03 | 0.000 | 2.86 |
| C | 1 | 0.00454 | 0.004538 | 2.36 | 0.131 | 0.29 |
| TT | 1 | 0.22298 | 0.222980 | 116.19 | 0.000 | 14.44 |
| **Square** | 3 | 0.17064 | 0.056880 | 29.64 | 0.000 | 11.05 |
| f×f | 1 | 0.01815 | 0.018148 | 9.46 | 0.004 | 1.18 |
| d×d | 1 | 0.08140 | 0.081400 | 42.41 | 0.000 | 5.27 |
| C×C | 1 | 0.05245 | 0.052448 | 27.33 | 0.000 | 3.40 |
| Error | 45 | 0.08636 | 0.001919 | | | 5.59 |
| **Lack-of-Fit** | 41 | 0.07683 | 0.001874 | 0.79 | 0.703 | 4.97 |
| **Pure Error** | 4 | 0.00953 | 0.002383 | | | 0.62 |
| **Total** | 53 | 1.54456 | | | | 100.00 |

**Model Summary**

S=0.0438083 $R^2$=94.41% $R^2$ (adj)= 93.41% $R^2$ (pred)= 91.93%

4 in 1 residual plot for different responses has been presented in Fig.3.1. Fig.3.1 (a) has been shown the residual plots for the temperature. In the normal probability plot, most of the points have been fall along the straight line although there was some clumping in the data. The histogram depicts a fairly normal distribution of the residuals. No skewness and outlier of the data were observed and tails were found clearly in the histogram of residuals. In the residual versus fitted value plot, the residuals have been allocated fairly evenly and randomly across all the fitted (estimated) values and the residual points appear to be randomly distributed on both sides of the line representing 0 residual value with constant variance and so specific pattern was observed. In the residual versus observation order plot, no particular trend or pattern has not been evident for all the data points. The residuals have fluctuated randomly around the centerline which confirms the non-significance of the experiment order on the residual. It can be concluded that the normality and the randomness of the residual values confirmed by the previously mentioned plots, verified the characteristics of a good model and reliable experimental data. Fig.3.1 (b) and (c) have been shown the residual plots for cutting force and surface roughness. From these plots, similar conclusions can be drawn.

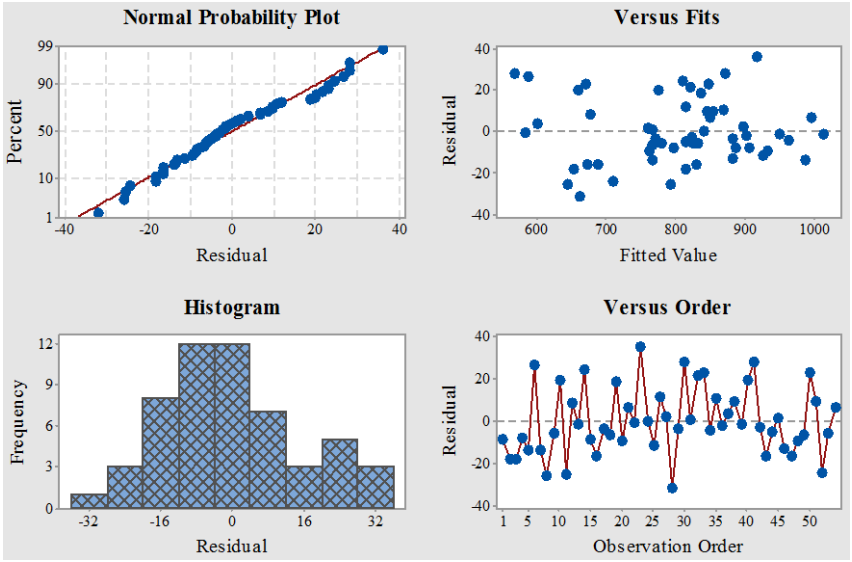


**(a) Cutting temperature**

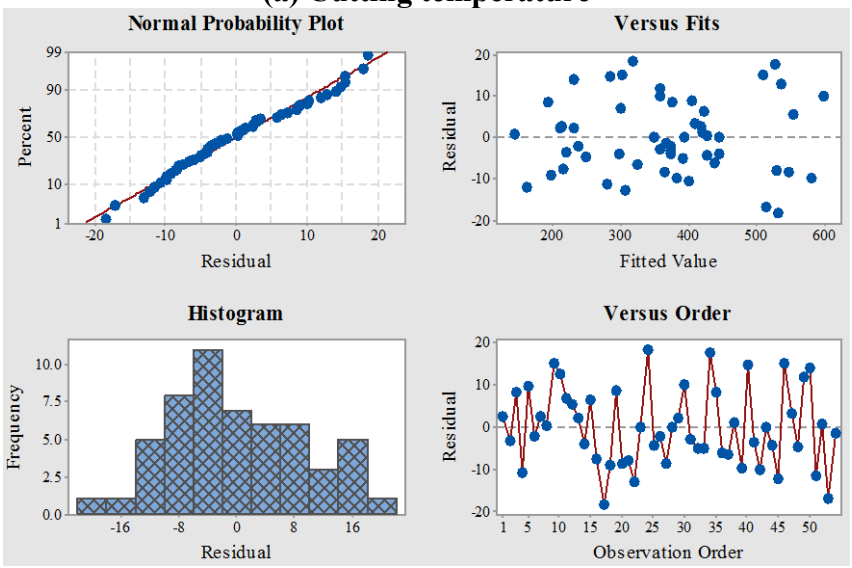


**(b) Cutting force**

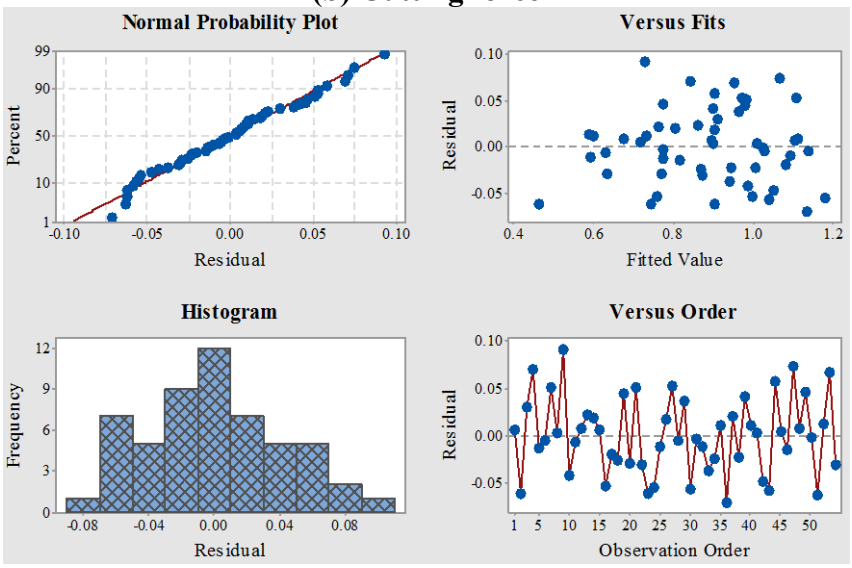


**(c) Surface roughness**

**Fig.3.1** Residual plots for (a) cutting temperature, (b) cutting force and (c) surface roughness.

For any model formulation, experimental validity is very important. The process parameters settings for the validity test have been shown in Table 3.6.

**Table 3.6** Parameter settings for validity test

| Run | V | f | d | C | TT |
|---|---|---|---|---|---|
| **1** | 40 | 0.10 | 0.5 | 1.0 | C |
| **2** | 40 | 0.10 | 1.5 | 1.0 | UC |
| **3** | 40 | 0.18 | 0.5 | 1.0 | C |
| **4** | 40 | 0.18 | 1.5 | 0.5 | UC |
| **5** | 75 | 0.14 | 0.5 | 1.5 | C |
| **6** | 75 | 0.14 | 1.0 | 1.5 | UC |
| **7** | 75 | 0.14 | 1.5 | 1.5 | C |
| **8** | 110 | 0.10 | 1.5 | 0.5 | C |
| **9** | 110 | 0.10 | 1.5 | 1.5 | UC |
| **10** | 110 | 0.14 | 0.5 | 1.0 | C |
| **11** | 110 | 0.18 | 1.5 | 1.0 | UC |

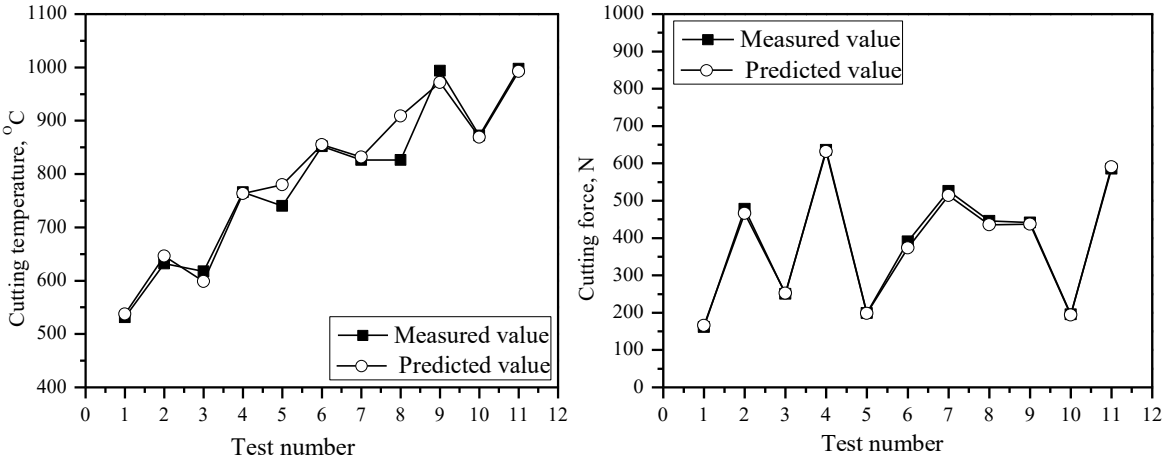


**(a) Cutting temperature** **(b) Cutting force**

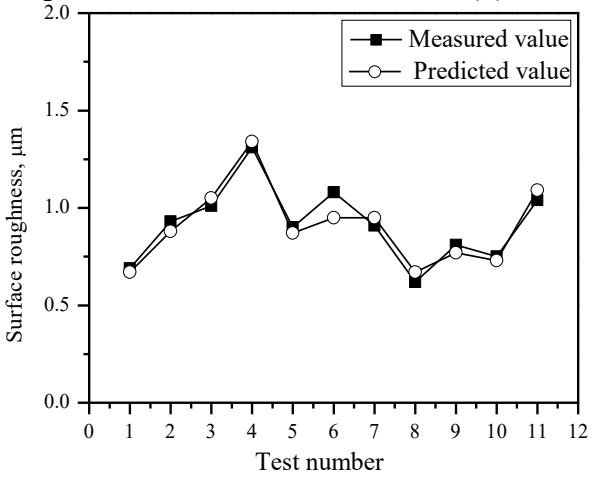


**(c) Surface roughness**

**Fig.3.2** Comparison of measured and predicted (a) cutting temperature (b) cutting force and (c) surface roughness

The actual values of the temperature, force and surface roughness and respective predicted values acquired from the empirical models of these responses have been graphically presented in Fig.3.2. Actual and predicted values were very close to each other. MAPE value for the cutting temperature was found as 2.39%, for cutting force 1.75% and for roughness 4.98%. These MAPE values were found realistic for RSM-based empirical model formulation of different manufacturing responses since similar MAPE values were previously found in the literature [Gupta et al., 2020; Zaman and Dhar, 2020]. Based on this error analysis it can be concluded that all the models are acceptable for correlating the responses with the process inputs with a reasonable error.

Different turning process parameters, nanoparticle concentration and tool types have different effects on different machining responses. Cutting speed, feed rate and depth of cut are the turning parameters that have been varied in this experiment. After analyzing their effect on the machinability, optimum parameter settings have been determined. All the process inputs and also their interactions have a significant effect on all the responses. Heat in the cutting zone negatively affects the tool life and machined surface. This negative effect is tried to be controlled by reducing heat generation and removing heat from the cutting zone through an appropriate selection of process parameters, cutting tools and cutting fluids along with their application methods [Ezugwu and Wang, 1997; Kosaraju and Anne, 2013; Settineri and Faga, 2008]. Usually, with the increase of nanoparticle concentration, the beneficial effects would increase. But sometimes, an excess concentration of nanoparticles in nano-fluids can increase the cutting force and the tool wear. Consequently, surface integrity can be hampered. So, depending on the machining operation, workpiece material, tool material, base fluid, the nano-particle type and concentration should be cautiously selected [Said et al., 2019].

The main effect and interaction plot of the cutting temperature for turning Ti-6AL-4V alloy regarding various cutting parameters (speed, feed rate and depth of cut), nano-particle concentration and tool-type is shown in Fig.3.3 and Fig.3.4. The main effect plot revealed that temperature is linearly increased with the increase in cutting speed. Because shearing of the work metal and the frictions at the tool-chip and work-tool interfaces is increased at the higher cutting speed [Kumar et al., 2013]. Moreover, the generated heat cannot be conducted to the workpiece, tool holder and chips due to shorter cutting time. In all, it can be said that cutting speed is the most prominent factor for increasing temperature which is previously claimed by [Abukhshim et al., 2006]. With the increase of feed rate

and depth of cut, cutting force is increased due to an increase of shear plane area which causes higher heat generation at the tool [Stephenson and Agapiou, 2016]. Additionally, with the increase of feed rate and depth of cut, the chip-tool and the work-tool contact area are increased which eventually increases the friction and further increases the cutting temperature. On the other hand, at a higher feed rate and depth of cut, the cross-sectional area of the chip is increased and more heat is carried away by the chip which reduces the total amount of heat in the tooltip [Pal et al., 2014]. Therefore, feed rate and depth of cut are less significant factors in controlling the cutting temperature. Previously, a similar trend has been shown during machining Ti-6Al-4V alloy [Işik and Kentli, 2014].

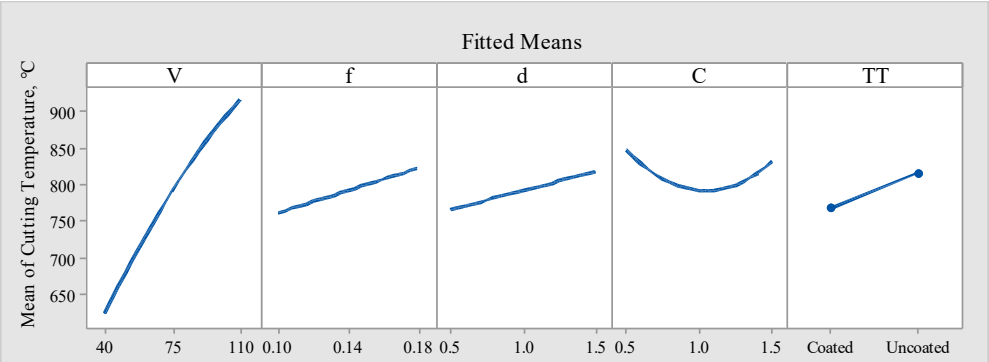


**Fig.3.3** Main effect plot for cutting temperature

With the increase of nanoparticle concentration, thermal conductivity and viscosity are generally increased [Shah et al., 2017]. Higher thermal conductivity facilitates the enhancement of heat transfer performance. Whereas, higher viscosity of cutting fluid aid the higher boundary layer thickness, which leads to a decrease in heat transfer performance. But a certain amount of viscosity is helpful for proper lubrication. Up to a certain concentration, the effect of thermal conductivity overcome the effect of viscosity and heat transfer is maximum at this point. Afterward, heat transfer is reduced because of the higher viscosity of the nano-fluid, which restricts the natural flow of cutting fluid to enter the chip-tool and work-tool interfaces. In this present research, heat transfer is maximum at 1% of concentration and minimum cutting temperature has been achieved in this condition. A similar trend of cutting temperature against nanoparticle concentration was reported by Rao et al. [2011].

From the main effect plot, it can be seen that the average cutting temperature obtained by using the coated carbide insert is 766.03°C, whereas, for the uncoated carbide insert the average temperature is 815.13°C. The substrate tungsten carbide provides major

toughness required for the cutting and the coatings (TiN-TiCN-$Al_2O_3$-TiN) provides additional strength, hardness and wear protection of the cutting tool. A multi-layer coated tool is more efficient than a monolayer coated tool [Grzesik and Nieslony, 2003]. Titanium nitride (TiN) is a general-purpose coating that is used as the initial layer and also the finishing layer. This coating ensures high hardness, excellent corrosion, wear and heat resistance. The outer golden layer also helps easy wear detection of the cutting tool. Titanium Carbo-Nitride (TiCN) is used as an inner layer that offers good abrasive wear resistance and adherence to a carbide substrate. It has higher surface hardness and also better lubricity because of the carbon content on it. The aluminum oxide ($Al_2O_3$) layer in the coating acts as a solid lubricant and also as a thermal and chemical barrier for the carbide insert. These coatings reduce the friction between the chip-tool and work-tool interfaces, chips easily slide off the tool rake surface which reduces heat generation. Additionally, this coating prevents the heat to diffuse into the tool. These above-mentioned actions of the coating are responsible for reducing the tool temperature. As stated by Grzesik [2016], the TiN-TiCN-$Al_2O_3$-TiN coating created an effective thermal barrier and harder cutting edge. Better performance of the TiN-TiCN-$Al_2O_3$-TiN coated carbide tool compared to the uncoated tool regarding less temperature during turning has also been previously observed in the literature [Zaman et al., 2020].

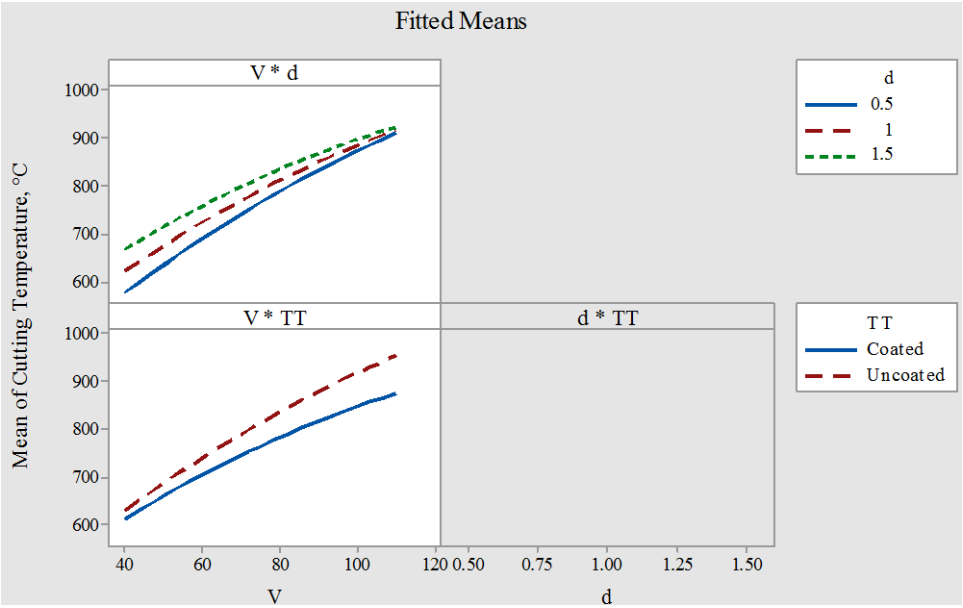


**Fig.3.4** Interaction plot for cutting temperature

There were interaction effects of speed with a depth of cut and tool-type. That means, with the increase of cutting speed, the temperature was increased but differently for

different depths of cut and tool-type. For a higher depth of cut, the rate of temperature increment is slower. As the uncoated tool wear out quickly, the temperature increased at a higher rate with speed compared to the coated tool.

Cutting force is an important index of machinability which is directly related to the power consumption of the machining process. From different experimental analyses, it was previously shown that cutting force decreased due to an increase in cutting speed. This is because, with the increase of cutting speed, shear and frictional energy increases and temperature at the cutting zone is increased which softens the work material and facilitates easy material removal with low cutting force. On the contrary, cutting force is increased with the feed rate and depth of cut due to the increase of shear plane area and chip load [André Stefenon et al., 2015; Gowd et al., 2014; Pal et al., 2014]. From Fig.3.5 it can be revealed that, with the increase of speed, cutting force decreases and with the increase of feed rate and depth of cut cutting force increases. Here, the depth of cut affects the maximum followed by feed rate. Cutting speed has the lowest effect on cutting force. With the increase of depth of cut, the cutting force increases linearly with a high slope, because the volume of material removal is increased significantly at a higher depth of cut. Whereas, with the feed rate the rate of increment of cutting force is moderate. For cutting speed, the cutting force slowly decreases with its increment. Similar interpretations were reported in previous literature during the dry turning of Ti-6Al-4V alloy [Sun et al., 2009].

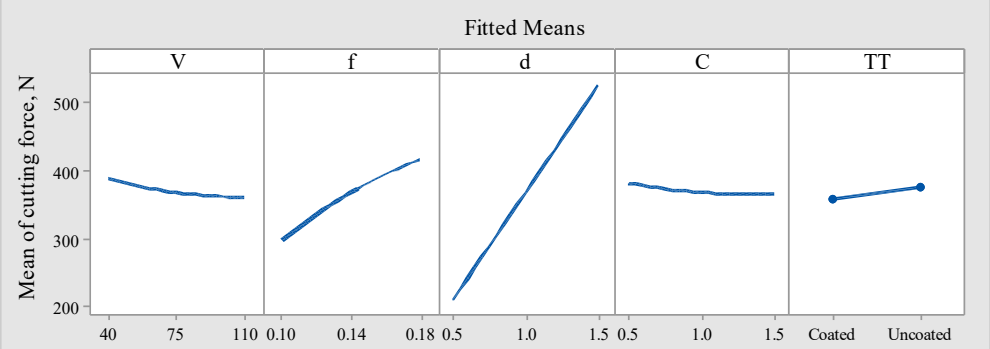


**Fig.3.5** Main effect plot for cutting force

Nano-particles presented in the nano-fluid reduce the force by its ball-bearing effect. The higher the nanoparticle concentration, the cutting force is reduced due to reduce the friction at the cutting interfaces. With the increase of nanoparticle concentration viscosity is increased. Due to increased viscosity the lubrication at the chip-tool and work-tool interfaces is increased, but the penetration of the cutting fluid into the interface may hamper due to higher viscosity. Additionally, as described earlier, up to 1% concentration

of $Al_2O_3$-MWCNT nano-particles thermal conductivity overcomes the effect of viscosity in cooling performance, then it becomes slower. For that reason, after a 1% concentration temperature at the cutting zone is increased. Due to the higher temperature, higher tool wear also occurred. So, ultimately, the cutting force is reduced with the increase of nanoparticle concentration up to about 1.3% but increased afterward.

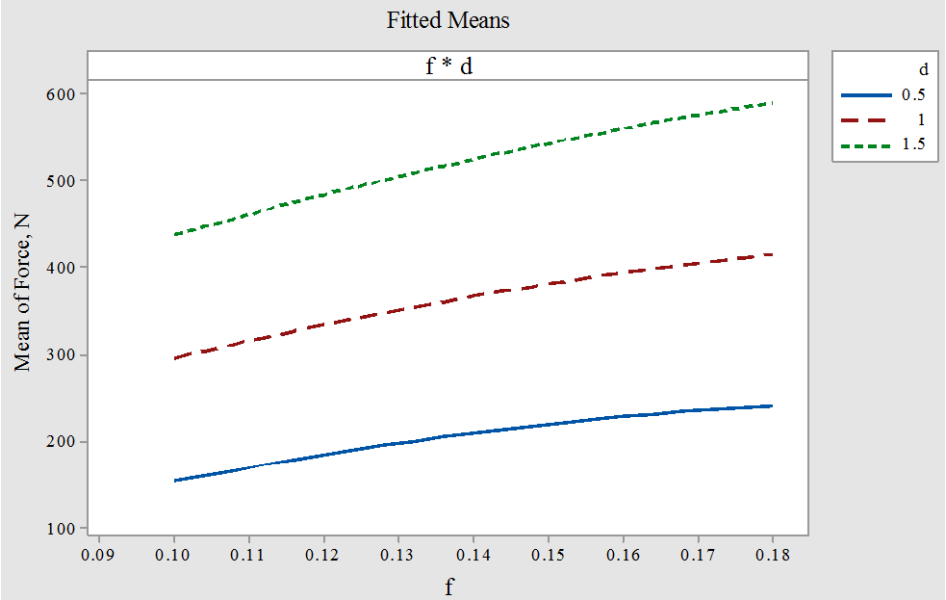


**Fig.3.6** Interaction plot for cutting force

The tool type has no significant interaction with other parameters investigated. So, the effect of all the factors on the cutting force is irrelevant to the tool type. During nanofluid-based MQL turning of Ti-6Al-4V alloy, the cutting force caused by the coated carbide tool is less compared to the uncoated carbide tool for identical machining conditions. From the main effect plot, it can be revealed that the average cutting force obtained by using the coated carbide insert is 357.57 N, whereas, for uncoated carbide insert the average force is 374.63 N. Coating material acts as a solid lubricant on the carbide insert. The coefficient of friction is lower for the coated carbide tool compared to the uncoated tool. These coatings reduce the friction between the chip-tool and work-tool interfaces, chips easily slide off the tool rake surface which reduces heat generation and also reduces frictional force. On the other hand, the low cutting temperature at the cutting zone maintains the work-piece hardness, for which cutting force can be slightly increased. For these reasons, the reduction of cutting force in the case of the coated tool is small. During the turning of TC11 titanium alloy under MQL condition, the coated tool has outperformed the uncoated carbide tool regarding cutting force [Qin et al., 2016]. There is a very little interaction effect between feed rate and depth of cut, which is shown in

Fig.5.8. The increase in cutting temperature with the increase of depth of cut but the rate of temperature increment is lower at lower feed rate.

Surface roughness is an important machining response that is extremely correlated with the cutting tool wear. So, it is also influenced by the cutting temperature and force during machining. The performance and life of a product highly depend on its surface integrity. The tool-work combination and cutting parameters affect the surface roughness directly. The main effect plot for surface roughness concerning input factors (cutting parameters, nanoparticle concentration and tool-type) has been illustrated in Fig.3.7. At high speed, thermal softening can happen and for this reason, the cutting force required for machining was reduced, which indirectly reduce the roughness of the machined surface. Additionally, BUE removal at a higher speed helps to reduce the roughness [Mia and Dhar, 2016]. A similar finding was previously reported during the machining of Ti-6Al-4V [Che-Haron and Jawaid, 2005]. Feed rate affects the most on roughness. Because a higher feed rate produced a higher amount of feed tool mark, which is a key cause for surface roughness [Thandra and Choudhury, 2010]. Similar results were claimed in previous literature during turning Ti-6Al-4V [Nithyanandam et al., 2015].

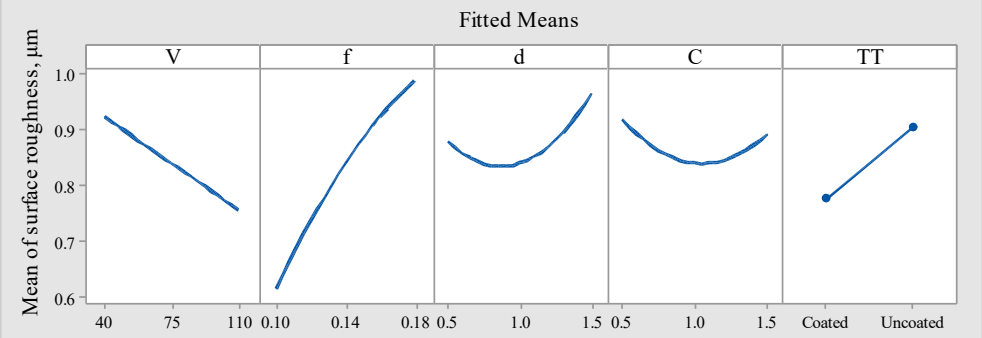


**Fig.3.7** Main effect plot for surface roughness

Usually, roughness increases with the increase of depth of cut and at lowest roughness are achieved for the lowest depth of cut. But, if the depth of cut is less than the nose radius of the tool, then a vibration in the tool may occur which is responsible for the higher roughness. In this research, turning by 0.5 mm of the depth of cut (< nose radius 0.8), the higher surface roughness of the product was achieved. For 1 mm of the depth of cut vibration became stable and roughness was reduced. After that, 1.5 mm of the depth of cut, roughness has increased again. For higher material engagement higher machining vibration could occur. This type of incident was also evident in different works [Vijay and Krishnaraj, 2013]. With the increase of nanoparticle concentration, the roughness is

reduced due to its polishing and mending effect [Virdi et al., 2020]. Reduced friction at the work-tool interface due to rolling and formation of the surface protecting film may also help to improve roughness. But after a specific C, nano-particles act as abrasives during the cutting and affect negatively the surface finish [Lee et al., 2017]. In this research, work roughness was reduced up to around 1% but then roughness was increased with the increase of nanoparticle concentration. Roughness was increased by around 6% when the particle concentration was increased from 1% to 1.5%. This may be due to the sedimentation of an excess particle, which restricts the fluid to enter the chip-tool and work-tool interfaces. Similar findings have been identified by Srikant et al. [2014].

Coating material acts as a solid lubricant on the carbide insert and reduces the friction between the chip-tool and work-tool interfaces. Chips easily slide off the coated tool rake surface which reduces heat generation and also reduces frictional force. Additionally, the coatings act as thermal and chemical insulation for the carbide tool, which prevents the heat to diffuse into the tool and reduces tool temperature. The higher force and temperature for the uncoated tool can cause higher tool wear [Qin et al., 2016], which is responsible for higher surface roughness when the cutting parameters are fixed. In this work, the surface roughness produced by the coated carbide tool is less compared to the uncoated carbide tool for the same machining conditions. From the main effect plot, it can be revealed that the average surface roughness obtained by using the coated carbide insert is 0.77 μm, whereas, for the uncoated carbide insert the average surface roughness is 0.9 μm. In previous research, the dry turning of Ti6Al4V alloy roughness for all combinations of cutting parameters by coated carbide is less than the uncoated tool [Patil and Sawant, 2014]. There is no significant interaction effect of the input parameters for surface roughness.

## 3.2 Optimum Process Parameters Selection by Desirability Approach

Process parameters optimization in manufacturing is very important because it emboldens productivity enhancement, time-cost reduction, hazard-free operation [Xiong et al., 2016]. Recently the concept of optimization becomes very popular due to achieve economical and environmental sustainability in manufacturing [Abubakr et al., 2020].

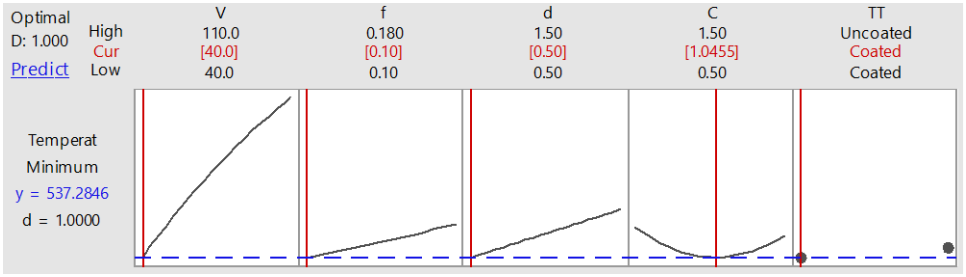


(a)

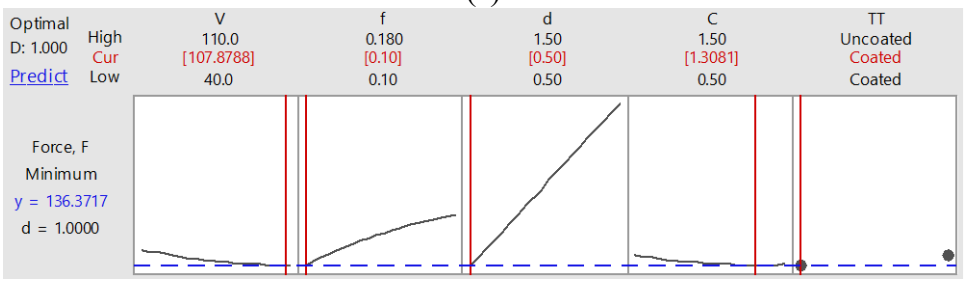


(b)

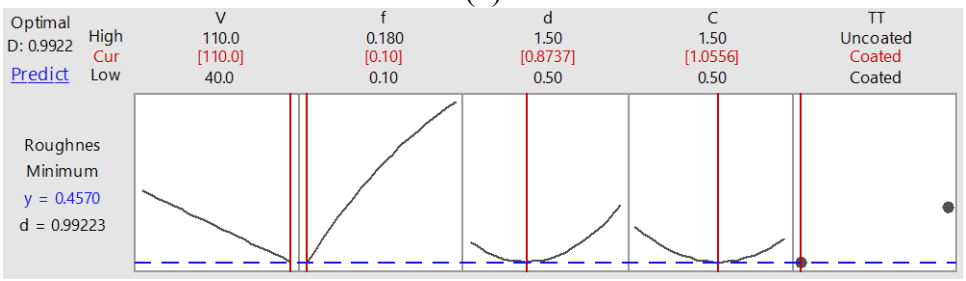


(c)

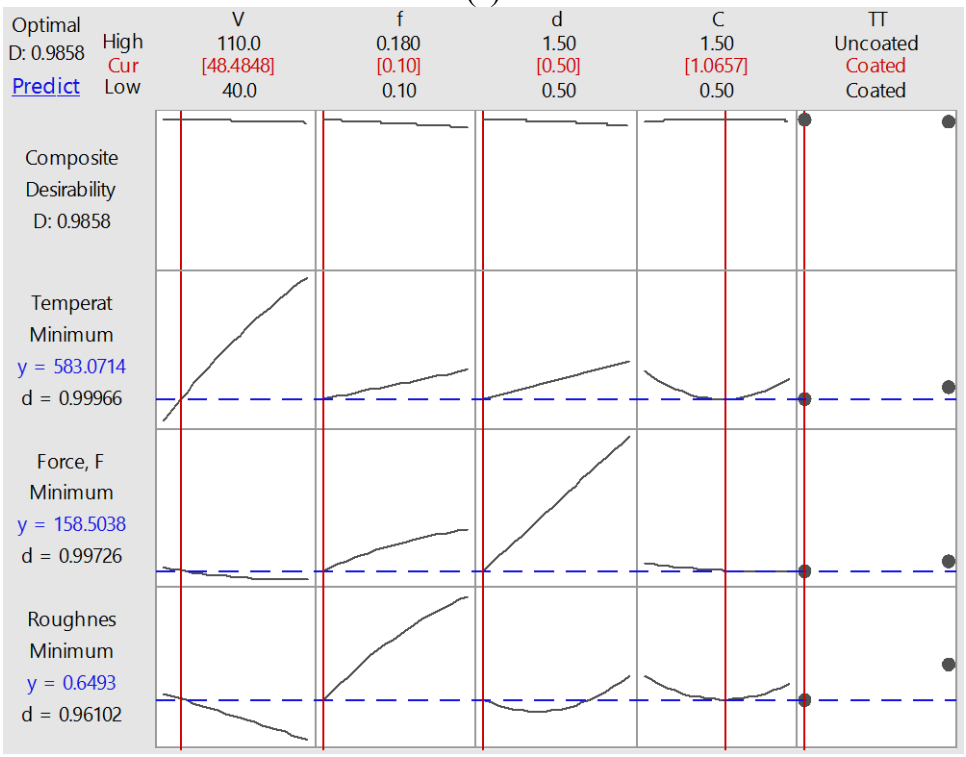


(d)

**Fig.3.8** Process parameters optimization considering (a) cutting temperature, (b) cutting force, (c) surface roughness and (d) multiple responses.

Moreover, multi-response optimization is very common in any engineering problem and it facilitates improving the system performance on the whole [Amrita et al., 2020]. The desirability-based RSM approach was selected for the optimization purpose of this research. Using the 'RSM Response Optimizer' of MINITAB 17, the combination of process inputs has been identified for the minimum value of temperature and roughness individually and simultaneously based on their empirical models. A composite desirability-based approach has been used in this research for a single objective and multiple objectives parameters optimizations. The weight and importance values can be assigned within a range of 0.1~10. In this work, weight and importance values for all the responses have been assigned as 0.1 and 1 respectively. The lowest and equal weight was selected as it provided the highest composite desirability. As well as the relative importance of different responses was considered to be equal. Here, any equal value of relative importance for all the responses provides the same results. Based on the authors' previous work the above-mentioned values were selected [Zaman and Dhar, 2021]. The optimization plots for selecting the optimum process parameters settings have been shown in Fig.3.8. From Fig.3.8 (a) it can be concluded that for achieving minimum cutting temperature 40 m/min of speed, 0.1 mm/rev of feed rate, 0.5 mm of the depth of cut, 1.0455 vol % of nano-particle concentration and coated tool-type were required. For minimum cutting force 107.88 m/min of speed, 0.1 mm/rev of feed rate, 0.5 mm of the depth of cut, 1.3081 vol % of nano-particle concentration and coated tool-type were found favorable and presented in Fig.3.3 (b). Additionally, in Fig.3.3 (c), 110 m/min of speed, 0.1 mm/rev of feed rate, 0.8737 mm of the depth of cut, 1.0556 vol % of nano-particle concentration and coated tool-type were detected to produce minimum surface roughness. On the other hand, when these three conflicting objectives have to be minimized concurrently, then a trade-off among these single optimization results is required. Finally, Fig.3.3 (d) reveals that 48.48 m/min of speed, 0.1 mm/rev of feed rate, 0.5 mm of the depth of cut, 1.0657 vol % of nano-particle concentration and coated tool-type were appropriate for minimizing temperature, force and roughness concurrently. In the case of multi-objective optimization individual desirability of temperature, force and roughness were 0.999, 0.997 and 0.961 respectively, which confirms that these settings of parameters were homogeneously effective for achieving all of the objectives. Composite desirability of 0.9858 was achieved by the final optimization, which is very close to 1 indicates that this setting can acquire favorable results for optimizing multiple responses altogether [Ola et al., 2019].

# Chapter 4

## Numerical Evaluation of Cutting Temperature and Chip

Finite Element Modeling (FEM) is one of the most popular numerical modeling approaches for metal cutting in recent times. In 1973 Klamecki developed the first FE models for the metal cutting process [Klamecki, 1973]. After that FEM has been progressively utilized for simulating different metal cutting processes. Various output responses such as the cutting force, stresses, tool wear, temperatures, chip geometry, etc. can be predicted by FEM with reasonable accuracy. Efficient quantitative and predictive models that establish the relationship between a big group of independent parameters and output variables have reduced the burden of extensive experimentation in understanding the behavior of machining. Finite element modeling is one of the effective and efficient modeling techniques by which a wide spectrum of manufacturing processes, cutting tools and engineering materials currently used in the industry can be modeled and it is the subject of intense research nowadays. Various numerical research in which serrated chip formation, cutting temperature, cutting force, tool wear and surface roughness during machining of hard-to-cut material Ti-6Al-4V alloy under various environments have already been carried out.

Chip morphology and segmentation during the machining of titanium alloys is necessary to study because it plays a most important role in determining machinability. Serrated chips cause serious vibrations and cyclic cutting force during machining. The thermo-mechanical behavior at the workpiece/tool interface is also influenced by chip morphology, which in turn affects the tool life. Hua and Shivpuri [2004] formulated and experimentally validated an FE model for chip formation and segmentation. Wang and Liu [2014] also develop a chip formation model for high-speed machining of Ti-6Al-4V alloy. Finite element analysis software ABAQUS /Explicit was used, in which the Johnson-Cook (JC) fracture model with an energy-based ductile failure criterion is adopted. The influence

of material constitutive models and finite element formulation on serrated chip formation for modeling of machining Ti-6Al-4V titanium alloy is investigated by Özel et al. [2010]. The finite element model was validated with the orthogonal cutting experiments with uncoated carbide tools using measured cutting forces and chip morphology. A FE model aiming to study of constitutive parameters definition effect on simulation of the machining of Ti-6Al-4V alloy has been proposed by Yaich et al. [2017]. Serrated chip segmentation frequency, chip curvature radius, shear band spacing, chip serration sensitivity and intensity, accumulated plastic strain in the formed chip segments, and cutting forces levels were determined. A numerical model developed in ABAQUS/explicit by Miguélez et al. [2013]for analyzing the adiabatic shear banding in orthogonal cutting of Ti-6Al-4Valloy. Due to adiabatic shear banding, segmented chips are formed, depending on thermal softening and strain and strain rate hardening. The consequences of cutting velocity and feed in the chip segmentation were analyzed. The effect of the sliding friction coefficient at the tool-chip interface on the chip segmentation and cutting force and the effect of rheological parameters of the constitutive equation on shear flow stability and chip morphology have been investigated.

Nikawa et al. [2016], have formulated a FEM simulation for the orthogonal cutting of Ti-6Al-4V alloy by using DEFORM-2D and AdvantEdge which were commercial software. Johnson-Cook‘s model was used for a flow stress equation of material suitable for milling simulation of Ti-6Al-4V. The calculated results of the chip shape and tool temperature were found to be similar to the actual value. Zhang et al. [2015] performed a numerical analysis for predicting chip geometry, chip compression ratio, forces (cutting force and thrust forces) and the distributions of temperature and equivalent plastic strain during orthogonal machining of the Ti-6Al-4V. Zanger and Schulze [2013] have developed a Finite element model for the machining of Ti-6Al-4V alloy with uncoated carbide (WC/Co) by using a self-developed continuous re-meshing method to form segmented chips. Different responses that are generally influencing the tool wear in machining, like stresses, temperatures and relative velocities between the tool face and the chip along the cutting tool were investigated. Finite element models for cutting Ti–6Al–4V alloy under dry and different cooling environments have been done by various researchers [Rui et al., 2014; Zhang et al., 2011]. Jamaluddin et al. [2017] have developed a finite element model (DEFORM™-3D) to analyze the tribological and thermal effects of the minimum quantity lubrication in turning of mild steel by TiCN-

coated cermet tool in terms of cutting force and cutting temperature and further verified experimentally. MQL friction coefficient and chip thickness were obtained from the experiment. Heat convection coefficients based on the MQL types are used in the model. The model could be applied for estimating the cutting temperature and cutting force with a high degree of accuracy. Hegab et al.[2019] formulated an FE model to simulate the thermal characteristics of nanofluid-based MQL in turning Ti-6Al-4V. Pervaiz et al. [2015] was a temperature model by DEFORM-3D for Ti-6Al-4V alloy machining. Numerical metal cutting simulation under nanofluid conditions is very rare. Sharma et al. [2018] formulate a numerical model to predict temperature over the cutting tool with $Al_2O_3$-MWCNT hybrid nanofluid in turning AISI 304 steel by coated cemented carbide insert. In this chapter, a finite element model (FEM) has been developed to observe chip morphology and temperature distribution in turning Ti-6Al-4V alloy by carbide insert under various cooling environment (Dry, MQL with cutting oil and MQL with hybrid nanofluid). A fully coupled thermal-stress analysis module of ABAQUS/Explicit version 6.14 has been employed to perform the analysis. ABAQUS is one of the various commercial FEM software packages has been popularly used for metal cutting simulation [Priyadarshini et al., 2012]. In ABAQUS, there is no specific module for machining simulation. Users have to define the tool and the workpiece geometry and material explicitly. Process parameters and simulation controls (boundary condition and mesh geometry) also have to define by the user. Several input values are demanded by FEM commercial software to predict the thermomechanical behavior of the machining process. The values of different input parameters of the FE model which can represent the actual deformation behavior during the metal cutting process efficiently confirm the accuracy of the FE model.

## 4.1 Temperature and Chip Formation Modelling Using FEM

In this research, an ALE FE model has been built to simulate the turning process of Ti-6Al-4V by carbide insert under various cooling conditions. From the actual machining viewpoint, the FE model is a restrictive approach that requires less computational time significantly and offers satisfactory results.

**Workpiece and Tool Modeling:** The 2D FE model comprises only a small segment of the workpiece and cutting tool which takes part in turning. A plane strain condition has been assumed because the feed rate value is generally very less as compared to the depth of cut.

In this study thermo-visco-plastic behavior of the workpiece has been expressed using the J-C constitutive material model. This model can be used to describe material behavior in the plastic regime over large strains, high strain rates and high temperatures [Duan et al., 2009]. The flow stress can be expressed as:

$$\sigma=(A+B\varepsilon^{n})\left[1+C\ln\left(\frac{\dot{\varepsilon}}{\dot{\varepsilon}_{o}}\right)\right]\left[1-\left(\frac{T-T_{R}}{T_{M}-T_{R}}\right)^{m}\right] \quad \text{.....} \quad \textbf{(4.1)}$$

where,

ε = equivalent plastic strain

$\dot{\varepsilon}$= strain rate normalized with a reference strain rate $\dot{\varepsilon}_{0}$

T = instantaneous temperature

$T_M$ = melting temperature

$T_R$ = reference temperature

Here, the first bracketed term called elastoplastic term represents strain hardening of the yield stress that is given the stress as a function of strain. The next term (visco-plasticity term) models the increase in the yield stress at elevated strain rates and the final term is softening of the yield stress due to local thermal effects. The above yield strength portion of the J-C model has five material constants. A is the yield stress, B and n represent the effect of strain hardening determine $\dot{\varepsilon}_{0}$. C is the strain rate constant. A, B, C, n and m are measured at $T_R$ or below $T_R$.

Moreover, the J-C damage model was used for initializing the chip separation. This model is suitable for progressive damage to high strain rate deformation such as high-speed machining. According to the J-C damage criterion the expression for fracture strain is:

$$\varepsilon^{f}=\left(D_{1}+D_{2}\exp D_{3}\frac{\sigma_{m}}{\bar{\sigma}}\right)\left(1+D_{4}\ln\frac{\dot{\varepsilon}}{\dot{\varepsilon}_{o}}\right)\left(1+D_{5}\frac{T-T_{R}}{T_{M}-T_{R}}\right) \quad \text{.....(4.2)}$$

where,

$D_1$= Initial fracture strain

$D_2$= Exponential factor

$D_3$= Triaxiality factor

$D_4$= Strain rate factor

$D_5$= Temperature factor

$\sigma_m$= Average of the three normal stress

$\bar{\sigma}$= Von-Mises equivalent stress

Here the first, mid and last bracketed term in the J-C damage model includes the effect of stress triaxiality, strain rate and local heating respectively. Damage initiation begins according to standard damage law,

$$W = \sum \frac{\Delta \varepsilon}{\varepsilon^f} \quad \text{(4.3)}$$

where W is the damage parameter and Δε is the accumulated increment of equivalent plastic strain during an increment step. According to this model, damage initiation is followed by the damage evolution criterion which governs the propagation of plastic strain until an ultimate failure happens. For crack initiation, the fracture energy was used as damage evolution. In the following Table, Johnson-Cook model parameters and progressive damage model parameters for Ti-6Al-4V alloy have been presented.

**Table 4.1** Johnson-Cook model and progressive damage parameters for Ti-6Al-4V [Wang and Liu, 2014]

| Johnson-Cook model parameters | | Johnson-Cook progressive damage parameters | |
|---|---|---|---|
| A (MPa) | 862 | $D_1$ | -0.09 |
| B (MPa) | 331 | $D_2$ | 0.25 |
| C | 0.012 | $D_3$ | -0.5 |
| n | 0.34 | $D_4$ | 0.014 |
| m | 0.8 | $D_5$ | 3.87 |
| $T_{melt}$ (°C) | 1878 | - | - |

The thermal and mechanical properties of Ti-6Al-4V, tungsten carbide and coating materials (TiN, TiCN, $Al_2O_3$) adopted in the numerical models are given in Table 7.2 and 7.3. In this research, multiple-layer coatings are represented by a composite single layer. _Equivalent‘ coating properties of the composite layer have been calculated according to the method utilized in a study by Yen et al. [2004] and defined as the coating properties.

**Table 4.2** Material properties of Ti-6Al4V alloy [Wang and Liu, 2014]

| Density, ρ ($Kg/m^3$) | Elastic modulus, E (GPa) | Poisson‘s ratio, ν | Thermal conductivity, λ (W/m/°C) | Specific heat, Cp (J/kg/°C) |
|---|---|---|---|---|
| 4,430 | 109 (323 K) | 0.34 | 6.8 (293 K) | 611 (293 K) |
| | 91 (523 K) | - | 7.4 (373 K) | 624 (373 K) |
| | 75 (723 K) | - | 9.8 (573 K) | 674 (573 K) |
| | - | - | 11.8 (773 K) | 703 (773 K) |

**Table 4.3** Material properties of tool substrate and coatings [Fahad et al., 2011]

| Materials | Density, ρ (Kg/m$^3$) | Thermal conductivity, λ (W/m/°C) | Specific heat, Cp (J/kg/°C) |
|---|---|---|---|
| Tungsten Carbide | 14700 | 100 | 203 |
| TiN | 5420 | 21 (373 K) | 702.6 (373 K) |
| | | 22 (573 K) | 783.4 (573 K) |
| | | 23 (773 K) | 818.9 (773 K) |
| TiCN | 4180 | 29 (373 K) | 1030 (373 K) |
| | | 30.6 (573 K) | 1040 (573 K) |
| | | 32 (773 K) | 1120 (773 K) |
| $Al_2O_3$ | 3780 | 17 (373 K) | 903 (373 K) |
| | | 12.5 (573 K) | 1089 (573 K) |
| | | 7.75 (773 K) | 1176 (773 K) |
| Composite layer | 4268 | 21.35 (373 K) | 913.72 (373 K) |
| | | 18.46 (573 K) | 1008.28 (573 K) |
| | | 14.95 (773 K) | 1082.18 (773 K) |

With the above mentioned properties, the material directory has been created for the analysis. The geometry of the workpiece and tool have been sketched considering the real dimension and the materials have been assigned. Then the geometry of the assembly was defined by creating instances of a part and positioned the instances relative to each other in a global coordinate system. Afterward, instances were merged to create a total metal cutting model. Fig.4.1 shows the assembly model of the work piece-tool.

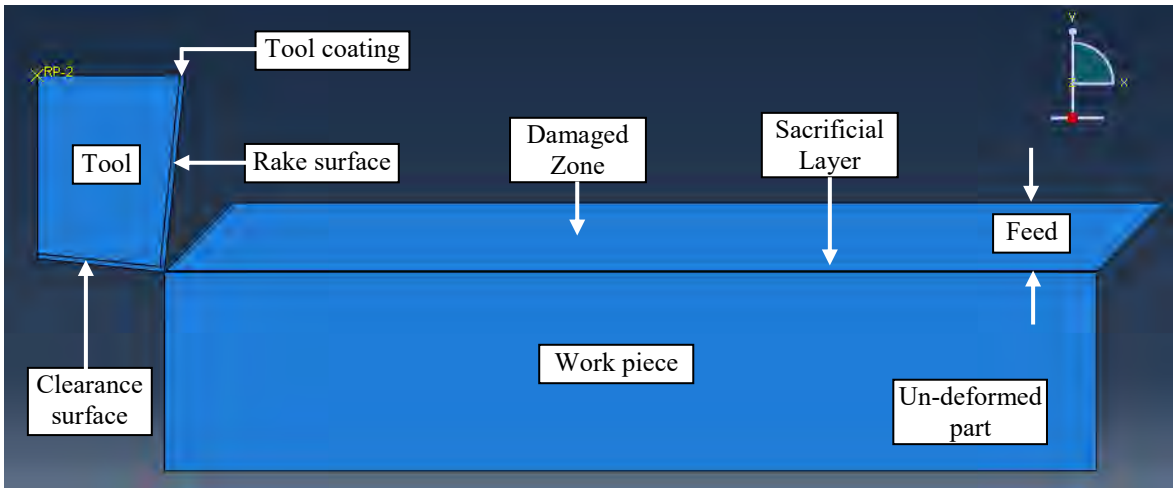


**Fig.4.1** Assembly model of work piece-tool

An intermediate layer known as the sacrificial layer has been considered in the workpiece. This layer defines the path of separation between the chip back surface and machined surface which is going to take place with the tool progression. The upper portion of this layer is equal to the uncut chip thickness or feed for the 2D simulation modeling. In this particular machining process, two edges of the tool are involved in cutting, such as the

rake face and clearance face. At the two faces, a negative rake angle of $6^{o}$ and a clearance angle of $6^{o}$ were drawn as real geometry of the cutting tool. The applied mesh consisted of CPE4RT elements with plane strain conditions. CPE4RT means 4 node bilinear displacement and temperature, reduced integration with hourglass control. The tool is composed of the CPE4RT and some triangular elements, but of variable length. The mesh distribution of the assembly is shown in Fig.4.2, where the different densities can be seen.

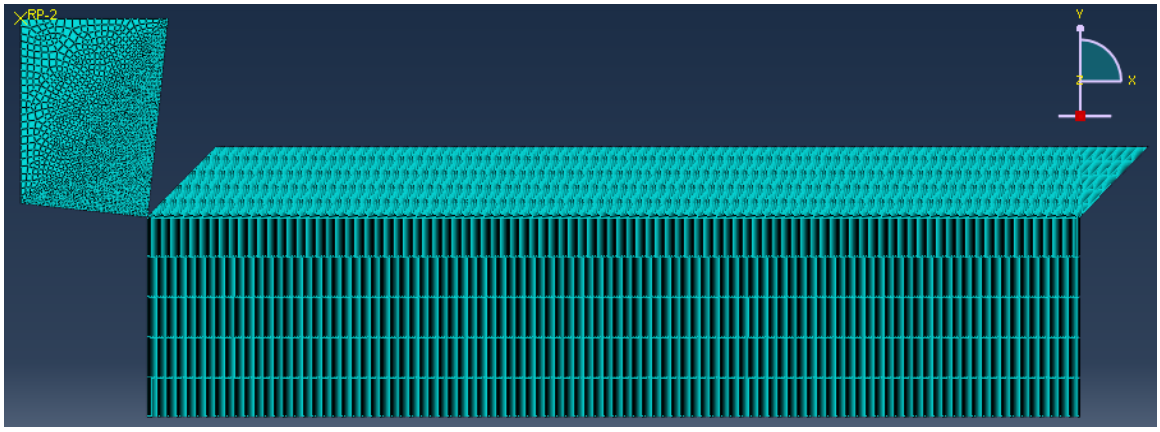


**Fig.4.2** Mesh structure of workpiece and tool

**Interaction Modeling:** Mechanical and thermal interaction between the tool and workpiece was modeled with a surface-to-surface contact. It consists of two surfaces expected to come into contact during the tool-workpiece interaction. These contact surfaces are designated by the master surface (edges of a tool) and node-based slave surface (node region of the top portion of the workpiece). Further, a self-contact was assigned to the top edge of the workpiece due to considering the possibility of the chips can be folded onto themselves during high deformation. Both types of contacts are shown in Fig.4.3. In this study, the contact areas have been modeled based on Coulomb‘s friction law, which is widely used in metal cutting simulations [Özel, 2006]. In the previous studies, friction coefficient 0.2 [Zhang et al., 2015], 0.3 [Shao et al., 2010], 0.5 [Sima and Özel, 2010], etc have been used when machining Ti-6Al-4V ally by carbide insert under dry condition. In this analysis, the friction coefficient has been selected within 0.2~0.5 for dry machining. Heat radiation and convection were neglected in the cutting model, as they are negligible compared to conduction. High speeds allow no time for heat transfer between integration points with which the process is treated as an adiabatic process. In this work, 100% of the frictional energy has been supposed to be transformed into heat and the fraction of heat distributed to the tool has been considered here as 0.75 for Ti-6Al-4V alloy machining by carbide tool, which is based on previous research. Tanveer et al. [2017]

showed that in machining Ti-6Al-4V alloy by carbide insert with 80 m/min, around 75% heat is transferred to the tool. A wide range of thermal conductance between 20 ~$10^4$ W/$m^2$/K at the tool-workpiece contact surface was utilized by different researchers [Sadeghifar et al., 2018]. Here, the thermal conductance value for turning Ti-6Al-4V alloy by coated and uncoated carbide inserts was used within this range. This conductance was imposed for the distance in the contact pair is less than $10^{-7}$ m.

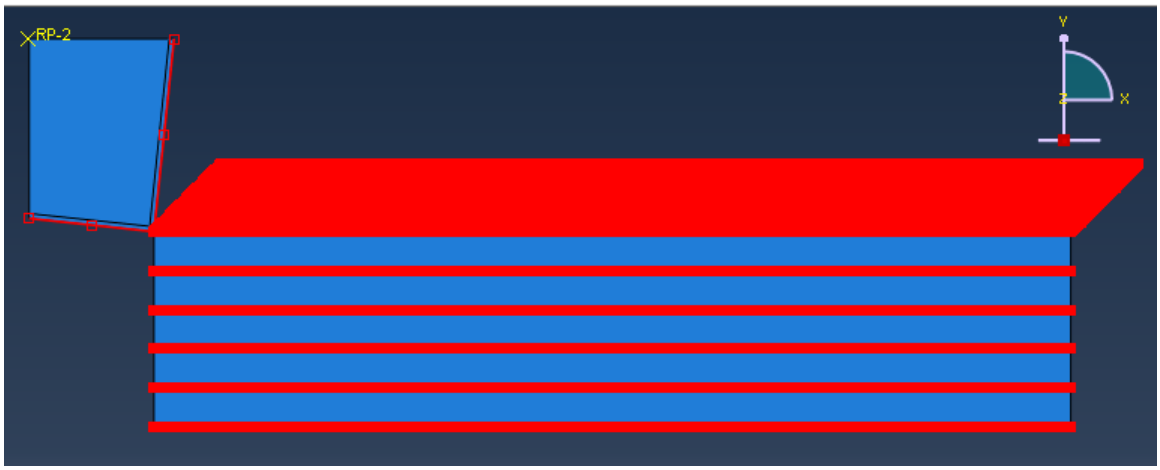


(a) Surface to surface contact

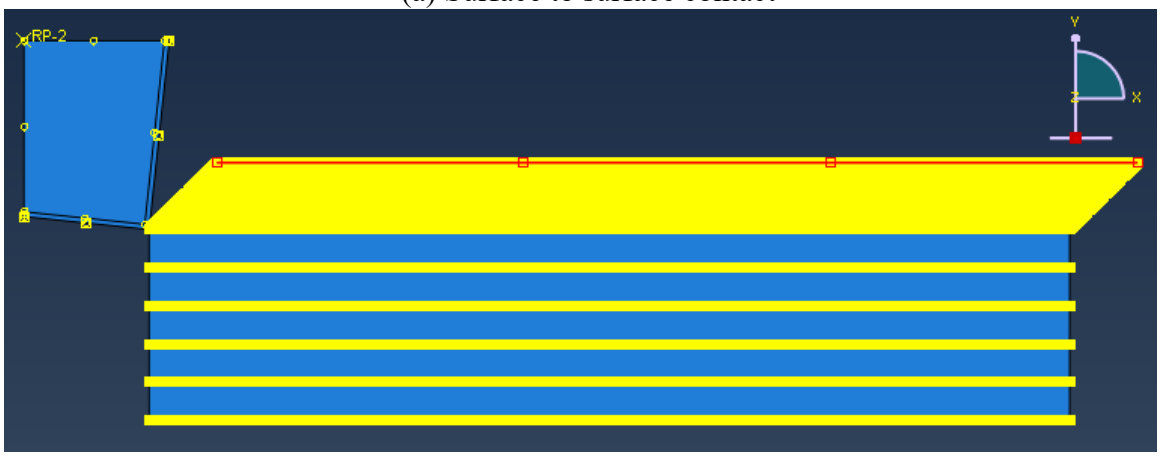


(b) Self-contact

**Fig.4.3** Contact model of workpiece and tool (a) Surface to surface contact and (b) Self-contact

In the case of MQL application with different coolants, the effect of the mist jet has been integrated into the model by a convective heat-transfer coefficient [Jamaluddin et al., 2017]. For this case, a surface film condition interaction in addition to thermal/ mechanical contact was generated and applied on the rake and flank surfaces of the cutting tool which are expected to come into contact with the workpiece during machining. The MQL effect was modeled by setting surface film conditions at the tool rake and flank surfaces. The

local temperature inside was set equal to 25 °C. The surfaces for the surface film interaction are highlighted in Fig.4.4.

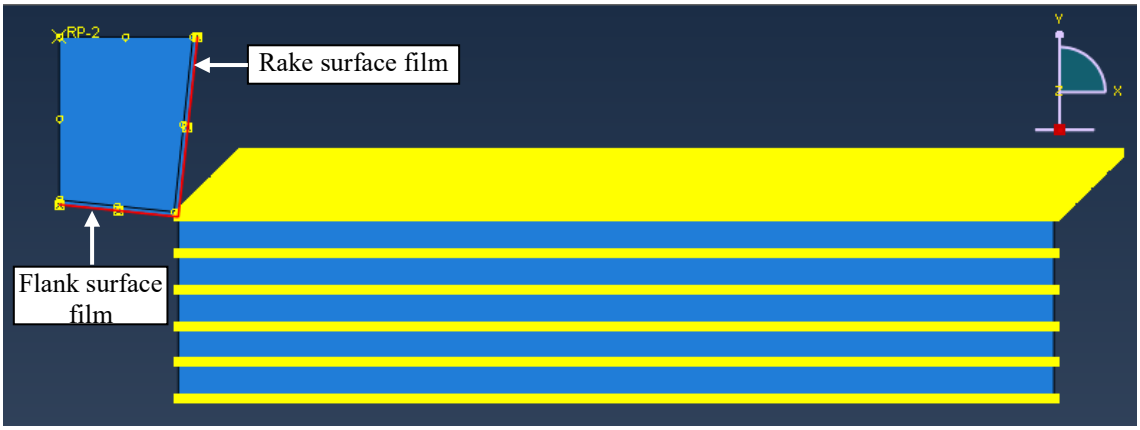


**Fig.4.4** Surface film condition for MQL at rake and flank surface of the tool

The VG 68 cutting oil and hybrid nanofluid was used as an MQL fluid in this study. Fluids have been mixed with compressed air and applied as a fine mist into the interface. Therefore, to study the effect of MQL, mist with cutting oil and hybrid nano-fluid characteristics have been calculated considering 50:50 air and oil mixture. The necessary parameters to calculate the film coefficient of MQL mists are tabulated in Table 4.4 and 4.5. Here, the properties of nano-fluid have been calculated theoretically or experimentally determined.

**Table 4.4** MQL fluid thermo-physical characteristics

| Parameters | VG 68 cutting oil | Hybrid nanofluid (1 vol %) | Air |
|---|---|---|---|
| Density ρ (kg/m3) | 850 | 876.82 | 23.48 |
| Dynamic Viscosity μ (N-s/m2) | 0.061 | 0.09 | $1.81\times10^{-5}$ |
| Thermal conductivity λ (W/m/°C) | 0.161 | 0.208 | $2.70\times10^{-2}$ |
| Specific heat, Cp (J/°C/kg) | 1670 | 1677 | 1038 |

**Table 4.5** MQL application parameters

| Parameters | Corresponding Value |
|---|---|
| Diameter of the nozzle injector (mm) | 1 |
| Diameter of outlet nozzle (mm) | 0.5 |
| Pressure inside nozzle (bar) | 20 |
| Angle of the spray pattern | $20^{o}$ |
| Flow rate of cutting fluid (ml/hr) | 50 |

Afterward, the film coefficient utilized for this interaction condition was calculated for the cutting oil mist and hybrid nanofluid mist. The traditional correlations for forced convection use a heat transfer co-efficient (film coefficient, *h*) of the form:

$$h = \frac{k_{mist} Nu}{L_c} \quad \text{(4.4)}$$

For cylindrical workpiece, the Reynolds number (Re), Prandtl number (Pr) and Nusselt number (Nu) are given below:

$$Re_{Lc,mist} = \frac{\rho_{mist} L_c V_{mist}}{\mu_{mist}} \quad \text{(4.5)}$$

$$Pr = \frac{C_{mist} \mu_{mist}}{k_{mist}} \quad \text{(4.6)}$$

$$G(Pr) = 0.60105\ Pr^{0.333} - 0.05084 \qquad for, Pr \geq 3.0 \quad \text{(4.7)}$$

$$Nu = G(Pr) Re_{Lc,mist}^{0.5} \sqrt{B'} \quad \text{(4.8)}$$

Re depends on mist density ($\rho_{mist}$), dynamic viscosity ($\mu_{mist}$), velocity ($V_{mist}$), and characteristics length ($L_c$). $L_c$ is the distance between the nozzle and the target plane. Pr depends only on the dynamic viscosity ($\mu$), specific heat (Cp) and thermal conductivity (k) of fluid. Pr number function (G(Pr)) can be calculated by using Eq. 4.7. Nu depends on G(Pr), Re and velocity gradient ($B'$). The dimensionless velocity gradient value $B'$=1.486 has been selected from previous literature [Liu et al., 1993]. After finding out the Nu value of the cutting oil and hybrid nanofluid mist, the heat convection coefficients and film coefficient values have been calculated by utilizing Eq. 4.4. All the characteristics values for both of the mists have been given in Table 4.6.

**Table 4.6** MQL mist characteristics for different fluid

| Parameters | Base fluid mist | Hybrid nanofluid mist |
|---|---|---|
| Density ρ (kg/m3) | 436.74 | 450.15 |
| Dynamic Viscosity μ (N-s/m2) | 0.031 | 0.045 |
| Thermal conductivity λ (W/m/°C) | 0.094 | 0.1190 |
| Specific heat, Cp (J/°C/kg) | 1354 | 1357.5 |
| Prandtl number (Pr) | $4.39\times10^{2}$ | $5.20\times10^{2}$ |
| Reynolds number (Re) | 6.87 | 4.81 |
| Average Nusselt number (Nu) | 4.51 | 4.77 |
| Heat convection coefficient, h | 14.67 | 12.98 |
| Film coefficient, G | 168.70 | 192.87 |

**Simulation environment and boundary conditions:** The work-piece was modeled as an elastic-plastic body with strain hardening properties, while the tool was modeled as an

elastic body. In this work, a FEM simulation model with an ALE scheme with pure Lagrangian boundaries is designed and kinematic penalty contact conditions between the tool and the workpiece are defined. This model allows a FEM simulation scheme to simulate the chip formation from the incipient to steady-state as it was proposed by the authors in reference [Özel and Zeren, 2005]. The boundary conditions for the 2D ALE Lagrangian base model along with the geometry of the system are shown in Fig.4.5. For the boundary conditions, ENCASTRE (fully built-in) applied to the workpiece at its left and bottom surfaces, restricting the workpiece in the X and Y direction, respectively. The tool is moved against the workpiece by applying constant cutting velocity. The tool moves in the–X-direction. The element deletion technique is used to allow element separation to form a chip.

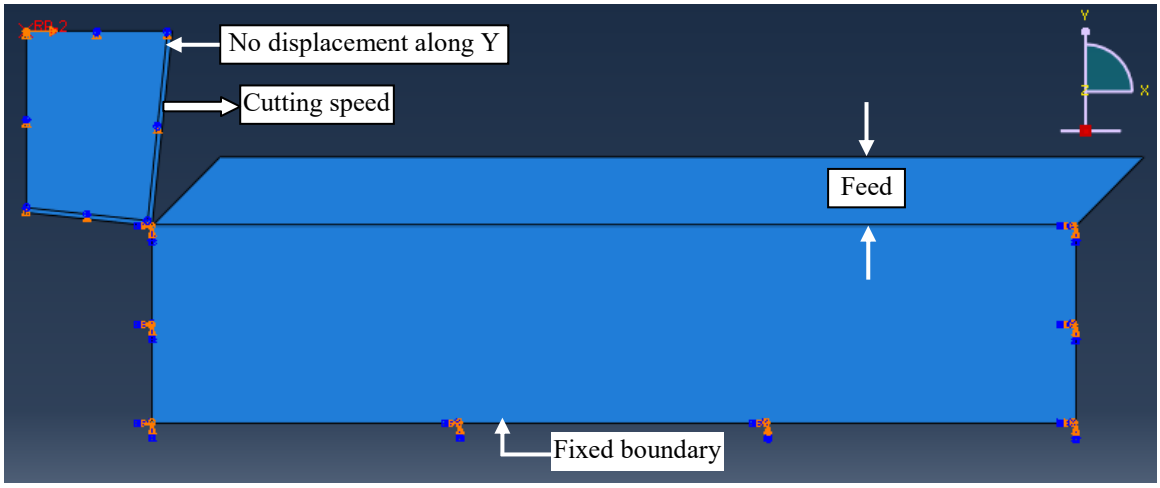


**Fig.4.5** Boundary conditions of workpiece and tool

The ALE adaptive meshing technique is used to reduce element distortion in cases of extreme deformation and applied at the top portion of the workpiece. So that, in this region the associated nodes move with the material in the direction normal to the material‘s surface and nodes are allowed to adapt (adjust their position) tangent to the free surface. The ALE re-mesh was used with a frequency of 2 and 1 re-meshing sweeps per increment. The adaptive mesh was controlled by a volume-based smoothing algorithm and the mesh motion was constrained to follow the underlying material.

## 4.2 Experimental validation of the FE model

Finite element modeling is another useful method, where the real case can be simulated to know the output responses without performing the experimental run. In this work, a 2D finite element model (FEM) for turning Ti-6Al-4V alloy by coated and uncoated carbide inserts under dry conditions, MQL with cutting oil and MQL with nano-fluid has been formulated, which was focused on chip morphology and cutting temperature distribution. The formulated FE model has been validated by comparing the simulated average chip-tool interface temperature (cutting temperature) and chip morphology with the experimental results. During the turning of Ti-6Al-4V alloy by carbide inserts under different cooling environments, the cutting speed of 73 m/min, the feed rate of 0.14 mm/rev and depth of cut of 1 mm have been used. Total 6 (six) machining runs have been carried out, which has been described in Table. 4.7.

**Table 4.7** Machining conditions for the simulation

| Runs | Environment | Cutting fluid | Cutting tool |
|---|---|---|---|
| 1 (DRY-UNCOATED) | Dry | - | Uncoated |
| 2 (CMQL-UNCOATED) | MQL | Cutting oil | Uncoated |
| 3 (NFMQL-UNCOATED) | MQL | Hybrid nano-fluid | Uncoated |
| 4 (DRY-COATED) | Dry | - | Coated |
| 5 (CMQL-COATED) | MQL | Cutting oil | Coated |
| 6 (NFMQL-COATED) | MQL | Hybrid nano-fluid | Coated |

### 7.2.1 Average chip-tool interface temperature

Fig.4.6 illustrates the temperature distribution along with the chip-tool interface under different environments and different tools. It is noticed from the figure that the cooling environment and cutting tool type have a substantial effect on the intensity and distribution of temperature when turning Ti-6Al-4V alloy. In the case of dry machining by coated and uncoated carbide inserts, a high temperature was generated. When machining with MQL, temperature intensity and distribution along the chip-tool interface is reduced compared to the dry condition for both types of tools. Additionally, compared to conventional MQL, nano-fluid-based MQL shows a lower temperature for both types of inserts.

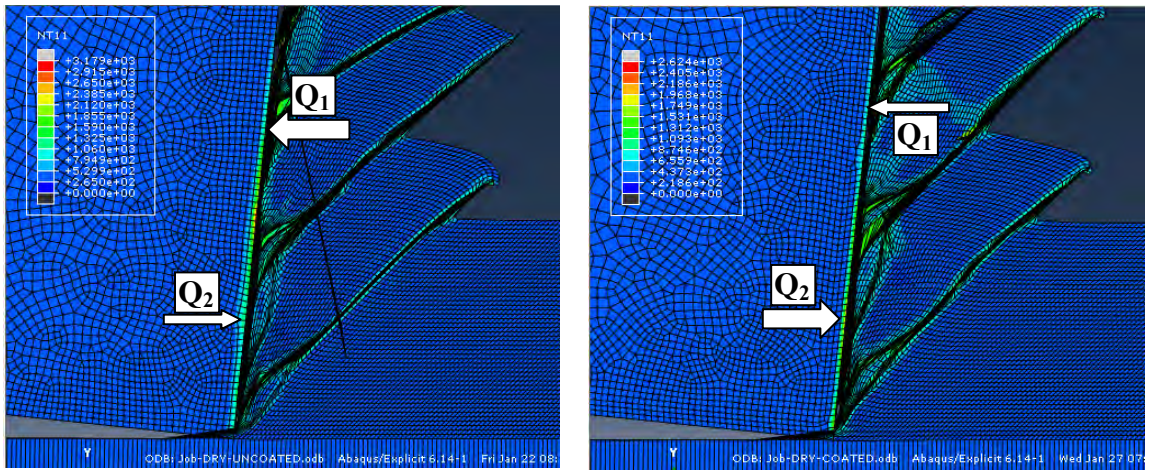


**Uncoated insert** **Coated insert**

**(a) Dry condition**

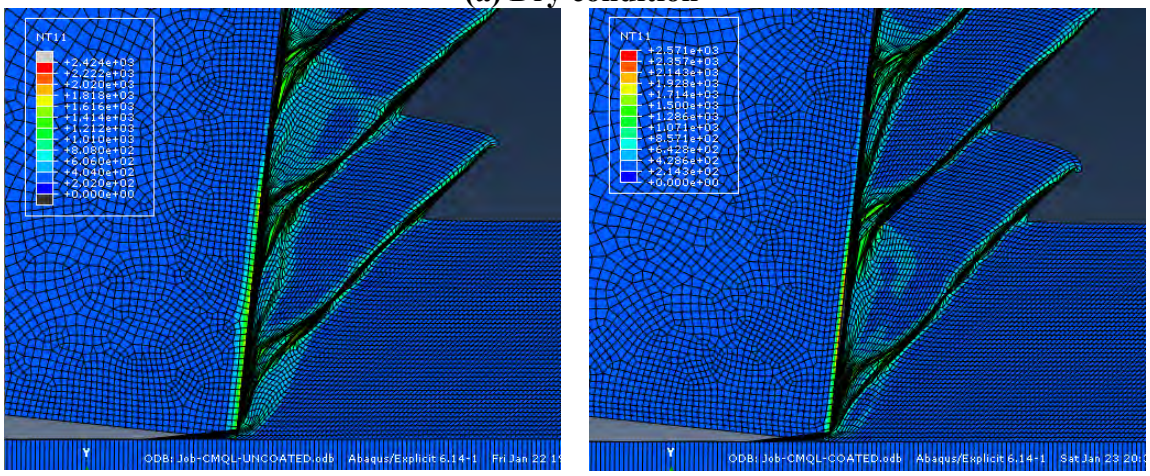


**Uncoated insert** **Coated insert**

**(b) MQL with cutting fluid**

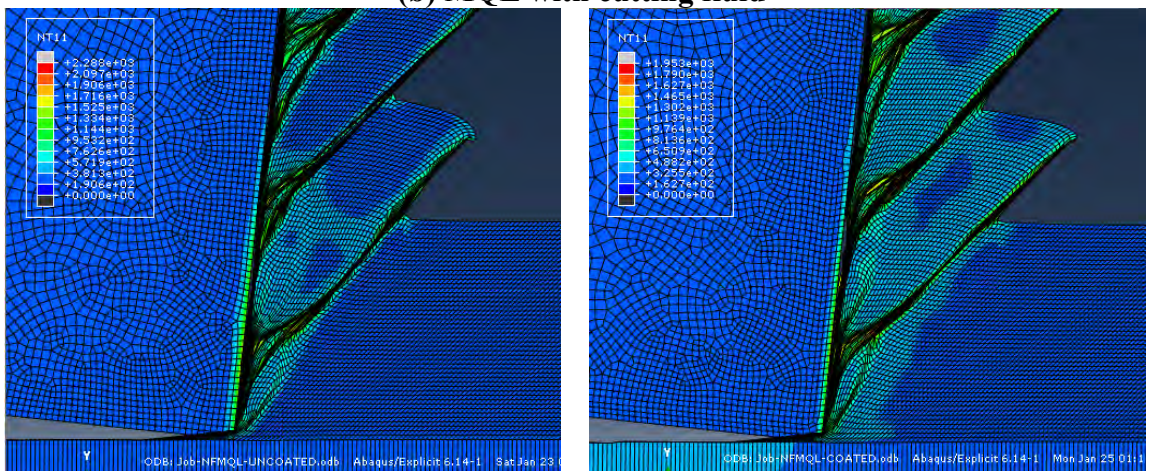


**Uncoated insert** **Coated insert**

**(c) MQL with nano-fluid**

**Fig.4.6** Chip-tool interface temperature under (a) dry, (b) MQL with cutting fluid and (c) MQL with nano-fluid conditions in turning Ti-6Al-4V alloy by uncoated and coated carbide inserts.

It can also be observed from Fig.4.6 that there is a clear difference in cutting temperature distribution when machining by the uncoated and coated carbide inserts. In the case of coated tool fraction of thermal energy towards the tool was decreased compared to the uncoated tool and heat flow towards the chip and workpiece is higher. Mechanical and thermal loads on the carbide tool were also decreased for the coating layer. Due to the low thermal conductivity of the coating layer, it acted as a thermal insulator to protect the tool substrate from penetration of the high heat generated during cutting and consequently, the tool substrate remained cooler. Whereas for uncoated tools, comparatively a higher amount of heat is transferred to the cutting tool and therefore chip-tool interface temperature rises significantly. In machining with an uncoated tool maximum temperature was observed in the tool and for coated tool maximum temperature was observed in the chip. In Fig. 4.6 $Q_1$ is the heat transferred towards the tool whereas $Q_2$ is the heat transferred towards the chip. These characteristics of the coating layer were evidenced in previous literature [Bouzakis et al., 2012; Grzesik et al., 2005].

The cooling environment during machining has a significant influence on the cutting temperature. The experimental cutting temperature has been measured for machining under various environments for different tool materials during machining by using the tool-work thermocouple technique, which measured the average chip-tool interface temperature. This average chip-tool interface temperature has been used to validate the formulated FEM. In FEM, temperature distribution at the chip-tool interface can be observed and average chip-tool interface temperature has been calculated. The variation of average chip-tool interface temperature generated during machining and FEM for turning Ti-6Al-4V alloy by uncoated and coated carbide inserts have been shown in Fig.4.7. From Fig. 4.7, it can be revealed that the simulation values are very close to the experimental values. The maximum discrepancy in average chip-tool interface temperature by uncoated and coated carbide insert was computed and found as 6.6% and 8.6% respectively, which are within the acceptable range (< 10%).

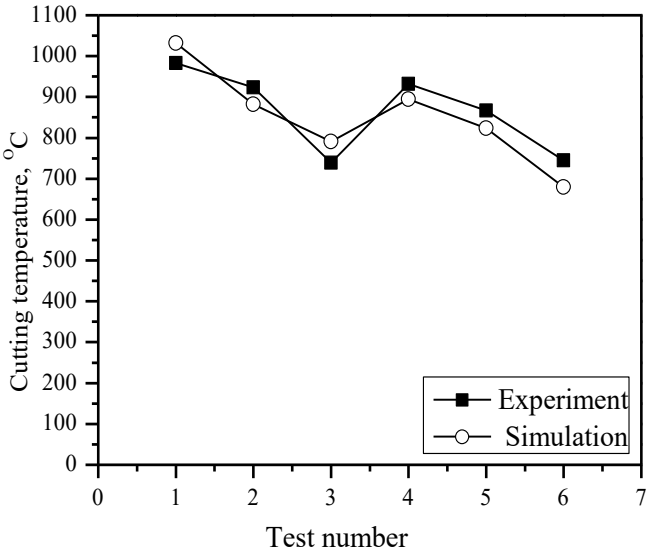


**Fig.4.7** Comparison of experimental and simulated cutting temperature for turning Ti-6Al-4V alloy

### 7.2.2 Chip morphology

Chip morphology is another important parameter for determining the machinability of Ti-6Al-4V alloy. The simulated and experimental chips (SEM) for machining under various environments for different tool materials have been presented in Fig.4.8 and Fig.4.9. When machining Ti-6Al-4V alloy by coated and uncoated insert under various cutting conditions, the serrated chip was observed in the simulation which was similar as observed in the experiment. When machining under dry condition chips was more deformed compared to the MQL machining for both types of inserts.

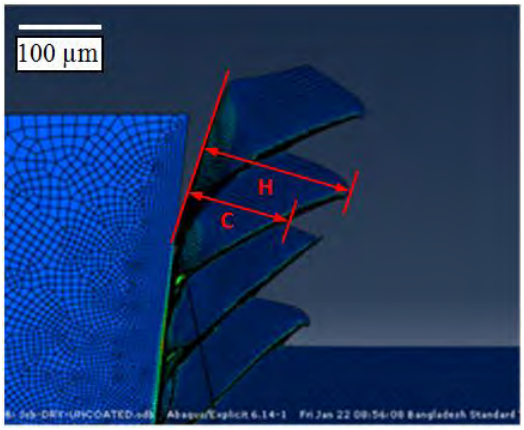


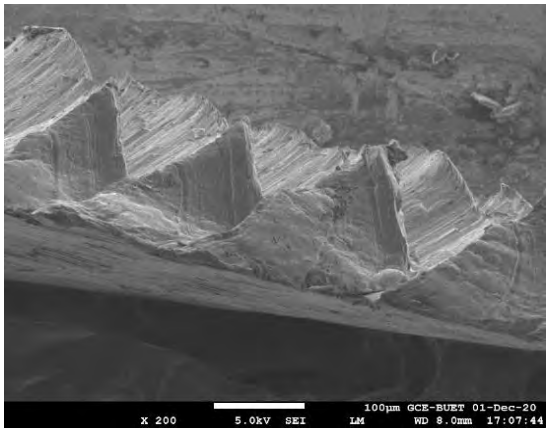


**Simulated** **Experimental**

**(a) Dry cutting**

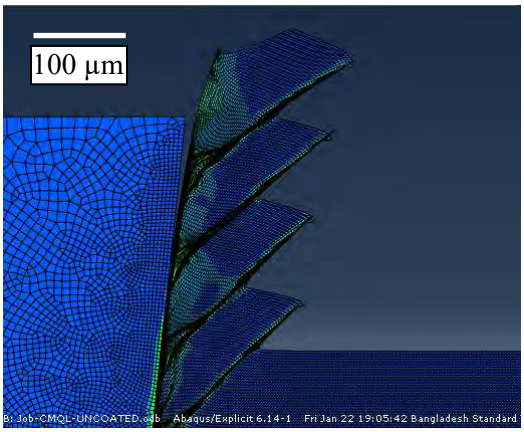


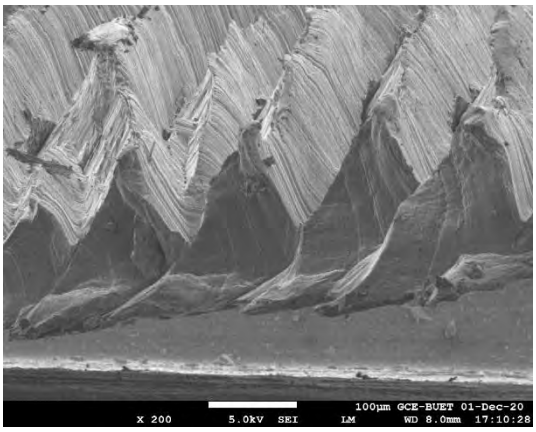


**Simulated** **Experimental**

**(b) MQL with cutting oil**

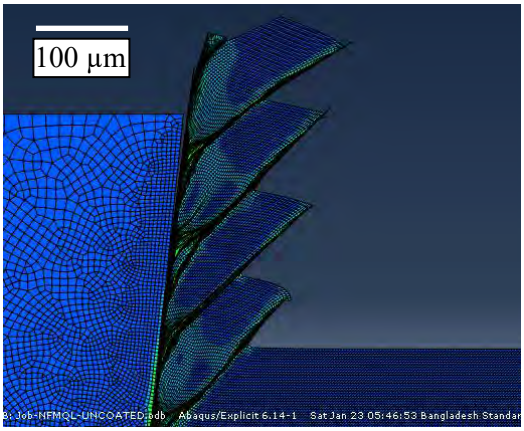


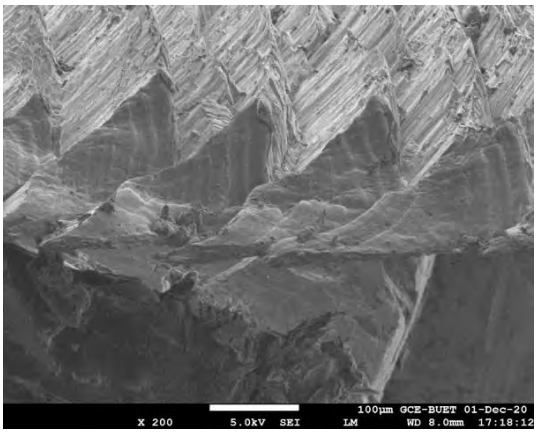


**Simulated** **Experimental**

**(c) MQL with nano-fluid**

Fig.4.8 Simulated and experimental chip morphology under (a) dry, (b) MQL with cutting fluid and (c) MQL with nano-fluid conditions in turning Ti-6Al-4V alloy by uncoated carbide insert

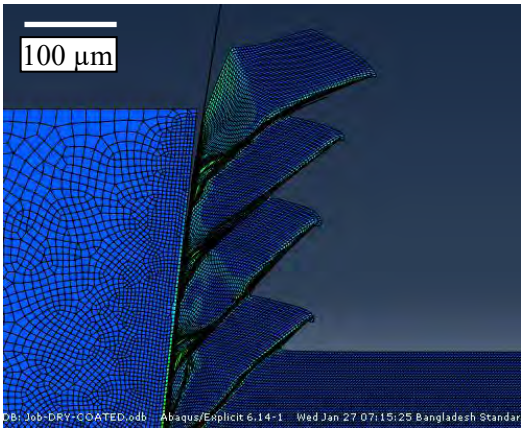


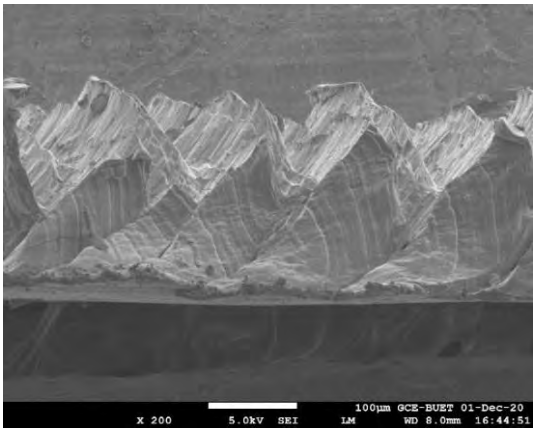


**Simulated** **Experimental**

**(a) Dry cutting**

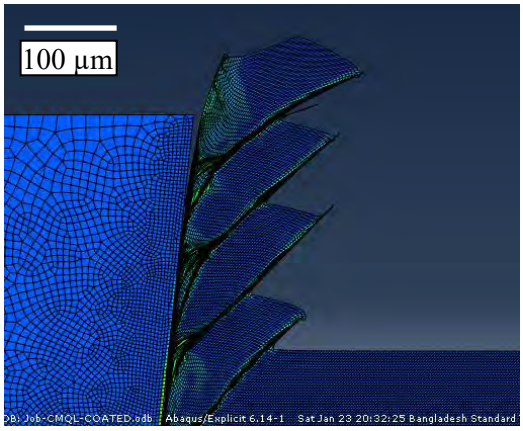


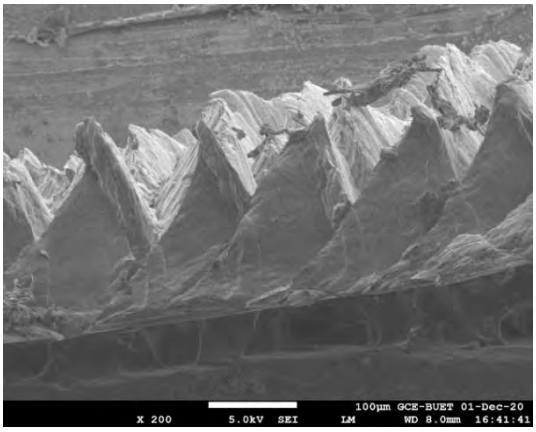


**Simulated** **Experimental**

**(b) MQL with cutting oil**

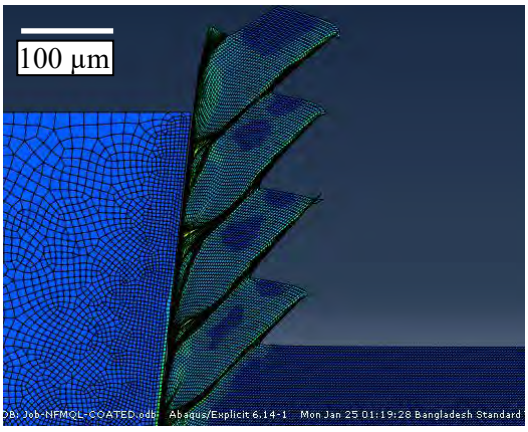


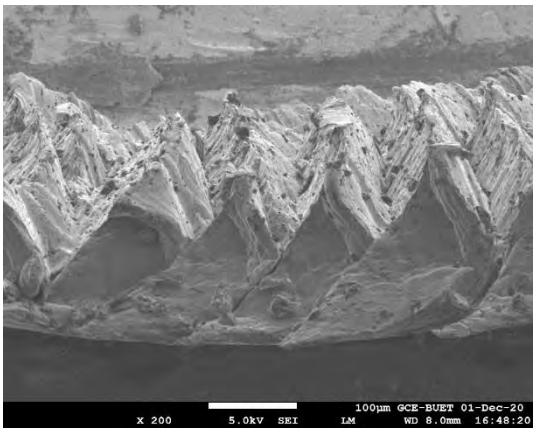


**Simulated** **Experimental**

**(c) MQL with nano-fluid**

Fig.4.9 Simulated and experimental chip morphology under (a) dry, (b) MQL with cutting fluid and (c) MQL with nano-fluid conditions in turning Ti-6Al-4V alloy by coated carbide insert

For the validity of the FE model regarding chip formation, the chip segmentation degree of the experimental and simulated chips for all the runs have been calculated and compared. Cooling environments and tool type significantly affect the chip morphology. In

Fig.4.10, the chip segmentation degree for all the experimental and simulation runs has shown.

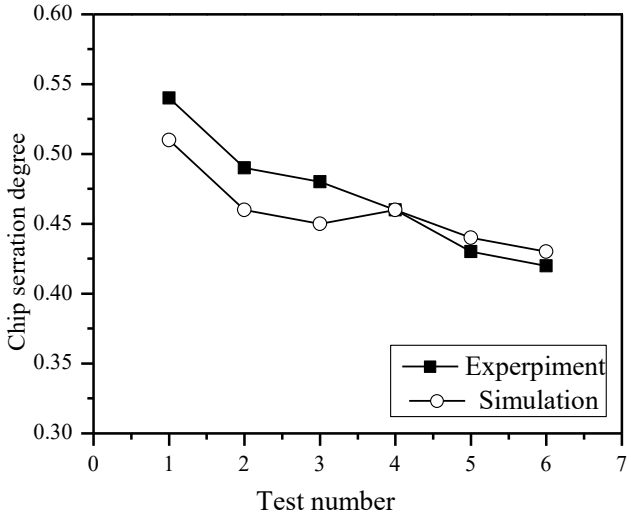


**Fig.4.10** Comparison of experimental and simulated chip serration degree for turning Ti-6Al-4V alloy

The difference between simulation experimental chip segmentation degree values is very small. The chip segmentation degree for experimental and simulated chips has been calculated by using Eq. 2.1. The maximum variation in average temperature by uncoated and coated carbide insert was calculated and found as 6.7% and 2% respectively, which are less than 10%. Based on the error analysis for cutting temperature and chip formation, it can be concluded that formulated FE model is acceptable and effective for predicting various responses with a reasonable error. These errors were found realistic for FEM-based model formulation of different manufacturing responses since similar percent error values were previously found in the literature [Zhang et al., 2019].

# Chapter 5

## Discussions on Experimental Results

MQL method is invented duo to reduce the metalworking fluid consumption by a considerable amount, which confirms the environmental safety and also reduces the expense of coolant/lubricant. Besides being eco-friendly and economical, MQL is an easy to handle and effective method for various operations [Da Silva et al., 2017; Ezugwu et al., 2019]. MQL method can be considered as a promising alternative to conventional cooling and dry machining. Though, flood cooling, HPC, cryogenic cooling was efficiently utilized during machining but, due to their respective problems simple MQL technique gained popularity over other techniques. Machining under the MQL method is far better than dry machining and its performance is similar or sometimes better than the conventional wet cooling method [Morgan et al., 2012].

In conventional flood cooling huge amount of oil is used but in the case of high-speed machining, coolant can‘t reach the chip-tool and work-tool interfaces due to the low speed of the liquid flow. In the MQL method, an aerosol is formed by mixing a very tiny amount of cutting fluid with the compressed air and applied towards the cutting zone by an external nozzle or internally through the tool [Ekinovic et al., 2015]. High-velocity aerosol can break the vapor blanket formed near the cutting zone and reach the heat-affected zone [Varadarajan et al., 2002], where the aerosol can effectively reduce the frictional temperature and frictional coefficient of the matting surfaces through the formation of oil films [Duc and Long, 2016]. In MQL condition, chip flushing is occurred by the action of high-pressure air which is very important to clear the cutting zone. Though lubrication is the main strategy for improving the machinability, a medium cooling effect during MQL machining is happened due to evaporative and convective heat transfer by the air-oil mist, whereas, in flood cooling, only convection occurs [Sen et al., 2019b]. A tribo-chemical layer was formed on the cutting tool insert during MQL machining. This protective layer formation along with the cooling lubrication effects of MQL eventually protects the tool. Due to these combined effects of MQL, machinability is radically improved or remains

similar compared to that of traditional flood cooling [Barczak et al., 2010; Morgan et al., 2012]. Due to the rebinder effect of MQL, mist droplets adhered with the machined surface and the back of the chips, which promotes the easier plastic flow of the materials, curled the chips more, reduced chip-tool contact length and consequently improved the machinability [Astakhov, 2010; Khan et al., 2009]. In MQL machining due to the full evaporation of coolant, dry chips were produced and also work-piece remains drier, which makes it green machining because no extra coolant will gather for environmental pollution [Lee et al., 2012]. Additionally, there is no need for maintenance, circulation, recycle and disposal of the cutting fluid and the costs associated with these actions are eliminated due to the evaporation of coolant [Sales et al., 2009]. Moreover, the risk of an accident is reduced due to clear visibility of the machining area in contrast to conventional cooling and provision for skin diseases of the operator is also eliminated [Madhukar et al., 2016].

It becomes less effective in machining difficult-to-cut materials where severe heat generation is the main concern. So, different techniques are needed to be hybridized with the MQL method. In this research, multi-jet MQL delivery and hybrid nano-fluid were used to enhance the MQL performance. The design and fabrication of a double jet MQL delivery system for the machinability improvement of Ti-6Al-4V alloy have been thoroughly described in chapter 2. With the newly designed MQL system, the mist can be impinged as close to the chip-tool and work-tool interfaces as possible and cools the above-mentioned interfaces and both the rake and auxiliary flank of the tool effectively as well. Oil mist supplied from two nozzles (along with the rake and flank surface of the cutting tool) should work better compared to the single nozzle system. For improving the performance of MQL further, nano-fluid can be used as an alternative to the cutting fluid. In the case of manufacturing, nano-fluids were used for their enhanced lubricating and cooling properties over an extensive range of temperatures. Nano-fluids can be applied to the machining area through a simple nozzle as flood cooling or through the MQL technique, which can reduce the friction between two contact surfaces and cool the heat-affected zone during machining. Nanoparticles present in the nano-fluid can easily penetrate the contacting surfaces and create an elastohydrodynamic lubrication effect. Besides, the enhanced thermal conductivity of the nano-fluid helps to easily cool the cutting zone. For that reason, highly efficient nano-lubricants can reduce the cutting fluid amount required for machining, which eventually reduces the cost and saves the environment as well as ensures improved machining performance [Sayuti et al., 2014].

Recently, nano-fluid is mostly used incorporation with the MQL system to further enhance the performances of MQL machining. With MQL the nano-fluid provide the following effect when applied into the machining zone [Hegab et al., 2019, 2018a]:

- By employing compressed air with the MQL method, nano-fluid can be converted into fine mist similar to other cutting fluids. Tiny nanoparticles in the mist are covered with a base fluid layer.
- When the high-velocity mist is applied during machining, nano-particles slide and rolled in the chip-tool and work-tool interfaces usually act as a separator for the matting surfaces and facilitate the access of cutting fluid.
- Nanoparticles in between the matting surface can bear the compressive force and reduce the stress concentration.
- Nano-particles and cutting fluid formed a tribofilm in between the mating surfaces, which reduced the friction and frictional heat generation. Moreover, heat transfer from the interfaces is increased for appropriate penetration of cutting fluid.
- The formation of tribofilm protects the tool and work surfaces, which can reduce the tool wear and cutting force with an improved surface finish.
- Improved thermal conductivity of nano-fluid facilitates the enhanced heat transfer from the cutting zone. Consequently, tool wear, force and surface roughness were reduced.
- Due to some surface modification effects, such as the mending and polishing effect of the nanoparticles provide better surface integrity during machining.

The direct effect and surface enhancement effect of nano-particles presented in the cutting oil can be visualized in the following manner [Lee et al., 2009]:

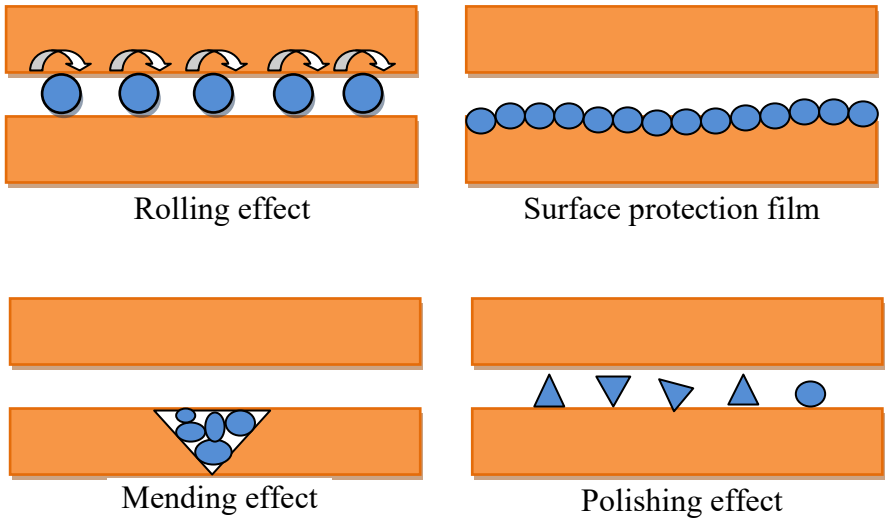


**Fig.5.1** Lubrication mechanism of nano-fluid

Hybrid nanofluid is an extension of nanofluid, which can be obtained by dispersing composite nano-powder or two different nanoparticles in the base fluid. It is believed that hybrid nanofluid will offer good thermal characteristics as compared to the base fluid and nanofluid containing single nanoparticles as a result of synergistic effects. In this research, hybrid $Al_2O_3$-MWCNT based nano-fluid has been prepared for utilizing as MQL fluid. The process of preparing the hybrid nanofluid along with their characterizations has been thoroughly described in chapter 2.

In this chapter, the performance of hybrid nano-fluid-based MQL with a specially designed double jet micro nozzle has been evaluated compared to dry and conventional MQL regarding various machinability indices. Turning of Ti-6Al-4V alloy by coated and uncoated carbide inserts has been carried out under dry machining, single jet MQL, double jet MQL and double jet MQL with nano-fluid. Chips morphology, cutting temperature, cutting forces, tool wear, tool life, surface roughness and dimensional accuracy have been analyzed for all the machining conditions. For this evaluation, cutting process parameters and nano-fluid concentration have been set at fixed values, such as cutting speed of 73 m/min, a feed rate of 0.14 mm/rev, depth of cut of 1 mm and nano-particle concentration of 1vol% have been fixed throughout the experiment.

## 6.1 Chip Morphology

Chip morphology is an important machinability index for assessing machinability. The cooling environment and tool type has a huge influence on the chip production process. Table 2.11 shows that when Ti-6Al-4V alloy has been turned by coated and uncoated carbide insert under dry condition ribbon type chips was produced. Their color was golden and the back surface was slightly rough. The color indicates high temperature and roughness indicates BUE formation on the rake surface of the tool. Single jet MQL produced helical and sometimes short ribbon type of chips. The color of chips for SJMQL becomes metallic for both types of inserts. For double jet MQL with conventional cutting oil and nano-fluid chips become helical and short helical respectively.

From Fig.2.20 and Fig.2.21, it can be observed that all the chips produced during Ti-6Al-4V alloy machining by coated and uncoated carbide inserts under various cooling conditions were serrated in nature. But they have some basic differences. For both of the tools chips for dry machining shown nonuniform chip segmentation. Which causes

nonuniform periodic cutting force. Slip angle was also high for dry cutting chips for both types of inserts, which is due to the high friction and deformation during dry cutting. Chip serration was also nonuniform when machining with uncoated and coated inserts under single jet MQL. In this present condition, the slip angles were also high but less than dry cutting. Because of cooling and lubrication action during MQL machining, chip formation was easy and slip angle was reduced. Less slip angle means less tool wear, cutting force and surface roughness, so, less slip angle is favorable [Ramana and Rao, 2014]. In the case of double jet MQL application with cutting oil and nanofluid, the produced serrated chips become more uniform. The slip angle for serrated chips was reduced more for these cases. Both types of inserts show the same pattern of chips but when nanofluid was applied by double jet MQL for coated carbide insert the chips were slightly curled. A high chip segmentation degree was observed for dry cutting and reduced for MQL conditions. Among all the MQL lowest segmentation degree was seen in the case of nanofluid-based MQL for both inserts. Additionally, chip segmentation degree was less for turning by coated tool compared to the uncoated tool. So, it can be concluded from the chip morphology analysis that turning by coated insert under nano-fluid-based double jet MQL was the most favorable machining environment among all the environments studied for turning Ti-6Al-4V alloy. Variation of chip serration degree and slip angle of serrated chips for turning Ti-6Al-4V alloy by coated and uncoated inserts under different cooling conditions have been presented in Fig.2.22.

## 6.2 Cutting Temperature

For assessing the machinability of any work material, cutting temperature can be used as an important index. Though it has some positive effects on machining, it is the main cause of an unproductive and inefficient machining process. Usually, the production of high cutting temperature limits various cutting process parameters for achieving controlled tool wear, power consumption and surface finish. The temperature at different deformation zone increased due to the heat generation during machining, which occurred mainly for the plastic deformation of the work material along with friction between the chip-tool and work-tool interface. Managing the cutting temperature is extremely necessary, owing to its most unfavorable effects. It is evident from Fig.2.23 that; the temperature is reduced under single jet (towards the rake) MQL condition compared to dry cutting for both of the inserts during turning Ti-6Al-4V alloy. The impinged aerosol form

an oil film at the interface which lubricates the chip-tool interface and reduces the frictional temperature [Duc and Long 2016]. Moreover, due to fluid vaporization in the area of impingement and conduction in the course of compressed air flow, temperature reduction can happen [Ekinovic et al., 2015]. A similar tendency was evident for turning TC11 titanium alloy by coated and uncoated carbide inserts [Qin et al., 2016].

When a specially designed double jet MQL delivery system was used to deliver two well-controlled and focused MQL jets, it works better than the previous one for both types of inserts. The main purpose of this multiple mist delivery system is to impinge the mist in the region of the chip-tool and work-tool interfaces simultaneously due to cool and lubricate the above-mentioned interfaces and the rake and flank surface effectively as well. Double-jet MQL performed better which has produced lower temperatures than the external single jet nozzle. A similar result was reported during turning AISI 4140 steel [Hadad and Sadeghi, 2013]. Additionally, a double jet nozzle provides consistent cooling throughout the machining time, since the fixed nozzle position never changed.

NFMQL through the double jet micro nozzle has been performed better than conventional MQL conditions. Heat dissipation was higher for NFMQL. The cooling and lubrication performance of cutting fluid depends on the thermo-physical properties of nano-fluid. Thermal conductivity and viscosity of nanofluid compared to the conventional cutting fluid are higher [Hegab et al., 2018b], for which cutting temperature is significantly reduced with the action of nanofluid instead of conventional fluid [B. Li et al., 2017; Maria, 2016]. In this work, better heat removal by hybrid nano-fluid-based MQL, consequently low cutting temperature has been observed. Coated carbide insert has been shown less temperature compared to uncoated one but the effect of MQL compared to dry has been less for coated carbide insert.

## 6.3 Cutting Force

The cutting force is one of the most important machinability indices. Due to this reason cutting force is also needs to be controlled. Higher tool wear which is caused by higher cutting temperatures usually causes higher cutting force. Where in some cases higher temperature softens the work material and eases the machining operation, which reduces the required cutting force. So, these interrelated machining indices jointly affect cutting force. From Fig.2.24 it can be said that single jet MQL produces less cutting force

compared to dry cutting. Due to effective coolant incursion at the chip-tool interface and rebinder effect, the chip-tool contact length was reduced during the MQL application. Consequently, friction was reduced and which subsequently reduce the main cutting force [Upadhyay et al., 2013]. A similar result was evident for the machining of Ti-6Al-4V alloy [Krishnaraj et al., 2017]. The MQL with a double jet nozzle seems to be more effective in cooling the cutting zone and ultimately reducing the main cutting force. By the secondary nozzle, the mist impinges into the work-tool interface, which reduces the friction on that interface. Ultimately, the frictional force is reduced in conjunction with reducing the temperature and improving the machined surface. For machining of turning of AISI 1045 steel, multiple MQL mist flow in the heat-affected zones during machining was proved to be more effective than single mist flow regarding cutting force [Masoudi et al., 2018].

Nano-particles present in the nano-fluid enhance its lubricating and heat transfer properties [Zhang et al., 2017]. For better lubrication friction at the interfaces was reduced. Eventually cutting temperature and force were also reduced due to less friction and better heat transfer properties of nano-fluid. This can be confirmed by measuring the cutting force in various cooling environments. The cutting force was reduced in the case of NFMQL, which confirms less required energy in machining [Anurag et al., 2018]. The average main cutting force exerted by coated carbide insert is less compared to uncoated carbide insert and this is definitely for the coating multi-layers where $Al_2O_3$ and TiN layer lubricates the interface plane of tool flank and workpiece resulting in reduced frictional co-efficient. During milling of the Ti-6Al-4V alloy, the coated tool has shown better performance than the uncoated carbide tool at each cooling condition [Sharif et al., 2014].

## 6.4 Tool Wear and Tool Life

Generally, in the turning operation, the cutting inserts fail by progressive wear depend on the tool-work combination, cutting conditions and also coolant type with application methods. It can be concluded from Fig.2.25 and Fig.2.26 that average principal and auxiliary flank wear have been decreased by using MQL compared to dry machining. In the case of the dry cutting nose of the tool was significantly affected. MQL mist decreases the cutting temperature, force and coefficient of friction which facilitates lower tool wears. Nose wear was slightly reduced compared to dry cutting. Furthermore, it can be evident from the previous analysis that double jet MQL works better than a single jet in the case of other responses. So, tool wear also decreased further when using double jet

MQL. The main contribution of the double jet nozzle was seen in reducing the auxiliary flank wear because the secondary nozzle works on reducing the rubbing of the workpiece and tool auxiliary flank surface. When uncoated and coated tools were compared it can be shown that tool coating prevents the tool to be wear out.

The performance of MQL with nano-fluid was better compared to the usual cutting fluid concerning tool wear. Due to better thermal conductivity and viscosity of nano-fluid, which confirms significant temperature reduction compared to conventional fluid [B. Li et al., 2017; Maria, 2016]. Due to less cutting temperature and friction, tool wear was also reduced for nano-fluid-based MQL machining. Moreover, hybrid nano-fluid was expected to be more effective in enhancing the machinability of Ti-6Al-4V alloy. Based on principal flank wear criteria, uncoated carbide tool life calculated for dry machining, single jet MQL and double jet MQL (with cutting oil and nano-fluid) were 5.25 min, 6.5 min, 8.55 min and 11 min respectively. So, the tool cost was reduced respectively for different cooling environments compared to dry machining. In the case of a single jet, double jet with cutting oil and double jet with hybrid nano-fluid MQL tool life increased by 23.8 %, 62.86 % and 109.5 % compared to dry machining. For coated carbide insert, calculated tool life for dry cutting, single jet, double jet with cutting oil and double jet with hybrid nano-fluid MQL were 8.65, 10,12.5 and 15.5 min. In the case of a single jet, double jet with cutting oil and double jet with hybrid nano-fluid MQL coated carbide tool life increased by 15.6 %, 44.5 % and 79.2 % compared to dry machining. The effect of different MQL cooling conditions compared to dry cutting regarding tool life increment was better for uncoated carbide insert.

From the SEM of tool wear for different cooling environments when machining Ti-6Al-4V alloy using uncoated and coated carbide inserts presented in Fig.2.27 and Fig.2.28, it can be observed that in the case of Ti-6Al-4V machining the width of crater wear was small but the crater was quite deep. High chemical reactivity, stress and temperature accelerate the crater wear. Crater wear extends up to the cutting edge and meets the flank wear, which causes the depression of the cutting edge. Flank wear was wide and deep towards the nose and gradually decrease along the cutting edge. Notching was absent for flank wear. When machining with uncoated carbide severe BUE was observed. The nose was deformed after a specific time. For SJMQL the severity was slightly decreased, which was due to temperature reduction to some extent. Wear at auxiliary flank and nose occurs due to high temperature and rubbing of the workpiece with the tool. These two wear cause

lower surface finish and high dimensional inaccuracy. For DJMQL tool wear was reduced and the nose was not damaged. BUE was also reduced. For the secondary mist jet towards the auxiliary flank surface, nose wear was reduced and shifted towards the principal flank. In the case of DJMQL with nano-fluid nose wear was shifted towards the principal flank surface. This provides lower surface roughness of the machined part.

In the case of machining with coated carbide insert similar crater and flank wear were observed but the nose was intact. Moreover, BUE formation was reduced for all types of environments. Auxiliary flank wear was shifted towards the principal flank surface for this type of tool also. From dry cutting to SJMQL and DJMQL the extent of flank and crater wear was decreased gradually. In the case of DJMQL with nano-fluid crater and flank wear was reduced most for the combined lubrication action of tool coating and nano-particles. So, in this case, only coating delamination was evident at the rake and flank surface after a long time of machining.

## 6.5 Surface Roughness

Surface roughness is a sign of better performance and life of a product and it is an important tool for evaluating the machinability of a specific work material by a specific tool. The surface roughness of a machined product is extremely allied with the cutting tool wear. Cutting temperature and cutting force also have relations with the surface roughness. It depends on the tool-work combination, cooling environment and cutting parameters. From Fig.2.29, it is clearly shown that roughness decreases for MQL compared to dry cutting conditions. Single jet MQL impinged oil mist towards the chip-tool interface, which is the secondary heat production zone. The heat from this zone was reduced due to MQL and the tool wear was reduced. So, ultimately the quality of the product surface was improved. A similar result during turning Ti-6Al-4V alloy was reported where MQL provides better machining performance with reduced surface roughness [Ramana and Aditya 2017]. MQL with a specially designed double jet nozzle showed extra effectiveness for improving the surface finish compared to single jet MQL. In this case, the secondary jet directed towards the work-tool interface may prevent the auxiliary flank face from rubbing with the machined surface and stop deteriorating the surface. A similar conclusion was found in previous literature, where surface roughness was reduced by the simultaneous application of two MQL nozzles [Masoudi et al., 2018].

When nano-fluid enhanced MQL was applied, the surface finish was further improved. Formation of the tribo-film produced from the nano-fluid used during machining protects the tool and work surfaces, which can reduce the tool wear and cutting force with an improved surface finish. Improved thermal conductivity of nano-fluid facilitates the enhanced heat transfer from the cutting zone. Consequently, tool wear, force and surface roughness were reduced. Due to the mending and polishing effect of the nanoparticles, provide a better quality of the machined surface. Ultimately, it can be concluded that the reduction of roughness in the case of MQL with NF compared to dry was very high than the conventional MQL condition. A similar conclusion was drawn for machining AISI 4140 steel, where twin jet SQL with nano-fluid performs better than soluble oil regarding surface roughness [Roy and Ghosh, 2013].

## 6.6 Dimensional Deviation

The dimensional deviation is another important product quality criterion, which has a significant influence on the machining cost and time. Excessive deviation required an additional machining operation for the final product. For turning operation, the finished workpiece diameter generally deviates from its desired value with the progress of machining time along the workpiece length. This may happen for the change of effective depth of cut due to various reasons which include wear of the tool nose, overall compliance of the Machine-Fixture-Tool-Work (M-F-T-W) system and thermal expansion and subsequent cooling of the job when the job temperature rises significantly during machining. In the case of a rigid M-F-T-W system, variation in diameter would be governed mainly by the heat generation during machining. This heat causes the increase of auxiliary flank wear and thermal expansion of the job. The application of coolant eradicates the major portion of the heat, which diminishes the cutting temperature and eventually, a dimensional deviation is reduced radically.

From Fig.2.30 it can be seen that using MQL dimensional deviation has been reduced compared to dry machining. As previously seen, single jet MQL is capable of reducing the cutting temperature and heat-induced tool wear. So, by this cooling method dimensional deviation has also been reduced. This result is inclined with previous literature [Dhar et al., 2006a]. MQL with a specially designed double jet nozzle showed better performance compared to conventional single jet MQL. Double jet MQL was effective for reducing the auxiliary flank wear caused by the rubbing action of the tool and

finished workpiece surface. And for this reason, the dimensional deviation was also reduced. Finally, when nano-fluid was utilized as MQL fluid, it has been reduced the dimensional deviation significantly. Because nano-fluid has improved thermal conductivity and viscosity compared to the base fluid. Tribo-film formed by this nano-fluid at the chip-tool and work tool interfaces reduces the heat from the cutting zone and also reduces the friction. Finally, cutting temperature and tool wear have been reduced, which is the main reason for the reduction of dimensional deviation. The effect of double jet MQL and nano-fluid-based MQL on dimensional deviation was not found in the previous literature.

From this chapter, it can be concluded that, with the increase of time and cutting length, chip morphology, cutting temperature, cutting forces, tool wear, tool life, surface roughness and dimensional accuracy were changed but differently for different tools and environments. Single jet MQL outperformed dry machining during turning Ti-6Al-4V alloy for both types of inserts. When a newly designed and fabricated double jet nozzle was used for MQL delivery it reduces the friction between the work-tool interface and eventually reduces temperature, force, roughness tool flank wear and dimensional deviation further. When hybrid nano-fluid has been used as MQL liquid, offers promising results concerning all the responses mentioned earlier. For improved thermal and tribological properties of the resultant nano-fluid, promising cooling and lubrication were observed during the turning of the Ti-6Al-4V alloy. For both inserts, different environments perform similarly. But, for all the responses coated tools perform better than uncoated one.

# Chapter-6

# Conclusions and Recommendations

## 6.1 Conclusions

The purpose of this research is to design and develop an effective, efficient and eco-friendly cooling system for the machinability enhancement of Ti-6Al-4V alloy. A double jet MQL with a hybrid nano-fluid-based cooling system has been experimentally and numerically investigated for turning this alloy. The main contributions of this research are as follow:

(i) A suitable double jet MQL delivery system integrated with the turning tool holder has been designed and developed which can deliver uninterrupted MQL with hybrid nano-fluid towards the rake and flank surface of the cutting tool simultaneously during machining. Appropriate MQL parameters have been found as, nozzle diameter of 0.5 mm, primary nozzle angle of 20°, secondary nozzle angle of 15°, air pressure of 20 bar and oil flow rate of 50 ml/hr.

(ii) A stable hybrid nano-fluid ($Al_2O_3$-MWCNT) with a concentration of 0.5%, 1% and 1.5% have been prepared by dispersing 80% $Al_2O_3$ and 20% MWCNT into the base fluid and uniformly dispersed by magnetic stirring and ultra-sonic agitation method. Thermal conductivity and viscosity of the prepared nano-fluids have been improved compared to the base fluid and they have a positive relationship with the volume concentration of the nanoparticles.

(iii) The effect of double jet MQL delivery system and hybrid nano-fluid on the machinability of Ti-6Al-4V alloy by coated and uncoated carbide insert has been evaluated in respect of chips morphology, cutting temperature, cutting forces, tool wear, tool life, surface roughness and dimensional accuracy. The application of double jet MQL can significantly improve the machinability of

Ti-6Al-4V alloy compared to single jet MQL. In addition, MQL with hybrid nano-fluid performs better compared to MQL with conventional cutting oil.

(iv) Statistical analysis pointed out that process inputs (cutting speed, feed rate, depth of cut, nanoparticle concentration and tool type) have a significant effect on cutting temperature, cutting force and surface roughness when turning Ti-6Al-4V alloy under hybrid nano-fluid based MQL. Empirical models for predicting the responses as a function of significant process inputs have been formulated and validated based on the experimental data. Optimum cutting speed, feed rate, depth of cut and particle concentration and the tool-type combination has been found as, 48.48 m/min, 0.1 mm/rev, 0.5 mm, 1.07 vol % and coated tool for improving the machinability of Ti-6Al-4V alloy considering multi-objectives.

(v) A finite element model (FEM) for turning Ti-6Al-4V alloy by carbide insert under different cooling environments has been formulated and experimentally validated. From this model, cutting temperature and chip morphology can be predicted with reasonable accuracy (error < 10%). For cutting temperature, simulated responses for turning by uncoated insert shows better agreement with the experimental results. Whereas, for chip morphology, simulated responses for turning by coated insert show better agreement with the experimental results.

## 6.2 Recommendations

There are some recommendations for future study which are briefly presented below:

(i) In the case of designing a double jet MQL delivery system, the nozzle number, distance and position were kept fixed based on literature. Variation of these parameters was not analyzed throughout the research, which can be thoroughly analyzed in further study.

(ii) In this research, only one type of coated tool has been used and compared with the uncoated tool. So, the effect of coating materials, thickness, and the number of layers on the responses cannot be discussed. Different types of coated tools can be used in future study.

(iii) Sustainability assessment of the machining processes has not been conducted

for this research work, which is necessary before the practical implementation of the developed process. This assessment can be conducted in the future.

(iv) In this research, all of the responses have been given equal importance in the case of multi-response optimization. But practically different responses may have different importance. So, the importance of responses can be incorporated in future studies.

(v) Optimization of the process parameters for multi-response can be carried out by using other optimization techniques, such as genetic algorithm, particle swarm optimization, etc.

# References


Abbas, A.T., Gupta, M.K., Soliman, M.S., Mia, M., Hegab, H., Luqman, M., Pimenov, D.Y., (2019), "Sustainability assessment associated with surface roughness and power consumption characteristics in nanofluid MQL-assisted turning of AISI 1045 steel", Int. J. of Adv. Manuf. Technology, Vol. 105 (1-4), pp. 1311-1327.

Abubakr, M., Abbas, A.T., Tomaz, I., Soliman, M.S., Luqman, M., Hegab, H., (2020), "Sustainable and smart manufacturing: An integrated approach", Sustainability, Vol. 12 (6), pp. 1-19.

Abukhshim, N.A., Mativenga, P.T., Sheikh, M.A., (2006), "Heat generation and temperature prediction in metal cutting: A review and implications for high-speed machining", Int. J. of Machine Tools and Manufacture, Vol. 46 (7-8), pp. 782-800.

Ahmed, L.S., Kumar, M.P., (2016), "Cryogenic Drilling of Ti-6Al-4V Alloy Under Liquid Nitrogen Cooling", Materials and Manufacturing Processes, Vol. 31 (7), pp. 951-959.

Ahmed, L.S., Pradeep Kumar, M., (2017), "Investigation of cryogenic cooling effect in reaming Ti-6AL-4V alloy", Journal of Materials and Manufacturing Processes, Vol. 32 (9), pp. 970-978.

Ali, M.H., Khidhir, B.A., Ansari, M.N.M., Mohamed, B., (2013), "Finite element modelling to predict cutting parameters for milling on titanium alloy (Ti-6Al-4V)", Australian Journal of Mechanical Engineering, Vol. 11 (2), pp. 83-92.

Amini, S., Khakbaz, H., Barani, A., (2015), "Improvement of near-dry machining and its effect on tool wear in turning of AISI 4142", Materials and Manufacturing Processes, Vol. 30 (2), pp. 241-247.

Amrita, M., Rukmini Srikant, R., Venkataramana, V.S.N., (2020), "Optimisation of cutting parameters for cutting temperature and tool wear in turning AISI4140 under different cooling conditions", Advances in Materials and Processing Technologies, DOI: 10.1080/2374068X.2020.1795794.

André Stefenon, Guilherme Cortelini da Rosa, André João de Souza, (2015), "A Qualitative analysis of cutting parameters influence in turning process temperature of stainless steel AISI 420C", in: Proceedings of the 23rd ABCM International Congress of Mechanical Engineering.

Anurag, A., Kumar, R., Joshi, K.K., Das, R.K., (2018), "Analysis of Chip Reduction Coefficient in Turning of Ti-6Al-4V ELI", in: IOP Conference Series: Materials Science and Engineering, Vol. 390 (1), pp. 012113 (1-7).

Arai, M., Ogawa, M., (1997), "Effects of high pressure supply of coolant in drilling of titanium alloy", Journal of Japan Institute of Light Metals, Vol. 47 (3), pp. 139-144.

Aramcharoen, A., (2016), "Influence of Cryogenic Cooling on Tool Wear and Chip Formation in Turning of Titanium Alloy", in: Procedia CIRP. Procedia CIRP, Vol. 46, pp. 83-86.

Armendia, M., Garay, A., Iriarte, L.M., Arrazola, P.J., (2010), "Comparison of the machinabilities of Ti6Al4V and TIMETAL® 54M using uncoated WC-Co tools", Journal of Materials Processing Technology, Vol. 210 (2), pp. 197-203.

Arulraj, J.G.A., Wins, K.L.D., Raj, A., (2014), "Artificial Neural Network Assisted Sensor Fusion Model for Predicting Surface Roughness During Hard Turning of H13 Steel with Minimal Cutting Fluid Application", Procedia Materials Science, Vol. 5, pp. 2338-2346.

Asadi, A., Asadi, M., Rezaniakolaei, A., Rosendahl, L. A., Afrand, M., Wongwises, S., (2018), "Heat transfer efficiency of $Al_2O_3$-MWCNT/thermal oil hybrid nanofluid as a cooling fluid in thermal and energy management applications", Int. J. Heat Mass Transf, Vol. 117, pp. 474–486.

Astakhov, V.P., (2010), "Metal cutting theory foundations of near-dry (MQL) machining", Int. J. of Machining and Machinability of Materials, Vol. 7 (1-2), pp. 1-16.

Astakhov, V.P., (2008), "Ecological machining: Near-dry machining", in: Machining: Fundamentals and Recent Advances, Springer London, pp. 195–223.

Attanasio, A., Gelfi, M., Giardini, C., Remino, C., (2006),"Minimal quantity lubrication in turning: Effect on tool wear", Wear, Vol. 260, pp. 333–338.

Banerjee, N., Sharma, A., (2019), "Improving machining performance of Ti-6Al-4V through multi-point minimum quantity lubrication method", Proc. Inst. Mech. Eng. Part B J. Eng. Manuf, Vol. 233, pp. 321–336.

Barczak, L.M., Batako, A.D.L., Morgan, M.N., (2010), "A study of plane surface grinding under minimum quantity lubrication (MQL) conditions", International Journal of Machine Tools and Manufacture, Vol. 50 (11), pp. 977-985.

Bermingham, M.J., Palanisamy, S., Kent, D., Dargusch, M.S., (2012), "A comparison of cryogenic and high pressure emulsion cooling technologies on tool life and chip morphology in Ti-6Al-4V cutting", Journal of Materials Processing Technology, Vol. 212 (4), pp. 752-765.

Bermingham, M.J., Palanisamy, S., Morr, D., Andrews, R., Dargusch, M.S., (2014), "Advantages of milling and drilling Ti-6Al-4V components with high-pressure coolant", Int. J. of Advanced Manufacturing Technology, Vol. 72 (1-4), pp. 77-88.

Biermann, D., Abrahams, H., Metzger, M., (2015), "Experimental investigation of tool wear and chip formation in cryogenic machining of titanium alloys", Advances in Manufacturing, Vol. 3 (4), pp. 292-299.

Black, J.T., Payton, L.N., (2003), "Metal cutting and forming", in: Smithells Metals Reference Book. Elsevier Ltd., pp. 1–16.

Bordin, A., Imbrogno, S., Rotella, G., Bruschi, S., Ghiotti, A., Umbrello, D., (2015), "Finite element simulation of semi-finishing turning of Electron Beam Melted Ti6Al4V under dry and cryogenic cooling", in: Procedia CIRP, Vol. 31, pp. 551-556.

Boswell, B., Chandratilleke, T.T., (2009), "Air-cooling used for metal cutting", American Journal of Applied Sciences, Vol. 6 (2), pp. 251-262.

Boswell, B., Islam, M.N., (2016), "Sustainable cooling method for machining titanium alloy", IOP Conference Series: Materials Science and Engineering, Vol. 114 (1), pp. 012021 (1-12).

Bouzakis, K.D., Michailidis, N., Skordaris, G., Bouzakis, E., Biermann, D., M'Saoubi, R., (2012), "Cutting with coated tools: Coating technologies, characterization methods and performance optimization", CIRP Annals-Manufacturing Technology, Vol. 61 (2), pp. 703-723.

Box, G.E.P., Wilson, K.B., (1951), "On the Experimental Attainment of Optimum Conditions", J. R. Stat. Soc. Ser. B. Vol.XIII (1), pp. 1-38.

Boyaci, I.H., (2005), "A new approach for determination of enzyme kinetic constants using response surface methodology", Biochem. Engineering, Vol. 25(1), pp.55–62.

Boyd, G., Na, D., Li, Z., Snowling, S., Zhang, Q., and Zhou, P., (2019), "Influent Forecasting for Wastewater Treatment Plants in North America", Sustainability, 11(6), 1764 (1-14).

Brinksmeier, E., Walter, A., Janssen, R., Diersen, P., (1999), "Aspects of cooling lubrication reduction in machining advanced materials", Proceedings of the Institution of Mechanical Engineers, Part B: J. of Eng. Manufacture, Vol. 213(8), pp. 769-778.

Calamaz, M., Coupard, D., Girot, F., (2008), "A new material model for 2D numerical simulation of serrated chip formation when machining titanium alloy Ti-6Al-4V", International Journal of Machine Tools and Manufacture, Vol. 48 (3-4), pp. 275-288.

Cantero, J.L., Tardío, M.M., Canteli, J.A., Marcos, M., Miguélez, M.H., (2005), "Dry drilling of alloy Ti-6Al-4V", International Journal of Machine Tools and Manufacture, Vol. 45 (11), pp. 1246-1255.

Caudill, J., Huang, B., Arvin, C., Schoop, J., Meyer, K., Jawahir, I.S., (2014), "Enhancing the surface integrity of Ti-6Al-4V alloy through cryogenic burnishing", in: Procedia CIRP, Vol. 13, pp. 243-248.

Chattopadhyay, A.K., Chattopadhyay, A.B., (1982), "Wear and performance of coated carbide and ceramic tools", Wear, Vol. 80 (2), pp. 239-258.

Che-Haron, C.H., (2001), "Tool life and surface integrity in turning titanium alloy", in: Journal of Materials Processing Technology, Vol. 118 (1–30), pp. 231-237.

Che-Haron, C.H., Jawaid, A., (2005), "The effect of machining on surface integrity of titanium alloy Ti-6Al-4V", J. Mater. Process. Technol, Vol. 166, pp. 188–192.

Chetan, Ghosh, S., Rao, P. V., (2016), "Environment friendly machining of ni-cr-co based super alloy using different sustainable techniques", Materials and Manufacturing Processes, Vol. 31 (7), pp. 852-859.

Choi, S.U.S., Eastman, J.A., (2001), "Enhanced heat transfer using nanofluids", Patent No.: US6221275B1, pp.1-7.

Choi, S.U.S., Eastman, J.A., (1995), "Enhancing thermal conductivity of fluids with nanoparticles", in: ASME International Mechanical Engineering Congress & Exposition, San Francisco, CA.

Choudhary, A., Paul, S., (2019), "Performance evaluation of PVD TIALN coated carbide tools vis-à-vis uncoated carbide tool in turning of titanium alloy (Ti-6Al-4V) by simultaneous minimization of cutting energy, dimensional deviation and tool wear", Machining Science and Technology, Vol. 23 (3), pp. 368-384.

Cordes, S., Hübner, F., Schaarschmidt, T., (2014), "Next generation high performance cutting by use of carbon dioxide as cryogenics", in: Procedia CIRP. Elsevier, Vol. 14, pp. 401–405.

Corduan, N., Himbert, T., Poulachon, G., Dessoly, M., Lambertin, M., Vigneau, J., Payoux, B., (2003), "Wear mechanisms of new tool materials for Ti-6Al-4V high performance machining", CIRP Annals-Manuf. Technology, Vol. 52 (1), pp. 73-76.

Courbon, C., Sajn, V., Kramar, D., Rech, J., Kosel, F., Kopac, J., (2011), "Investigation of machining performance in high pressure jet assisted turning of Inconel 718: A numerical model", J. of Mat. Processing Technology, Vol. 211 (11), pp. 1834-1851.

Cui, C., Hu, B.M., Zhao, L., Liu, S., (2011), "Titanium alloy production technology, market prospects and industry development", Materials and Design, Vol. 32 (3), pp. 1684-1691.

Da Silva, R.B., MacHado, Á.R., Ezugwu, E.O., Bonney, J., Sales, W.F., (2013),"Tool life and wear mechanisms in high speed machining of Ti-6Al-4V alloy with PCD tools under various coolant pressures", Journal of Materials Processing Technology, Vol. 213 (8), pp. 1459-1464.

Da Silva, R.B., Sales, W.F., Costa, E.S., Ezugwu, E.O., Bonney, J., Da Silva, M.B., Machado, Á.R., (2017), "Surface integrity and tool life when turning of Ti-6Al-4V with coolant applied by different methods", International Journal of Advanced Manufacturing Technology, Vol. 93 (5-8), pp. 1893-1902.

Damir, A., Sadek, A., Attia, H., Tendolkar, A., (2017), "Characterization and Optimization of Machinability and Environmental Impact of Machining of Ti-6Al-4V with Minimum Quantity Lubrication", International Journal of Mechatronics and Manufacturing Systems, Vol. 7 (4), pp. 296-310.

Das, M.K., Kumar, K., Barman, T.K., Sahoo, P., (2014), "Investigation on electrochemical machining of EN31 steel for optimization of MRR and surface roughness using artificial bee colony algorithm", in: Procedia Engineering, Vol. 97, pp. 1587-1596.

Das, S.K., Putra, N., Thiesen, P., Roetzel, W., (2003), "Temperature dependence of thermal conductivity enhancement for nanofluids", Journal of Heat Transfer, Vol. 125 (4), pp. 567-574.

Davim, J.P., (2014), "Machining of Titanium Alloys: Materials Forming, Machining and Tribology", Springer-Verlag, pp. 1–153.

de Mello, A.V., de Silva, R.B., Machado, Á.R., Gelamo, R.V., Diniz, A.E., de Oliveira, R.F.M., (2017), "Surface Grinding of Ti-6Al-4V Alloy with SiC Abrasive Wheel at Various Cutting Conditions", Procedia Manuf., Vol. 10, pp. 590-600.

de Myttenaere, A., Golden, B., Le Grand, B., Rossi, F., (2016), "Mean Absolute Percentage Error for regression models", Neurocomputing, Vol. 192, pp. 38–48.

Deiab, I., Raza, S.W., Pervaiz, S., (2014), "Analysis of lubrication strategies for sustainable machining during turning of titanium ti-6al-4v alloy", in: Procedia CIRP. Procedia CIRP, Vol. 17, pp. 766-771.

Deng, J., Li, Y., Song, W., (2008), "Diffusion wear in dry cutting of Ti-6Al-4V with WC/Co carbide tools", Wear, Vol. 265, pp. 1776–1783.

Derringer, G., Suich, R., (1980), ―Simultaneous Optimization of Several Response Variables", J. Qual. Technol. Vol. 12 (4), pp. 214-219.

Derringer, G.C., (1994), ―A Balancing Act : Optimizing a Product's Properties", Qual. Prog. Vol. 27, pp. 51–58.

Devarajan, M., Krishnamurthy, N. P., Balasubramanian, M., Ramani, B., Wongwises, S., Abd El-Naby, K., Sathyamurthy, R., (2018), "Thermophysical properties of CNT and CNT/$Al_2O_3$ hybrid nanofluid", Micro Nano Lett, Vol. 13, pp. 617–621.

Dhar, N.R., Islam, M.W., Islam, S., Mithu, M.A.H., (2006a), "The influence of minimum quantity of lubrication (MQL) on cutting temperature, chip and dimensional accuracy in turning AISI-1040 steel", J. of Mat. Proc. Technology, Vol.171 (1), pp. 93-99.

Dhar, N. R., Kamruzzaman, M., Ahmed, M., (2006b), ―Effect of minimum quantity lubrication (MQL) on tool wear and surface roughness in turning AISI-4340 steel", Journal of Materials Processing Technology, Vol. 172(2), pp. 299–304.

Dhar, N. R., Islam, S., Kamruzzaman, M., & Paul, S., (2006c), ―Wear behavior of uncoated carbide inserts under dry, wet and cryogenic cooling conditions in turning C-60 steel", Journal of the Brazilian Society of Mechanical Sciences and Engineering, Vol. 28(2), pp. 146–152.

Dhar, N. R., Kamruzzaman, M., Khan, M. M. A., and Chattopadhyay, A. B., (2006d), ―Effects of cryogenic cooling by liquid nitrogen jets on tool wear, surface finish and dimensional deviation in turning different steels. International Journal of Machining and Machinability of Materials, Vol. 1(1), pp. 115-131.

Dhar, N.R., Siddiqui, A.T., Rashid, M.H., (2006e), "Effect of High-Pressure Coolant Jet on Grinding Temperature, Chip and Surface Roughness in Grinding AISI-1040 Steel", Journal of Engineering and Applied Sciences, Vol. 1, pp. 22–28.

Dhar, N.R., Nanda Kishore, S. V., Paul, S., Chattopadhyay, A.B., (2002a), "The effects of cryogenic cooling on chips and cutting forces in turning AISI 1040 and AISI 4320 steels", in: Proceedings of the Institution of Mechanical Engineers, Part B: Journal of Engineering Manufacture, Vol. 216 (5), pp. 713–724.

Dhar, N. R., Paul, S., & Chattopadhyay, A. B., (2002b), "Role of Cryogenic Cooling on Cutting Temperature in Turning Steel", Journal of Manufacturing Science and Engineering, Vol. 124(1), pp. 146-154.

Dhar, N.R., Khan, M.M.A., (2010), "Effects of minimum quantity lubrication (MQL) by vegetable oil-based cutting fluid on machinability of AISI 9310 steel", International Journal of Machining and Machinability of Materials, Vol. 7, pp. 17–38.

Donachie, M.J., (2000), "Titanium – A Technical Guide", 2nd Ed, ASM Int., Pages: 381.

Donea, J., Huerta, A., Ponthot, J.-P., Rodrïguez-Ferran, A., (2004), "Arbitrary Lagrangian-Eulerian Methods", in: Encyclopedia of Computational Mechanics, John Wiley & Sons, Ltd, pp. 413-437.

Duan, C., Dou, T., Cai, Y., Li, Y., (2009), "Finite element simulation and experiment of chip formation process during high speed machining of AISI 1045 hardened steel", Int. Journal on Production and Industrial Engineering, Vol. 02 (01), pp. 28-32.

Duchosal, A., Leroy, R., Vecellio, L., Louste, C., Ranganathan, N., (2013), "An experimental investigation on oil mist characterization used in MQL milling process", Int. J. Adv. Manuf. Technol, Vol. 66, pp. 1003–1014.

Dureja, J.S., Singh, R., Singh, T., Singh, P., Dogra, M., Bhatti, M.S., (2015), "Performance evaluation of coated carbide tool in machining of stainless steel (AISI 202) under minimum quantity lubrication (MQL)", International Journal of Precision Engineering and Manufacturing - Green Technology, Vol. 2 (2), pp. 123-129.

Eastman, J.A., Choi, S.U.S., Li, S., Yu, W., Thompson, L.J., (2001),"Anomalously increased effective thermal conductivities of ethylene glycol-based nanofluids containing copper nanoparticles", Applied Physics Letters, Vol. 78 (6), pp. 718-720.

Eberhard, P., Gaugele, T., (2013), "Simulation of cutting processes using mesh-free Lagrangian particle methods", Computational Mechanics, Vol. 51 (3), pp. 261-278.

Ehrgott, M., (2005), "Multicriteria optimization", Multicriteria Optimization: Second Edition. Springer Berlin Heidelberg, pp. 1-323.

Ekinovic, S., Prcanovic, H., Begovic, E., (2015), "Investigation of Influence of MQL Machining Parameters on Cutting Forces during MQL Turning of Carbon Steel St52-3", in: Procedia Engineering, Elsevier Ltd, Vol. 132, pp. 608-614.

Elmagrabi, N., Che Hassan, C.H., Jaharah, A.G., Shuaeib, F.M., (2008), "High speed milling of Ti-6Al-4V using coated carbide tools", European Journal of Scientific Research, Vol. 22 (2), pp. 153-162.

Eltaggaz, A., Deiab, I., (2018), "The Effect Of Nanoparticle Concentration On Mql Performance When Machining Ti-6Al-4V Titanium Alloy", CSME International Congress 2018 Toronto, Canada, pp. 1-4.

Ezugwu, E.O., Bonney, J., Da Silva, R.B., Machado, A.R., Ugwoha, E., (2009), "High productivity rough turning of ti-6al-4v alloy, with flood and high-pressure cooling", Tribology Transactions, Vol. 52 (3), pp. 395-400.

Ezugwu, E.O., Bonney, J., Yamane, Y., (2003), "An overview of the machinability of aeroengine alloys", J. of Materials Processing Technology, Vol. 134 (2), pp. 233-253.

Ezugwu, E.O., Da Silva, R.B., Bonney, J., Costa, E.S., Sales, W.F., Machado, A.R., (2019), "Evaluation of performance of various coolant grades when turning Ti-6Al-4V alloy with uncoated carbide tools under high-pressure coolant supplies", ASME Journal of Manufacturing Science and Engineering, Vol. 141 (1), 014503.

Ezugwu, E.O., Da Silva, R.B., Bonney, J., Machado, Á.R., (2005), "The effect of argon-enriched environment in high-speed machining of titanium alloy", Tribology Transactions, Vol. 48 (1), pp. 18-23.

Ezugwu, E.O., Wang, Z.M., (1997), "Titanium alloys and their machinability - A review", Journal of Materials Processing Technology, Vol. 68, pp. 262–274.

Fahad, M., Mativenga, P.T., Sheikh, M.A., 2011. An investigation of multilayer coated (TiCN/Al 2O 3-TiN) tungsten carbide tools in high speed cutting using a hybrid finite element and experimental technique, in: Proceedings of the Institution of Mechanical Engineers, Part B: Journal of Engineering Manufacture, pp. 1835–1850.

Feng, X., Johnson, D.W., (2012),. "Mass transfer in SiO 2 nanofluids: A case against purported nanoparticle convection effects", International Journal of Heat and Mass Transfer, Vol. 55 (13-14), pp. 3447-3453.

Froes, F., Qian, M., Niinomi, M., (2019), "Titanium for Consumer Applications", Titanium for Consumer Applications, Elsevier.

Geoffrey, B., Winston, A.K., Chattopadhyay, A.B., (1989), "Fundamentals of Machining and Machine Tools, Machining: Fundamentals and Recent Advances", John Wiley & Sons.

Gilbert, W.W., (1950), "Economics of Machining", in: In Machining Theory and Practice. American Society of Metals, Materials Park, pp. 465–485.

Goindi, G.S., Sarkar, P., (2017), "Dry machining: A step towards sustainable machining – Challenges and future directions", J. of Cleaner Production, Vol. 165, pp. 1557-1571.

Gowd, G.H., Vali, S.S., Ajay, V., Mahesh, G.G., (2014), "Experimental Investigations &Effects of Cutting Variables on MRR and Tool Wear for AISI S2 Tool Steel", Procedia Materials Science, Vol. 5, pp. 1398–1407.

Grzesik, W., (2016), ―Advanced Machining Processes of Metallic Materials: Theory, Modelling, and Applications", Second Edition.

Grzesik, W., Bartoszuk, M., Nieslony, P., (2005), "Finite element modelling of temperature distribution in the cutting zone in turning processes with differently coated tools", J. of Materials Processing Technology, Vol. 164–165, pp. 1204-1211.

Grzesik, W., Nieslony, P., (2003), "A computational approach to evaluate temperature and heat partition in machining with multilayer coated tools", International Journal of Machine Tools and Manufacture, Vol. 43 (13), pp. 1311-1317.

Gupta, K., Laubscher, R.F., (2017), "Sustainable machining of titanium alloys: A critical review", Proceedings of the Institution of Mechanical Engineers, Part B: Journal of Engineering Manufacture, Vol 231 (14), pp.1-18.

Gupta, M.K., Mia, M., Pruncu, C.I., Khan, A.M., Rahman, M.A., Jamil, M., Sharma, V.S., (2020), "Modeling and performance evaluation of $Al_2O_3$, $MoS_2$ and graphite nanoparticle-assisted MQL in turning titanium alloy: an intelligent approach", J. of the Brazilian Society of Mechanical Sciences and Eng., Vol. 42 (4), pp. 207 (1-21).

Gupta, M.K., Sood, P.K., Sharma, V.S., (2016), "Machining Parameters Optimization of Titanium Alloy using Response Surface Methodology and Particle Swarm Optimization under Minimum-Quantity Lubrication Environment" Mater. Manuf. Process, Vol. 31, pp. 1671–1682.

Hadad, M., Sadeghi, B., (2013), "Minimum quantity lubrication-MQL turning of AISI 4140 steel alloy", Journal of Cleaner Production, Vol. 54, pp. 332–343.

Hadad, M., Sharbati, A., (2016), "Thermal Aspects of Environmentally Friendly-MQL Grinding Process", in: Procedia CIRP, Vol. 40, pp. 509-515.

Hadzley, A.B.M., Izamshah, R.A.R., Amran, M.A.M., Kamaruzaman, J., Sivaraos, Hambali, A., Izan, S.H.N., Hasrulnizzam, W.M.W., Abu, A., Mariana, Y., Meysam, S., (2013), "Machining performance of Ti-6Al-4V titanium alloy assisted by High Pressure Waterjet", World Applied Sciences Journal, Vol. 21, pp. 98–104.

Hammond, D.R., Koen, D., Oosthuizen, G.A., (2011), "The investigation and design of a focused high pressure cooling technique for the milling of Ti6Al4V", in: ISEM 2011 Proceedings, pp. 1-20.

Hassanpour, H., Sadeghi, M.H., Rezaei, H., Rasti, A., (2016), "Experimental Study of Cutting Force, Microhardness, Surface Roughness, and Burr Size on Micro milling of Ti6Al4V in Minimum Quantity Lubrication", Materials and Manufacturing Processes, Vol. 31 (13), pp. 1654-1662.

Hegab, H., Kishawy, H.A., Gadallah, M.H., Umer, U., Deiab, I., (2018a),"On machining of Ti-6Al-4V using multi-walled carbon nanotubes-based nano-fluid under minimum quantity lubrication", International Journal of Advanced Manufacturing Technology, Vol. 97 (5-8), pp. 1593-1603.

Hegab, H., Kishawy, H.A., Umer, U., Mohany, A., (2019), "A model for machining with nano-additives based minimum quantity lubrication", International Journal of Advanced Manufacturing Technology, Vol. 102 (5-8), pp. 2013-2028.

Hegab, H., Umer, U., Deiab, I., Kishawy, H., (2018b), "Performance evaluation of Ti–6Al–4V machining using nano-cutting fluids under minimum quantity lubrication", Int. Journal of Advanced Manufacturing Technology, Vol. 95 (9-12), pp. 4229-4241.

Heisel, U., Lutz, D., Wassmer, S., (1998), "The minimum quantity lubricant technique and its application in cutting process", Machines and Metals Mag., Vol. 386, pp. 22–38.

Hernández, Y.S., Vilches, F.J.T., Gamboa, C.B., Hurtado, L.S., (2018),"Experimental parametric relationships for chip geometry in dry machining of the Ti6Al4V alloy", Materials, Vol. 11, pp. 1260 (1-17).

Hong, S.Y., Markus, I., Jeong, W.-C., (2001), "New cooling approach and tool life improvement in cryogenic machining of titanium alloy Ti-6Al-4V", International Journal of Machine Tools and Manufacture, Vol. 41 (15), pp. 2245-2260.

Hosseini Kordkheili, S.A., Bahai, H., Mirtaheri, M., (2011), "An updated Lagrangian finite element formulation for large displacement dynamic analysis of three-dimensional flexible riser structures". Ocean Engineering, Vol. 38 (5-6), pp. 793-803.

Hua, J., Shivpuri, R., (2004), "Prediction of chip morphology and segmentation during the machining of titanium alloys", Journal of Materials Processing Technology. Vol. 150 (1-2), pp. 124-133.

Huang, S., Lv, T., Wang, M., Xu, X., (2018), "Effects of Machining and Oil Mist Parameters on Electrostatic Minimum Quantity Lubrication–EMQL Turning Process", International Journal of Precision Engineering and Manufacturing - Green Technology, Vol. 5 (2), pp. 317-326.

Hutchison, J.L., Kiselev, N.A., Krinichnaya, E.P., Krestinin, A.V., Loutfy, R.O., Morawsky, A.P., Muradyan, V.E., Obraztsova, E.D., Sloan, J., Terekhov, S.V., Zakharov, D.N., (2001), "Double-walled carbon nanotubes fabricated by a hydrogen arc discharge method", Carbon N. Y. Vol. 39, pp. 761–770.

Imbrogno, S., Sartori, S., Bordin, A., Bruschi, S., Umbrello, D., (2017), "Machining Simulation of Ti6Al4V under Dry and Cryogenic Conditions", in: Procedia CIRP, Vol. 58, pp. 475-480.

Inasaki, I., (1998), "Principles of Abrasive Processing", Machining Science and Technology, Vol. 2 (1), pp. 155-156.

Işik, B., Kentli, A., (2014), "The prediction of surface temperature in drilling of Ti6Al4V", Archives of Metallurgy and Materials, Vol. 59 (2), pp. 467-471.

Antonialli, A.I.S., Diniz, A.E., Pederiva, R., (2010), "Vibration analysis of cutting force in titanium alloy milling", International Journal of Machine Tools and Manufacture, Vol. 50 (1), pp. 65-74.

Jacobus, K., DeVor, R.E., Kapoor, S.G., (2000), "Machining-induced residual stress: Experimentation and modeling", International Journal of Machine Tools and Manufacture, Vol. 51 (2011), pp. 250–280.

Jama, M., Singh, T., Gamaleldin, S.M., Koc, M., Samara, A., Isaifan, R.J., Atieh, M.A., (2016), "Critical Review on Nanofluids: Preparation, Characterization, and Applications", Journal of Nanomaterials, Vol. 2016, pp. 6717624 (1-22).

Jamaludin, A.S., Hosokawa, A., Furumoto, T., Koyano, T., Hashimoto, Y., (2017), "Evaluation of the minimum quantity lubrication in orthogonal cutting with the application of finite element method", International Journal of Mechanical and Mechatronics Engineering, Vol. 17 (1), pp. 104-109.

Jamil, M., Khan, A.M., Hegab, H., Gong, L., Mia, M., Gupta, M.K., He, N., (2019), "Effects of hybrid $Al_2O_3$-CNT nanofluids and cryogenic cooling on machining of Ti–6Al–4V", International Journal of Advanced Manufacturing Technology, Vol. 102 (9-12), pp. 3895-3909.

Jatti, V.S., Singh, T.P., (2015), "Copper oxide nano-particles as friction-reduction and anti-wear additives in lubricating oil", Journal of Mechanical Science and Technology, Vol. 29 (2), pp. 793-798.

Jawaid, A., Sharif, S., Koksal, S., (2000), "Evaluation of wear mechanisms of coated carbide tools when face milling titanium alloy", Journal of Materials Processing Technology, Vol. 99 (1), pp. 266-274.

Jia, Y., Zhu, L., (2018), "Technics Research on Polycrystalline Cubic Boron Nitride Cutting Tools Dry Turning Ti-6AL-4V Alloy Based on Orthogonal Experimental Design", in: MATEC Web of Conferences. MATEC Web of Conferences, Vol. 142, pp. 03002 (1-6).

Joshi, V.A., (2006), "Titanium Alloys - An Atlas of Structures and Fracture Features", CRC Press.

Karkade, H.B., Patil, N.G., (2018), "Comparative investigations into high speed machining of A-B titanium alloy (Ti-6al-4v) under dry and compressed $CO_2$ gas cooling environment", in: AIP Conference Proceedings, pp. 020009 (1-9).

Ke, Y. Lin, Dong, H. Yue, Liu, G., Zhang, M., (2009), "Use of nitrogen gas in high-speed milling of Ti-6Al-4V", Transactions of Nonferrous Metals Society of China (English Edition), Vol. 19 (3), pp. 530-534.

Kechagias, J.D., Aslani, K.E., Fountas, N.A., Vaxevanidis, N.M., Manolakos, D.E., (2020),"A comparative investigation of Taguchi and full factorial design for machinability prediction in turning of a titanium alloy", Measurement: Journal of the International Measurement Confederation, Vol. 151, pp. 107213 (1-11).

Khan, M.A. (2015), "Effect of high pressure coolant jets in turning ti-6al-4v alloy with specialized designed nozzle", M.Sc. Thesis, Bangladesh University of Engineering and Technology.

Khan, M.A., Mia, M., Dhar, N.R., (2017), "High-pressure coolant on flank and rake surfaces of tool in turning of Ti-6Al-4V: investigations on forces, temperature, and chips", International Journal of Advanced Manufacturing Technology, Vol. 90 (5-8), pp. 1977-1991.

Khan, M.M.A., Mithu, M.A.H., Dhar, N.R., (2009), "Effects of minimum quantity lubrication on turning AISI 9310 alloy steel using vegetable oil-based cutting fluid", Journal of Materials Processing Technology, Vol. 209 (15-16), pp. 5573-5583.

Khanna, N., Agrawal, C., Gupta, M.K., Song, Q., (2019), "Tool wear and hole quality evaluation in cryogenic Drilling of Inconel 718 superalloy", Tribology International, Vol. 143, pp. 106084 (1-10).

Khatri, A., Jahan, M.P., (2018), "Investigating tool wear mechanisms in machining of Ti-6Al-4V in flood coolant, dry and MQL conditions", in: Procedia Manufacturing, Vol.26, pp. 434-445.

Kim, D.H., Lee, P.-H., Kim, J.S., Lee, S.W., (2015), "Machinability on Micro-End Milling Process of Ti-6Al-4V with Nanofluid Minimum Quantity Lubrication using Hexagonal Boron Nitride Particles", Proceedings of the 4M/ICOMM2015 Conference, pp. 158–161.

Kim, J.S., Kim, J.W., Lee, S.W., (2017), "Experimental characterization on micro-end milling of titanium alloy using nanofluid minimum quantity lubrication with chilly gas", International Journal of Advanced Manufacturing Technology, Vol. 91 (5-8), pp. 2741-2749.

Kim, J.S.J.W., Kim, J.S.J.W., Lee, S.W., (2017), "Experimental Characterization of Turning Process of Titanium Alloy Using Cryogenic Cooling and Nanofluid Minimum Quantity Lubrication", Journal of the Korean Society for Precision Engineering, Vol. 34 (3), pp. 185-189.

Klamecki, B.E., (1973), "Incipient chip formation in metal cutting a three dimension finite element analysis", Ph.D. thesis. Univ. Illinois.

Klocke, F., Döbbeler, B., Peng, B., Lakner, T., (2017), "FE-simulation of the Cutting Process under Consideration of Cutting Fluid", in: Proc. CIRP, Vol. 58, pp. 341-346.

Klocke, F., Eisenblaetter, G., (1997), "Dry cutting", CIRP Annals - Manufacturing Technology, Vol. 46 (2), pp. 519-526.

Klocke, F., Krämer, A., Sangermann, H., Lung, D., (2012), "Thermo-mechanical tool load during high performance cutting of hard-to-cut materials", in: Proc. CIRP, Vol. 1 (1), pp. 295-300.

Koenig, W., (1979), "Applied Research on the Machinability of Titanium and Its Alloys", in: Proceeding 47th Meeting of AGARD Structural and Materials Panel Vol. CP256. AGARD, London, pp. 1–10.

Komanduri, R., Hou, Z.B.,(2002), "On thermoplastic shear instability in the machining of a titanium alloy (Ti-6Al-4V)", Metallurgical and Materials Transactions A: Physical Metallurgy and Materials Science, Vol. 33 (9), pp. 2995-3010.

Kopac, J., (2009), "Achievements of sustainable manufacturing by machining", Journal of Achievements in Materials and Manufacturing Engineering, Vol. 34 (2), pp. 180-187.

Kosa, T. and Ney, R. P., (1989), –Metals Handbook", Vol.16, ASM, pp.681-707.

Kosaraju, S., Anne, V.G., (2013), "Optimal machining conditions for turning Ti-6Al-4V using response surface methodology", Adv. in Manuf., Vol. 1 (4), pp. 329-339.

Kosaraju, S., Gopal, V., Bangaru, A.&, Popuri, B., (2012), "Taguchi Analysis on Cutting Forces and Temperature in Turning Titanium Ti-6Al-4V", International Journal of Mechanical and Industrial Engineering, Vol.1 (4), pp. 2231–6477.

Krishna, A.G., Rao, T.B., (2016), "Performance Assessment of Carbon Nano Tube Based Cutting Fluid in Machining Process", International Journal of Science, Engineering and Technology, Vol. 10, pp. 1059–1062.

Krishnaraj, V., Krishna, B.H., Ahmad, J.Y.S., (2017), "An experimental study on end milling of titanium alloy (Ti-6Al-4V) under dry and minimum quantity lubrication conditions", International Journal of Machining and Machinability of Materials, Vol. 19 (4), pp. 325-342.

Krolczyk, G.M., Maruda, R.W., Krolczyk, J.B., Wojciechowski, S., Mia, M., Nieslony, P., Budzik, G., (2019),"Ecological trends in machining as a key factor in sustainable production – A review", Journal of Cleaner Production, Volume 218, pp. 601-615.

Krolczyk, G.M., Nieslony, P., Maruda, R.W., Wojciechowski, S., (2017), "Dry cutting effect in turning of a duplex stainless steel as a key factor in clean production', Journal of Cleaner Production, Vol. 142 (4), pp. 3343-3354.

Kumar, M.P., Jerold, B.D., (2013), "Effect of Cryogenic Cutting Coolants on Cutting Forces and Chip Morphology in Machining Ti-6Al-4V Alloy", International Journal of Applied Science and Technology, Vol. 6 (2), pp. 1-7.

Kumar, R., Kumar Sahooa, A., Satyanarayana, K., Venkateswara Rao, G., (2013), "Some studies on cutting force and temperature in machining Ti-6AL-4V alloy using regression analysis and ANOVA", International Journal of Industrial Engineering Computations, Vol. 4 (3), pp. 427-436.

Kumar, V.P.S., Manikandan, N., Subakaran, C., Jeso, Y.G.S., (2018), "An Experimental Effect of ZnO Nanoparticles in SAE 20W50 Oil", International Research Journal of Engineering and Technology, Vol. 05 (03), pp. 1069–1073.

Lee, G.J., Park, J.J., Lee, M.K., Rhee, C.K., (2017), "Stable dispersion of nanodiamonds in oil and their tribological properties as lubricant additives", Applied Surface Science, Vol. 415, pp. 24–27.

Lee, I., Bajpai, V., Moon, S., Byun, J., Lee, Y., Park, H.W., (2015), "Tool life improvement in cryogenic cooled milling of the preheated Ti–6Al–4V", International Journal of Advanced Manufacturing Technology, Vol. 79 (1-4), pp. 665-673.

Lee, K., Hwang, Y., Cheong, S., Choi, Y., Kwon, L., Lee, J., Kim, S.H., (2009), "Understanding the role of nanoparticles in nano-oil lubrication", Tribology Letters, Vol. 35 (2), pp. 127-131.

Lee, P.H., Nam, J.S., Li, C., Lee, S.W., (2012), "An experimental study on micro-grinding process with nanofluid minimum quantity lubrication (MQL)", International Journal of Precision Engineering and Manufacturing, Vol. 13 (3), pp. 331-338.

Lee, P.H., Nam, T.S., Li, C., Lee, S.W., (2010), "Environmentally-friendly nano-fluid minimum quantity lubrication (MQL) meso-scale grinding process using nano-diamond particles", in: Proceedings - 2010 International Conference on Manufacturing Automation, ICMA 2010, pp. 44-49.

Lee, S.W., Park, S.D., Kang, S., Bang, I.C., Kim, J.H., (2011), "Investigation of viscosity and thermal conductivity of SiC nanofluids for heat transfer applications", International Journal of Heat and Mass Transfer, Vol. 54 (1-3), pp. 433-438.

Lee, W.Y., Kim, K.W., Sin, H.C., (2002), "Cutting conditions for finish turning process aiming: The use of dry cutting", International Journal of Machine Tools and Manufacture, Vol. 42 (8), pp. 899-904.

Leong, K.Y., Mohd Hanafi, N., Mohd Sohaimi, R., Amer, N.H., (2016), "The effect of surfactant on stability and thermal conductivity of carbon nanotube based nanofluids", Thermal Science, Vol. 20 (2), pp. 429-436.

Lepicka, M., Gradzka-Hahlke, M.,(2016), "Surface Modification of Ti6al4v Titanium Alloy for Biomedical Applications and its Effect", Reviews on Advanced Materials Science, Vol. 46 (1), pp. 86-103.

Li, A., Zhao, J., Hou, G., (2017), "Effect of cutting speed on chip formation and wear mechanisms of coated carbide tools when ultra-high-speed face milling titanium alloy Ti-6Al-4V", Advances in Mechanical Engineering, Vol. 9 (7), pp.1-13.

Li, A., Zhao, J., Zhou, Y., Chen, X., Wang, D., (2012), "Experimental investigation on chip morphologies in high-speed dry milling of titanium alloy Ti-6Al-4V", Int. Journal of Advanced Manufacturing Technology, Vol. 62 (9-12), pp. 933-942.

Li, B., Li, C., Zhang, Y., Wang, Y., Jia, D., Yang, M., Zhang, N., Wu, Q., Han, Z., Sun, K., (2017), "Heat transfer performance of MQL grinding with different nanofluids for Ni-based alloys using vegetable oil", J. of Cleaner Production, Vol. 154, pp. 1-11

Liang, X., Liu, Z., Liu, W., Li, X., (2019), "Sustainability assessment of dry turning Ti-6Al-4V employing uncoated cemented carbide tools as clean manufacturing process", Journal of Cleaner Production, Vol. 214, pp. 279-289.

Liang, Z., Gao, P., Wang, X., Li, S., Zhou, T., Xiang, J., (2018), "Cutting performance of different coated micro end mills in machining of Ti-6Al-4V", Micro machines, Vol. 9 (11), pp. 568 (1-12).

Lienhard V. and Jhon, H., (2006), ―Heat Transfer by Impingement of Circular Free-Surface Liquid Jets", 18th National & 7th ISHMT-ASME Heat and Mass Transfer Conference, 16.

Lin, Z.C., Ho, C.Y., (2003), "Analysis and application of grey relation and ANOVA in chemical-mechanical polishing process parameters", International Journal of Advanced Manufacturing Technology, Vol. 21, pp. 10–14.

Liu, G.R., Quek, S.S., (2003), "Finite Element Method: A Practical Course", pp. 1–348.

Liu, S., Shin, Y.C., (2019), "Additive manufacturing of Ti6Al4V alloy: A review", Materials and Design, Vol. 164, pp. 107552 (1-64).

Liu, W., Liu, Z., (2018), "High-pressure coolant effect on the surface integrity of machining titanium alloy Ti-6Al-4V: A review", Materials Research Express, Vol. 5 (3), pp. 032001 (1-50).

Liu, Z., An, Q., Xu, J., Chen, M., Han, S., (2013), "Wear performance of (nc-AlTiN)/(a-Si3N4) coating and (nc-AlCrN)/(a-Si3N4) coating in high-speed machining of titanium alloys under dry and minimum quantity lubrication (MQL) conditions", Wear, Vol. 305 (1-2), pp. 249-259.

Liu, Z.Q., Cai, X.J., Chen, M., An, Q.L., (2011), "Investigation of cutting force and temperature of end-milling Ti-6Al-4V with different minimum quantity lubrication (MQL) parameters", in: Proceedings of the Institution of Mechanical Engineers, Part B: Journal of Engineering Manufacture, Vol. 225 (8), pp. 1273-1279.

López De Lacalle, L.N., Pérez, J., Llorente, J.I., Sánchez, J.A., (2000), "Advanced cutting conditions for the milling of aeronautical alloys", Journal of Materials Processing Technology, Vol. 100 (1), pp. 1-11.

Lorza, R., Calvo, M., Labari, C., Fuente, P., (2018), "Using the Multi-Response Method with Desirability Functions to Optimize the Zinc Electroplating of Steel Screws", Metals, Vol. 8 (9), pp. 711 (1-20).

M. Venkata Ramana, G. Krishna Mohan Rao, D.H.R., (2014), "Chip Morphology in Turning of Ti-6al-4v Alloy under Different Machining Conditions", Journal of Production Engineering, Vol. 17 (1), pp. 27–32.

M.J. Donachie, (2000), "Titanium: A Technical Guide", ASM International.

Machado, A.R., J Wallbank, J., (1990), "Machining of Titanium and its Alloys—a Review", Proceedings of the Institution of Mechanical Engineers, Part B: Journal of Engineering Manufacture, SAGE Publications Ltd, Vol. 204, pp. 53-60.

Madhukar, S., Shravan, A., G Sreeram Reddy, Vidyanand, P., (2016), "A Critical review on Minimum Quantity Lubrication (MQL) Coolant System for Machining Operations", International Journal of Current Engineering and Technology, Vol. 6 (5), pp.1745-1751.

Mahbubul, I.M., Saidur, R., Amalina, M.A., (2012), "Latest developments on the viscosity of nanofluids", Int. Journal of Heat and Mass Transfer, Vol. 55 (4), pp. 874-885.

Manjaiah, M., Deenashree, K.N., Basavarajappa, S., (2019), "WED-machining characteristics of Ti6Al4V alloy based on central composite design", International Journal of Materials and Product Technology, Vol. 59 (2), pp. 121-139.

Mannekote, J.K., Kailas, S. V., (2012), "The effect of oxidation on the tribological performance of few vegetable oils", Journal of Materials Research and Technology, Vol. 1 (2), pp. 91–95.

Maria, R., (2016), "Heat transfer coefficient of nanofluid", Mech. System Design, pp. 1-6.

Marigoudar R and Kanakuppi S, (2013), ―Investigation of tool wear and surface roughness during machining of ZA43-SiCp composite using full factorial approach", Proceedings of the Institution of Mechanical Engineers, Part B: Journal of Engineering Manufacture, Vol. 227 (6), pp. 821-831.

Martin, H., (1977), "Heat and Mass Transfer between Impinging Gas Jets and Solid Surfaces", Advances in Heat Transfer, Vol. 13 (C), pp. 1-60.

Masoudi, S., Vafadar, A., Hadad, M., Jafarian, F., (2018), "Experimental investigation into the effects of nozzle position, workpiece hardness, and tool type in MQL turning of AISI 1045 steel", Materials and Manufacturing Processes, Vol. 33, pp. 1011–1019.

Matthew J. Donachie, J., (2003),"Titanium A Technical guide", ASM International, Vol. 99, pp. 171–182.

Merchant, M.E., (1945), "Mechanics of the metal cutting process. II. Plasticity conditions in orthogonal cutting", Journal of Applied Physics, Vol. 16 (6), pp. 318-324.

Mhamdi, M.-B., Boujelbene, M., Bayraktar, E., Zghal, A., (2012), "Surface Integrity of Titanium Alloy Ti-6Al-4V in Ball end Milling", Physics Proc., Vol. 25, pp. 355-362.

Mia, M., Dhar, N.R., (2019), "Influence of single and dual cryogenic jets on machinability characteristics in turning of Ti-6Al-4V", Proceedings of the Institution of Mechanical Engineers, Part B: Journal of Engineering Manufacture, Vol. 233 (3), pp. 711-726.

Mia, M., Dhar, N.R., (2016b), "Prediction of surface roughness in hard turning under high pressure coolant using Artificial Neural Network", Measurement: Journal of the International Measurement Confederation, Vol. 92, pp. 464-474.

Mia, M., Khan, M.A., Dhar, N.R., (2017), "High-pressure coolant on flank and rake surfaces of tool in turning of Ti-6Al-4V: investigations on surface roughness and tool wear", Int. J. of Advanced Manufacturing Technology, Vol. 90 (5-8), pp. 1825-1834.

Miguélez, M.H., Soldani, X., Molinari, A., (2013), "Analysis of adiabatic shear banding in orthogonal cutting of Ti alloy", Int. J. of Mechanical Sciences, Vol. 75, pp. 212-222.

Minea, A.A., Moldoveanu, M.G., (2018), "Overview of Hybrid Nanofluids Development and Benefits", Journal of Engineering Thermophysics, Vol. 27 (4), pp. 507-514.

Mirmohammadi, S.A., Behi, M., Gan, Y., Shen, L., (2019), "Particle-shape-, temperature-, and concentration-dependent thermal conductivity and viscosity of nanofluids", Physical Review E, Vol. 99 (4), pp. 043109 (1-15).

Mishra, P.C., Mukherjee, S., Nayak, S.K., Panda, A., (2014), "A brief review on viscosity of nanofluids". Int. Nano Lett, Vol. 4, pp. 109–120.

Mondal, A., Roy, P., Mitra, S., (2020), "Experimental investigation on electro discharge machining of Ti6Al4V alloy", Advances in Materials and Processing Technologies, DOI: 10.1080/2374068X.2020.1759913, pp.1-11.

Morgan, M.N., Barczak, L., Batako, A., (2012), "Temperatures in fine grinding with minimum quantity lubrication (MQL)", International Journal of Advanced Manufacturing Technology, Vol. 60 (9-12), pp. 951-958.

Mosleh, M., Shirvani, K., Smith, S., Belk, J., Lipczynski, G., (2019), "A Study of Minimum Quantity Lubrication (MQL) by Nanofluids in Orbital Drilling and Tribological Testing", J. of Manuf. and Materials Processing, Vol. 3 (1), pp. 5 (1-12).

Nabhani, F., (2001), "Wear mechanisms of ultra-hard cutting tools materials", Journal of Materials Processing Technology, Vol. 115 (3), pp. 402-412.

Nam, J., Lee, S.W., (2018), "Machinability of titanium alloy (Ti-6Al-4V) in environmentally-friendly micro-drilling process with nanofluid minimum quantity lubrication using nanodiamond particles", International Journal of Precision Engineering and Manufacturing - Green Technology, Vol. 5 (1), pp. 29-35.

Namb, M., Paulo, D., (2011), "Influence of Coolant in Machinability of Titanium Alloy (Ti-6Al-4V)", Journal of Surface Engineered Materials and Advanced Technology, Vol. 01 (01), pp. 9-14.

Nandy, A.K., Gowrishankar, M.C., Paul, S., (2009), "Some studies on high-pressure cooling in turning of Ti-6Al-4V", International Journal of Machine Tools and Manufacture, Vol. 49 (2), pp. 182-198.

Nasr, M.N.A., Ng, E.G., Elbestawi, M.A., (2008), "A modified time-efficient FE approach for predicting machining-induced residual stresses", Finite Elements in Analysis and Design, Vol. 44 (4), pp. 149-161.

Nguyen, T., Nguyen, D., Howes, P., Kwon, P., Park, K.-H.H., (2015), "Minimum quantity lubrication (MQL) using vegetable oil with nano-platelet solid lubricant in milling titanium alloy", in: ASME 2015 International Manufacturing Science and Engineering Conference, MSEC 2015, Vol. 2, pp. 9466 (1-10).

Nikawa, M., Mori, H., Kitagawa, Y., Okada, M., (2016), "FEM simulation for orthogonal cutting of Titanium-alloy considering ductile fracture to Johnson-Cook model", Mechanical Engineering Journal, Vol. 3 (2), pp. 15-00536 (1-10).

Nimel Sworna Ross, K., Ganesh, M., (2019), "Performance Analysis of Machining Ti–6Al–4V Under Cryogenic $CO_2$ Using PVD-TiN Coated Tool", Journal of Failure Analysis and Prevention, Vol. 19 (3), pp. 821-831.

Nithyanandam, J., Das, S.L., Palanikumar, K., (2015), "Influence of Cutting Parameters in Machining of Titanium Alloy", Indian Journal of Science and Technology, Vol. 8 (S8), pp. 556–562.

Obikawa, T., Kamata, Y., Asano, Y., Nakayama, K., Otieno, A.W., (2008), "Micro-liter lubrication machining of Inconel 718", International Journal of Machine Tools and Manufacture, Vol. 48, pp. 1605–1612.

Obikawa, T., Kamata, Y., Shinozuka, J., (2006), "High-speed grooving with applying MQL", Int. Journal of Machine Tools and Manufacture, Vol. 46, pp. 1854–1861.

Ola, O.T., Valdez, R.L., Oluwasegun, K.M., Ojo, O.A., Chan, K., Birur, A., Cuddy, J., (2019), "Process variable optimization in the cold metal transfer weld repair of aerospace ZE41A-T5 alloy using central composite design", International Journal of Advanced Manufacturing Technology, Vol. 105 (11), pp. 4827-4835.

Öpöz, T.T., Chen, X., (2016), "Chip formation mechanism using finite element simulation", Journal of Mechanical Engineering, Vol. 62 (11), pp. 636-646.

Osman, K.A., Ünver, H.Ö., Şeker, U., (2019), "Application of minimum quantity lubrication techniques in machining process of titanium alloy for sustainability: a review", The International Journal of Advanced Manufacturing Technology, Vol. 100, pp. 2311–2332.

Özel, T., (2006), "The influence of friction models on finite element simulations of machining", Int. J. of Machine Tools and Manufacture, Vol. 46(5), pp. 518-530.

Özel, T., Sima, M., Srivastava, A.K., (2010), "Finite element simulation of high speed machining Ti-6Ai-4V alloy using modified material models", in: Transactions of the North American Manufacturing Research Institution of SME, Vol. 38, pp. 49-56.

Özel, T., Zeren, E., (2005), "Finite element method simulation of machining of AISI 1045 steel with a round edge cutting tool", Proceedings of 8th CIRP International Workshop on Modeling of Machining Operations, Chemnitz, Germany, pp. 533-542.

Pal, A., Choudhury, S.K., Chinchanikar, S., (2014), "Machinability Assessment through Experimental Investigation during Hard and Soft Turning of Hardened Steel", Procedia Materials Science, Vol. 6, pp. 80-91.

Palanisamy, S., McDonald, S.D., Dargusch, M.S., (2009a), "Effects of coolant pressure on chip formation while turning Ti6Al4V alloy", International Journal of Machine Tools and Manufacture, Vol. 49(9), pp. 739-743.

Palanisamy, S., Townsend, D., Scherrer, M., Andrews, R., Dargusch, M.S., (2009b), "High Pressure Coolant Application in Milling Titanium", Materials Science Forum Vol. 618-619, pp. 89-92.

Park, K.H., Olortegui-Yume, J., Yoon, M.C., Kwon, P., (2010), "A study on droplets and their distribution for minimum quantity lubrication (MQL)", International Journal of Machine Tools and Manufacture, Vol. 50(9), pp. 824-833.

Park, K.H., Suhaimi, M.A., Yang, G.D., Lee, D.Y., Lee, S.W., Kwon, P., (2017), "Milling of titanium alloy with cryogenic cooling and minimum quantity lubrication (MQL)", Int. Journal of Precision Engineering and Manufacturing, Vol. 18(1), pp. 5-14.

Pastoriza-Gallego, M.J., Lugo, L., Legido, J.L., Piñeiro, M.M., (2011), "Thermal conductivity and viscosity measurements of ethylene glycol-based $Al_2O_3$ nanofluids", Nanoscale Research Letters, Vol. 6, pp. 221 (1-11).

Patil, D.K., Sawant, S.M., (2014), "A Parametric Study on Performance of Titanium Alloy Using Coated and Uncoated Carbide Insert in CNC Turning", International Journal of Advanced Mechanical Engineering, Vol. 4 (5), pp. 557-564.

Paul, G., Chopkar, M., Manna, I., Das, P.K.,(2010), "Techniques for measuring the thermal conductivity of nanofluids: A review", Renewable and Sustainable Energy Reviews, Vol. 14 (7), pp. 1913-1924.

Pervaiz, S., Anwar, S., Qureshi, I., Ahmed, N., (2019), "Recent Advances in the Machining of Titanium Alloys using Minimum Quantity Lubrication (MQL) Based Techniques", International Journal of Precision Engineering and Manufacturing-Green Technology, Vol.6 (1–2), pp. 133–145.

Pervaiz, S., Deiab, I., Wahba, E., Rashid, A., Nicolescu, C.M., (2015), "A novel numerical modeling approach to determine the temperature distribution in the cutting tool using conjugate heat transfer (CHT) analysis", International Journal of Advanced Manufacturing Technology, Vol. 80, pp. 1039–1047.

Pittalà, G.M., (2018), "A study of the effect of CO2 cryogenic coolant in end milling of Ti-6Al-4V", in: Procedia CIRP, Vol. 77, pp. 445-448.

Pittalà, G.M., Monno, M., (2011), "A new approach to the prediction of temperature of the workpiece of face milling operations of Ti-6Al-4V", Applied Thermal Engineering, Vol. 31(2–3), pp. 173-180.

Pradhan, S., Singh, S., Prakash, C., Królczyk, G., Pramanik, A., Pruncu, C.I., (2019), "Investigation of machining characteristics of hard-to-machine Ti-6Al-4V-ELI alloy for biomedical applications", J. of Mat. Res. and Tech., Vol. 8 (5), pp. 4849-4862.

Priyadarshini, A., Pal, S.K., Samantaray, A.K., (2012), "Finite element modeling of chip formation in orthogonal machining", in: Statistical and Computational Techniques in Manufacturing, pp.101-144.

Proudian, J., (2012), "Simulating Residual Stress in Machining; from Post Process Measurement to Pre-Process Predictions", M.Sc. thesis, KTH Royal Ins. of Tech.

Qin, S., Li, Z., Guo, G., An, Q., Chen, M., Ming, W., (2016), "Analysis of minimum quantity lubrication (MQL) for different coating tools during turning of TC11 titanium alloy", Materials, Vol.9 (10), pp. 804 (1-13).

Raczy, A., Elmadagli, M., Altenhof, W.J., Alpas, A.T., (2004), "An Eulerian finite-element model for determination of deformation state of a copper subjected to orthogonal cutting", Metallurgical and Materials Transactions A: Physical Metallurgy and Materials Science, Vol. 35 A (8), pp. 2393-2400.

Ramana, M.V., Aditya, Y.S., (2017), "Optimization and influence of process parameters on surface roughness in turning of titanium alloy", in: Materials Today: Proceedings. Vol. 4 (2-Part A), pp. 1843-1851.

Ramana, M.V., Srinivasulub, K., Gurram, K.M.R., (2011), "Performance Evaluation and Selection of Optimal Parameters in Turning of Ti-6Al-4V Alloy Under Different Cooling Conditions", International Journal of Innovative Technology & Creative Engineering, Vol. 1 (5), pp. 10–21.

Ranjan, P., Hiremath, S.S., (2019), "Role of textured tool in improving machining performance: A review", Journal of Manufacturing Processes, Vol. 43, pp. 47-73.

Rao, S.N., Satyanarayana, B., Venkatasubbaiah, K., (2011), "Experimental Estimation of Tool Wear and Cutting Temperatures in MQL Using Cutting Fluids With CNT Inclusion", Int. J. of Engineering Science & Technology, Vol. 3 (4), pp. 2928-2931.

Rapeti, P., Pasam, V.K., Rao Gurram, K.M., Revuru, R.S., (2016), "Performance evaluation of vegetable oil based nano cutting fluids in machining using grey relational analysis-A step towards sustainable manufacturing", Journal of Cleaner Production, Vol. 172, pp. 2862-2875.

Reed, R. P. and Clark, A. F., (1983), –Materials at Low Temperatures", American Society for Metals, Carnes Publication, Metal Park, OH, pp. 294-296.

Revankar, G.D., Shetty, R., Rao, S.S., Gaitonde, V.N., (2014), "Analysis of surface roughness and hardness in titanium alloy machining with polycrystalline diamond tool under different lubricating modes", Mater. Res., Vol. 17 (4), pp. 1010-1022.

Revuru, R.S., Posinasetti, N.R., Vsn, V.R., Amrita, M., (2017), "Application of cutting fluids in machining of titanium alloys—a review", International Journal of Advanced Manufacturing Technology, Vol. 91, pp. 2477–2498.

Revuru, R.S., Zhang, J.Z., Posinasetti, N.R., Kidd, T., (2018), "Optimization of titanium alloys turning operation in varied cutting fluid conditions with multiple machining performance characteristics", International Journal of Advanced Manufacturing Technology, Vol. 95 (1-4), pp. 1451-1463.

Rohit, J.N., Surendra Kumar, K., Sura Reddy, N., Kuppan, P., Balan, A.S.S., (2018), "Computational Fluid Dynamics Analysis of MQL Spray Parameters and Its Influence on MQL Milling of SS304", Sim. for Design and Manufacturing, pp.45-78.

Rotella, G., Dillon, O.W., Umbrello, D., Settineri, L., Jawahir, I.S., (2014), "The effects of cooling conditions on surface integrity in machining of Ti6Al4V alloy", Int International Journal of Advanced Manufacturing Technology, Vol.71, pp. 47–55.

Roy, S., Ghosh, A., (2013), "High speed turning of AISI 4140 steel using nanofluid through twin jet SQL system", ASME 2013 International Manufacturing Science and Engineering Conference Collocated with the 41st North American Manufacturing Research Conference, MSEC 2013, Vol. 2, pp. 1-6.

Rui, T., Li, H., Qi, Z., Bo, Z., (2014), "Cutting properties analysis of titanium alloy (Ti-6Al-4V) base on cryogenic cooling", Open Mat. Sci. Journal, Vol. 8(1), pp. 122-126.

Sachin, B., Narendranath, S., Chakradhar, D., (2019), "Enhancement of surface integrity by cryogenic diamond burnishing toward the improved functional performance of the components", Journal of the Brazilian Society of Mechanical Sciences and Engineering, Vol. 41, pp. 396 (1-13).

Sadeghifar, M., Sedaghati, R., Jomaa, W., Songmene, V., (2018), "A comprehensive review of finite element modeling of orthogonal machining process: chip formation and surface integrity predictions", Int. J. Adv. Manuf. Tech.., Vol.96, pp. 3747–379.

Sadik, M.I., Isakson, S., Malakizadi, A., Nyborg, L., (2016), "Influence of Coolant Flow Rate on Tool Life and Wear Development in Cryogenic and Wet Milling of Ti-6Al-4V", in: Procedia CIRP, Vol. 46, pp. 91-94.

Buruaga, M.S., Esnaola, J.A., Aristimuno, P., Soler, D., Björk, T., Arrazola, P.J., (2017), "A Coupled Eulerian Lagrangian Model to Predict Fundamental Process Variables and Wear Rate on Ferrite-pearlite Steels", Proc. CIRP, Vol. 58, pp. 251-256.

Saha, A., Mondal, S.C., (2016), "Multi-objective optimization in WEDM process of nanostructured hard facing materials through hybrid techniques", Measurement: Journal of the International Measurement Confederation, Vol. 94, pp. 46-59.

Said, Z., Gupta, M., Hegab, H., Arora, N., Khan, A.M., Jamil, M., Bellos, E., (2019), "A comprehensive review on minimum quantity lubrication (MQL) in machining processes using nano-cutting fluids", International Journal of Advanced Manufacturing Technology, Vol. 105 (5-6), pp. 2057-2086.

Sales, W., Becker, M., Barcellos, C.S., Landre, J., Bonney, J., Ezugwu, E.O., (2009), "Tribological behaviour when face milling AISI 4140 steel with minimum quantity fluid application". Industrial Lubrication and Tribology, Vol. 61 (2), pp. 84-90.

Sarikaya, M., Güllü, A., (2015), "Multi-response optimization of minimum quantity lubrication parameters using Taguchi-based grey relational analysis in turning of difficult-to-cut alloy Haynes 25", J. of Cleaner Production, Vol. 91, pp. 347-357.

Sarikaya, M., Güllü, A., (2014), "Taguchi design and response surface methodology based analysis of machining parameters in CNC turning under MQL", Journal of Cleaner Production, Vol. 65, pp. 604-616.

Sarıkaya, M., Yılmaz, V., Güllü, A., (2016), "Analysis of cutting parameters and cooling/lubrication methods for sustainable machining in turning of Haynes 25", superalloy Journal of Cleaner Production, Vol. 133, pp. 172–181.

Sartori, S., Taccin, M., Pavese, G., Ghiotti, A., Bruschi, S., (2018), "Wear mechanisms of uncoated and coated carbide tools when machining Ti6Al4V using LN2 and cooled N2", International Journal of Advanced Manufacturing Technology, Vol. 95 (1-4), pp. 1255-1264.

Sayuti, M., Sarhan, A.A.D., Salem, F., (2014), "Novel uses of SiO2 nano-lubrication system in hard turning process of hardened steel AISI4140 for less tool wear, surface roughness and oil consumption", J. of Cleaner Production, Vol. 67, pp. 265–276.

Sen, B., Mia, M., Gupta, M.K., Rahman, M.A., Mandal, U.K., Mondal, S.P., (2019a), "Influence of $Al_2O_3$ and palm oil–mixed nano-fluid on machining performances of Inconel-690: IF-THEN rules–based FIS model in eco-benign milling", International Journal of Advanced Manufacturing Technology, Vol. 103, pp. 3389–3403.

Sen, B., Mia, M., Krolczyk, G.M., Mandal, U.K., Mondal, S.P., (2019b), "Eco-Friendly Cutting Fluids in Minimum Quantity Lubrication Assisted Machining: A Review on the Perception of Sustainable Manufacturing", International Journal of Precision Engineering and Manufacturing - Green Technology Vol. 8, pp. 249-280.

Setti, D., Ghosh, S., Rao, P. V., (2012), "Application of Nano Cutting Fluid under Minimum Quantity Lubrication (MQL) Technique to Improve Grinding of Ti – 6Al – 4V Alloy", International Journal of Mechanical, Aerospace, Industrial, Mechatronic and Manufacturing Engineering, Vol. 6 (10), pp. 2107 - 2111.

Setti, D., Sinha, M.K., Ghosh, S., Rao, P.V., (2015a), "An investigation into the application of $Al_2O_3$nanofluid-based minimum quantity lubrication technique for grinding of Ti-6Al-4V", Int. J. of Precision Technology, Vol. 4 (3/4), pp. 268-279.

Setti, D., Sinha, M.K., Ghosh, S., Venkateswara Rao, P., (2015b), "Performance evaluation of Ti-6Al-4V grinding using chip formation and coefficient of friction under the influence of nanofluids", International Journal of Machine Tools and Manufacture, Vol. 88, pp. 237-248.

Settineri, L., Faga, M.G., (2008), "Nanostructured cutting tools coatings for machining titanium", Machining Science and Technology, Vol. 12 (2), pp. 158-169.

Seyedzavvar, M., Shabgard, M., Mohammadpourfard, M., (2019), "Investigation into the performance of eco-friendly graphite nanofluid as lubricant in MQL grinding", Mach. Sci. Technol, Vol.23 (4), pp. 569-594.

Shah, J., Ranjan, M., Davariya, V., Gupta, S.K., Sonvane, Y., (2017), "Temperature-dependent thermal conductivity and viscosity of synthesized a-alumina nanofluids", Applied Nanoscience (Switzerland), Vol. 7(8), pp. 803-813.

Shankar, M.C.G., Jayashree, P.K., Shivaprakash, Y., Gurumurthy, B.., Shettar, M., Sharma, S.S., (2015),"Machinability study on turning of Ti-6Al-4V alloy under high-pressure", Glob. J. Eng. Sci. Res. Manag. 2, 169–181.

Shao, F., Liu, Z., Wan, Y., Shi, Z., (2010), "Finite element simulation of machining of Ti-6Al-4V alloy with thermo dynamical constitutive equation", Int. J. Adv. Manuf. Technol, Vol. 9, pp. 431–439.

Sharif, S., Safari, H., Izman, S., Kurniawan, D., (2014), "Effect of high speed dry end milling on surface roughness and cutting forces of Ti-6Al-4V ELI", Applied Mechanics and Materials, Vol. 493, pp. 546-551.

Sharma, A.K., Tiwari, A.K., Dixit, A.R., (2018), "Prediction of temperature distribution over cutting tool with alumina-MWCNT hybrid nanofluid using computational fluid dynamics (CFD) analysis", International Journal of Advanced Manufacturing Technology, Vol. 97(1-4), pp. 427-439.

Sharma, A.K., Tiwari, A.K., Dixit, A.R., (2016), "Effects of Minimum Quantity Lubrication (MQL) in machining processes using conventional and nanofluid based cutting fluids: A comprehensive review", J. of Cleaner Prod., Vol. 127, pp. 1-18.

Sharma, V.S., Dogra, M., Suri, N.M., (2009), "Cooling techniques for improved productivity in turning", International Journal of Machine Tools and Manufacture, Vol. 49 (6), pp. 435-453.

Shet, C., Deng, X., (2003), "Residual stresses and strains in orthogonal metal cutting", International Journal of Machine Tools and Manufacture, Vol. 43 (6), pp. 573-587.

Shokrani, A., Dhokia, V., Newman, S.T., (2016a), "Comparative investigation on using cryogenic machining in CNC milling of Ti-6Al-4V titanium alloy", Machining Science and Technology, Vol. 20(3), pp. 475-494.

Shokrani, A., Dhokia, V., Newman, S.T., (2016b), "Investigation of the effects of cryogenic machining on surface integrity in CNC end milling of Ti-6Al-4V titanium alloy", Journal of Manufacturing Processes, Vol. 21, pp. 172-179.

Shokrani, A., Dhokia, V., Newman, S.T., (2016c), "Cryogenic High Speed Machining of Cobalt Chromium Alloy", Procedia CIRP, Vol. 46, pp. 404-407.

Silva, L.R., Bianchi, E.C., Catai, R.E., Fusse, R.Y., França, T. V., Aguiar, P.R., (2005), "Study on the behavior of the minimum quantity lubricant - MQL technique under different lubricating and cooling conditions when grinding ABNT 4340 steel", J. of the Braz. Society of Mechanical Sciences and Engineering, Vol. 27(2), pp. 192-199.

Sima, M., Özel, T., (2010), "Modified material constitutive models for serrated chip formation simulations and experimental validation in machining of titanium alloy Ti-6Al-4V", Int. J. of Machine Tools & Manufacture, Vol. 50, pp. 943-960.

Singh, G., Gupta, M.K., Hegab, H., Khan, A.M., Song, Q., Liu, Z., Mia, M., Jamil, M., Sharma, V.S., Sarikaya, M., Pruncu, C.I., (2020), "Progress for sustainability in the mist assisted cooling techniques: a critical review", Int. J. Adv. Manuf. Technol.The Int. J. of Advanced Manufacturing Technology, Vol. 109, pp. 345–376.

Singh, R., Dureja, J.S., Dogra, M., Gupta, M.K., Mia, M., (2019a), "Influence of graphene-enriched nanofluids and textured tool on machining behavior of Ti-6Al-4V alloy", Int. J. of Advanced Manufacturing Technology, Vol. 105(1-4), pp. 1685-1697.

Singh, R., Dureja, J.S., Dogra, M., Randhawa, J.S., (2019b), "Optimization of machining parameters under MQL turning of Ti-6Al-4V alloy with textured tool using multi-attribute decision-making methods", World J. of Eng., Vol. 16(5), pp. 648-659.

Songmei, Y., Xuebo, H., Guangyuan, Z., Amin, M., (2017), "A novel approach of applying copper nanoparticles in minimum quantity lubrication for milling of Ti-6Al-4V", Advances in Production Engineering and Management, Vol. 12(2), pp. 139–150.

Sreejith, P.S., Ngoi, B.K.A., (2000), "Dry machining: Machining of the future", J. Mater. Process. Technol, Vol. 101, pp. 287–291.

Srikant, R.R., Prasad, M.M.S., Amrita, M., Sitaramaraju, A. V., Krishna, P.V., (2014), "Nanofluids as a potential solution for Minimum Quantity Lubrication: A review", Proceedings of the Institution of Mechanical Engineers Part B Journal of Engineering Manufacture, Vol. 228 (1), pp. 3-20.

Stephenson, D.A., Agapiou, J.S., (2016), "Metal cutting theory and practice", Third edition.

Su, Y., He, N., Li, L., Iqbal, A., Xiao, M.H., Xu, S., Qiu, B.G., (2007), "Refrigerated cooling air cutting of difficult-to-cut materials", International Journal of Machine Tools and Manufacture, Vol. 47(6), pp. 927-933.

Sun, S., Brandt, M., Dargusch, M.S., (2009), "Characteristics of cutting forces and chip formation in machining of titanium alloys", International Journal of Machine Tools and Manufacture, Vol. 49(7-8), pp. 561-568.

Sun, S., Brandt, M., Palanisamy, S., Dargusch, M.S., (2015), "Effect of cryogenic compressed air on the evolution of cutting force and tool wear during machining of Ti-6Al-4V alloy", J. of Materials Processing Technology, Vol. 221, pp. 243-254.

Suryanarayana, C., Prabhu, B., (2006), "Synthesis of Nanostructured Materials by Inert-Gas Condensation Methods", in: Nanostructured Materials: Processing, Properties, and Applications: Second Edition. Elsevier Inc., (2006), 47-90

Tanveer, A., Marla, D., Kapoor, S.G., (2017), "A Thermal Model to Predict Tool Temperature in Machining of Ti-6Al-4V Alloy With an Atomization-Based Cutting Fluid Spray System", J. Manuf. Sci. Eng. Trans, ASME, Vol. 139, pp. 071016 (1-9).

Tapoglou, N., Lopez, M.I.A., Cook, I., Taylor, C.M., (2017), "Investigation of the Influence of CO2 Cryogenic Coolant Application on Tool Wear", Procedia CIRP, Vol. 63, pp. 745-749.

Taylor, C.M., Hernandez, S.G.A., Marshall, M., Broderick, M., (2018), "Cutting fluid application for titanium alloys Ti-6Al-4V and Ti-10V-2Fe-3Al in a finish turning process", Procedia CIRP, pp. 441–444.

Taylor, R., Coulombe, S., Otanicar, T., Phelan, P., Gunawan, A., Lv, W., Rosengarten, G., Prasher, R., Tyagi, H., (2013), "Small particles, big impacts: A review of the diverse applications of nanofluids", J. of Applied Physics, Vol. 113 (1), pp. 011301(1-60)

Thandra, S.K., Choudhury, S.K., (2010), "Effect of cutting parameters on cutting force, surface finish and tool wear in hot machining", International Journal of Machining and Machinability of Materials, Vol. 7(3), pp. 278.

Tirelli, S., Chiappini, E., Strano, M., Monno, M., Semeraro, Q., (2014), "Experimental Comparison between Traditional and Cryogenic Cooling Conditions in Rough Turning of Ti-6Al-4V", Key Engineering Materials, Vol. 611-612, pp. 1174-1185.

Tool Life Testing With Single-Point Turning Tools, 1976. Mec. Mater. Electr.

Tran Minh Duc, Tran The Long, (2016), "Investigation of MQL-Employed Hard-Milling Process of S60C Steel Using Coated-Cermented Carbide Tools", Journal of Mechanics Engineering and Automation, Vol. 6(3), pp. 128-132.

Upadhyay, V., Jain, P.K., Mehta, N.K., (2013), "Machining with minimum quantity lubrication: a step towards green manufacturing", International Journal of Machining and Machinability of Materials, Vol. 13(4), pp. 349-371.

Upadhyay, V., Jain, P.K., Mehta, N.K., (2012), "Minimum Quantity Lubrication Assisted Turning - An Overview", DAAAM International Scientific Book 2012. DAAAM International Vienna, pp. 463-478.

Vajjha, R.S., Das, D.K., (2009), "Experimental determination of thermal conductivity of three nanofluids and development of new correlations"International Journal of Heat and Mass Transfer, Vol. 52(21-22), pp. 4675-4682.

Varadarajan, A.S., Philip, P.K., Ramamoorthy, B., (2002), "Investigations on hard turning with minimal cutting fluid application (HTMF) and its comparison with dry and wet turning", Int. J. of Machine Tools and Manufacture, Vol. 42(2), pp. 193-200.

Veiga, C., Davim, J.P., Loureiro, A.J.R., (2013a), "Review on machinability of titanium alloys: The process perspective", Rev. on adv. Mat. science, Vol. 34(2), pp. 148-164.

Venkata Ramana, M., (2017), "Optimization and Influence of Process Parameters on Surface Roughness in Turning of Titanium Alloy under Different Lubricant Conditions", Materials Today: Proceedings. Elsevier Ltd, pp. 8328–8335.

Venugopal, K.A., Paul, S., Chattopadhyay, A.B., (2007a), "Tool wear in cryogenic turning of Ti-6Al-4V alloy". Cryogenics, Vol.47(1), pp. 12-18.

Venugopal, K.A., Paul, S., Chattopadhyay, A.B.,( 2007b), "Growth of tool wear in turning of Ti-6Al-4V alloy under cryogenic cooling", Wear, Vol.262(9), pp. 1071-1078.

Vijay, S., Krishnaraj, V., (2013), "Machining parameters optimization in end milling of Ti-6A1-4V", Procedia Engineering, Vol.64, pp. 1079-1088.

Virdi, R.L., Chatha, S.S., Singh, H., (2020.), "Processing Characteristics of Different Vegetable Oil-based Nanofluid MQL for Grinding of Ni-Cr Alloy", Adv. Mater. Process. Technol. International Journal of Precision Engineering and Manufacturing - Green Technology (2018) 5(2) 327-339

Wang, B., Liu, Z., (2015), "Shear localization sensitivity analysis for Johnson-Cook constitutive parameters on serrated chips in high speed machining of Ti6Al4V", Simulation Modelling Practice and Theory, Vol. 55, pp. 63-76.

Wang, B., Liu, Z., (2014), "Investigations on the chip formation mechanism and shear localization sensitivity of high-speed machining Ti6Al4V", International Journal of Advanced Manufacturing Technology, Vol. 75(5-8), pp. 1065-1076.

Wang, X., Xu, X., Choi, S.U.S., (1999), "Thermal conductivity of nanoparticle-fluid mixture", Journal of Thermophysics and Heat Transfer, Vol. 13(13), pp. 474-480.

Wang, Z.M., Ezugwu, E.O., (1997), "Performance of PVD-coated carbide tools when machining Ti-6Al-4V", Tribology Transactions, Vol. 40(1), pp. 81-86.

Wu, Z., Deng, J., Zhao, J., (2012), "Study on tool life of surface textured tool in dry cutting of Ti-6Al-4V alloys", Advanced Materials Research, pp. 1245–1249.

Wyen, C.F., Wegener, K., (2010), "Influence of cutting edge radius on cutting forces in machining titanium", CIRP Annals – Manuf. Technology, Vol. 59(1), pp. 93-96.

Xie, H., Jiang, B., Liu, B., Wang, Q., Xu, J., Pan, F., (2016), "An Investigation on the Tribological Performances of the SiO2/MoS2 Hybrid Nanofluids for Magnesium Alloy-Steel Contacts", Nanoscale Research Letters, Vol. 11, pp. 329 (1-17).

Xie, H., Wang, J., Xi, T., Liu, Y., Ai, F., Wu, Q., (2002), "Thermal conductivity enhancement of suspensions containing nanosized alumina particles", Journal of Applied Physics, Vol. 91 (7), pp. 4568-4572.

Xiong, Y., Wu, J., Deng, C., Wang, Y., (2016), "Machining process parameters optimization for heavy-duty CNC machine tools in sustainable manufacturing", Int. Journal of Advanced Manufacturing Technology, Vol. 87 (5-8), pp. 1237-1246.

Yaich, M., Ayed, Y., Bouaziz, Z., Germain, G., (2017), "Numerical analysis of constitutive coefficients effects on FE simulation of the 2D orthogonal cutting process: application to the Ti6Al4V", International Journal of Advanced Manufacturing Technology, Vol. 93 (1-4), pp. 283-303.

Yan, L., Yuan, S., Liu, Q., (2012), "Influence of minimum quantity lubrication parameters on tool wear and surface roughness in milling of forged steel", Chinese Journal of Mechanical Engineering, Vol. 25 (3), pp. 419-429.

Yan, P., Rong, Y., Wang, G., (2016), "The effect of cutting fluids applied in metal cutting process", Proceedings of the Institution of Mechanical Engineers, Part B: Journal of Engineering Manufacture, Vol. 230 (1), DOI: 10.1177/0954405415590993, pp. 1-19.

Yang, L., Ji, W., Mao, M., Huang, J. nan, (2020), "An updated review on the properties, fabrication and application of hybrid-nanofluids along with their environmental effects", Journal of Cleaner Production, Vol. 257, pp. 120408.

Yang, X., Liu, C.R., (1999), "Machining titanium and its alloys", Machining Science and Technology, Vol. 3(1), pp. 107-139.

Yasa, E., Pilatin, S., Çolak, O., (2012), "Overview of cryogenic cooling in machining of Ti alloys and a case study", Journal of Production Engineering, Vol. 2, pp. 1-9.

Yen, Y.C., Jain, A., Chigurupati, P., Wu, W.T., Altan, T., (2004), "Computer simulation of orthogonal cutting using a tool with multiple coatings", An International Journal of Machining Science and Technology, Vol. 8 (2), pp. 305-326.

Yousfi, M., Outeiro, J.C., Nouveau, C., Marcon, B., Zouhair, B., (2017), "Tribological Behavior of PVD Hard Coated Cutting Tools under Cryogenic Cooling Conditions", Procedia CIRP, Vol. 58, pp. 561-565.

Yu, W., France, D.M., Routbort, J.L., Choi, S.U.S., (2008), "Review and comparison of nanofluid thermal conductivity and heat transfer enhancements", Heat Transfer Engineering, Vol. 29(5), pp. 432-460.

Yu, W., Xie, H., (2012), "A review on nanofluids: Preparation, stability mechanisms, and applications", Journal of Nanomaterials, Vol. 2012, Article ID 435873 (1-17).

Zaman, P., Dhar, N., (2021), "Multi-criteria Process Optimization for better machinability in Turning Medium Carbon Steel using Composite Desirability Approach", International Journal of Manufacturing Research, Vol. 16, pp.1.

Zaman, P.B., Dhar, N.R., (2020), "Multi-objective Optimization of Double-Jet MQL System Parameters Meant for Enhancing the Turning Performance of Ti–6Al–4V Alloy", Arabian Journal for Science and Engineering, Vol. 45, pp. 9505–9526.

Zaman, P.B., Sultana, N., Dhar, N.R., (2020), "Quantifying the effects of cooling condition, tool type and cutting parameters on machinability of turning AISI 4140 steel using full factorial DOE", Journal of Production System & Manufacturing Science, Vol. 1 (2), pp. 0009 (1-17).

Zanger, F., Schulze, V., (2013), "Investigations on mechanisms of tool wear in machining of Ti-6Al-4V using FEM simulation", Procedia CIRP, Vol. 8, pp. 158-163.

Ze, W., Jianxin, D., Yang, C., Youqiang, X., Jun, Z., (2012), "Performance of the self-lubricating textured tools in dry cutting of Ti-6Al-4V", International Journal of Advanced Manufacturing Technology, Vol. 62 (9-12), pp. 943-951.

Zeilmann, R.P., Weingaertner, W.L., (2006), "Analysis of temperature during drilling of Ti6Al4V with minimal quantity of lubricant", Journal of Materials Processing Technology, Vol. 179 (1-3), pp. 124–127.

Zhang, S., Zhang, W., Wang, P., Liu, Y., Ma, F., Yang, D., Sha, Z., (2019), "Simulation of material removal process in EDM with composite tools", Advances in Materials Science and Engineering, Vol. 2019, pp. 1321780 (1-11).

Zhang, Y., Outeiro, J.C., Mabrouki, T., (2015), "On the selection of Johnson-Cook constitutive model parameters for Ti-6Al-4V using three types of numerical models of orthogonal cutting", Procedia CIRP, Vol. 31, pp. 112-117.

Zhang, Y.C., Mabrouki, T., Nelias, D., Gong, Y.D., (2011), "Chip formation in orthogonal cutting considering interface limiting shear stress and damage evolution based on fracture energy approach", Finite Elem. in Anal. and Design, Vol. 47(7), pp. 850-863.

Zhang, N., Yang, F., Liu, G., (2020), "Cutting performance of micro-textured WC/Co tools in the dry cutting of Ti-6Al-4V alloy", International Journal of Advanced Manufacturing Technology, Vol. 107(5–8), pp. 1-13.

Zhang, Xianpeng, Li, C., Zhang, Y., Jia, D., Li, B., Wang, Y., Yang, M., Hou, Y., Zhang, Xiaowei, (2016), "Performances of $Al_2O_3$/SiC hybrid nanofluids in minimum-quantity lubrication grinding", International Journal of Advanced Manufacturing Technology, Vol. 86, pp. 3427–3441.

Zhang, Y., Li, C., Ji, H., Yang, X., Yang, M., Jia, D., Zhang, X., Li, R., Wang, J., (2017), "Analysis of grinding mechanics and improved predictive force model based on material-removal and plastic-stacking mechanisms", International Journal of Machine Tools and Manufacture, Vol. 122, pp. 81-97.

Zhu, H., Zhang, C., Liu, S., Tang, Y., Yin, Y., (2006), "Effects of nanoparticle clustering and alignment on thermal conductivities of Fe3O4 aqueous nanofluids", Applied Physics Letters, Vol. 89 (2), pp. 023123-023123-3.

# List of Publications


01. **Zaman, P.B.** and Dhar, N.R. (2019), "Design and Evaluation of an Embedded Double Jet Nozzle for MQL Delivery Intending Machinability Improvement in Turning Operation". Journal of Manufacturing Processes, V ol.44, pp. 179–196.

02. Sultana, M.N., Dhar, N.R. and **Zaman, P.B.,**(2019), "A Review on Different Cooling /Lubrication Techniques in Metal Cutting", American Journal of Mechanics and Applications, Vol .7(4), Pp. 71–87.

03. **Zaman, P.B.,** Saha, S., Dhar, N.R., (2020), ‗Hybrid Taguchi-GRA-PCA Approach for Multi-Response Optimization of Turning Process Parameters Under HPC Condition', Int. J. Machining and Mach. of Materials, Vol. 22 (3/4), pp. 281-308.

04. **Zaman, P.B.** and Dhar, N.R., (2021), ‗Multi-Criteria Process Optimization for Better Machinability in Turning Medium Carbon Steel using Composite Desirability Approach', Int. J. of Manufacturing Research, Vol 16 (1), pp. 1

05. **Zaman, P.B.** and Dhar, N.R., (2020), "Multi-Objective Optimization of Double Jet MQL System Parameters Meant for Enhancing the Turning Performance of Ti-6Al-4V Alloy", Arabian Journal for Science and Engineering, Vol. 45, pp. 9505–9526.

06. **Zaman, P.B.,** Sultana, M.N., and Dhar, N.R., (2020), "Quantifying the Effects of Cooling Condition, Tool Type and Cutting Parameters on Machinability of Turning AISI 4140 Steel using Full Factorial DOE", Journal of Production System & Manufacturing Science, Vol. 1(2), pp. 0009 (1-17).

07. Sultana, M.N., **Zaman, P.B.** and Dhar, N.R., (2020), "Multi-Response Optimization of Turning Process Parameters for Low Alloy Steel AISI 4140 under Cryogenic Cooling using Hybrid Taguchi-GRA-PCA", Journal of Production System & Manufacturing Science, Vol. 1(2), pp. 0010 (1-23).

08. **Zaman, P.B.,** Tusar, I.H.M and Dhar, N.R., (2020), "Selection of Appropriate Process Inputs for Turning Ti-6al-4v Alloy using Uncoated and Coated Carbide Inserts under Hybrid $Al_2O_3$-MWCNT Nano-Fluid Based MQL", Advances in Materials and Processing Technologies, Vol. 6(3), pp. 1-21.

09. Sultana, M.N., **Zaman, P.B.** and Dhar, N.R., (2020), "Effects of Nano-Fluids Assisted MQL in Machining Processes: A Review", 6th Int. Conf. on Mechanical, Industrial and Energy Engineering 2020 (ICMIEE 2020], Khulna, Bangladesh.

10. Sultana, M.N., **Zaman, P.B.** and Dhar, N.R., (2020), "Process Parameter Optimization of Cryogenic Turning of Ni-Cr Steel using Taguchi Grey Relational Analysis", 6th Int. Conf. on Mechanical, Industrial and Energy Engineering 2020 (ICMIEE 2020], Khulna, Bangladesh.

11. **Zaman, P.B.** and Dhar, N.R., (2020), "Current Research Trends in Coolant Application for Machining Ti-6Al-4V Alloy: A State-of-the-Art Review", Advances in Materials and Processing Technologies, *(Accepted subject to revision).*

12. **Zaman, P.B.,** Sultana, M.N., and Dhar, N.R., **"**Multi-Variant Hybrid Techniques Coupled with Taguchi in Multi-Response Parameter Optimization for Better Machinability of Turning Alloy Steel**",** Advances in Materials and Processing Technologies, *(Accepted subject to revision).*.

13. Sultana, M.N., **Zaman, P.B.** and Dhar, N.R., "Hybrid Taguchi-PCA-Utility Approach for Simultaneous Optimisation of Multiple Responses in Turning AISI E4340C Steel", Decision Science Letters, *(Under Review).*

14. Tusar, I.H.M, **Zaman, P.B.,** Mia, M., Saha, S., Sultana, M.N. and Dhar, N.R., ―Influence of Grinding Parameters on Surface Roughness and Temperature under Carbon Nanotube assisted MQL", Measurement, *(Submitted).*